Effects and mechanistic targets of blueberry administered before and/or after stressors on neuroinflammation, oxidative stress, and cognitive deficits

A Dissertation Submitted by:

Danielle S. Cahoon

Presented to the Faculty of

The Gerald J. and Dorothy R. Friedman School of Nutrition Science and Policy at Tufts University

In partial fulfillment of the requirements for the Degree of Doctor of Philosophy in Biochemical and Molecular Nutrition

May 2022

Thesis Advisor:

Dayong Wu, M.D., Ph.D.

Thesis Committee Members:

Barbara Shukitt-Hale, Ph.D.

Tong Zheng, M.D., Ph.D.

Stefania Lamon-Fava, M.D., Ph.D.

ACKNOWLEDGEMENTS

I am extremely grateful to many individuals whose expertise, guidance, and moral support were invaluable for the completion of my doctoral thesis. I was privileged to have completed my doctoral training in the Neuroscience & Aging Laboratory, under the guidance of Dr. Barbara Shukitt-Hale. Her expertise in nutritional neuroscience and the effects of radiation on the central nervous system were instrumental in shaping, refining, and executing my thesis work. Despite the many challenges the COVID-19 pandemic, Barbara taught me to perform cognitive tests in rodents and journeyed to Brookhaven National Laboratory with me for on several occasions for experimental irradiations. She thoroughly reviewed all my work, trusted my ideas, and always kept my best interest at heart. Without her persistence and dedication to my technical and professional development, this dissertation and my growth as a scientist would not have been possible.

I would like to express my sincere appreciation to the members of my thesis committee who provided insightful feedback at all stages of this thesis work, reviewed manuscripts with a critical eye, devoted their time and expertise to teaching me laboratory techniques, and gave unwavering support and encouragement. Dr. Dayong Wu graciously served as my academic and thesis advisor and provided valuable insight on immunology throughout this work. Dr. Tong Zheng taught me to perform immunohistochemistry and imaging analyses and was always willing to answer my many technical and/or scientific questions related to neuroscience. Dr. Stefania Lamon-Fava taught me to perform quantitative PCR and has been a kind and thoughtful mentor since the beginning of my time at the Friedman school.

I am thankful for the support of individuals in the Neuroscience & Aging Laboratory and the HNRCA. Derek Fisher guided me through cell culture and Western blotting experiments and was essential to trouble-shooting many challenges we encountered. Dr. Donna Bielinski taught me molecular biology techniques with incredible patience and kept my days light-hearted before she began a well-deserved retirement. Dr. Grant Rutledge was a wonderful sounding board for scientific ideas and queries, even after moving on from his post-doctoral position. I would also like to thank Dr. Sarah Booth for her support of my thesis work, including her careful review and constructive criticism of my abstracts and manuscripts. I am extremely grateful to Dr. Donald Smith and the Comparative Biology Unit who were critical to maintaining our animal experiment during the pandemic. The expertise of Dr. Bernie Rabin and individuals at the Brookhaven National Laboratory were essential to understanding and performing the radiation aspect of this work.

I also benefited greatly from many members of the Tufts community who contributed to my growth outside of the laboratory, including the professors who took me on as a teaching assistant and various other projects. Dr. Stefania Lamon-Fava, Dr. Lynne Ausman, Dr. Tammy Scott, Dr. Paul Jacques, Dr. Alice Lichtenstein, Dr. Mei Chung, and Dr. Nangurini Nirmala taught me to think critically, collaborate and communicate with confidence and grace, and pursue research with integrity. Additionally, my Friedman school friends kept me motivated and inspired during countless hours in library study rooms and beyond as we navigated the setbacks and successes of graduate school together. Finally, I would like to thank my family for their patience and overwhelming support as I completed my graduate education, who trusted my path and believed in me unconditionally.

ABSTRACT

Background & Objective: Neuroinflammation and oxidative stress (OS) increase following a range of pathological stressors, and have been implicated in development of neurodegeneration and cognitive decline. The molecular mechanisms underlying stressor-induced deficits in the central nervous system (CNS) are not fully understood, limiting the development of therapeutic strategies. Dietary interventions using foods with anti-inflammatory and antioxidant properties, such as blueberries (BB), can attenuate neuroinflammation, OS, and cognitive deficits when administered before stressors such as high energy and charge (HZE) particle radiation. However, the effects and mechanistic targets of anti-inflammatory/antioxidant foods administered after stressors on these outcomes are not well established. The objective of this research was to evaluate the differential effects, and mechanistic targets of pre- and/or post-stressor BB on neuroinflammation, OS, and cognitive deficits.

Methods: *In vitro*, rat microglia were incubated with 0.5 mg/mL BB for 24 hours before and/or after stressor exposure to lipopolysaccharide (LPS) or HZE particles (20 cGy ^{4}He or 2 Gy ^{56}Fe), and inflammation and OS biomarkers were assessed. *In vivo*, male Sprague-Dawley rats were fed a 2% BB-supplemented diet for 45 days before and/or after whole-body exposure to HZE particles (150 cGy ^{56}Fe) and memory-related functions were evaluated at the end of the post-treatment interval. Following euthanasia, the mRNA and protein expression of neuroinflammation, OS, and glial cell activation indicators were analyzed in the frontal cortex and hippocampus.

Results: *In vitro* exposure to LPS, but not HZE particles, induced inflammation and OS in rat microglia. All BB treatments (pre-, post-, and pre-/post) attenuated LPS-induced inflammation and OS. In rats, HZE particle irradiation increased neuroinflammation, OS, and glial activation in the frontal cortex and hippocampus and produced deficits in recognition memory. All dietary BB treatments attenuated irradiation-induced neuroinflammation, OS, glial activation, and memory deficits, and the mitigating effects of pre- and/or post-BB were not different. Changes in neuroinflammation, OS, and glial activation were positively correlated with each other and negatively correlated with recognition memory function.

Conclusions: The attenuating effects of BB treatments, even when administered after LPS or HZE particle exposures, supports the role of neuroinflammation and OS in stressor-induced CNS deficits. Results indicate that activated glial cells may contribute to stressor-induced neuroinflammation, OS, and cognitive deficits, and can be targeted by dietary post-treatments. Correlation analyses suggest that a self-propelling cycle of glial cell activation, neuroinflammation, and OS mediates HZE particle-induced CNS damage and memory deficits. Future work should identify the primary targets of antioxidant/anti-inflammatory post-treatments in this cycle and the optimal post-stressor duration to administer therapeutics. Overall, our findings support the use of dietary post-treatments to reduce the risk of neurodegenerative disease following neuroinflammatory/OS-inducing stressors, such as HZE particle irradiation, and potentially other unpredictable insults involving neuroinflammation and OS such as stroke and traumatic brain injury.

TABLE OF CONTENTS

Acknowledgements ..... **i**

Abstract ..... **ii**

List of Abbreviations ..... **iv**

Figures and Tables ..... **v**

1 INTRODUCTION **1**

1.1 Significance of proposed research 1

1.2 Hypotheses and specific aims 3

2 LITERATURE REVIEW **8**

2.1 Neurodegenerative Diseases 8

2.2 Neuroinflammation, Oxidative Stress & Microglia 8

2.3 Blueberries & Anthocyanins 12

2.4 Pre vs. Post-Treatments 13

2.5 Conclusions and areas of opportunity for research 23

3 MANUSCRIPTS/CHAPTERS **34**

3.1 Blueberry treatment administered before and/or after lipopolysaccharide stimulation attenuates inflammation and oxidative stress in rat microglial cells 34

3.2 Galactic cosmic ray particle exposure does not increase inflammation or oxidative stress in rat microglial cells *in vitro* 57

3.3 Dietary blueberry before and/or after exposure to HZE particle radiation attenuates neuroinflammation, oxidative stress, and cognitive deficits in rats ... 74

4 SUMMARY AND DISCUSSION **133**

4.1 Research summary 133

4.2 Discussion and future directions 136

5 APPENDICES **144**

5.1 Dose-response effects of blueberry on LPS-induced nitric oxide release in rat microglia 144

5.2 Without a radiation effect, pre- and/or post-treatment with blueberry does not alter inflammation or oxidative stress biomarkers in rat microglia exposed to ^{56}Fe *in vitro* 147

5.3 Animal diet composition 151

5.4 Sample size calculation for adequate power *in vivo* 153

5.5 Methods 154

LIST OF ABBREVIATIONS

ANOVA	analysis of variance
BB	blueberry
BNL	Brookhaven National Laboratory
CNS	central nervous system
COX-2	cyclooxygenase-2
CSF-1	colony-stimulating factor 1
ELISA	enzyme-linked immunosorbent assay
GAPDH	glyceraldehyde 3-phosphate dehydrogenase
GCR	galactic cosmic ray
GFAP	glial fibrillary acidic protein
HNRCA	Human Nutrition Research Center on Aging
HZE particles	high energy and charge particles
Iba-1	ionized calcium-binding adaptor molecule 1
iNOS	inducible nitric oxide synthase
IoR	ionizing radiation
IκB-α	inhibitor kappa-B-α
LET	linear energy transfer
LPS	lipopolysaccharide
MPTP	1-methyl-4-phenyl-1,2,3,6- tetrahydropyridine
NF-κB	nuclear factor kappa-B
NO	nitric oxide
NO_2^-	nitrite
NOR	novel object recognition
NOX2	NADPH oxidase
Nrf2	nuclear factor erythroid 2-related factor 2
NSRL	NASA Space Radiation Laboratory
OS	oxidative stress
PD	Parkinson's disease
PGE_2,	prostaglandin E_2
RAWM	radial arm water maze
RNS	reactive nitrogen species
ROS	reactive oxygen species
SEM	standard error of the mean
SOD	superoxide dismutase
TBI	traumatic brain injury
TLR4	toll-like receptor-4
TNFα	tumor necrosis factor-α.

FIGURES AND TABLES

Figures

Section	Figure	Figure Title	Page
2	1	Reactive gliosis	18
3.1	-	Graphical abstract	51
	1	Experimental design (aim 1a)	52
	2	Effect of pre- and/or post-BB on microglia viability.	53
	3	Effect of pre- and/or post-BB on LPS-induced nitrite and TNFα production in microglia.	54
	4	Effect of pre- and/or post-BB on LPS-induced protein expression of iNOS, COX-2, and pIκB-α in microglia.	55
	5	Effect of pre- and/or post-BB on LPS-induced OS and antioxidant defense enzymes.	56
3.2	1	No significant effect of 20 cGy ^{4}He or 2 Gy ^{56}Fe on protein expression of pro-inflammatory enzymes in microglia.	71
	2	No significant effect of 2 Gy ^{56}Fe on extracellular release of soluble pro-inflammatory factors in microglia.	72
	3	No significant effect of 20 cGy ^{4}He or 2 Gy ^{56}Fe on protein expression of oxidative stress-mediating enzyme NOX2 in microglia.	73
3.3	1	Experimental design (aim 2)	81
	2	Body weight and food intake in non-irradiated and irradiated rats fed control and/or blueberry-supplemented diets.	87
	3	Effect of pre- and/or post-BB on novel object recognition performance in non-irradiated and irradiated rats.	87
	4	No effect of irradiation and/or of pre- and/or post-BB on RAWM performance on trial 5 in non-irradiated and irradiated rats.	88
	5	Effect of pre- and/or post-BB on ^{56}Fe-induced protein expression of inducible inflammatory factors, iNOS, COX-2, and pIκB-α, and an indicator of astrocyte activation, GFAP in the frontal cortex and hippocampus.	90
	6	Effect of pre- and/or post-BB on ^{56}Fe-induced protein expression of oxidative stresses mediators, NOX2, SOD, and Nrf2 in the frontal cortex and hippocampus.	93
	7	Effect of pre- and/or post-BB on ^{56}Fe-induced relative mRNA levels of inducible inflammatory enzymes, iNOS, COX-2, pro-inflammatory cytokine TNFα, and an indicator of microglia activation, CD68 in the frontal cortex and hippocampus.	95
	8	Effect of pre- and/or post-BB on ^{56}Fe-induced relative mRNA expression of oxidative stresses mediator, NOX2 in the frontal cortex and hippocampus.	98

	9	No effect of ^{56}Fe irradiation or of pre- and/or post-BB on Iba-1 immunolabeled cells in the frontal cortex and	99
	10	Cascade of inflammatory and OS-inducing events associated with ^{56}Fe irradiation and the attenuating effects of pre- and/or post- ^{56}Fe BB.	113
	S1	Latency to find the platform on the RAWM task by trial and day.	123
	S2	Iba-1 labeled microglia in the frontal cortex and hippocampus.	124
	S3	Correlation between protein expression of neuroinflammatory enzymes and recognition memory function.	129
	S4	Correlation between protein expression of neuroinflammatory transcriptional regulator pIκB-α or mRNA levels of pro-inflammatory cytokine TNFα and recognition memory function.	130
	S5	Correlation between glial cell activation indicators and recognition memory function.	131
	S6	Correlation between OS-inducing enzyme NOX2 and recognition memory function.	132
4	1	Proposed mechanisms for stressor-induced neuroinflammation, OS, and cognitive decline, mediated by reactive gliosis, and the observed attenuating effects of BB.	136
5	1	Experimental design of dose-response experiment to determine the minimum optimal dose of BB that reduces LPS-induced nitrite production in microglia.	144
	2	The effects of 0, 0.125, 0.25, 0.5, and 1.0 mg/mL BB administered before and/or after LPS on nitrite production in microglia.	145
	3	Neither irradiation with ^{56}Fe nor 0.5 mg/mL BB (pre- and/or post-treatment) produces significant effects on protein expression of inflammation and oxidative stress biomarkers in microglia.	149

Tables

Section	Table	Table Title	Page
5.1	1	Correlation between indicators of neuroinflammation, OS, and glial cell activation in the frontal cortex, and memory function.	100
	2	Correlation between indicators of neuroinflammation, OS, and glial cell activation in the hippocampus, and memory function.	101
	S1	Correlation between indicators of neuroinflammation, OS, and glial cell activation in the frontal cortex, and memory	124

		function in irradiated and non-irradiated animals fed a control diet.	
	S2	Correlation between indicators of neuroinflammation, OS, and glial cell activation in the hippocampus, and memory function in irradiated and non-irradiated animals fed a control diet.	125
	S3	All data for correlations between indicators of neuroinflammation, OS, glial cell activation, and memory function (i.e., Pearson r, p-values, number of observations).	126
5.2	1	Macronutrient composition of control and 2% BB diets	151
	2	Ingredient composition of control and 2% BB diets	151

1 INTRODUCTION

1.1 Significance of proposed research

Neuroinflammation and oxidative stress (OS) have been implicated in the development of cognitive decline and neurodegenerative diseases, which place significant personal, medical, and financial burdens on those affected. The cellular drivers and mechanisms underlying neurodegeneration are not fully understood and therapeutic strategies for Alzheimer's and Parkinson's disease are limited. Neuroinflammation, OS, and the associated risk for cognitive decline and neurodegenerative conditions increase with age and following exposure to a variety of acute stressors such as ionizing radiation (IoR), including high energy and charge (HZE) particles (1-5), ischemic stroke (6, 7), traumatic brain injury (TBI) (6, 8, 9), pharmacologic neurotoxins (8, 10-12), and pesticides (8). A common stress response following acute insults may involve activation of microglia, the primary immune cells of the central nervous system (CNS). Microglia release free radicals (e.g., reactive oxygen and nitrogen species, ROS/RNS) and inflammatory cytokines (e.g., tumor necrosis factor-α, TNFα) when activated. In excess, these molecules can be neurotoxic and promote neuronal damage beyond the site of an inflammatory insult (13). A self-sustaining cycle of microglial activation and neuronal damage known as reactive microgliosis ensues, leading to chronic neuroinflammation, OS, and other effects associated with neurodegeneration (14). Therefore, targeting stressor-induced neuroinflammation, OS, and microglial activation may be important to prevent the progression of neurodegeneration.

Studies have demonstrated that anti-inflammatory/antioxidant foods can be neuroprotective when administered *before* the onset of stressor-induced neuroinflammation and OS (i.e., as pre-treatments). For example, blueberries (BB), which are rich in antioxidant and anti-inflammatory polyphenols, can attenuate neuroinflammation, OS, and/or cognitive deficits when administered *before* the cellular stress induced by bacterial endotoxin lipopolysaccharide (LPS) (15, 16), HZE-particle irradiation (4, 17-21), stroke (22), and the neurotoxin kainic acid (23). However, the beneficial effects and mechanistic targets of antioxidant/anti-inflammatory foods administered *after* stressors (i.e., post-treatments) on neuroinflammation, OS, and cognitive deficits are not well established. More specifically, to our knowledge, the effects

of dietary antioxidant/anti-inflammatory strategies after HZE particle exposure on neuroinflammation, OS, and cognitive deficits have not been explored.

Post-treatments may be necessary countermeasures to attenuate neuroinflammation, OS, and the resulting disease risk, particularly when administration of pre-treatments is not feasible (e.g., with unpredictable stressors: urgent radiotherapy, occupational irradiation, TBI, and stroke). Additionally, when possible, the protection afforded by pre-treatments may not be sufficient to reduce the progression of CNS deficits that continues after neuroinflammatory/OS-inducing stressors have ended. This could be because many therapeutics, including dietary components, have short half-lives; pre-treatments may be partially or fully metabolized by the time stressor exposures occur, while post-treatments, delivered after the onset of the stress response, provide a higher dose of active agent to interact with elevated OS/inflammation (24). Furthermore, secondary mechanisms triggered by the initial stressor, such as reactive microgliosis, may require prolonged treatment to prevent the development of neurodegenerative disease, which can present with clinical symptoms many years after stressor exposure.

Despite the need for post-treatment strategies, current therapeutic options for the residual effects of neuroinflammatory/OS-inducing stressors are limited. Long-term stroke treatments aim to prevent another stroke (e.g., anti-coagulants), rather than targeting the progressive effects of the initial stroke (7). Additionally, there are no established strategies to ameliorate the cognitive deficits and other detrimental CNS effects that progress after radiation exposure (25). Pharmacological treatments targeting biochemical deficits in the CNS such as neuroinflammation and OS are associated with side effects, particularly with prolonged administration (26). Therefore, there is a need for safe, effective, and sustainable post-stressor therapeutic strategies for CNS deficits. Post-stressor nutritional treatments such as dietary BB consumption could be easily implemented as a safe and accessible long-term neuroprotective lifestyle strategy.

Overall, there is a gap in knowledge regarding the efficacy of post-treatments on stressor-induced damage to the CNS, and how the potential attenuating effects of post-treatments compare to pre-treatments and pre-/post-treatments. The development of post-stressor strategies is in part limited by a lack of understanding of the cellular and molecular mechanisms of stressor-induced neurodegeneration. Examining the effects of

antioxidant/anti-inflammatory post-treatments can identify mechanisms involved in post-stressor neurodegeneration, including cellular and molecular mediators. Furthermore, findings could provide guidance for future countermeasures by differentiating targets responsive to preventative strategies versus post-stressor treatments. Lastly, results could support the use of nutritional interventions after initiation of neuroinflammation/OS, which could contribute to reducing the risk of neurodegenerative disease associated with aging and following exposure to unpredictable stressors such as IoR, stroke, and TBI.

This research evaluates whether post-stressor BB is more, less, or similarly effective as pre-stressor BB and pre-/post-stressor BB at attenuating neuroinflammation, OS, and cognitive deficits. Stressor-induced cellular and molecular targets were investigated *in vitro* (microglia), using bacterial endotoxin LPS and HZE particles as stressors, in addition to *in vivo* (Sprague-Dawley rats) using HZE irradiation as the stressor. Correlation analyses were performed to assess linear associations between neuroinflammation, OS, glial activation, and cognitive outcomes.

1.2 Hypotheses and specific aims

The **overall objective** of this research is to evaluate the effects and mechanistic targets of post-stressor BB on neuroinflammation, OS, glial cell activation, and cognitive deficits, relative to no BB, pre-stressor BB, and pre-/post-stressor BB. Our **central hypothesis** is that post-stressor BB will mitigate stressor-induced neuroinflammation, OS, glial activation, and cognitive deficits compared to no BB. Additionally, we predict that both pre- and post-stressor BB will have beneficial effects on these outcomes, but less beneficial than pre/post-stressor BB. We investigated our hypotheses by addressing the following aims:

Aim 1a: Evaluate the effects of post-stressor BB on inflammation and OS in rat microglia cells stressed with LPS *in vitro*, relative to no BB, pre-stressor BB, and pre-/post-stressor BB.

Aim 1b: Evaluate the effects of post-stressor BB on inflammation and OS in rat microglia cells stressed with HZE particle irradiation *in vitro*, relative to no BB, pre-stressor BB, and pre-/post-stressor BB.

Aim 2: Evaluate the effects of a post-stressor BB-supplemented diet on neuroinflammation, OS, glial activation, and memory function deficits in rats stressed with HZE particle irradiation, relative to no BB, pre-stressor BB, and pre-/post-stressor BB.

References:

1. Joseph JA, Shukitt-Hale B, McEwen J, Rabin BM. CNS-induced deficits of heavy particle irradiation in space: The aging connection. Advances in Space Research 2000;25(10):2057-64. doi: 10.1016/S0273-1177(99)01013-3.
2. Greene-Schloesser D, Robbins ME, Peiffer AM, Shaw EG, Wheeler KT, Chan MD. Radiation-induced brain injury: A review. Frontiers in Oncology 2012;2 JUL(July):1-18. doi: 10.3389/fonc.2012.00073.
3. Rabin BM, Shukitt-Hale B. A voyage to Mars: Space radiation, aging, and nutrition. Nutrition and Aging 2014;2(4):233-41. doi: 10.3233/nua-140045.
4. Poulose SM, Bielinski DF, Carrihill-Knoll KL, Rabin BM, Shukitt-Hale B. Protective effects of blueberry- and strawberry diets on neuronal stress following exposure to 56Fe particles. Brain Research 2014;1593:9-18. doi: 10.1016/j.brainres.2014.10.028.
5. Parihar VK, Maroso M, Syage A, Allen BD, Angulo MC, Soltesz I, Limoli CL. Persistent nature of alterations in cognition and neuronal circuit excitability after exposure to simulated cosmic radiation in mice. Neuroscience Letters 2018;305(2018):44-55. doi: 10.1016/j.expneurol.2018.03.009.
6. Slemmer JE, Shacka JJ, Sweeney MI, Weber JT. Antioxidants and free radical scavengers for the treatment of stroke, traumatic brain injury and aging. Current Medicinal Chemistry 2008;15(4):404-14. doi: 10.2174/092986708783497337.
7. Weinstein JR, Koerner IP, Mller T. Microglia in ischemic brain injury. Future Neurology 2010;5(2):227-46. doi: 10.2217/fnl.10.1.
8. Liu B, Gao HM, Hong JS. Parkinson's disease and exposure to infectious agents and pesticides and the occurrence of brain injuries: role of neuroinflammation. Environmental Health Perspectives 2003;111(8):1065-73. doi: 10.1289/ehp.6361.
9. Loane DJ, Byrnes KR. Role of Microglia in Neurotrauma. Neurotherapeutics 2010;7(4):366-77. doi: 10.1016/j.nurt.2010.07.002.

10. Klegeris A, McGeer EG, McGeer PL. Therapeutic approaches to inflammation in neurodegenerative disease. Current Opinion in Neurology 2007;20(3):351-7. doi: 10.1097/WCO.0b013e3280adc943.
11. Gao HM, Hong JS. Why neurodegenerative diseases are progressive: uncontrolled inflammation drives disease progression. Trends in Immunology 2008;29(8):357-65. doi: 10.1016/j.it.2008.05.002.
12. Sundaram RS, Gowtham L, Manikandan P, Venugopal V. The Role Of Reactive Microglia In Neurodegenerative Disease: Multiple Triggers With A Common Mechanism. International Journal of Recent Advances in Pharmaceutical Research 2012;2:29-40.
13. Lyman M, Lloyd DG, Ji X, Vizcaychipi MP, Ma D. Neuroinflammation: The role and consequences. Neuroscience Research 2014;79(1):1-12. doi: 10.1016/j.neures.2013.10.004.
14. Nam KN, Choi YS, Jung HJ, Park GH, Park JM, Moon SK, Cho KH, Kang C, Kang I, Oh MS, et al. Genipin inhibits the inflammatory response of rat brain microglial cells. International Immunopharmacology 2010;10(4):493-9. doi: 10.1016/j.intimp.2010.01.011.
15. Lau FC, Bielinski DF, Joseph JA. Inhibitory effects of blueberry extract on the production of inflammatory mediators in lipopolysaccharide-activated BV2 microglia. Journal of Neuroscience Research 2007;85(5):1010-7. doi: 10.1002/jnr.21205.
16. Joseph JA, Shukitt-Hale B, Brewer GJ, Weikel KA, Kalt W, Fisher DR. Differential protection among fractionated blueberry polyphenolic families against DA-, Aβ42- and LPS-Induced decrements in Ca2+ buffering in primary hippocampal cells. Journal of Agricultural and Food Chemistry 2010;58(14):8196-204. doi: 10.1021/jf100144y.
17. Rabin BM, Joseph JA, Shukitt-Hale B. Effects of age and diet on the heavy particle-induced disruption of operant responding produced by a ground-based model for exposure to cosmic rays. Brain Research 2005;1036(1-2):122-9. doi: 10.1016/j.brainres.2004.12.041.

18. Shukitt-Hale B, Carey AN, Jenkins D, Rabin BM, Joseph JA. Beneficial effects of fruit extracts on neuronal function and behavior in a rodent model of accelerated aging. Neurobiology of Aging 2007;28(8):1187-94. doi: 10.1016/j.neurobiolaging.2006.05.031.
19. Rabin BM, Carrihill-Knoll K, Hinchman M, Shukitt-Hale B, Joseph JA, Foster BC. Effects of heavy particle irradiation and diet on object recognition memory in rats. Advances in Space Research 2009;43(8):1193-9. doi: 10.1016/j.asr.2009.01.015.
20. Shukitt-Hale B, C. Lau F, Cheng V, Luskin K, N. Carey A, Carrihill-Knoll K, M. Rabin B, A. Joseph J. Changes in Gene Expression in the Rat Hippocampus Following Exposure to 56Fe Particles and Protection by Berry Diets. Central Nervous System Agents in Medicinal Chemistry 2013;13(1):36-42. doi: 10.2174/1871524911313010006.
21. Poulose SM, Rabin BM, Bielinski DF, Kelly ME, Miller MG, Thanthaeng N, Shukitt-Hale B. Neurochemical differences in learning and memory paradigms among rats supplemented with anthocyanin-rich blueberry diets and exposed to acute doses of (56)Fe particles. Life Sciences in Space Research 2017;12:16-23. doi: 10.1016/j.lssr.2016.12.002.
22. Slemmer J, Shacka J, Sweeney-Nixon M, Weber J. Do antioxidants and free radical scavengers still hold promise for the treatment of stroke, traumatic brain injury and aging? Journal of Chemical Information and Modeling 2019;53(9):1689-99. doi: 10.1017/CBO9781107415324.004.
23. Shukitt-Hale B, Lau FC, Carey AN, Galli RL, Spangler EL, Ingram DK, Joseph JA. Blueberry polyphenols attenuate kainic acid-induced decrements in cognition and alter inflammatory gene expression in rat hippocampus. Nutritional Neuroscience 2008;11(4):172-82. doi: 10.1179/147683008X301487.
24. Limoli CL, Giedzinski E, Baure J, Rola R, Fike JR. Redox changes induced in hippocampal precursor cells by heavy ion irradiation. Radiat Environ Biophys 2007;46(2):167-72. doi: 10.1007/s00411-006-0077-9.
25. Stone HB, Moulder JE, Coleman CN, Ang KK, Anscher MS, Barcellos-Hoff MH, Dynan WS, Fike JR, Grdina DJ, Greenberger JS, et al. Models for Evaluating

Agents Intended for the Prophylaxis, Mitigation and Treatment of Radiation Injuries Report of an NCI Workshop. Radiation Research 2006;162(6):711-28. doi: 10.1667/rr3276.

26. Pariset E, Malkani S, Cekanaviciute E, Costes SV. Ionizing radiation-induced risks to the central nervous system and countermeasures in cellular and rodent models. International Journal of Radiation Biology 2021;97(sup1):S132-S50. doi: 10.1080/09553002.2020.1820598.

2 LITERATURE REVIEW

2.1 Neurodegenerative Diseases

Neurodegenerative diseases pose significant personal and public health burdens worldwide, and the prevalence is expected to grow as life expectancy increases. The mechanisms underlying neurodegeneration are not fully understood, limiting the development and efficacy of therapeutic strategies. Therefore, it is critical to identify factors contributing to disease development to establish therapeutics and ultimately reduce the increasing burdens of these pathologies.

2.2 Neuroinflammation, Oxidative Stress & Microglia

Neuroinflammation and excess free radical production (i.e., OS) are implicated in the development of cognitive decline and neurodegenerative diseases (1). Neuroinflammation and OS increase with age and in response to a variety of neuropathogenic stressors such as irradiation (e.g., HZE particle exposure), TBI, stroke, infection, and neurotoxins. While the acute inflammatory response is a beneficial defense mechanism to restore homeostasis, uncontrolled and chronic neuroinflammation/OS produce damage to otherwise healthy neuronal cells and tissues (i.e., neurodegeneration). A common mechanism involving activation of inflammasomes in various cell types (e.g., microglia, astrocytes, neurons, and endothelial cells) has been identified in the development of neurogenerative diseases with age and following acute insults (2). However, because neuroinflammation and OS can both contribute to and cause neuronal death, the precise role of these processes in progressive neurodegeneration remains unclear.

Glial cells, particularly microglia and astrocytes, are key regulators of the inflammatory response and ROS/RNS production in the CNS. Microglial cells, the specialized macrophages and primary immune cells of the CNS, are believed to be the most active participants in initiating the neuroinflammatory response, and subsequently recruit astrocytes and other cellular mediators (3). In a quiescent state, microglia serve a neuroprotective role by clearing cellular debris and surveying the CNS for noxious stimuli (4). Stressor exposure and the resulting damage signals cause microglia to change from quiescent phenotype to an activated phenotype and produce cytotoxic mediators including cytokines (e.g., TNFα), ROS (e.g., superoxide), and RNS (e.g., nitric oxide, NO) to destroy

invading pathogens and initiate repair processes (4, 5). The excess production of these mediators can be neurotoxic to healthy neurons beyond the site of an inflammatory insult (4). NO and ROS at basal levels are important for intracellular signaling cascades. However, high levels of NO, produced by inducible nitric oxide synthase (iNOS) under inflammatory conditions, can induce neuronal apoptosis (e.g., by blocking mitochondrial respiration through inhibiting cytochrome oxidase) (3). Excess ROS production relative to available antioxidant defenses (e.g., superoxide dismutase, SOD) results in OS, which induces oxidative damage to neurons. These molecules and neuronal damage activate astrocytes and additional microglia to sustain the immune response. Therefore, if unchecked, a vicious cycle of glial activation and neurotoxicity known as reactive gliosis can result, leading to chronic inflammation, OS, and neurodegeneration, long after the initial stressor dissipates (4, 6). These processes and their associations with neurodegenerative disease have been observed following many acute stressors such as the neurotoxin 1-methyl-4-phenyl-1,2,3,6- tetrahydropyridine (MPTP) (4), peripheral lipopolysaccharide (LPS) (6), pesticides, TBI, stroke (7), and ionizing radiation (8).

The CNS is particularly susceptible to excess inflammation/OS relative to other tissues. The brain consumes 1/5 of total oxygen intake, accounting for >20% of the resting metabolic rate despite comprising 2% of body weight (9). This high metabolic rate results in greater production of free radicals, since an estimated 5% of cellular oxygen is converted to ROS/RNS (9). Therefore, stressor-induced free radical production, combined with the already elevated ROS/RNS in the brain, can easily overwhelm the antioxidant defense system, leading to OS. The brain is especially vulnerable to the detrimental effects of OS because the ability of neurons to regenerate is limited (10). Furthermore, neuronal membranes contain high proportions of polyunsaturated fatty acids, which are easily oxidized due to the presence of double bonds (9). As a result, inflammation, OS, and other processes associated with neurodegeneration occur in the CNS following stressor exposures.

2.2.1 Ionizing Radiation Exposure

IoR is one stressor that causes neuroinflammation, OS, and cognitive deficits (11-13), and is associated with increased neurodegenerative disease risk. IoR exposures include

environmental, occupational (e.g., nuclear workers and astronauts), and medical (e.g., radiotherapy patients) irradiation. IoR consists of electromagnetic waves or particles that cause detachment of electrons from atoms with which they interact, resulting in ROS/RNS, oxidative damage, and inflammatory cascades (14). These immediate processes trigger secondary perturbations and long-term cognitive deficits, although the precise mechanisms and cellular mediators are unclear (15). Radiation-induced brain injury, and the resulting cognitive decline, involves demyelination, direct neuronal damage, neural stem cell depletion in the hippocampus, microvascular damage, blood-brain-barrier (BBB) disruption, edema, changes in neurotransmission, and activated glial cells, all of which may be a cause and/or result of neuroinflammation and OS. The frontal cortex and hippocampus appear particularly sensitive to the effects of irradiation, and deficits in learning and memory functions mediated by these regions are often observed (15). However, there are no clinically approved strategies to attenuate the cognitive deficits and other neurodegenerative effects that progress after radiation exposure (16), and treatments targeting neurochemical deficits are associated with side effects, particularly with prolonged administration (17).

IoR types can be classified by linear energy transfer (LET). X-rays and γ-rays are considered low-LET particles. In contrast, high LET particles, including particles of high (H) charge (Z) and energy (E) (HZE; $Z \geq 2$) such as ^{56}Fe, produce a higher density of ionized matter per unit of volume at a given dose. Due to greater energy transfer, HZE particles are densely ionizing and highly penetrative (12). One source of HZE particles is cancer radiotherapy; charged particle therapy is rapidly increasing due to its superior tumor killing capacity compared to X-ray therapy (15). Another source of HZE particles is galactic cosmic rays (GCRs) and solar particle events in outer space. The majority of prior research investigating the detrimental effects of IoR on the CNS has been conducted in the context of radiotherapy. This thesis work (Chapters 3.2 and 3.3), on the other hand, primarily investigates the effects of HZE particle exposure in the context of cosmic radiation. Therefore, the reviewed literature includes findings from radiotherapy and cosmic radiation experiments. It should be noted that radiotherapy typically uses higher dose, lower-LET, and localized exposures of IoR compared to simulated cosmic radiation. Nonetheless, similar detrimental effects of cosmic radiation on the CNS have been

observed (15). Findings from radiotherapy experiments provide important insight on potential mechanisms involved in cosmic exposures to HZE particle radiation and highlight the need to develop therapeutic strategies for IoR exposures in both contexts.

2.2.1.1 HZE particles in cosmic radiation

A manned mission to Mars is considered the main goal of all national space agencies (18). Beyond the protection provided by Earth's magnetic field, which deflects charged particles, astronauts on exploratory missions will be exposed to HZE particles. HZE particles can penetrate both spacecraft shielding and human tissue, and exposure can form secondary radiation particles (e.g., neutrons and recoil nuclei) by nuclear reactions upon impact (19). Therefore, the ionization capacity of HZE particles makes them a major contributor to the biological risk of GCR exposures in space.

In cosmic radiation experiments using rodents, HZE particle irradiation can induce both acute and chronic deleterious CNS effects such as neuroinflammation and OS as well as cognitive deficits (20-23). Additionally, exposure to HZE particles may produce 'accelerated aging' in the CNS, as irradiated young animals exhibit biochemical changes in the brain and cognitive deficits similar to those observed in older animals (8). Because HZE particle exposures increase neuroinflammation and OS, both well-established contributors to neurodegenerative disease development, HZE particle irradiation may increase risk for and/or exacerbate neurodegenerative disease (12). Therefore, countermeasures are necessary to mitigate the detrimental effects of HZE exposure on the CNS during and after mission completion. However, as with neurodegenerative disease progression following radiotherapy and other stressor exposures, the cellular and molecular mediators responsible for HZE-induced biochemical changes in the brain and cognitive deficits are not well established, limiting the development of radioprotective and radio-mitigating strategies.

2.2.1.2 HZE-irradiation as a model stressor

In addition to the clinical and occupational relevance of studying the effects of HZE particles, HZE particle exposure can serve as a model for accelerated aging and other inflammatory/OS-inducing stressors with neurodegenerative effects (e.g., infection, stroke,

and TBI). Common mechanisms by which these stressors can drive neurodegeneration have been identified (24), including activation of glial cells as a potential mediating factor (25, 26). Several putative pharmacological countermeasures for IoR-induced CNS deficits (e.g., PPARy agonists) have been shown to improve outcomes in other neuroinflammatory/OS conditions such as stroke, Alzheimer's and Parkinson's disease, further suggesting that common mechanisms exist (27-29). In addition to biochemical similarities, irradiation-induced cognitive decline resembles that of neurodegenerative disease. A recent study found that 2/3 of the post-radiotherapy brain tumor survivors met criteria for mild cognitive decline (MCI), as defined by the National Institute on Aging and Alzheimer's Association (27). Of these, the majority were characterized as amnestic MCI-multiple domain, the subtype most commonly observed in Alzheimer's diseases.

2.3 Blueberries & Anthocyanins

Given the prominent role of neuroinflammation and OS in neurodegenerative disease pathology, interventions targeting these processes may help prevent, slow or reverse neurodegeneration. Nutritional strategies using foods with antioxidant and anti-inflammatory properties show potential to be safe, inexpensive and effective therapies to attenuate inflammation/OS-induced neurodegenerative effects. In particular, berry fruits containing high concentrations of polyphenolic compounds such as flavonoids can benefit the CNS via antioxidant and anti-inflammatory properties (30-32). Berry species have been shown to contain some of the highest levels of polyphenols relative to other plant species (32, 33), with blueberries (BBs) shown in several studies to be highly neuroprotective (30, 34).

The beneficial effects of BBs on neuroinflammation, OS, and cognitive function have been attributed to their high anthocyanin content (31, 32, 35, 36). Anthocyanins are flavonoid polyphenols that confer red, blue, and purple coloration to plant foods. Studies have shown that anthocyanins have anti-inflammatory activities, protect against OS, and may modulate other cellular processes such as apoptosis, autophagy and metabolism (31, 32). Additionally, anthocyanins from dietary BB consumption can cross the blood-brain-barrier and are thus neuroavailable (37). The benefits of anthocyanins observed in cells and animals translate to neuroprotective effects in humans. A recent study found that

individuals with the highest intakes of anthocyanins had a lower risk of developing Alzheimer's disease and related dementias relative to those with the lowest intake over a 20-year follow-up (38). Additionally, the inverse association between dementia risk and anthocyanin intake was stronger than that for other flavonoids.

Although anthocyanins contribute to the neuroprotective effects of BBs, studies show that the whole BB is more effective than individual polyphenol fractions at attenuating stressor induced CNS deficits (39). The superior benefit of the whole fruit may be due to synergistic interactions among blueberry polyphenols or unique properties of individual polyphenols other than anthocyanins (34). A whole-food, non-proprietary treatment such as BB could be more easily implemented as a therapeutic strategy than individual polyphenols.

In addition to the putative therapeutic value, evaluating the effects of BB treatments can be used to identify specific targets for dietary countermeasures and other mitigating strategies after stressor exposures. The biological effects of flavonoids (e.g., anthocyanins) have primarily been attributed to antioxidant and anti-inflammatory mechanisms such as directly scavenging ROS and inhibiting OS/inflammation-producing enzymes, resulting in the modulation of signaling cascades involving gene expression and cell survival Therefore, BB interventions can be used to evaluate the role of inflammation/OS in stressor-induced CNS changes, and identify which molecular factors can be targeted to prevent (i.e., with pre-treatments) or reduce the progression of (i.e., with post-treatments) neurodegeneration.

2.4 Pre vs. Post-Treatments

The majority of studies examining the beneficial effects of antioxidant/anti-inflammatory foods such as BBs on the CNS have investigated a preventative (i.e., pre-stressor) role in neuroinflammation, OS, and/or cognitive function. In the *in vitro studies* using microglial cells, BB pre-treatment can protect against inflammation and OS when administered to microglia and removed before stressors such as LPS (40-42), Beta-amyloid (42), glutamate, and alpha-synuclein (43). In dietary supplementation studies using rodent models, BBs can protect against neuroinflammation, OS, and/or cognitive deficits when administered before experimentally-induced stroke (33) and the neurotoxin kainic acid

(44). Few studies have assessed dietary radioprotectors for the effects of HZE particles, but nutritional radioprotectors (e.g., watermelon juice, vitamin E) have been identified for the neuroinflammatory/OS-inducing effects of γ-rays or X-rays in rodents (17). Of studies on HZE particles, the protective effects of blueberries and strawberries have been demonstrated as pre-treatments on HZE particle-induced acute biochemical changes in the brain (13, 20, 45) and prolonged cognitive deficits (21, 46), and as pre-/post-treatments on biochemical changes (13) and cognitive deficits (47) one month after irradiation. In humans, epidemiological studies have shown that BB consumption can lower risk of developing neurodegenerative diseases such as Alzheimer's disease (38) and stroke (48).

As reviewed, the neuroprotective effects of BBs and other antioxidant/anti-inflammatory dietary strategies have been demonstrated when introduced before a neuropathological stressor. However, in general, the effects and mechanistic targets of antioxidant/anti-inflammatory foods administered *after* stressors (i.e., post-treatments) on neuroinflammation, OS, and cognitive function are not well-established. Furthermore, the differential efficacy of pre-, post-, and pre-/post-stressor dietary treatments on biochemical changes in the brain (e.g., neuroinflammation, OS) and cognitive deficits has not been investigated. Examining the post-stressor effects of dietary strategies on neuroinflammation, OS, and cognitive function is important for several reasons which are discussed below. In brief, post-treatments may be necessary on a mechanistic level to repair damage from the initial stress response and prevent active progression of neurodegeneration long-term. From a clinical standpoint, assessing the effects of post-treatments is important to develop countermeasures for unpredictable stressors, and because current therapeutics for post-stressor neurodegeneration are limited.

2.4.1 The detrimental CNS effects of inflammatory/OS-inducing stressors can persist long after exposures end, which may be due to deficits in early reparative processes.

Pathogenic stressors can produce ROS/RNS and an inflammatory response that overwhelms endogenous defense mechanisms (10, 29, 48, 49). Due to the limited regenerative capacity of the CNS, this early imbalance can have lasting consequences; damage from the *initial* insult may not be fully repaired and impairments persist even after

the stress response subsides. For example, half of ischemic stroke patients who survive have moderate to severe impairments in brain function, and these have been attributed to the overproduction of ROS/RNS during stroke (33). Additionally, animal studies using simulated cosmic radiation have shown that short-term neuronal impairments and/or cognitive deficits remain present months to over a year after irradiation, suggesting that initial damage is not fully repaired (8, 13, 50-52).

Treatments that fortify defense mechanisms could accelerate post-stressor restoration of homeostasis and ultimately prevent irreversible damage. Although pre-stressor treatments can be protective by enhancing the endogenous defense system, they may not be sufficient to counteract stressor-induced inflammation/OS (9). Post-treatments may be more efficient countermeasures for the consequences of an overwhelmed endogenous defense system and the resulting persistent damage. One reason for this is that many therapeutics have short half-lives, so pre-stressor treatments are partially or fully metabolized by the time stressor exposures occur. Because post-treatments are delivered after the onset of the stress response, a higher dose of active agent is available to interact with elevated ROS/inflammatory processes. One study found that IoR-induced increases in ROS production by neural precursor cells were more effectively reduced by *post*-treatment with antioxidant lipoic acid (LA) than *pre*-treatment with LA (53). The authors postulated that pre-treatment efficacy was limited by a short half-life and that the superior benefit of post-IoR LA was due to maximized overlap with elevated ROS production.

Additionally, because physiological levels of inflammation and ROS/RNS are beneficial, antioxidant and/or anti-inflammatory pre-treatments could suppress the endogenous immune response, making it less effective at initiating repair processes when exposed to stressors (25, 54). Pharmacological radioprotectors (e.g., indralin) administered before or both before and after irradiation can have adverse effects on the hematopoietic system by inhibiting the early reparative processes (55), and it is possible that similar inhibition of endogenous defense mechanisms occur with pre-stressor treatments in the CNS. Therefore, by targeting inflammation/OS shortly *after* imbalances occur, post-treatments could more effectively complement endogenous defense mechanisms. As a result, post-treatments may reduce the severity and persistence of stressor-induced CNS damage.

2.4.2 The detrimental CNS effects of inflammatory/OS-inducing stressors can progress long after exposures end, and may require prolonged and sustained treatments.

Neuropathological stressors can initiate cascades that can result in progressive damage, and may ultimately lead to neurodegenerative disease. For example, MPTP, a by-product of heroin, can cause Parkinson's disease (PD) in both human and animal models. In humans, the time between MPTP exposure and manifestation of PD symptoms is ~8-10 years (56), and it is unlikely that toxins remain in the brain for this long. This suggests that the early pathogenic mechanisms initiated by toxin exposure are amplified years after exposure has ended, resulting in neurodegenerative disease. One study found activated microglia in the substantia nigra 10 years after MPTP exposure, implicating the role of glial cells and neuroinflammation in the neurodegenerative progression (10, 54).

Progressive CNS damage is also observed after exposure to IoR (57). For example, rodents exposed to simulated cosmic radiation (^{4}He) displayed increasing trends in cognitive deficits, neuroinflammation, and activated microglia from 6 weeks to one-year post-irradiation (8). Of brain tumor patients who survive >6 months post-radiotherapy, 50-90% exhibit lasting and often progressive signs of IoR-induced brain injury (26, 57), including brain atrophy and dementia (26). A study examining whole-brain radiotherapy patients post-IoR found that the percentage of patients with cognitive impairments and the severity of impairment increased over the 72-month study, further supporting the progressive nature of these effects (58). Studies have also demonstrated that neuroinflammation can occur in waves; early production of pro-inflammatory cytokines (e.g., TNFα) post-irradiation can precede subsequent waves of cytokine production weeks to months after irradiation (59). Therefore, in addition to targeting early inflammation/OS resulting from direct stressor exposure, post-treatments can attenuate secondary and/or delayed processes that continue in the absence of a stressor.

2.4.2.1 Microglia & Reactive Gliosis

The cellular and molecular mediators responsible for the progression of post-stressor CNS deficits, including neurodegeneration are unclear. However, research

describes an emerging role for microglia in the development and progressive nature of neurodegenerative diseases (3). Microglia activation by acute stressors was initially perceived as transient and self-limiting defense response, but research suggests that microglia activation can be self-sustaining and chronic (4, 56). For example, microglia activation following TBI has been detected up to 16 years after the insult in humans (60). Furthermore, TBI is a strong risk factor for Alzheimer's disease, and neuroinflammation is implicated in disease development (60).

The precise mechanisms by which microglia become and remain activated to promote neurodegeneration remain elusive, but may involve reactive gliosis (**Figure 2.1**) (4, 56). Reactive gliosis is initiated when stressors cause microglia activation through direct mechanisms such as irradiation-induced double strand breaks or ligand binding to pattern-recognition receptors. Receptor binding (e.g., LPS bound to toll-like receptor-4 [TLR4] *in vitro*) initiates a range of signal transduction cascades, including pathways involving NF-κB, resulting in the expression of pro-inflammatory enzymes and molecules. Microglia can also be indirectly activated when not directly exposed to stressors, but in response to changes in the CNS environment such as apoptosis of neurons, disruption of the blood-brain-barrier, and infiltration of peripheral immune cells/signals (61). Once activated, microglia upregulate inflammatory/OS-inducing enzymes including iNOS, NADPH oxidase-2 (NOX-2), and cyclooxygenase-2 (COX-2). The resulting production of cytotoxic factors such as NO, ROS, PGE_2, and TNFα can perpetuate neuroinflammation/OS when released in excess through mechanisms such as damaging neurons or activating astrocytes, which release signals for further microglial activation. A progressive cycle of neuronal damage and glial cell activation ensues, leading to chronic neuroinflammation, OS, and CNS damage.

Although reactive gliosis involves both microglia and astrocytes, it is hypothesized that microglia are the driving factor of this cycle, and astrocyte activation requires microglial-derived soluble factors. For example, an *in vitro* study found that X-ray irradiation produced no effect on astrocyte activation, but incubating astrocytes with cell conditioned media collected from irradiated microglia increased GFAP immunostaining and produced morphological changes indicating a reactive state (62). Similar changes were observed by incubating astrocytes with PGE_2 (produced by COX-2) and TNFα. Another

study found that microglia are neceessary for the neurotoxic effect of glial activation; astrocyte co-cultures with neurons treated with LPS/IFN-y did not reduce neuron viability, while cultures containing astrocytes, microglia, and neurons treated with LPS/IFN-y showed reduced neuron viability (63).

Furthermore, research has shown that microglial activation can be self-propelling in the absence of signals from other cells. In microglia stressed with LPS, increased levels of NO persisted at 24 hours after LPS removal relative to non-LPS treated cells (5). Subsequent knockdown and enzyme inhibitor experiments showed that NADPH oxidase (NOX2)-generated ROS upregulated inducible nitric oxide synthase (iNOS)-generated NO, and vice-versa. This study was the first to demonstrate that signals from activated microglia can propel reactive gliosis after stressor removal and direct neuronal damage and other external signals are not necessary.

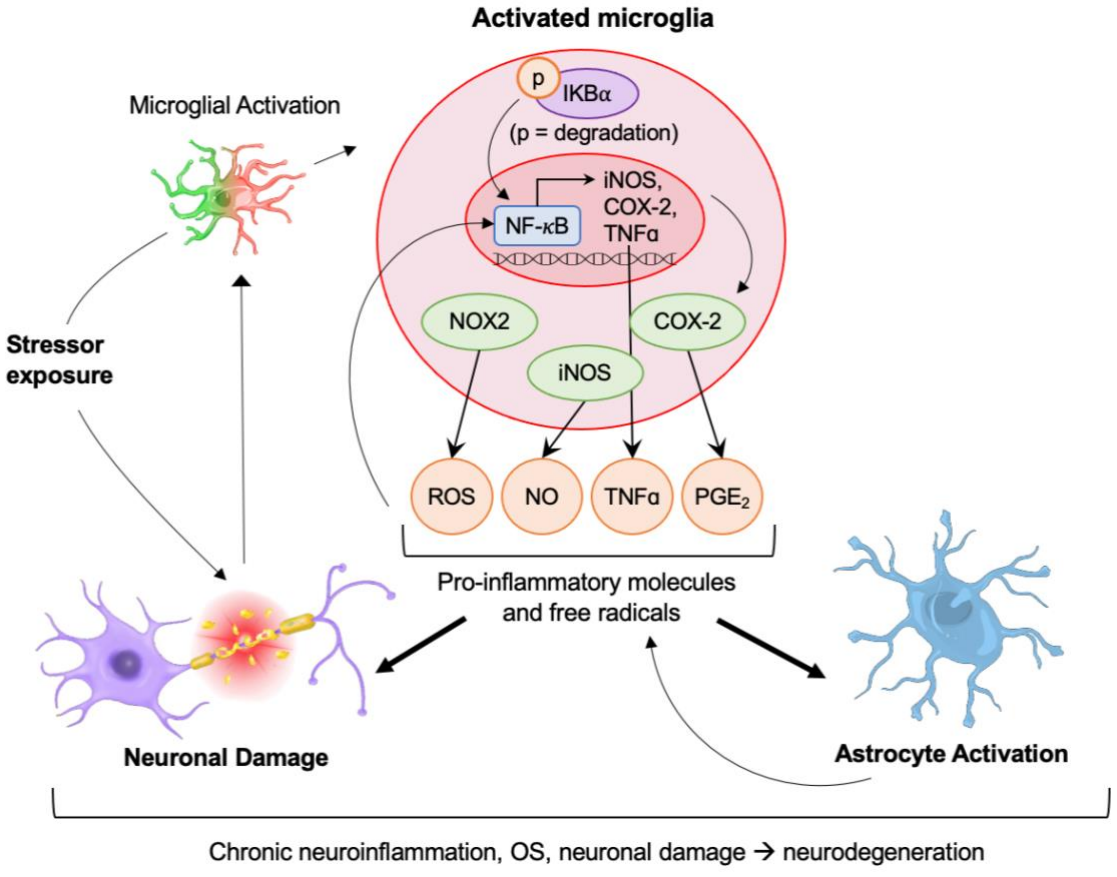

Figure 1. Reactive gliosis

Reactive gliosis is initiated when stressors activate microglia directly (e.g., LPS binds TLR4) or indirectly (e.g., damage signals released from neurons), resulting in signaling cascades (e.g., involving NF-κB activation) and the upregulation of pro-inflammatory and OS-inducing enzymes (e.g., iNOS, COX-2, NOX2). Activated microglia release pro-inflammatory molecules and free radicals (e.g., ROS, NO, TNFα, PGE_2), which in excess, damage neurons, activate astrocytes, and cause further microglia activation. A progressive cycle of neuronal damage and glial cell activation ensues, leading to chronic neuroinflammation, OS, and neurodegeneration. COX-2, cyclooxygenase-2; IκB-α, inhibitor kappa-B-α; iNOS, inducible nitric oxide synthase; NF-κB, nuclear factor kappa-B; NO, nitric oxide; NOX2, NADPH oxidase; OS, oxidative stress; PGE_2, prostaglandin E_2; ROS, reactive oxygen species; TNFα, tumor necrosis factor-α.

Overall, research suggests that activated microglia are important therapeutic targets to curb stressor-induced neuroinflammation, OS, and neurodegeneration. However, the interplay between glial cell activation, neuroinflammation, OS, and neurodegeneration is not well defined, and the primary molecular drivers of reactive gliosis for countermeasure targets have not been identified. In particular, the role of microglia in the detrimental CNS effects of HZE particle exposures remains elusive. Several studies in mice have demonstrated HZE-induced increases in microglia activation, as indicated by CD68/ED-1 expression (64, 65) and depletion of microglia (e.g., using small molecule inhibitor PLX3397) can attenuate irradiation-induced biochemical changes in the brain and cognitive deficits (66). Other studies did not find HZE-induced changes in CD68/ED-1 (23, 67-70) using a similar range of doses, HZE-particles, and post-irradiation durations. Reasons for the discrepancy in findings are unclear. Given that neuroinflammation and OS increase with HZE particle-irradiation, and that glial cells mediate neuroinflammation and OS, further study of microglial responses to HZE particle exposures is warranted. Findings could provide clarity on the relationship between these processes in the common response to neuropathological stressors.

Evaluating the molecular responses of microglia to stressors *in vitro,* and the extent to which these can be modulated after activation occurs, could suggest that microglia are a cellular target for attenuating stressor-induced neuroinflammation and OS *in vivo*. If reactive gliosis is a main contributor to persistent stressor-induced neuroinflammation, OS, and cognitive deficits, then anti-inflammatory and antioxidant post-treatments may provide beneficial effects even after stressor removal. Therefore, post-treatments can provide insight on the cellular and molecular mechanisms underlying progressive CNS damage and

whether this can be attenuated after stress exposure. By targeting reactive gliosis and other progressive mechanisms, post-treatments may be necessary to attenuate OS/inflammatory processes subsequent to microglial activation and reduce the development of post-stressor neurodegeneration.

2.4.3 Sufficient pre-stressor time may not be available to administer protective agents, such as with unpredictable inflammation/OS-inducing stressors.

Post-stressor treatments are necessary for clinical and occupational situations in which sufficient time is not available to administer protective agents pre-stressor. Patients who require urgent radiotherapy rely on post-irradiation therapeutics when the need for radiotherapy was not anticipated. Additionally, post-treatments are necessary to mitigate unexpected occupational exposures to populations such as nuclear plant workers, military personnel, and astronauts (29). For example, radiation exposure in deep space may occur without advance warning from solar particle events, which are unpredictable surges of HZE particles that can be quantified *after* exposure (71). Post-treatments are also important for other unpredictable inflammatory/OS-inducing brain injuries such as stroke and TBI. Due to the rapid onset and the spontaneous nature of these injuries, protective pre-treatments are not always feasible, raising a need for post-treatments. As discussed, post-treatments may be necessary even in situations when pre-treatments are feasible to attenuate delayed, persistent, and/or progressive effects. Findings from pre-clinical and clinical studies on putative treatments for post-stressor CNS deficits highlight a need to continue advancing research in this area.

2.4.4 Treatments for the detrimental CNS effects of inflammatory/OS-inducing stressors are lacking, in part due to unclear mechanisms in the post-stressor response.

Neuroinflammatory/OS-inducing stressors can trigger persistent and progressive CNS deficits, increasing risk for neurodegenerative disease. The causal pathway from these insults to neurodegeneration may involve a common stress response driven by self-propagating microglia activation, neuroinflammation, and OS. Therefore, targets in the cycle of reactive gliosis could be up or downregulated with therapeutics to curb chronic

neurodegeneration and cognitive deficits. However, the relationship (i.e., directionality and causality) between glial cell activation, neuroinflammation/OS, and neurodegeneration is not fully understood, and primary molecular targets have not been identified. As a result, treatments for the prolonged neurodegenerative effects of inflammation/OS-inducing stressors are lacking in number and efficacy, and are associated with side effects. For example, current ischemic stroke treatments are aimed at removing the clot and therefore serve to prevent acute damage rather than lasting effects. The gold standard treatment for stroke (tissue plasminogen activator IV) has side effects such as risk for intracerebral hemorrhage, which would exacerbate brain damage (33). Long term treatments aim to prevent another stroke (e.g., anti-coagulants), rather than targeting the residual effects of the initial stroke (72).

Additionally, there are no established strategies to attenuate the cognitive deficits and other neurodegenerative effects that progress after radiation exposure (16). Furthermore, the majority of countermeasures for irradiation-induced CNS deficits have been investigated in radiotherapy models, and the efficacy on space-like radiation exposures has not been assessed. To our knowledge, only four clinical trials have been completed investigating therapeutics for irradiation-induced cognitive decline. In brain tumor patients, concomitant administration of Memantine, an NMDA receptor blocker, did not preserve memory function (73), Methylphenidate, a CNS stimulant during and after radiotherapy, did not attenuate cognitive deficits (27), and Donepezil, an acetylcholinesterase inhibitor, did not improve overall cognitive function 6 months post-irradiation (74). Gingko Biloba, a plant extract with multiple mechanisms of action, improved cognitive function in several domains in patients who had completed radiotherapy 6 months prior, but was associated with side effects resulting in a high dropout rate (75). Pre-clinical studies have shown mixed effects of PPAR agonists (e.g., Fenofibrate and Pioglitazone) on irradiation-induced cognitive deficits, which may be due to anti-inflammatory mechanisms. Therefore, the effects of treatments targeting processes such as neuroinflammation and OS on irradiation-induced cognitive deficits should be investigated.

The only FDA-approved drug that has been shown to prevent irradiation-induced OS in the CNS is Amifostine (Ethylol ®), usually administered before radiation exposure

(17). Amifostine is dephosphorylated by alkaline phosphatase to a thiol metabolite in the body, which scavenges free radicals induced by ionizing radiation and chemotherapy agents (76). However, the neuroprotective effects have been demonstrated only in pre-clinical studies. The clinical use of Amifostine is limited to reduction of renal toxicity in ovarian cancer patients using cisplatin (chemotherapy) and protection against xerostomia (dry mouth) induced by radiotherapy for head and neck cancer patients. However, Amifostine use is frequently associated with severe side effects. Similarly, treatments for irradiation-induced inflammation have been reported to cause side effects, especially with prolonged administration. Inhibiting inflammatory mediators pharmacologically could be deleterious under conditions in which repair processes are necessary.

Selective targeting of microglia has been proposed as a promising approach to attenuate irradiation-induced CNS damage. Small molecule inhibitors of colony-stimulating factor 1 (CSF-1), a tyrosine kinase receptor that promotes the migration, differentiation, and survival of microglia, include PLX3397 and PLX5622. These pharmacological agents have been shown to reduce irradiation-induced memory deficits in animal studies and are now being investigated in clinical trials (61). However, systemic administration of CSF-1 receptor inhibitors is limited by a lack of specificity, and can suppress other cell populations in the body including macrophages, hematopoietic stem cells, and mast cells. Additionally, after treatments stop, microglia can quickly repopulate within several days.

Many studies evaluating the effects of pharmacological agents on neuroinflammation, OS, and cognitive deficits have administered treatments before stressors, and outcomes were assessed shortly after stressors end (10, 48). As a result, the efficacy of post-treatments alone, and the potential to attenuate delayed and progressive CNS damage following neuroinflammatory/OS-inducing stressors, has been minimally assessed. These limitations even apply to pre-clinical studies on the neurodegenerative effects of unpredictable stressors such as stroke and TBI, for which post-treatments are essential. Furthermore, whether post-treatments administered after stressor-induced initiation of neuroinflammation, OS, and other potentially neurodegenerative processes are less, more, or similarly effective as pre-treatments remains to be established.

Findings from studies on pharmacotherapies highlight a need to identify mechanistic targets involved in post-stressor neurodegeneration to advance the development of countermeasures. In particular, there is a need to establish therapeutic strategies with minimal side effects that can be administered over a prolonged duration. Dietary interventions using foods with antioxidant and anti-inflammatory properties could be safe and effective countermeasures for neuroprotection.

2.5 Conclusions and areas of opportunity for research

Neuroinflammation, and OS persist (i.e., remain elevated) and can progress (i.e., worsen) following exposure to acute stressors such as stroke, TBI, infection, and IoR (e.g., HZE particles), increasing associated cognitive deficits and risk for neurodegenerative disease. Because neuroinflammation/OS can both contribute to and cause neuronal death, the precise role of these processes in progressive neurodegeneration and/or cognitive decline has not been established. Furthermore, the relationship between neuroinflammation, OS, and various cell types in the common response to neuropathological stressors remains unclear. In particular, the mechanisms and cellular mediators involved in the detrimental effects of HZE particles on the CNS have not been elucidated. Given the increasing evidence for the deleterious CNS effects of HZE exposure and other neuroinflammation/OS-inducing stressors, there is a need to establish safe, effective, and maintainable countermeasure strategies.

The development of therapeutic strategies is in part limited by a lack of understanding of stressor-induced neurodegenerative effects Therefore, there is a gap in knowledge regarding the efficacy of post-treatments on stressor-induced neuroinflammation, OS, and cognitive deficits, and how the potential attenuating effects of post-treatments compare to the more widely investigated pre-treatments and pre-/post-treatments. Furthermore, mechanistic targets responsive to pre-treatments compared to those attenuated by post-treatments have not been established.

Examining the effects of post-treatments will provide insight on mechanisms underlying post-stressor neurodegeneration. Identifying targets responsive to pre- and/or post-stressor anti-inflammatory/antioxidant treatments would provide guidance for the development of future countermeasures. Furthermore, findings could support the use of

nutritional interventions after initiation of neuroinflammation/OS, which could reduce the risk of neurodegenerative disease with age and following exposure to stressors such as IoR, stroke, and TBI. Nutritional countermeasures could be easily implemented as a safe and accessible long-term neuroprotective lifestyle strategy. Therefore, the objective of this research is to evaluate the effects and mechanistic targets, of pre- and/or post-stressor BB on neuroinflammation, OS, and cognitive deficits.

References

1. Shukitt-Hale B, Thangthaeng N, Miller MG, Poulose SM, Carey AN, Fisher DR. Blueberries Improve Neuroinflammation and Cognition differentially Depending on Individual Cognitive baseline Status. Journals of Gerontology - Series A Biological Sciences and Medical Sciences 2019;74(7):977-83. doi: 10.1093/gerona/glz048.
2. Lumniczky K, Szatmári T, Sáfrány G. Ionizing radiation-induced immune and inflammatory reactions in the brain. Frontiers in Immunology 2017;8(MAY):1-13. doi: 10.3389/fimmu.2017.00517.
3. Cianciulli A, Porro C, Calvello R, Trotta T, Lofrumento DD, Panaro MA. Microglia mediated neuroinflammation: Focus on PI3K modulation. Biomolecules 2020;10(1):1-19. doi: 10.3390/biom10010137.
4. Lull ME, Block ML. Microglial activation and chronic neurodegeneration. Neurotherapeutics 2010;7(4):354-65. doi: 10.1016/j.nurt.2010.05.014.
5. Lijia Z, Zhao S, Wang X, Wu C, Yang J. A self-propelling cycle mediated by reactive oxide species and nitric oxide exists in LPS-activated microglia. Neurochemistry International 2012;61(7):1220-30. doi: 10.1016/j.neuint.2012.09.002.
6. Qin L, Wu X, Block ML, Liu Y, Breese GR, Hong JS, Knapp DJ, Crews FT. Systemic LPS causes chronic neuroinflammation and progressive neurodegeneration. Glia 2007;55(5):453-62. doi: 10.1002/glia.20467.
7. Liu B, Gao HM, Hong JS. Parkinson's disease and exposure to infectious agents and pesticides and the occurrence of brain injuries: role of neuroinflammation. Environmental Health Perspectives 2003;111(8):1065-73. doi: 10.1289/ehp.6361.

8. Parihar VK, Maroso M, Syage A, Allen BD, Angulo MC, Soltesz I, Limoli CL. Persistent nature of alterations in cognition and neuronal circuit excitability after exposure to simulated cosmic radiation in mice. Neuroscience Letters 2018;305(2018):44-55. doi: 10.1016/j.expneurol.2018.03.009.
9. Cui K, Luo X, Xu K, Ven Murthy MR. Role of oxidative stress in neurodegeneration: recent developments in assay methods for oxidative stress and nutraceutical antioxidants. Progress in Neuro-Psychopharmacology & Biological Psychiatry 2004;28(5):771-99. doi: 10.1016/j.pnpbp.2004.05.023.
10. Gao HM, Hong JS. Why neurodegenerative diseases are progressive: uncontrolled inflammation drives disease progression. Trends in Immunology 2008;29(8):357-65. doi: 10.1016/j.it.2008.05.002.
11. Joseph JA, Shukitt-Hale B, McEwen J, Rabin BM. CNS-induced deficits of heavy particle irradiation in space: The aging connection. Advances in Space Research 2000;25(10):2057-64. doi: 10.1016/S0273-1177(99)01013-3.
12. Rabin BM, Shukitt-Hale B. A voyage to Mars: Space radiation, aging, and nutrition. Nutrition and Aging 2014;2(4):233-41. doi: 10.3233/nua-140045.
13. Poulose SM, Bielinski DF, Carrihill-Knoll KL, Rabin BM, Shukitt-Hale B. Protective effects of blueberry- and strawberry diets on neuronal stress following exposure to 56Fe particles. Brain Research 2014;1593:9-18. doi: 10.1016/j.brainres.2014.10.028.
14. Yahyapour R, Motevaseli E, Rezaeyan A, Abdollahi H, Farhood B, Cheki M, Rezapoor S, Shabeeb D, Musa AE, Najafi M, et al. Reduction-oxidation (redox) system in radiation-induced normal tissue injury: molecular mechanisms and implications in radiation therapeutics. Clinical and Translational Oncology 2018;20(8):975-88. doi: 10.1007/s12094-017-1828-6.
15. Limoli C. Can a comparison of clinical and deep space irradiation scenarios shed light on the radiation response of the brain? British Journal of Radiology 2020;93(1115):20200245. doi: 10.1259/bjr.20200245.
16. Stone HB, Moulder JE, Coleman CN, Ang KK, Anscher MS, Barcellos-Hoff MH, Dynan WS, Fike JR, Grdina DJ, Greenberger JS, et al. Models for Evaluating Agents Intended for the Prophylaxis, Mitigation and Treatment of Radiation

Injuries Report of an NCI Workshop. Radiation Research 2006;162(6):711-28. doi: 10.1667/rr3276.

17. Pariset E, Malkani S, Cekanaviciute E, Costes SV. Ionizing radiation-induced risks to the central nervous system and countermeasures in cellular and rodent models. International Journal of Radiation Biology 2021;97(sup1):S132-S50. doi: 10.1080/09553002.2020.1820598.
18. Durante M. Space radiation protection: Destination Mars. Life Sciences in Space Research 2014;1(1):2-9. doi: 10.1016/j.lssr.2014.01.002.
19. Durante M, Cucinotta FA. Heavy ion carcinogenesis and human space exploration. Nature Reviews Cancer 2008;8(6):465-72. doi: 10.1038/nrc2391.
20. Poulose SM, Rabin BM, Bielinski DF, Kelly ME, Miller MG, Thanthaeng N, Shukitt-Hale B. Neurochemical differences in learning and memory paradigms among rats supplemented with anthocyanin-rich blueberry diets and exposed to acute doses of (56)Fe particles. Life Sciences in Space Research 2017;12:16-23. doi: 10.1016/j.lssr.2016.12.002.
21. Rabin BM, Carrihill-Knoll K, Hinchman M, Shukitt-Hale B, Joseph JA, Foster BC. Effects of heavy particle irradiation and diet on object recognition memory in rats. Advances in Space Research 2009;43(8):1193-9. doi: 10.1016/j.asr.2009.01.015.
22. Britten RA, Davis LK, Jewell JS, Miller VD, Hadley MM, Sanford LD, Machida M, Lonart G. Exposure to mission relevant doses of 1 GeV/Nucleon 56Fe particles leads to impairment of attentional set-shifting performance in socially mature rats. Radiation Research 2014;182(3):292-8. doi: 10.1667/RR3766.1.
23. Cherry JD, Liu B, Frost JL, Lemere CA, Williams JP, Olschowka JA, O'Banion MK. Galactic cosmic radiation leads to cognitive impairment and increased abeta plaque accumulation in a mouse model of Alzheimer's disease. PLoS ONE 2012;7(12):e53275. doi: 10.1371/journal.pone.0053275.
24. Betlazar C, Middleton RJ, Banati RB, Liu GJ. The impact of high and low dose ionising radiation on the central nervous system. Redox Biology 2016;9:144-56. doi: 10.1016/j.redox.2016.08.002.

25. Lee YW, Cho HJ, Lee WH, Sonntag WE. Whole brain radiation-induced cognitive impairment: Pathophysiological mechanisms and therapeutic targets. Biomolecules and Therapeutics 2012;20(4):357-70. doi: 10.4062/biomolther.2012.20.4.357.

26. Makale MT, McDonald CR, Hattangadi-Gluth JA, Kesari S. Mechanisms of radiotherapy-associated cognitive disability in patients with brain tumours. Nature Reviews Neurology 2016;13(1):52-64. doi: 10.1038/nrneurol.2016.185.

27. Cramer CK, Cummings TL, Andrews RN, Strowd R, Rapp SR, Shaw EG, Chan MD, Lesser GJ. Treatment of Radiation-Induced Cognitive Decline in Adult Brain Tumor Patients. Current Treatment Options in Oncology 2019;20(5). doi: 10.1007/s11864-019-0641-6.

28. Patel VN, Gupta S, Shareef MM, Ahmed MM. Contemporary radiation countermeasures. Defence Science Journal 2011;61:138-45. doi: 10.14429/dsj.61.834.

29. Dumont F, Roux AL, Bischoff P. Radiation countermeasure agents: an update. Expert Opinion on Therapeutic Patents 2010;20(1):73-101. doi: 10.1517/13543770903490429.

30. Shukitt-Hale B, Galli RL, Meterko V, Carey A, Bielinski DF, McGhie T, Joseph JA. Dietary supplementation with fruit polyphenolics ameliorates age-related deficits in behavior and neuronal markers of inflammation and oxidative stress. Age 2005;27(1):49-57. doi: 10.1007/s11357-005-4004-9.

31. Lau FC, Shukitt-Hale B, Joseph JA. Nutritional intervention in brain aging: reducing the effects of inflammation and oxidative stress. Subcellular Biochemistry 2007;42:299-318. doi: 10.1007/1-4020-5688-5.

32. Ma L, Sun Z, Zeng Y, Luo M, Yang J. Molecular Mechanism and Health Role of Functional Ingredients in Blueberry for Chronic Disease in Human Beings. International Journal of Molecular Sciences 2018;19(9):2785-. doi: 10.3390/ijms19092785.

33. Slemmer JE, Shacka JJ, Sweeney MI, Weber JT. Antioxidants and free radical scavengers for the treatment of stroke, traumatic brain injury and aging. Current Medicinal Chemistry 2008;15(4):404-14. doi: 10.2174/092986708783497337.

34. Ma H, Johnson S, Liu W, DaSilva N, Meschwitz S, Dain J, Seeram N. Evaluation of Polyphenol Anthocyanin-Enriched Extracts of Blackberry, Black Raspberry, Blueberry, Cranberry, Red Raspberry, and Strawberry for Free Radical Scavenging, Reactive Carbonyl Species Trapping, Anti-Glycation, Anti-β-Amyloid Aggregation, and Mic. International Journal of Molecular Sciences 2018;19(2):461-. doi: 10.3390/ijms19020461.

35. Galli RL, Shukitt-Hale B, Youdim KA, Joseph JA. Fruit polyphenolics and brain aging: nutritional interventions targeting age-related neuronal and behavioral deficits. Annals of the New York Academy of Sciences 2002;959:128-32. doi: 10.1111/j.1749-6632.2002.tb02089.x.

36. McNamara RK, Kalt W, Shidler MD, McDonald J, Summer SS, Stein AL, Stover AN, Krikorian R. Cognitive response to fish oil, blueberry, and combined supplementation in older adults with subjective cognitive impairment. Neurobiology of Aging 2018;64(2018):147-56. doi: 10.1016/j.neurobiolaging.2017.12.003.

37. Andres-Lacueva C, Shukitt-Hale B, Galli RL, Jauregui O, Lamuela-Raventos RM, Joseph JA. Anthocyanins in aged blueberry-fed rats are found centrally and may enhance memory. Nutritional Neuroscience 2005;8(2):111-20. doi: 10.1080/10284150500078117.

38. Shishtar E, Rogers GT, Blumberg JB, Au R, Jacques PF. Long-term dietary flavonoid intake and risk of Alzheimer disease and related dementias in the Framingham Offspring Cohort. The American Journal of Clinical Nutrition 2020;23(9):1576-88. doi: 10.1093/ajcn/nqaa079.

39. Joseph JA, Shukitt-Hale B, Brewer GJ, Weikel KA, Kalt W, Fisher DR. Differential protection among fractionated blueberry polyphenolic families against DA-, Aβ42- and LPS-Induced decrements in Ca2+ buffering in primary hippocampal cells. Journal of Agricultural and Food Chemistry 2010;58(14):8196-204. doi: 10.1021/jf100144y.

40. Lau FC, Bielinski DF, Joseph JA. Inhibitory effects of blueberry extract on the production of inflammatory mediators in lipopolysaccharide-activated BV2

microglia. Journal of Neuroscience Research 2007;85(5):1010-7. doi: 10.1002/jnr.21205.

41. Carey AN, Fisher DR, Rimando AM, Gomes SM, Bielinski DF, Shukitt-Hale B. Stilbenes and anthocyanins reduce stress signaling in BV-2 mouse microglia. Journal of Agricultural and Food Chemistry 2013;61(25):5979-86. doi: 10.1021/jf400342g.
42. Zhu Y, Bickford PC, Sanberg P, Giunta B, Tan J. Blueberry opposes beta-amyloid peptide-induced microglial activation via inhibition of p44/42 mitogen-activation protein kinase. Rejuvenation Research 2008;11(5):891-901. doi: 10.1089/rej.2008.0757.
43. Debnath-Canning M, Unruh S, Vyas P, Daneshtalab N, Igamberdiev AU, Weber JT. Fruits and leaves from wild blueberry plants contain diverse polyphenols and decrease neuroinflammatory responses in microglia. Journal of Functional Foods 2020;68(2020). doi: 10.1016/j.jff.2020.103906.
44. Shukitt-Hale B, Lau FC, Carey AN, Galli RL, Spangler EL, Ingram DK, Joseph JA. Blueberry polyphenols attenuate kainic acid-induced decrements in cognition and alter inflammatory gene expression in rat hippocampus. Nutritional Neuroscience 2008;11(4):172-82. doi: 10.1179/147683008X301487.
45. Shukitt-Hale B, C. Lau F, Cheng V, Luskin K, N. Carey A, Carrihill-Knoll K, M. Rabin B, A. Joseph J. Changes in Gene Expression in the Rat Hippocampus Following Exposure to 56Fe Particles and Protection by Berry Diets. Central Nervous System Agents in Medicinal Chemistry 2013;13(1):36-42. doi: 10.2174/1871524911313010006.
46. Rabin BM, Joseph JA, Shukitt-Hale B. Effects of age and diet on the heavy particle-induced disruption of operant responding produced by a ground-based model for exposure to cosmic rays. Brain Research 2005;1036(1-2):122-9. doi: 10.1016/j.brainres.2004.12.041.
47. Shukitt-Hale B, Carey AN, Jenkins D, Rabin BM, Joseph JA. Beneficial effects of fruit extracts on neuronal function and behavior in a rodent model of accelerated aging. Neurobiology of Aging 2007;28(8):1187-94. doi: 10.1016/j.neurobiolaging.2006.05.031.

48. Slemmer J, Shacka J, Sweeney-Nixon M, Weber J. Do antioxidants and free radical scavengers still hold promise for the treatment of stroke, traumatic brain injury and aging? Journal of Chemical Information and Modeling 2019;53(9):1689-99. doi: 10.1017/CBO9781107415324.004.

49. Spitz DR, Azzam EI, Li JJ, Gius D. Metabolic oxidation/reduction reactions and cellular responses to ionizing radiation: A unifying concept in stress response biology. Cancer and Metastasis Reviews 2004;23(3-4):311-22. doi: 10.1023/B:CANC.0000031769.14728.bc.

50. Poulose SM, Bielinski DF, Carrihill-Knoll K, Rabin BM, Shukitt-Hale B. Exposure to 16 O-Particle Radiation Causes Aging-Like Decrements in Rats through Increased Oxidative Stress, Inflammation and Loss of Autophagy. Radiation Research 2011;176(6):761-9. doi: 10.1667/rr2605.1.

51. Rabin BM, Carrihill-Knoll KL, Shukitt-Hale B. Comparison of the Effectiveness of Exposure to Low-LET Helium Particles (4He) and Gamma Rays (137Cs) on the Disruption of Cognitive Performance. Radiation Research 2015;184(3):266-72. doi: 10.1667/rr14001.1.

52. Rabin BM, Poulose SM, Bielinski DF, Shukitt-Hale B. Effects of head-only or whole-body exposure to very low doses of 4He (1000 MeV/n) particles on neuronal function and cognitive performance. Life Sciences in Space Research 2019;20(August):85-92. doi: 10.1016/j.lssr.2019.02.001.

53. Limoli CL, Giedzinski E, Baure J, Rola R, Fike JR. Redox changes induced in hippocampal precursor cells by heavy ion irradiation. Radiat Environ Biophys 2007;46(2):167-72. doi: 10.1007/s00411-006-0077-9.

54. Klegeris A, McGeer EG, McGeer PL. Therapeutic approaches to inflammation in neurodegenerative disease. Current Opinion in Neurology 2007;20(3):351-7. doi: 10.1097/WCO.0b013e3280adc943.

55. Ushakov IB, Vasin MV. Radiation protective agents in the radiation safety system for long-term exploration missions. Human Physiology 2014;40(7):695-703. doi: 10.1134/S0362119714070251.

56. Sundaram RS, Gowtham L, Manikandan P, Venugopal V. The Role Of Reactive Microglia In Neurodegenerative Disease: Multiple Triggers With A Common

Mechanism. International Journal of Recent Advances in Pharmaceutical Research 2012;2:29-40.

57. Greene-Schloesser D, Robbins ME, Peiffer AM, Shaw EG, Wheeler KT, Chan MD. Radiation-induced brain injury: A review. Frontiers in Oncology 2012;2 JUL(July):1-18. doi: 10.3389/fonc.2012.00073.

58. Nieder C, Leicht A, Motaref B, Nestle U, Niewald M, Schnabel K. Late Radiation Toxicity After Whole-Brain Radiotherapy: The Influence of Antiepileptic Drugs. American Journal of Clinical Oncology: Cancer Clinical Trials 1999;22(6):573-. doi: 10.1097/00000421-199912000-00007.

59. Stone HB, McBride WH, Coleman CN. Modifying normal tissue damage postirradiation. Report of a workshop sponsored by the Radiation Research Program, National Cancer Institute, Bethesda, Maryland, September 6-8, 2000. Radiiatioin Research 2002;157(2):204-23.

60. Loane DJ, Byrnes KR. Role of Microglia in Neurotrauma. Neurotherapeutics 2010;7(4):366-77. doi: 10.1016/j.nurt.2010.07.002.

61. Paladini MS, Feng X, Krukowski K, Rosi S. Microglia depletion and cognitive functions after brain injury: From trauma to galactic cosmic ray. Neuroscience Letters 2021;741:135462. doi: 10.1016/j.neulet.2020.135462.

62. Hwang SY, Jung JS, Kim TH, Lim SJ, Oh ES, Kim JY, Ji KA, Joe EH, Cho KH, Han IO. Ionizing radiation induces astrocyte gliosis through microglia activation. Neurobiology of Disease 2006;21(3):457-67. doi: 10.1016/j.nbd.2005.08.006.

63. Gresa-Arribas N, Vieitez C, Dentesano G, Serratosa J, Saura J, Sola C. Modelling neuroinflammation in vitro: a tool to test the potential neuroprotective effect of anti-inflammatory agents. PLoS ONE 2012;7(9):e45227. doi: 10.1371/journal.pone.0045227.

64. Parihar VK, Allen BD, Caressi C, Kwok S, Chu E, Tran KK, Chmielewski NN, Giedzinski E, Acharya MM, Britten RA, et al. Cosmic radiation exposure and persistent cognitive dysfunction. Scientific Reports 2016;6(June):1-14. doi: 10.1038/srep34774.

65. Rola R, Sarkissian V, Obenaus A, Nelson GA, Otsuka S, Limoli CL, Fike JR. High-LET radiation induces inflammation and persistent changes in markers of

hippocampal neurogenesis. Radiation Research 2005;164(4 Pt 2):556-60. doi: 10.1667/rr3412.1.

66. Acharya MM, Green KN, Allen BD, Najafi AR, Syage A, Minasyan H, Le MT, Kawashita T, Giedzinski E, Parihar VK, et al. Elimination of microglia improves cognitive function following cranial irradiation. Scientific Reports 2016;6:31545. doi: 10.1038/srep31545.
67. Liu B, Hinshaw RG, Le KX, Park MA, Wang S, Belanger AP, Dubey S, Frost JL, Shi Q, Holton P, et al. Space-like 56Fe irradiation manifests mild, early sex-specific behavioral and neuropathological changes in wildtype and Alzheimer's-like transgenic mice. Scientific Reports 2019;9(1):1-17. doi: 10.1038/s41598-019-48615-1.
68. Rola R, Fishman K, Baure J, Rosi S, Lamborn KR, Obenaus A, Nelson GA, Fike JR. Hippocampal Neurogenesis and Neuroinflammation after Cranial Irradiation with 56Fe Particles. Radiation Research 2008;169(6):626-32. doi: 10.1667/rr1263.1.
69. Raber J, Yamazaki J, Torres ERS, Kirchoff N, Stagaman K, Sharpton T, Turker MS, Kronenberg A. Combined Effects of Three High-Energy Charged Particle Beams Important for Space Flight on Brain, Behavioral and Cognitive Endpoints in B6D2F1 Female and Male Mice. Frontiers in Physiology 2019;10:179. doi: 10.3389/fphys.2019.00179.
70. Raber J, Fuentes Anaya A, Torres ERS, Lee J, Boutros S, Grygoryev D, Hammer A, Kasschau KD, Sharpton TJ, Turker MS, et al. Effects of Six Sequential Charged Particle Beams on Behavioral and Cognitive Performance in B6D2F1 Female and Male Mice. Frontiers in Physiology 2020;11:959. doi: 10.3389/fphys.2020.00959.
71. Mortazavi SMJ, Foadi M, Mozdarani H, Haghani M. Future role of vitamin C in radiation mitigation and its possible applications in manned deep space missions: survival study and the measurement of cell viability. European Journal of Medical Physics 2015;13(1):55-60. doi: 10.7508/ijrr.2015.01.007.
72. Weinstein JR, Koerner IP, Mller T. Microglia in ischemic brain injury. Future Neurology 2010;5(2):227-46. doi: 10.2217/fnl.10.1.

73. Brown PD, Pugh S, Laack NN, Wefel JS, Khuntia D, Meyers C, Choucair A, Fox S, Suh JH, Roberge D, et al. Memantine for the prevention of cognitive dysfunction in patients receiving whole-brain radiotherapy: a randomized, double-blind, placebo-controlled trial. Neuro-Oncology 2013;15(10):1429-37. doi: 10.1093/neuonc/not114.

74. Rapp SR, Case LD, Peiffer A, Naughton MM, Chan MD, Stieber VW, Moore DF, Jr., Falchuk SC, Piephoff JV, Edenfield WJ, et al. Donepezil for Irradiated Brain Tumor Survivors: A Phase III Randomized Placebo-Controlled Clinical Trial. Journal of Clinical Oncology 2015;33(15):1653-9. doi: 10.1200/JCO.2014.58.4508.

75. Attia A, Rapp SR, Case LD, D'Agostino R, Lesser G, Naughton M, McMullen K, Rosdhal R, Shaw EG. Phase II study of Ginkgo biloba in irradiated brain tumor patients: effect on cognitive function, quality of life, and mood. Journal of Neurooncology 2012;109(2):357-63. doi: 10.1007/s11060-012-0901-9.

76. Kouvaris JR, Kouloulias VE, Vlahos LJ. Amifostine: the first selective-target and broad-spectrum radioprotector. Oncologist 2007;12(6):738-47. doi: 10.1634/theoncologist.12-6-738.

3 MANUSCRIPTS/CHAPTERS

3.1 Blueberry treatment administered before and/or after lipopolysaccharide stimulation attenuates inflammation and oxidative stress in rat microglial cells

Danielle S. Cahoon[a], Derek R. Fisher[a], Stefania Lamon-Fava[a], Dayong Wu[a], Tong Zheng[a], and Barbara Shukitt-Hale[a,*]

[a]USDA-ARS, Jean Mayer Human Nutrition Research Center on Aging at Tufts University, Boston, MA, USA

Correspondence to:

Barbara Shukitt-Hale, Ph.D.

USDA, HNRCA at Tufts University

711 Washington Street

Boston, MA 02111

Tel: 617-556-3118; Fax: 617-556-3299

E-Mail: barbara.shukitthale@usda.gov

Published in *Nutritional Neuroscience* (2021), p. 1-11. doi:

10.1080/1028415x.2021.2020404.

Abstract

Microglia, the primary immune cells of the central nervous system (CNS), are key regulators of inflammation and oxidative stress (OS) in the CNS. Microglia activation can lead to chronic inflammation, OS, and neurodegeneration. Blueberries (BB) have been shown to reduce inflammation and OS when administered to microglia before stressors such as lipopolysaccharide (LPS), but the therapeutic value of BBs administered to microglia after activation by stressors has not been examined. Post-stressor treatments may be important to target chronic and progressive inflammation/OS following microglia activation. Therefore, this study investigated the differential effects of pre-, post-, and pre-/post-BB on inflammation and OS in LPS-activated microglia. Rat microglia were pre-treated with freeze-dried BB diluted in media (0.5 mg/mL) or control media (C) for 24 hours, incubated overnight with LPS (0 or 200 ng/mL), and post-treated with BB or C for 24 hours. Biomarkers of inflammation (e.g., nitrite [NO_2^-], tumor necrosis factor-α [TNFα], inducible nitric oxide synthase [iNOS], cyclooxygenase-2 [COX-2], phosphorylated IκB-α [pIκB-α]) and OS (e.g., NADPH oxidase [NOX2], nuclear factor erythroid 2-related factor 2 [Nrf2], superoxide dismutase [SOD]) were assessed. Results showed that LPS increased NO_2^-, TNFα, COX-2, iNOS, pIκB-α, and NOX2 compared to non-stressed control conditions ($P < 0.05$), however BB before and/or after LPS significantly reduced these markers compared to no BB ($P < 0.05$). Pre-BB was more effective than post-BB at reducing LPS-induced NO_2^-, TNFα, and COX-2 ($P < 0.05$). Pre-BB was also more effective than pre-/post-BB at attenuating LPS-induced NO_2^- and TNFα ($P < 0.05$). All BB treatments were equally effective in reducing LPS-induced iNOS, pIκB-α, and NOX2. Results suggest that BBs can target the downstream events of LPS-induced microglial activation and prevent stressor-induced neuroinflammation and OS. Furthermore, BBs may not need to be present prior to microglial activation for beneficial effects. These findings provide evidence suggesting that dietary interventions may be effective even after initiation of disease processes such as microglial-induced neuroinflammation and OS.

Keywords: neuroinflammation, oxidative stress, polyphenolics, microglia, blueberry

Introduction

Neuroinflammation and oxidative stress (OS) have been implicated as mediators of cognitive decline and neurodegenerative diseases [1]. Microglial cells, the specialized macrophages and primary immune cells of the central nervous system (CNS), are key regulators of the inflammatory response and free radical production in the CNS [2]. Under normal physiological conditions, microglia serve a neuroprotective role by clearing cellular debris and surveying the CNS for noxious stimuli [1]. In response to a range of pathogenic stressors, microglia change from quiescent phenotype to an activated phenotype and produce cytotoxic mediators including inflammatory cytokines (e.g., tumor necrosis factor-α [TNFα]), reactive oxygen species (ROS), and nitric oxide (NO) to initiate repair processes, destroy invading pathogens, and restore homeostasis [1, 3]. However, microglial activation has been considered a 'double-edged sword' as the excess and/or uncontrolled production of these mediators can be neurotoxic to healthy neurons beyond the site of an inflammatory insult [1, 4]. Collateral neuronal damage signals further microglial activation, resulting in a feed-forward amplification of inflammation and neuronal damage known as reactive microgliosis [1, 4]. Therefore, a vicious cycle of microglial activation and neurotoxicity can result, leading to chronic inflammation, OS, and neurodegeneration, long after the initial stressor dissipates [1, 4]. Chronic microglial activation, neuronal damage, and associated neurodegenerative processes have been observed following acute exposures to pathogenic stressors such as neurotoxin 1-methyl-4-phenyl-1,2,3,6-tetrahydropyridine (MPTP) [1], peripheral lipopolysaccharide (LPS) [4], pesticides [5], traumatic brain injury (TBI) [5], stroke [5], and ionizing radiation [6].

In addition to neuronal damage, Lijia and colleagues demonstrated that microglial activation can be self-propelling in the absence of signals from damaged neurons [3]. In microglia stressed with LPS, a potent endotoxin and activator of microglia [1], increased levels of NO persisted at 24 hours after LPS removal relative to non-LPS treated cells. Subsequent knockdown and enzyme inhibitor experiments showed that NADPH oxidase (NOX2)-generated ROS upregulated inducible nitric oxide synthase (iNOS)-generated NO, and vice-versa. This study was the first to demonstrate that signals from activated microglia can propel reactive microgliosis after stressor removal and direct neuronal damage is not necessary [3]. Therefore, interventions that target activated microglia, and

the resulting inflammatory processes, may help prevent, slow, or reverse neurodegeneration and cognitive decline.

Nutritional strategies using whole foods with antioxidant and anti-inflammatory properties show potential to be safe, inexpensive, and easily accessible therapies to attenuate microglial activation and the resulting neurodegenerative processes. As one of such cases, blueberries (BB) contain some of the highest levels of antioxidant and anti-inflammatory polyphenols relative to other plant species, such as the flavonoid anthocyanin [7]. Anthocyanins from dietary BB consumption can readily reach the CNS by crossing the blood-brain-barrier [8], and could therefore directly interact with activated microglia in the brain. The neuroprotective effects of BB have been previously demonstrated when introduced before a stressor. In animal studies, BBs can protect against neuroinflammation, OS, and/or cognitive deficits when administered before ionizing radiation [9], experimentally-induced stroke [10], and the neurotoxin kainic acid [11]. *In vitro*, BB pre-treatment can protect against inflammation and OS when administered to microglia and removed before stressors such as LPS [12-14], B-amyloid [14], glutamate, and a-synuclein [7]. In these studies, outcomes were assessed immediately after stressor removal, precluding any conclusions on whether BB pre-treatments can attenuate self-propelling microglial activation and the potential therapeutic efficacy of post-stressor treatments.

In addition to neuroprotective effects, antioxidant and anti-inflammatory compounds may also be effective at modulating prolonged microglia activation when stressors are no longer present by targeting reactive microgliosis and the self-amplifying cycle of microglial-derived ROS and inflammatory factors. However, to our knowledge, there are limited studies demonstrating the attenuating effects of therapeutics on self-propelling microglial activation, particularly when administered after the instigating stimulus ends. Additionally, the differential efficacy of pre- and/or post-stressor treatments on neuroinflammation and OS in microglia has not been explored. Given the antioxidant and anti-inflammatory neuroprotective properties of BBs, in this study we investigated the potential beneficial effects of pre- and/or post-stressor BB on increases in inflammation and OS in LPS-activated microglial cells.

Methods

Cell Culture and Treatments

The experimental design for this study is shown in Figure 1. Highly aggressively proliferating immortalized (HAPI) rat microglial cells (generously provided by Dr Grace Sun, University of Missouri, Columbia, MO) were maintained in Dulbecco's modified Eagle's medium (DMEM, Invitrogen, Grand Island, NY) supplemented with 10% fetal bovine serum (FBS), 100 U/mL penicillin, and 100 µg/mL streptomycin at 37 °C in a humidified incubator under 5% CO_2. Cells were maintained in 100 mm plates and then split into T25 flasks at a seeding density of 2.5 x 10^6 cells/flask for experimental treatments in DMEM without phenol red. Previous studies have shown that 0.5 mg/mL BB significantly attenuates LPS-induced inflammation in microglia with no cytotoxic effects [12, 13]. Additionally, preliminary dose-response experiments in HAPI cells using 0.125, 0.25, and 0.5 mg/mL BB showed that only 0.5 mg/mL BB for 24 hours before and/or after LPS significantly attenuated nitrite production, a well-known indicator of microglial activation [1, 15] relative to no BB ($P < 0.05$, data not shown). Therefore, 0.5 mg/mL BB was chosen to be used for experimental treatments. For pre-treatments, cells were incubated in the absence (control) or presence of freeze-dried BB extract (Tif-blue BB) prepared as described previously [12] and diluted in media to a concentration of 0.5 mg/mL for 24 hours. Pre-treatment media was removed, and cells were incubated in the absence (unstressed control) or presence of LPS (Sigma-Aldrich, St Louis, MO) in serum-free DMEM at 200 ng/mL for 18 hours, as this dose has been shown induce stress signaling without reducing viability [16]. Media was removed and cells were post-treated in the absence or presence of 0.5 mg/mL BB for 24 hours. A 24 hour treatment interval was chosen based on a study by Lijia and authors who demonstrated a self-propelling cycle of LPS-induced microglial activation 24 hours after LPS removal [3]. All outcomes were assessed at the end of the post-treatment period.

Cell Viability

Cell viability was assessed using the Trypan blue exclusion method [17]. In brief, microglial cells were seeded onto 6-well plates and experimental treatments were performed as above. Following treatments, cells were incubated with 500 µL trypsin/well

for 5 minutes for detachment, and 50 µL of cell suspension was mixed with 50 µL of Trypan blue. Only dead cells with damaged membranes are permeable to Trypan blue and can be identified by their blue stain. The cell suspension was added to a hemocytometer and the number of blue-stained and non-stained cells were counted under a light microscope to calculate percentage of viable cells (non-stained/total cells X 100).

Nitrite Quantification

To assess the production of free radical nitric oxide (NO) from HAPI cells, the extracellular release of nitrite (NO_2^-), a stable and nonvolatile breakdown product of NO, was measured in cell-conditioned supernatant by Greiss reagent kit (Invitrogen, Carlsbad, CA) according to manufacturer's instructions. In brief, 100 µl of supernatant from each flask was added in duplicate to a 96-well plate. Then, 25 µl of Griess reagent was added to each well and incubated at room temperature for 15 min. Absorbance was read at 548 nm and the concentration of NO_2^- in each sample was calculated with the linear equation derived from the standard curve generated by known concentrations of NO_2^-. Values were normalized by total protein levels in cell lysates quantified with the DC protein assay (BioRad, Hercules, CA).

TNFα Enzyme-linked Immunosorbent Assay (ELISA)

Secretion of inflammatory cytokine TNFα was quantified using ELISA according to manufacturer's instructions (Invitrogen, Carlsbad, CA). In brief, 50 µl of cell-conditioned supernatant or provided protein standards was added in duplicate to a 96-well plate and incubated for 2 hours. Following washing, peroxidase-conjugated detection antibody was added to each well and incubated for 1 hour. Wells were washed and substrate solution was added to each well for 15 min, followed by stop solution. Absorbance was read at 450 nm and the TNFα concentration in each sample was calculated from the linear equation derived from the standard curve of known concentrations of the cytokine. Values were normalized by total protein levels in cell lysates quantified with the DC protein assay (BioRad, Hercules, CA).

Western Blots

Following experimental treatments, cells were washed in ice-cold phosphate-buffered saline (PBS), resuspended and lysed by scraping in CelLytic-M Cell Lysis Reagent (Sigma-Aldrich, St Louis, MO) containing phenylmethylsulfonylfluoride (PMSF, 10 ug/mL), and centrifuged at 14,000 rpm for 10 min at 4 °C. The resultant supernatant lysate was used for blotting after total protein was quantified with the DC protein assay (BioRad, Hercules, CA). Western blots were performed as described previously [18], except that 10% polyacrylamide gels were used. Primary antibodies were used at 1:1000 dilutions for inflammatory markers cyclooxygenase-2 (COX-2, Santa Cruz, Dallas, TX), phospho- and total IκB-α (pIκB-α, IκB-α Santa Cruz, Dallas, TX), and iNOS (Millipore, Billerica, MA), and oxidative stress markers NOX2 (Santa Cruz, Dallas, TX), nuclear factor erythroid 2-related factor 2 (Nrf2, Santa Cruz, Dallas, TX), and superoxide dismutase (Cu/Zn-SOD, Santa Cruz, Dallas, TX) for incubation overnight at 4°C. Glyceraldehyde 3-phosphate dehydrogenase (GAPDH, Santa Cruz, Dallas, TX) was used as a protein loading control marker. The signal was detected using an electrochemiluminescence (ECL) detection kit (BioRad, Hercules, CA) and the optical density of antibody-specific bands was analyzed by the VisionWorks LS image acquisition and analysis software (UVP, Upland, CA). Values were normalized to GAPDH protein levels.

Statistical Analysis

Statistical analyses were conducted in R (*v*3.8) using RStudio (*v*1.0.153) and results were considered statistically significant if the observed significance level was $P \leq 0.05$. Two-way analysis of variance (ANOVA) was conducted using a general linear model with LPS exposure (no LPS or LPS) and BB treatment period (no BB, pre-BB, post-BB, pre-/post-BB) as experimental factors. If the LPS exposure by BB treatment period interaction was significant, post-hoc testing was performed with Tukey's honestly significant difference test to adjust for multiple comparisons and determine differences among groups. Data are expressed as mean ± standard error of the mean (SEM).

Results

Viability

Neither LPS ($F_{1,16} = 2.41$, $P = 0.14$) nor BB treatments ($F_{3,16} = 0.84$, $P = 0.49$) caused significant changes in viability **(Figure 2).** Cell viability was on average 95.7 ± 0.8%.

Inflammation

Nitrite (NO_2^-)

There were significant main effects of LPS ($F_{1,208} = 1{,}643.59$, $P < 0.001$) and BB ($F_{3,208} = 12.08$, $P < 0.001$), and an LPS x BB interaction ($F_{3,208} = 14.57$, $P < 0.001$) on NO_2^- production in microglia. Post-hoc testing showed that LPS exposure significantly increased NO_2^- production in all groups compared to non-stressed control conditions without LPS ($P < 0.001$) **(Figure 3).** BB treatments did not exert any effects on NO_2^- in non-stressed cells. However, BB treatment before and/or after LPS (i.e., pre-, post-, and pre-/post-BB) significantly reduced NO_2^- production compared to microglia incubated only with control media ($P < 0.01$). Additionally, pre-BB was more effective at reducing LPS-induced NO_2^- than post-BB and pre-/post-BB ($P < 0.01$), while post-BB and pre-/post-BB were not significantly different from each other.

TNFa

There were significant main effects of LPS ($F_{1,208} = 4{,}018.24$, $P < 0.001$) and BB ($F_{3,208} = 19.36$, $P < 0.001$), and an LPS x BB interaction ($F_{3,208} = 24.06$, $P < 0.001$) on TNFα production in microglia. Post-hoc testing showed that LPS significantly induced TNFα compared to non-stressed conditions ($P < 0.001$) **(Figure 3).** All BB treatments significantly reduced LPS-induced TNFα relative to no BB ($P < 0.01$), although BB did not exert any effects on TNFα in non-stressed cells. As with NO_2^- , pre-BB was more effective at reducing LPS-induced TNFα than post-BB and pre-/post-BB ($P < 0.01$), while post-BB and pre-/post-BB were not significantly different from each other.

iNOS

There were significant main effects of LPS ($F_{1,208} = 541.90$, $P < 0.001$) and BB ($F_{3,208} = 24.49$, $P < 0.001$), and an LPS x BB interaction ($F_{3,208} = 25.84$, $P < 0.001$) on

iNOS expression in microglia. Post-hoc testing showed that LPS significantly increased iNOS expression compared to non-stressed conditions ($P < 0.001$), and BB treatments did not affect iNOS expression in non-stressed cells compared to no BB **(Figure 4).** Results showed that BB treatment before and/or after LPS significantly reduced iNOS expression compared to no BB ($P < 0.01$). The timing of BB administration did not alter LPS-induced iNOS expression as levels following pre-, post-, and pre-/post-LPS BB treatments were not significantly different.

COX-2

There were significant main effects of LPS ($F_{1,208} = 529.94$, $P < 0.001$) and BB ($F_{3,208} = 9.99$, $P < 0.001$), and an LPS x BB interaction ($F_{3,208} = 11.38$, $P < 0.001$) on COX2 expression in microglia. Post-hoc testing showed that LPS exposure significantly increased COX-2 expression in microglia compared to non-stressed conditions ($P < 0.001$) **(Figure 4).** All BB treatments significantly reduced LPS-induced COX-2 relative to no BB ($P < 0.01$), although BB did not exert any effects on COX-2 in non-stressed cells. Pre-BB was more effective at reducing LPS-induced COX-2 expression than post-BB ($P < 0.01$), although neither was significantly different than pre-/post-BB.

pIκB-α/IκB-α

There were significant main effects of LPS ($F_{1,208} = 181.10$, $P < 0.001$) and BB ($F_{3,208} = 3.97$, $P < 0.01$), and an LPS x BB interaction ($F_{3,208} = 10.40$, $P < 0.001$) on IκB-α phosphorylation in microglia. Post-hoc testing showed that LPS significantly induced phosphorylation of IκB-α relative to no LPS ($P < 0.001$) **(Figure 4).** BB treatments did not significantly alter IκB-α phosphorylation in non-stressed cells. However, in LPS-treated cells, all BB treatments significantly reduced IκB-α phosphorylation relative to no BB ($P < 0.01$). The attenuating effects of pre-, post-, and pre-/post-BB on LPS-induced IKB phosphorylation were not significantly different.

Oxidative Stress

NOX2

There were significant main effects of LPS ($F_{1,208} = 1{,}915.53$, $P < 0.001$) and BB ($F_{3,208} = 5.64$, $P < 0.001$), and an LPS x BB interaction ($F_{3,208} = 4.63$, $P < 0.01$) on NOX2 expression in microglia. Post-hoc testing showed that LPS significantly increased NOX2 expression compared to non-stressed conditions ($P < 0.001$), and BB treatments did not significantly affect NOX2 expression in non-stressed cells compared to no BB **(Figure 5).** Results showed that BB treatment before and/or after LPS significantly reduced NOX2 expression compared to no BB ($P < 0.01$). However, the timing of BB administration did not alter LPS-induced NOX2 expression as levels following pre-, post-, and pre-/post-LPS BB treatments were not significantly different.

SOD

The overall ANOVA showed a significant main effect of BB treatment period on Cu/Zn-SOD expression ($F_{3,208} = 3.52$, $P = 0.016$) **(Figure 5).** However, neither the main effect of LPS ($F_{1,208} = 0.89$, $P = 0.35$) nor the LPS x BB interaction ($F_{1,208} = 0.69$, $P = 0.58$) were significant.

Nrf2

Neither LPS ($F_{1,208} = 0.15$, $P = 0.70$) nor BB ($F_{3,208} = 0.63$, $P = 0.60$) caused significant changes in Nrf2 expression **(Figure 5).**

Discussion

Activated microglia play a key role in the chronic neurodegenerative processes that continue after exposure to acute stressors end [1, 4], implicating activated microglia as therapeutic targets to curb the progression of stressor-induced neurodegeneration. Our study showed that all BB treatment periods (pre-, post-, and pre-/post) attenuated LPS-induced increases in the protein expression of inflammatory factors (NO_2^-, iNOS, COX-2, TNFα, pIκB-α), and one mediator of oxidative stress (NOX2) when assessed 24 hours after LPS washout. Pre-BB was more effective than post- or pre-/post-BB at attenuating some markers of inflammation and OS, while for other markers all BB treatments were similarly

effective. Because LPS and BB treatments did not alter cell viability, the observed effects cannot be attributed to differences in cell survival. LPS is a potent activator of microglia, and one hallmark of microglial activation is the production of pro-inflammatory mediators (e.g., TNFα, NO) [1, 15]. BBs were selected as a nutritional intervention agent in this study because they are a safe and easily accessible food, and studies have demonstrated the neuroprotective (i.e., pre-stressor) properties of BBs both *in vitro* [12, 13, 19, 20] and *in vivo* [9-11].

Previous studies in microglia have demonstrated similar effects of BB pre-treatments on molecular targets in the present study when outcomes were assessed immediately after LPS removal. For example, pre-treatment with BB attenuated LPS-induced NO_2^- [12, 13, 19, 20], TNFα [12, 13, 20], and ROS [12, 20], mRNA and/or protein expression of iNOS and COX-2 [12, 13, 19, 20], and NF-κB DNA binding activity [19, 20] in microglia. The present study shows that the effects of BB pre-treatments on these outcomes continue for 24 hours after stressor exposure, despite washout of pre-treatment media. While the effects of BB post-treatments on LPS-induced inflammation and OS have not been demonstrated in microglia, two studies in RAW 264.7 macrophages showed that post-treatment with BB polyphenols reduced LPS-induced inflammatory cytokines [21], NO_2^-, iNOS, COX-2, and p-NF-κB [22]. Similarly, our findings suggest that BB does not need to be present prior to microglial activation, and that post-stressor treatments can have beneficial effects on stressor-induced inflammation and OS.

Pre-treatments were more effective than post-treatments at reducing LPS-induced protein expression of 1) NO_2^-, a breakdown product of free radical NO, which has been shown to mediate the inflammatory processes associated with microglial activation [3], 2) TNFα, a pro-inflammatory cytokine that can trigger reactive microgliosis [4], and 3) COX-2, an enzyme that produces pro-inflammatory prostaglandins [22]. Additionally, there was a trend for lower iNOS expression, the enzyme responsible for producing NO [3], with pre-treatment relative to post-treatment (P = 0.08). The mechanisms responsible for the differential efficacy of pre- and post-LPS BB treatments on inflammatory markers in microglia are unclear. However, in support of these findings, Ebenezer and colleagues found that pre-feeding a BB-enriched diet before stress induction in an animal model of

post-traumatic stress disorder had a greater attenuating effect on brain levels of ROS and cytokines than feeding BB after stress exposure [23].

One possible explanation for the greater attenuating effects of pre-treatments relative to post-treatments is that blocking transcription of inflammatory genes before activation by stressors may be more effective than modulating transcription or inducing protein degradation after stressor-induced initiation of these processes. Previous work has attributed the anti-inflammatory effects of polyphenols found in BBs such as quercetin and resveratrol primarily to the inhibition of gene transcription [24, 25]. An additional possible explanation for the greater anti-inflammatory efficacy of pre-treatments relative to post-treatments is that BB phytochemicals act through hormesis [26]. Phytochemicals in BB pre-treatments may initially activate mild stress signaling that later prevents overactivation of microglia in response to pathogenic stressors [27], such as LPS in the current study. Without the benefit of pre-conditioning, post-treatments may not be as effective at attenuating microglial overactivation. Further investigation is necessary to determine whether the greater efficacy of pre-BB relative to post-BB on LPS-induced microglial activation can be attributed to inhibition of inflammatory gene transcription or hormesis.

Pre-treatments were also more effective than pre-/post-treatments at attenuating LPS-induced NO_2^- and TNFα. This observation could be attributed to hormesis, as excess exposures of hormetic chemicals can have adverse effects (e.g., by inducing stress signaling beyond the threshold for adaptive effects) [27]. Studies have shown that in LPS-stimulated macrophages, treatment with BB polyphenols for longer durations or higher concentrations increased pro-inflammatory cytokines relative to shorter durations [21] or lower concentrations [28]. Therefore, the addition of post-treatments after pre-treatments may induce additional stress which may or may not be beneficial (i.e., adaptive) long-term. An alternative speculation is that relative to pre-treatments, the continuous presence of pre-/post-BB phytochemicals may interfere with degradation of inflammatory proteins, as many phytochemicals possess proteasome inhibitory activity [29]. Therefore, pre-/post-treatments may be less effective than pre-treatments at attenuating LPS-induced NO_2^- and TNFα not only by altering production, but also by slowing down degradation.

In contrast, the timing of BB administration did not produce different attenuating effects on the protein expression of 1) iNOS, 2) NOX2, a ROS generating enzyme that can

perpetuate reactive microgliosis [1, 3], and 3) pIκB-α, an indicator of increased activation of NF-κB, a transcription factor responsible for inducing the expression of inflammatory genes [22]. As pre-/post-treatments did not provide additional benefit beyond pre- or post-treatments, there may be a dose and/or duration threshold for the beneficial effects of BB, depending on the biomarker. In support of this hypothesis, Cheng and colleagues found that in LPS-activated macrophages, treatment with BB polyphenols for 24 hours did not produce different effects on iNOS expression compared to 48 or 72 hours [22].

The finding that all BB treatments attenuated the same markers of inflammation and OS, and that BB treatment period did not differentially affect some of these markers, suggests that BBs target similar pathways before and after microglial activation by LPS. This study showed that BB reduces phosphorylation, and therefore degradation, of IκB-α, an inhibitor of NF-κB. Upon activation, NF-κB enters the nucleus where it initiates transcription of inflammatory genes, including TNFα, iNOS and COX-2 [22]. Therefore, pre- and/or post-BB may suppress TNFα, NO, iNOS, and COX-2 by reducing IκB-α phosphorylation, thus inhibiting NF-κB activation. Furthermore, high levels of NO, TNFα, and NOX2-derived superoxide can induce further NF-κB signaling [2, 15] and NO can modulate NOX2 activity in a feed-forward process [3]. Therefore, along with directly blocking the expression of inflammatory factors, BB may additionally or alternatively exert effects on this pathway by scavenging downstream mediators. The potential differential efficacy of pre- and/or post-stressor BB at targeting these processes may underlie the observed differences in protein levels of inflammatory markers.

In the present study, LPS did not induce significant changes in Nrf2, an antioxidant transcription factor [30] or Cu/Zn-SOD, a cytoplasmic antioxidant enzyme [2]. While studies have shown increased Nrf2 immediately after LPS [30], it is possible that Nrf2 does not remain activated for 24 hours after LPS removal. Additionally, mitochondrial MnSOD may be primarily induced by LPS [2, 15], while Cu/Zn-SOD is less responsive [2]. Despite null findings on Nrf2 and Cu/Zn-SOD in the present study, research has shown that OS plays a role in microglial-mediated neurodegeneration following stressors [1]. While BBs may reduce OS by attenuating NOX2 as observed in the present study, future studies should assess the pre-/post-stressor effects of BBs on additional endogenous defense markers and indicators of OS in microglia.

One limitation of this research is that it was conducted *in vitro* using microglia to obtain cell-specific effects. Therefore, results cannot be extrapolated to *in vivo* conditions. However, findings implicate microglia and associated biomarkers as targets for future *in vivo* studies investigating the differential effects of pre- and/or post-stressor BB. Additionally, the BB dose of 0.5 mg/mL used in this study translates to a 1% BB diet for adult rats [12, 31], and to 0.5-1 cups/day in humans [9], an attainable dietary target. An additional limitation is that only protein expression of inflammation and OS biomarkers was assessed. Although results provide insight on the pathways involved, future study of gene transcription is necessary to better understand the mechanisms responsible for the potential differential effects of pre- and/or post-stressor BB. Studies should also include additional indicators of microglial activation, including surface receptors and morphological changes.

To conclude, we found that persistent increases in LPS-induced inflammation and OS can be attenuated by administering BB before, after, or both before and after LPS exposure. Pre-treatments may have a greater effect on reducing stressor-induced inflammation relative to post-treatments and pre-/post-treatments, possibly due to differences in transcriptional modulation, protein degradation, and/or hormetic effects, although mechanisms are unclear. Regardless of these differences, results suggest that in addition to a neuroprotective role, BBs can also have therapeutic effects. These findings provide evidence to support that dietary interventions, using foods such as BBs, may be beneficial even after neurodegenerative diseases processes such as microglial-induced inflammation and OS are initiated. Post-treatments would be particularly important when pre-stressor time is not available to administer protective agents such as with unpredictable, spontaneous inflammatory brain injuries (e.g., urgent radiotherapy, TBI, stroke). Nevertheless, future studies both *in vitro* and *in vivo* are necessary to evaluate the therapeutic potential and mechanisms of BB against microglial activation and other neurodegenerative processes.

Financial Support

This work was supported by USDA intramural funding and NASA Grants NNJ16HP45I and NNX16AE06G.

Disclosure of Interest

The authors report no conflict of interest.

Data Availability Statement

All data are available upon request.

References

1. Lull, M.E. and M.L. Block, *Microglial activation and chronic neurodegeneration.* Neurotherapeutics, 2010. **7**(4): p. 354-65.
2. Dringen, R., *Oxidative and antioxidative potential of brain microglial cells.* Antioxid Redox Signal, 2005. **7**(9-10): p. 1223-33.
3. Lijia, Z., et al., *A self-propelling cycle mediated by reactive oxide species and nitric oxide exists in LPS-activated microglia.* Neurochem Int, 2012. **61**(7): p. 1220-30.
4. Qin, L., et al., *Systemic LPS causes chronic neuroinflammation and progressive neurodegeneration.* Glia, 2007. **55**(5): p. 453-62.
5. Liu, B., H.M. Gao, and J.S. Hong, *Parkinson's disease and exposure to infectious agents and pesticides and the occurrence of brain injuries: role of neuroinflammation.* Environ Health Perspect, 2003. **111**(8): p. 1065-73.
6. Parihar, V.K., et al., *Persistent nature of alterations in cognition and neuronal circuit excitability after exposure to simulated cosmic radiation in mice.* Exp Neurol, 2018. **305**(2018): p. 44-55.
7. Debnath-Canning, M., et al., *Fruits and leaves from wild blueberry plants contain diverse polyphenols and decrease neuroinflammatory responses in microglia.* Journal of Functional Foods, 2020. **68**(2020).
8. Andres-Lacueva, C., et al., *Anthocyanins in aged blueberry-fed rats are found centrally and may enhance memory.* Nutr Neurosci, 2005. **8**(2): p. 111-20.
9. Rabin, B.M. and B. Shukitt-Hale, *A voyage to Mars: Space radiation, aging, and nutrition.* Nutrition and Aging, 2014. **2**(4): p. 233-241.
10. Slemmer, J.E., et al., *Antioxidants and free radical scavengers for the treatment of stroke, traumatic brain injury and aging.* Curr Med Chem, 2008. **15**(4): p. 404-14.

11. Shukitt-Hale, B., et al., *Blueberry polyphenols attenuate kainic acid-induced decrements in cognition and alter inflammatory gene expression in rat hippocampus.* Nutr Neurosci, 2008. **11**(4): p. 172-82.
12. Lau, F.C., D.F. Bielinski, and J.A. Joseph, *Inhibitory effects of blueberry extract on the production of inflammatory mediators in lipopolysaccharide-activated BV2 microglia.* J Neurosci Res, 2007. **85**(5): p. 1010-7.
13. Carey, A.N., et al., *Stilbenes and anthocyanins reduce stress signaling in BV-2 mouse microglia.* J Agric Food Chem, 2013. **61**(25): p. 5979-86.
14. Zhu, Y., et al., *Blueberry opposes beta-amyloid peptide-induced microglial activation via inhibition of p44/42 mitogen-activation protein kinase.* Rejuvenation Res, 2008. **11**(5): p. 891-901.
15. Bozic, I., et al., *Benfotiamine attenuates inflammatory response in LPS stimulated BV-2 microglia.* PLoS One, 2015. **10**(2): p. e0118372.
16. Zhou, X., et al., *Antiinflammatory effects of orientin-2"-O-galactopyranoside on lipopolysaccharide-stimulated microglia.* Biol Pharm Bull, 2014. **37**(8): p. 1282-94.
17. Strober, W., *Trypan Blue Exclusion Test of Cell Viability.* Curr Protoc Immunol, 2015. **111**(1): p. A3 B 1-A3 B 3.
18. Poulose, S.M., et al., *Anthocyanin-rich acai (Euterpe oleracea Mart.) fruit pulp fractions attenuate inflammatory stress signaling in mouse brain BV-2 microglial cells.* J Agric Food Chem, 2012. **60**(4): p. 1084-93.
19. Lau, F.C., et al., *Attenuation of iNOS and COX2 by blueberry polyphenols is mediated through the suppression of NF-κB activation.* Journal of Functional Foods, 2009. **1**(3): p. 274-283.
20. Serra, D., et al., *An Anthocyanin-Rich Extract Obtained from Portuguese Blueberries Maintains Its Efficacy in Reducing Microglia-Driven Neuroinflammation after Simulated Digestion.* Nutrients, 2020. **12**(12).
21. Cheng, A., et al., *Polyphenols from blueberries modulate inflammation cytokines in LPS-induced RAW264.7 macrophages.* Int J Biol Macromol, 2014. **69**(2014): p. 382-7.

22. Cheng, A., et al., *Extractable and non-extractable polyphenols from blueberries modulate LPS-induced expression of iNOS and COX-2 in RAW264.7 macrophages via the NF-kappaB signalling pathway.* J Sci Food Agric, 2016. **96**(10): p. 3393-400.

23. Ebenezer, P.J., et al., *The Anti-Inflammatory Effects of Blueberries in an Animal Model of Post-Traumatic Stress Disorder (PTSD).* PLoS One, 2016. **11**(9): p. e0160923.

24. Wadsworth, T.L., T.L. McDonald, and D.R. Koop, *Effects of Ginkgo biloba extract (EGb 761) and quercetin on lipopolysaccharide-induced signaling pathways involved in the release of tumor necrosis factor-alpha.* Biochem Pharmacol, 2001. **62**(7): p. 963-74.

25. Panaro, M.A., et al., *Anti-inflammatory effects of resveratrol occur via inhibition of lipopolysaccharide-induced NF-kappaB activation in Caco-2 and SW480 human colon cancer cells.* Br J Nutr, 2012. **108**(9): p. 1623-32.

26. Elks, C.M., et al., *A blueberry-enriched diet attenuates nephropathy in a rat model of hypertension via reduction in oxidative stress.* PLoS One, 2011. **6**(9): p. e24028.

27. Murugaiyah, V. and M.P. Mattson, *Neurohormetic phytochemicals: An evolutionary-bioenergetic perspective.* Neurochem Int, 2015. **89**: p. 271-80.

28. Wang, J. and G. Mazza, *Effects of anthocyanins and other phenolic compounds on the production of tumor necrosis factor alpha in LPS/IFN-gamma-activated RAW 264.7 macrophages.* J Agric Food Chem, 2002. **50**(15): p. 4183-9.

29. Shen, M., T.H. Chan, and Q.P. Dou, *Targeting tumor ubiquitin-proteasome pathway with polyphenols for chemosensitization.* Anticancer Agents Med Chem, 2012. **12**(8): p. 891-901.

30. Sun, G.Y., et al., *Quercetin Attenuates Inflammatory Responses in BV-2 Microglial Cells: Role of MAPKs on the Nrf2 Pathway and Induction of Heme Oxygenase-1.* PLoS One, 2015. **10**(10): p. e0141509.

31. Goyarzu, P., et al., *Blueberry supplemented diet: Effects on object recognition memory and nuclear factor-kappa B levels in aged rats.* Nutritional Neuroscience, 2004. **7**(2): p. 75-83.

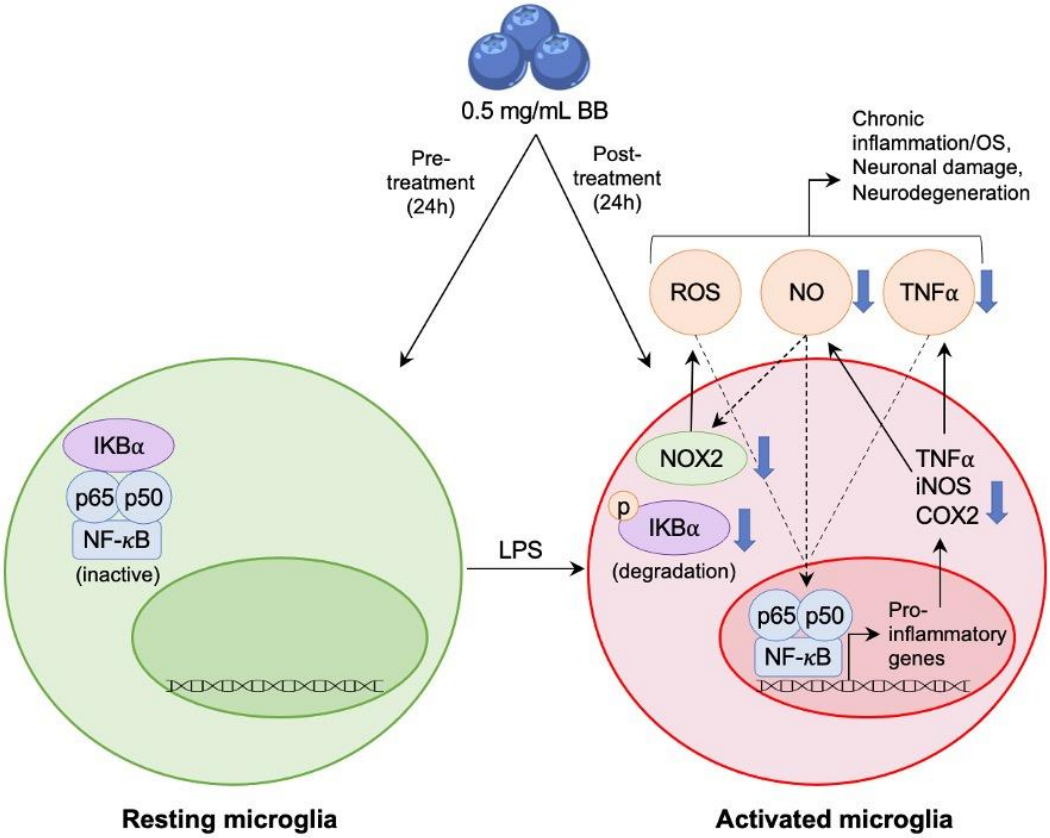

Graphical Abstract.

Cascade of inflammatory and OS-inducing events associated with self-propelling microglial activation by LPS and the effects of blueberry (0.5 mg/mL) administered before and/or after LPS on these processes (blue arrows). BB, blueberry; COX2, cyclooxygenase-2; IκB-α, inhibitor kappa-B-α; iNOS, inducible nitric oxide synthase; LPS, lipopolysaccharide; NF-κB, nuclear factor kappa-B; NO, nitric oxide; NOX2, NADPH oxidase; OS, oxidative stress; ROS, reactive oxygen species; TNFα, tumor necrosis factor-α

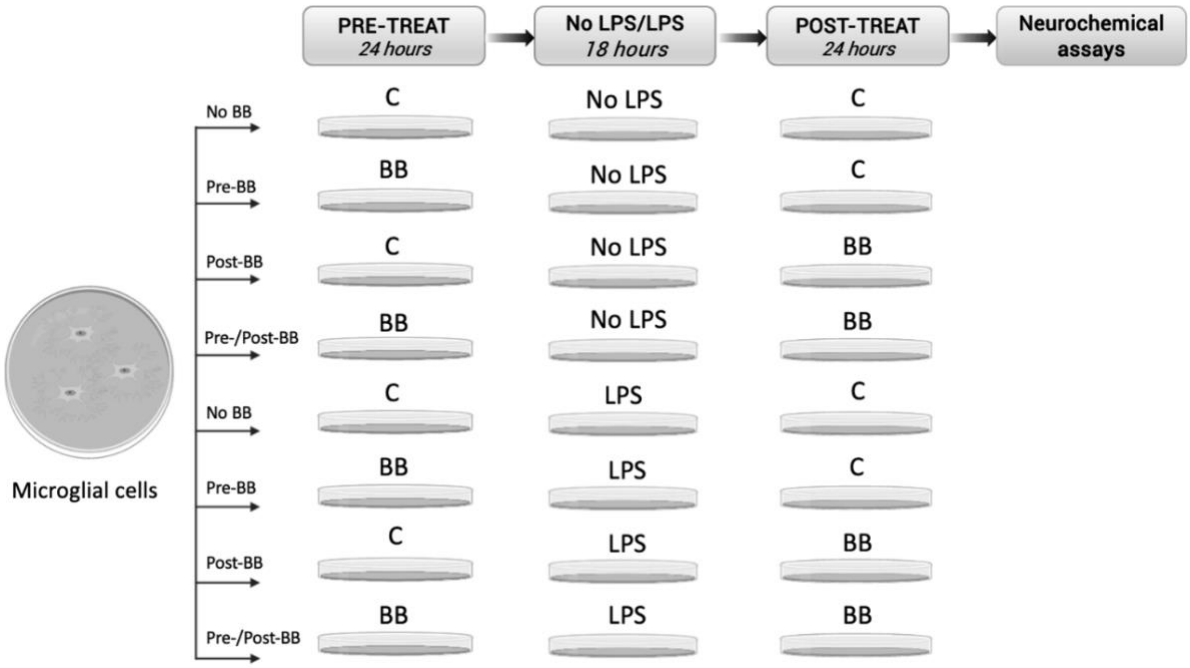

Figure 1. Experimental design.

Rat microglial cells were pre-treated in the absence (control) or presence of BB (0.5 mg/mL) for 24 hours. Pre-treatment media was removed and cells were incubated in the absence (unstressed control) or presence of LPS (200 ng/mL) for 18 hours. Media was removed and cells were post-treated in the absence (control) or presence of BB (0.5 mg/mL) for 24 hours. Outcomes were assessed following the post-treatment period. C, control media; BB, blueberry; LPS, lipopolysaccharide.

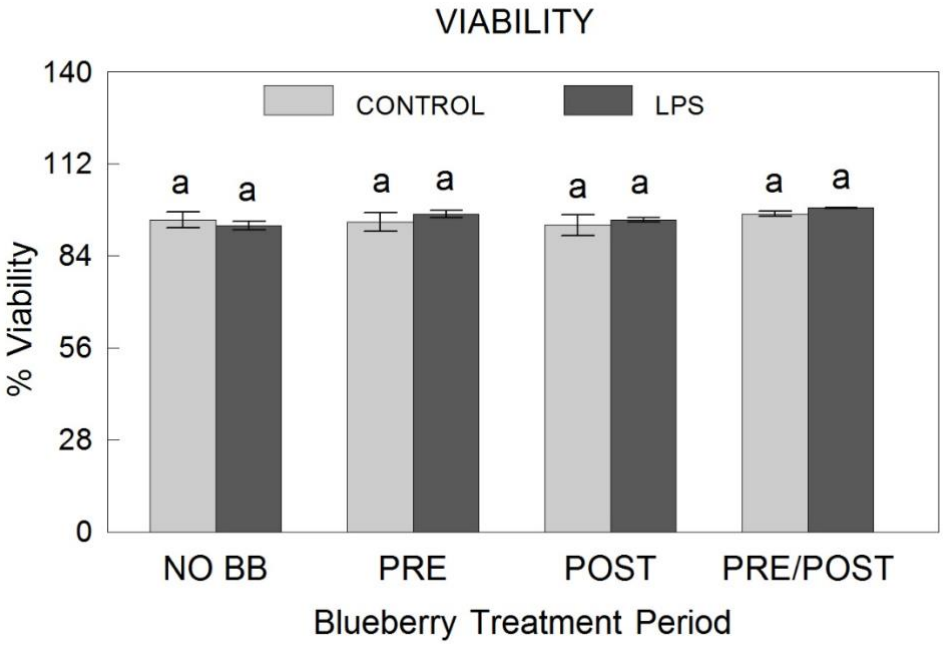

Figure 2. Effect of pre- and/or post-BB on microglia viability.

Microglia were pre-treated in the absence or presence of BB (0.5 mg/mL), then incubated in the absence (unstressed control) or presence of LPS (200 ng/mL), and post-treated with or without BB. Cell viability was assessed as % viability by the Trypan blue method after the post-treatment period for the following groups with or without LPS: NO BB, neither pre- nor post-treatment with BB; PRE: only pre-treatment with BB; POST, only post-treatment with BB; PRE/POST, both pre- and post-treatment with BB. Data are presented as the mean ± SEM of three independent experiments (i.e., flasks). Bars with different letters are significantly different from each other ($P < 0.05$). No difference in cell viability was observed.

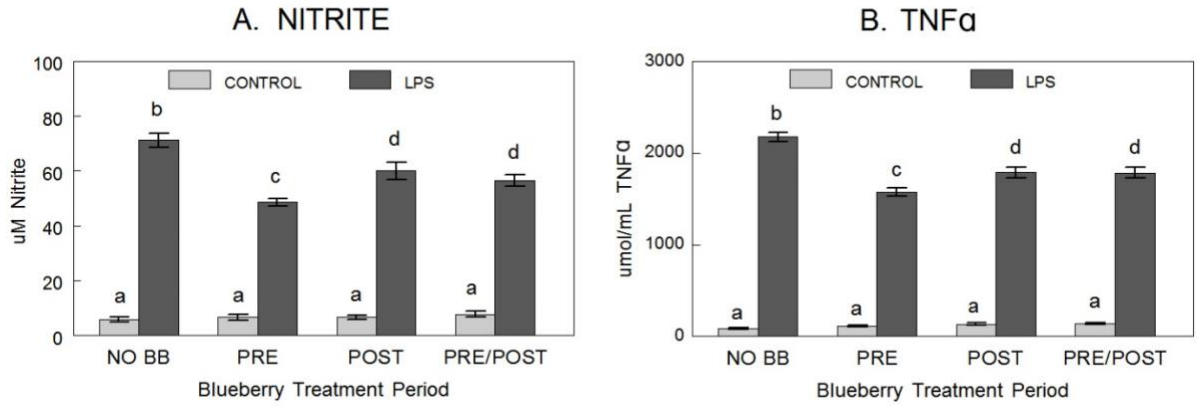

Figure 3. Effect of pre- and/or post-BB on LPS-induced nitrite and TNFα production in microglia.

Microglia were pre-treated in the absence or presence of BB (0.5 mg/mL), then incubated in the absence (unstressed control) or presence of LPS (200 ng/mL), and post-treated with or without BB. The following outcomes were assessed after the post-treatment period: A) nitrite concentrations determined by Griess methods and B) TNFα concentrations determined by ELISA. Data are presented as the mean ± SEM of nine independent experiments (i.e, flasks) assessed in triplicate. Bars with different letters are significantly different from each other ($P < 0.05$). NO BB, neither pre- nor post-treatment with BB; PRE: only pre-treatment with BB; POST, only post-treatment with BB; PRE/POST, both pre- and post-treatment with BB.

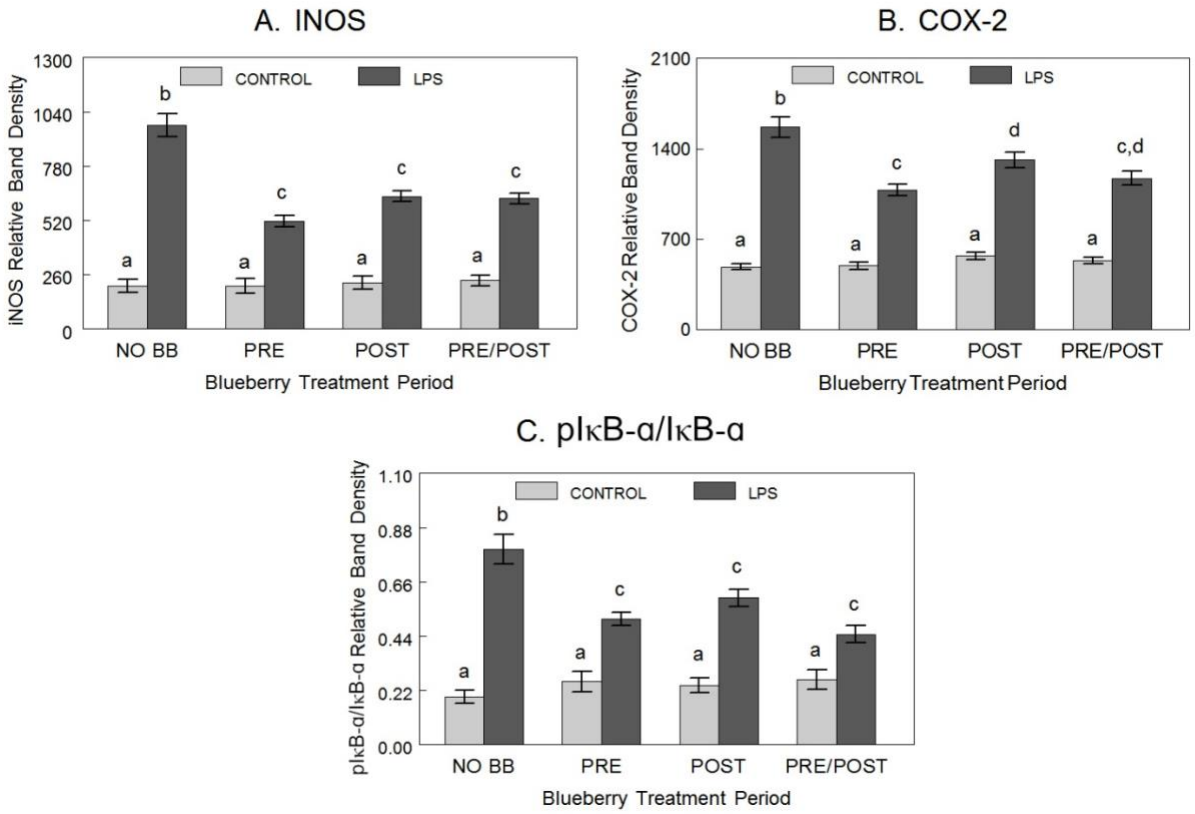

Figure 4. Effect of pre- and/or post-BB on LPS-induced protein expression of iNOS, COX-2, and pIκB-α in microglia.

Microglia were pre-treated in the absence or presence of BB (0.5 mg/mL), then incubated in the absence (unstressed control) or presence of LPS (200 ng/mL), and post-treated with or without BB. The following outcomes were assessed after the post-treatment period using Western blot: A) iNOS protein expression, B) COX-2 protein expression, and C) phosphorylated IκB-α protein expression, expressed as a ratio of total IκB-α. Data are presented as the mean ± SEM of nine independent experiments (i.e, flasks) assessed in triplicate. Bars with different letters are significantly different from each other ($P < 0.05$). NO BB, neither pre- nor post-treatment with BB; PRE: only pre-treatment with BB; POST, only post-treatment with BB; PRE/POST, both pre- and post-treatment with BB.

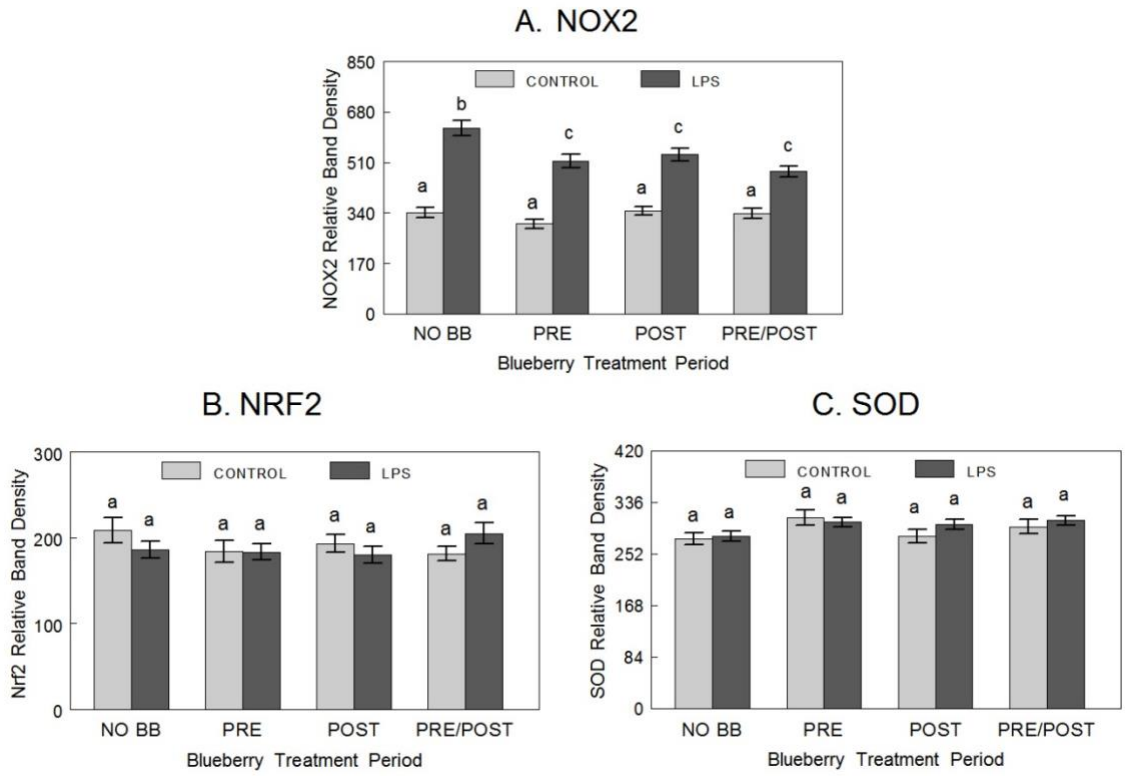

Figure 5. Effect of pre- and/or post-BB on LPS-induced OS and antioxidant defense enzymes.

HAPI cells were pre-treated in the absence or presence of BB (0.5 mg/mL), then incubated in the absence (unstressed control) or presence of LPS (200 ng/mL), and post-treated with or without BB. The following outcomes were assessed after the post-treatment period using Western blot: A) NOX2 protein expression, B) Nrf2 protein expression, and C) SOD protein expression. Data are presented as the mean ± SEM from nine independent experiments (i.e, flasks) assessed in triplicate. Bars with different letters are significantly different from each other ($P < 0.05$). NO BB, neither pre- nor post-treatment with BB; PRE: only pre-treatment with BB; POST, only post-treatment with BB; PRE/POST, both pre- and post-treatment with BB.

3.2 Galactic cosmic ray particle exposure does not increase inflammation or oxidative stress in rat microglial cells *in vitro*

Danielle S. Cahoon[a], Derek R. Fisher[a], Bernard M. Rabin[b], Stefania Lamon-Fava[a], Dayong Wu[a], Tong Zheng[a], and Barbara Shukitt-Hale[a,*]

[a]USDA-ARS, Jean Mayer Human Nutrition Research Center on Aging at Tufts University, Boston, MA, USA

[b]Department of Psychology, UMBC, Baltimore, MD, USA

Correspondence to:

Barbara Shukitt-Hale, Ph.D.

USDA, HNRCA at Tufts University

711 Washington Street

Boston, MA 02111

Tel: 617-556-3118; Fax: 617-556-3299

E-Mail: barbara.shukitthale@usda.gov

Abstract

Astronauts on exploratory missions will be exposed to galactic cosmic rays (GCR), which include helium (^{4}He) and ^{56}Fe particles. Exposure to GCR can induce neuroinflammation and oxidative stress (OS) and may increase risk for neurodegenerative disease. As key regulators of inflammation and OS in the central nervous system (CNS), microglial cells may be involved in GCR-induced deficits, and therefore could be a target for neuroprotection. This study assessed the effects of exposure to ^{4}He and ^{56}Fe particles on inflammation and OS in microglia *in vitro*, with the goal of establishing a model for testing countermeasure efficacy. Rat microglia were exposed to a single dose of 20 cGy (300 MeV/n) ^{4}He or 2 Gy ^{56}Fe (600 MeV/n), while control cells were not exposed to radiation (0 cGy). Immediately following irradiation, fresh media was applied to the cells, and outcomes were assessed 24 hours later. Biomarkers of inflammation (cyclooxygenase-2 [COX-2], nitric oxide synthase [iNOS], phosphorylated IκB-α [pIκB-α], tumor necrosis factor-α [TNFα], and nitrite [NO_2^-]) and OS (NADPH oxidase [NOX2]) were assessed using standard immunochemical techniques. Results showed that radiation did not increase protein expression of COX-2, iNOS, pIκB-α, TNFα, NO_2^- or NOX2 compared to non-irradiated control conditions in microglial cells ($P > 0.05$). These findings suggest that GCR exposures under our experimental conditions may not induce neuroinflammation and OS in isolated microglia. Future work identifying alternative cellular mechanisms is necessary to advance the development of countermeasures against the detrimental CNS effects of GCR particle exposure.

Keywords: neuroinflammation, oxidative stress, microglia, space-radiation

1. Introduction

On exploratory missions, such as to Mars, astronauts will be exposed to galactic cosmic rays (GCR) which are composed of protons, alpha particles, helium (^{4}He), and particles of high energy and charge (HZE particles), including iron (^{56}Fe) and ^{4}He. Although HZE particles are less abundant than protons in the space environment, their high linear energy transfer (LET) makes them major contributors to the total dose and biological effects of exposures *(1)*. GCR particles are densely ionizing in contrast to other forms of ionizing radiation (IoR, e.g., γ-rays and x-rays) *(2)*, and exposure can induce neuroinflammation, oxidative stress (OS) *(3)*, and cognitive deficits *(2-4)* at low doses. Furthermore, exposure to GCR particles may produce 'accelerated aging' in the central nervous system (CNS) *(5)* and increase risk for neurodegenerative disease *(2)*. However, the mechanisms underlying the progression of GCR-induced biochemical changes in the brain and cognitive deficits are unclear. Consequently, research on therapeutic strategies to attenuate the detrimental CNS effects that progress after radiation exposure is limited. Identifying cellular mechanisms is necessary to advance the development of countermeasures against the detrimental CNS effects of GCR particle exposure.

Microglial cells, the resident macrophages of the central nervous system (CNS), are key regulators of neuroinflammation and OS in the CNS *(6)*. In response to a range of pathogenic stressors, microglia can change from a quiescent phenotype to an activated phenotype and produce cytotoxic mediators including pro-inflammatory cytokines (e.g., tumor necrosis factor-α [TNFα]), reactive oxygen species (ROS), and nitric oxide (NO) *(7, 8)*. The excess production of these mediators can produce collateral damage to tissues beyond the site of the initial insult and promote further microglial activation *(8, 9)*. Therefore, a vicious cycle of microglial activation and neurotoxicity can result, leading to chronic inflammation, OS, and neurodegeneration, long after the initial stressor dissipates.

Given that neuroinflammation and OS increase following exposure to the types of radiation encountered in space, microglial cells are a putative target in mediating GCR-induced biochemical changes in the brain and cognitive deficits. However, research on microglial responses to GCR particles *in vitro* and *in vivo* is equivocal. While some animal studies using low to moderate dose (5 cGy-3 Gy) exposures to GCR particles (protons, ^{4}He, ^{56}Fe, ^{16}O, ^{48}Ti, and combined particles) have demonstrated microglial activation

following irradiation *(5, 10-13)*, other studies found no such effects on microglial activation *in vivo (14-19)*. Additionally, to the best of our knowledge, microglial responses to GCR particles have not been assessed *in vitro.* Instead, *in vitro* research assessing the effects of radiation on microglia has used γ-rays and x-rays, which have different radiophysics and biological effects than heavier particles in GCRs due to different patterns of energy deposition *(20-22)*. Investigating microglial responses to GCR particles is needed to better understand and target radiation-induced neuroinflammation and OS following GCR exposures such as on exploratory missions beyond Earth's magentic field. As such, this study was designed as a proof-of-concept, preliminary study to establish an *in vitro* model for testing anti-inflammatory and antioxidant countermeasures against GCR-induced neuroinflammation and OS in microglia. In this study, we assessed the effects of two GCR particles, ^{4}He and ^{56}Fe, on inflammation and OS in a microglial cell model 24 hours after exposure.

2. Methods

2.1 Cell Culture and Irradiation Procedure

Highly aggressively proliferating immortalized (HAPI) rat microglial cells (generously provided by Dr Grace Sun, University of Missouri, Columbia, MO) were maintained in Dulbecco's modified Eagle's medium (DMEM, Invitrogen, Grand Island, NY) supplemented with 10% fetal bovine serum (FBS), 100 U/mL penicillin, and 100 µg/mL streptomycin at 37 °C in a humidified incubator under 5% CO_2. Cells were transported by vehicle in T75 flasks from the Human Nutrition Research Center on Aging (HNRCA) to the NASA Space Radiation Laboratory (NSRL) at Brookhaven National Laboratory (BNL). Cells were then split into T25 flasks at a seeding density of 2.5 x 10^6 cells/flask in DMEM without phenol red for 24 hours prior to irradiation. During two separate runs, cells were exposed to a single dose of either 20 cGy (300 MeV/n) ^{4}He or 2 Gy (600 MeV/n) ^{56}Fe. Irradiations were performed at room temperature using a beam of ^{4}He or ^{56}Fe ions perpendicular to the plane of cells. Because the beam is horizontal, flasks were upended to a vertical position during irradiation. Dosimetry was provided by the NSRL staff using parallel plate ionizing chambers *(23)*. Doses were selected within the ranges of *in vivo* studies demonstrating increased microglial activation (up to 30 cGy ^{4}He,

up to 3 cGy ^{56}Fe), while minimizing the time required for flasks to be upended at room-temperature for irradiations.

Control cells for each run were not exposed to radiation (n=6 flasks/group) but were treated similarly to those cells which were radiated (e.g., placed in a vertical position at room temperature), except they were not placed in the beam. Immediately following irradiation procedures, media was removed and cells were incubated in fresh media for 24 hours. A 24 hour post-irradiation interval was selected based on previous studies in microglia demonstrating increased inflammation (e.g., TNFα) 24 hours after γ-ray or x-ray exposures *(24-27)*. After the 24 hour post-irradiation period, cell lysates were prepared as described below, and transported back to the HNRCA by vehicle on ice. Samples were stored at -80°C before processing for analysis of inflammation and OS biomarkers.

2.2 Cell Viability

Cell viability was assessed using the Trypan blue exclusion method *(28)*. In brief, microglial cells were seeded onto T25 flasks and experimental procedures were performed as above. Following the post-irradiation period, cells were incubated with 500 µL trypsin/well for 5 minutes for detachment, and 50 µL of cell suspension was mixed with 50 µL of Trypan blue. Only dead cells with damaged membranes are permeable to Trypan blue and can be identified by their blue stain. The cell suspension was added to a hemocytometer and the number of blue-stained and non-stained cells were counted under a light microscope to calculate percentage of viable cells (non-stained/total cells X 100).

2.3 Western Blots

Cells were washed in ice-cold phosphate-buffered saline (PBS), resuspended and lysed by scraping in CelLytic-M Cell Lysis Reagent (Sigma-Aldrich, St Louis, MO) containing phenylmethylsulfonylfluoride (PMSF, 10 ug/mL), and centrifuged at 14,000 rpm for 10 min at 4 °C. The resultant supernatant lysate was used for blotting after total protein was quantified with the DC (detergent compatible) protein assay (BioRad, Hercules, CA). Western blots were performed as described previously *(29)*, except that 10% polyacrylamide gels were used. Primary antibodies were used at 1:1000 dilutions for inflammatory markers cyclooxygenase-2 (COX-2, Santa Cruz, Dallas, TX), phospho- and

total IκB-α (pIκB-α, IκB-α Santa Cruz, Dallas, TX), and inducible nitric oxide synthase (iNOS, Millipore, Billerica, MA), and oxidative stress marker NADPH oxidase (NOX2, Santa Cruz, Dallas, TX), for incubation overnight at 4°C. Glyceraldehyde 3-phosphate dehydrogenase (GAPDH, Santa Cruz, Dallas, TX) was used as a protein loading control marker. The signal was detected using an electrochemiluminescence (ECL) detection kit (BioRad, Hercules, CA) and the optical density of antibody-specific bands was analyzed by the VisionWorks LS image acquisition and analysis software (UVP, Upland, CA). Values were normalized to GAPDH protein levels.

2.4 TNFα Enzyme-linked Immunosorbent Assay (ELISA)

Secretion of inflammatory cytokine TNFα was quantified using ELISA according to manufacturer's instructions (Invitrogen, Carlsbad, CA). In brief, 50 µl of cell-conditioned supernatant or provided protein standards was added in duplicate to a 96-well plate and incubated for 2 hours. Following washing, peroxidase-conjugated detection antibody was added to each well and incubated for 1 hour. Wells were washed and substrate solution was added to each well for 15 min, followed by stop solution. Absorbance was read at 450 nm and the TNFα concentration in each sample was calculated from the linear equation derived from the standard curve of known concentrations of the cytokine. Values were normalized by total protein levels in cell lysates quantified with the DC protein assay (BioRad, Hercules, CA).

2.5 Nitrite Quantification

To assess the production of free radical nitric oxide (NO) from HAPI cells, the extracellular release of nitrite (NO_2^-), a stable and nonvolatile breakdown product of NO, was measured in cell-conditioned supernatant by Greiss reagent kit (Invitrogen, Carlsbad, CA) according to manufacturer's instructions. In brief, 100 µl of supernatant from each flask was added in duplicate to a 96-well plate. Then, 25 µl of Griess reagent was added to each well and incubated at room temperature for 15 min. Absorbance was read at 548 nm and the concentration of NO_2^- in each sample was calculated with the linear equation derived from the standard curve generated by known concentrations of NO_2^-. Values were normalized

by total protein levels in cell lysates quantified with the DC protein assay (BioRad, Hercules, CA).

2.6 Statistical Analysis

Statistical analyses were conducted in R (*v*3.8) using RStudio (*v*1.0.153) and results were considered statistically significant if the observed significance level was $P < 0.05$. One-way analysis of variance (ANOVA) was used to determine differences between irradiated and non-irradiated groups for each particle (^{4}He or ^{56}Fe) separately. Data are expressed as mean ± standard error of the mean (SEM).

3. Results

3.1 Viability

Cell viability was on average 94.65 ± 0.93%, and exposure to ^{4}He or ^{56}Fe did not produce changes in cell viability (data not shown).

3.2 Inflammation

To assess the effects of ^{4}He and ^{56}Fe on inflammation, we quantified the protein expression of COX-2 and iNOS, the intracellular enzymes responsible for producing pro-inflammatory prostaglandins *(30)* and nitric oxide (NO) *(7)*, respectively. Additionally, we quantified protein expression of pIκB-α, an indicator of increased activation of NF-κB, a transcription factor responsible for inducing the expression of inflammatory genes such as COX-2 and iNOS *(30)*. As shown in Figure 1, compared to non-irradiated cells, exposure to 20 cGy ^{4}He did not have significant effects on COX-2 ($F_{1,34} = 14$, $P = 0.71$), iNOS ($F_{1,34} = 0.00$, $P = 0.98$), or pIκB-α/IκB-α ($F_{1,34} = 0.84$, $P = 0.84$). Similarly, 2 Gy ^{56}Fe did not have significant effects on COX-2 ($F_{1,34} = 0.09$, $P = 0.77$), iNOS ($F_{1,34} = 0.10$, $P = 0.75$), or pIκB-α/IκB-α ($F_{1,34} = 0.33$, $P = 0.57$).

For the experiment using ^{56}Fe, we assessed extracellular release of NO_2^-, a breakdown product of free radical NO and TNFα, a pro-inflammatory cytokine *(9)*, both of which are hallmarks of microglial activation *(8, 31)*. As shown in Figure 2, compared to non-irradiated cells, exposure to 2 Gy ^{56}Fe did not have significant effects on NO_2^- ($F_{1,34} = 0.18$, $P = 0.68$), or TNFα ($F_{1,34} = 0.07$, $P = 0.79$).

3.3 Oxidative Stress

To assess the effects of ^{4}He and ^{56}Fe on oxidative stress, we quantified the protein expression of NOX2, a ROS generating enzyme in microglia *(6, 7)*. Relative to non-irradiated controls, no significant changes in NOX2 were observed following exposure to 20 cGy ^{4}He ($F_{1,34} = 0.005$, $P = 0.94$) or 2 cGy ^{56}Fe ($F_{1,34} = 0.22$, $P = 0.64$) (Figure 3).

4. Discussion

In this *in vitro* study, neither exposure to ^{4}He (20 cGy) nor ^{56}Fe (2 Gy) significantly altered the protein expression of inflammation (COX-2, iNOS, pIκB-α, TNFα, NO_2^-) or OS (NOX2) biomarkers in HAPI rat microglia compared to no irradiation. To our knowledge, this study is the first to assess the effects of exposure to GCR particles on inflammation and OS in microglia *in vitro*. Despite null findings, results contribute to a body of research examining the effects of space-like radiation on the CNS, and highlight the need to evaluate alternative mechanisms involved in the neuroinflammation and OS associated with particles in GCRs.

Previous work in rodents has shown that particles in GCRs, including ^{4}He and ^{56}Fe, can induce neuroinflammation, OS, and behavioral deficits *(2-4)*. However, the cellular mediators responsible for these changes have not been established. As key regulators of neuroinflammation and OS in the CNS *(6)*, we hypothesized that microglia play a pivotal role in the biochemical changes in the brain and cognitive deficits that result from radiation exposure. Several *in vivo* studies with rodents have demonstrated increased microglial activation indicated by expression of ionized calcium-binding adaptor molecule 1 (Iba-1) and/or CD68/ED-1 in brain tissue at acute and long-term durations following exposures to GCR particles *(5, 10-13)*. Additionally, depletion of microglia has been shown to limit irradiation-induced neuronal and cognitive deficits *(32)*. However, other studies did not find effects of GCR particles at a range of post-exposure durations on microglial activation as measured by Iba and/or CD68/ED-1, despite increases in inflammation, OS, and/or other neuronal changes *(14-17)*.

Although *in vivo* studies provide important insight on integrated systemic responses, we assessed microglial responses to GCR particle radiation *in vitro* to isolate

the putative role of this specific cell type in neuroinflammation and OS. Previous work on microglial responses to ionizing radiation *in vitro* has been limited to high dose x-ray or γ-ray exposures. As with *in vivo* studies, findings on the effects of x-ray and γ-ray exposures on microglia activation, inflammation, and OS are inconsistent. For example, 10 Gy of ^{137}Cs γ-ray has been shown to increase COX-2 protein expression and TNFα mRNA up to 24 hours post-radiation, with or without changes in pIκB-α or NF-κB activity *(26, 33, 34)*. Another set of studies using ^{137}Cs-137 γ-rays found increased COX-2 mRNA levels 24 hours after higher doses (25 and 35 Gy) *(35)*, but not with lower doses of 5, 15, or 16 Gy *(35, 36)*. Irradiation with x-rays increased TNFα protein 24 hours after 4 to 10 Gy, but not 2 Gy *(37)*. Another study found that 24 hours after x-ray irradiation increased mRNA of COX-2 and TNFα at 2, 4, 6, 8, and 10 Gy, but did not produce any changes in iNOS or nitrite *(25)*

These mixed findings from *in vitro* studies using γ-ray and x-ray radiation in microglia highlight the gap in knowledge of microglial responses to radiation exposure. However, data from γ-ray and x-ray irradiation should not be extrapolated to predict responses to heavier particle radiation due to differences in energy distribution; γ-ray and x-rays are low linear energy transfer (LET) particles and deposit energy uniformly in cells and tissues, whereas higher LET particles, such as helium and HZE particles deposit energy along linear tracks in addition to scattering energy as delta rays outside the track *(38)*. Therefore, additional *in vitro* studies using high-LET particles in GCRs are necessary to understand the potential role of microglia in mediating responses to space-radiation.

Our findings suggest that microglia in isolation may be resistant to the effects of ^{4}He and ^{56}Fe exposures. However, because this was a proof-of-concept, preliminary study with the goal of establishing a model for countermeasure testing, results should be interpreted with caution. In this study, only protein expression of inflammation and OS biomarkers was assessed. Changes may occur in mRNA expression, post-translational regulation, and functionality of these indicators, and also at shorter or longer post-irradiation durations than at 24 hours in this study. Furthermore, we assessed the effects of a single dose each for two particles in GCRs; higher doses may be necessary to cause microglial activation *in vitro*. Future studies should assess the effects of additional GCR particles, doses, combined particles, and post-irradiation time-points on inflammation and OS in microglia.

Additionally, alternative indicators of microglial activation, such as morphology changes, can provide further insight on microglial responses to radiation.

Acknowledging these limitations, and based on our consistent findings in an *in vitro* model, it is possible that microglia are not primarily responsible for irradiation-induced increases in neuroinflammation and OS with GCR exposures. Instead, these effects could be mediated by other cells in the CNS, such as astrocytes, or could be due to peripheral mechanisms such as activation of the vagus nerve or a compromised blood-brain-barrier *(38)*. For example, studies have shown that exposure of just the body, but not the head, to GCR particles can produce neuroinflammation and OS in the brain, suggesting that peripheral mechanism may mediate CNS effects *(39, 40)*. Additionally, the response of microglia to GCR exposure may depend on the brain's environment. In other words, microglia activation in response to radiation may require signals produced by other cells such as ROS, apoptosis signals, and damaged dendrites *(38)*. Therefore, future work should assess the effects of GCR particles on inflammation and OS in co-cultures of brain cells (e.g., neurons, astrocytes, and microglia).

Financial Support

This work was supported by USDA intramural funding (USDA ARS Project Number 8050-51000-102-000-D) and NASA Grants NNJ16HP45I and NNX16AE06G.

Disclosure of Interest

The authors report no conflict of interest.

Disclaimer

The mention of trade names or commercial products in this publication is solely for the purpose of providing specific information and does not imply recommendation or endorsement by the USDA. USDA is an equal opportunity provider and employer. Source of Support: USDA ARS Project Number 8050-51000-102-000-D.

Data Availability Statement

All data are available upon request.

Acknowledgements

The authors wish to thank Peter Guida, Adam Rusek, Michael Sivertz, Paula Bennett, and their staff for guidance and assistance with irradiations at the NSRL.

References

1. Durante M, Cucinotta FA. Heavy ion carcinogenesis and human space exploration. Nat Rev Cancer. 2008;8(6):465-72.

2. Rabin BM, Shukitt-Hale B. A voyage to Mars: Space radiation, aging, and nutrition. Nutrition and Aging. 2014;2(4):233-41.

3. Joseph JA, Shukitt-Hale B, McEwen J, Rabin BM. CNS-induced deficits of heavy particle irradiation in space: The aging connection. Advances in Space Research. 2000;25(10):2057-64.

4. Poulose SM, Bielinski DF, Carrihill-Knoll KL, Rabin BM, Shukitt-Hale B. Protective effects of blueberry- and strawberry diets on neuronal stress following exposure to 56Fe particles. Brain Res. 2014;1593:9-18.

5. Parihar VK, Maroso M, Syage A, Allen BD, Angulo MC, Soltesz I, et al. Persistent nature of alterations in cognition and neuronal circuit excitability after exposure to simulated cosmic radiation in mice. Exp Neurol. 2018;305(2018):44-55.

6. Dringen R. Oxidative and antioxidative potential of brain microglial cells. Antioxid Redox Signal. 2005;7(9-10):1223-33.

7. Lijia Z, Zhao S, Wang X, Wu C, Yang J. A self-propelling cycle mediated by reactive oxide species and nitric oxide exists in LPS-activated microglia. Neurochem Int. 2012;61(7):1220-30.

8. Lull ME, Block ML. Microglial activation and chronic neurodegeneration. Neurotherapeutics. 2010;7(4):354-65.

9. Qin L, Wu X, Block ML, Liu Y, Breese GR, Hong JS, et al. Systemic LPS causes chronic neuroinflammation and progressive neurodegeneration. Glia. 2007;55(5):453-62.

10. Parihar VK, Allen BD, Caressi C, Kwok S, Chu E, Tran KK, et al. Cosmic radiation exposure and persistent cognitive dysfunction. Scientific Reports. 2016;6(June):1-14.

11. Krukowski K, Grue K, Frias ES, Pietrykowski J, Jones T, Nelson G, et al. Female mice are protected from space radiation-induced maladaptive responses. Brain, Behavior, and Immunity. 2018;74(August):106-20.

12. Allen BD, Syage AR, Maroso M, Baddour AAD, Luong V, Minasyan H, et al. Mitigation of helium irradiation-induced brain injury by microglia depletion. Journal of Neuroinflammation. 2020;17(1):159-.

13. Rola R, Sarkissian V, Obenaus A, Nelson GA, Otsuka S, Limoli CL, et al. High-LET radiation induces inflammation and persistent changes in markers of hippocampal neurogenesis. Radiat Res. 2005;164(4 Pt 2):556-60.

14. Cherry JD, Liu B, Frost JL, Lemere CA, Williams JP, Olschowka JA, et al. Galactic cosmic radiation leads to cognitive impairment and increased abeta plaque accumulation in a mouse model of Alzheimer's disease. PLoS One. 2012;7(12):e53275.

15. Liu B, Hinshaw RG, Le KX, Park MA, Wang S, Belanger AP, et al. Space-like 56Fe irradiation manifests mild, early sex-specific behavioral and neuropathological changes in wildtype and Alzheimer's-like transgenic mice. Scientific Reports. 2019;9(1):1-17.

16. Raber J, Yamazaki J, Torres ERS, Kirchoff N, Stagaman K, Sharpton T, et al. Combined Effects of Three High-Energy Charged Particle Beams Important for Space Flight on Brain, Behavioral and Cognitive Endpoints in B6D2F1 Female and Male Mice. Front Physiol. 2019;10:179.

17. Raber J, Fuentes Anaya A, Torres ERS, Lee J, Boutros S, Grygoryev D, et al. Effects of Six Sequential Charged Particle Beams on Behavioral and Cognitive Performance in B6D2F1 Female and Male Mice. Front Physiol. 2020;11:959.

18. Sweet TB, Panda N, Hein AM, Das SL, Hurley SD, Olschowka JA, et al. Central Nervous System Effects of Whole-Body Proton Irradiation. Radiation Research. 2014;182(1):18-34.

19. Rola R, Fishman K, Baure J, Rosi S, Lamborn KR, Obenaus A, et al. Hippocampal Neurogenesis and Neuroinflammation after Cranial Irradiation with 56 Fe Particles. Radiation Research. 2008;169(6):626-32.

20. Chew MT, Nisbet A, Jones B, Suzuki M, Matsufuji N, Murakami T, et al. Ion beams for space radiation radiobiological effect studies. Radiation Physics and Chemistry. 2019:108373-.

21. Cucinotta FA, Cacao E. Risks of cognitive detriments after low dose heavy ion and proton exposures. International Journal of Radiation Biology. 2019;95(7):985-98.

22. Betlazar C, Middleton RJ, Banati RB, Liu GJ. The impact of high and low dose ionising radiation on the central nervous system. Redox Biology. 2016;9:144-56.

23. La Tessa C, Sivertz M, Chiang IH, Lowenstein D, Rusek A. Overview of the NASA space radiation laboratory. Life Sciences in Space Research. 2016;11:18-23.

24. Dong X, Luo M, Huang G, Zhang J, Tong F, Cheng Y, et al. Relationship between irradiation-induced neuro-inflammatory environments and impaired cognitive function in the developing brain of mice. Int J Radiat Biol. 2015;91(3):224-39.

25. Hwang SY, Jung JS, Kim TH, Lim SJ, Oh ES, Kim JY, et al. Ionizing radiation induces astrocyte gliosis through microglia activation. Neurobiology of Disease. 2006;21(3):457-67.

26. Ramanan S, Kooshki M, Zhao W, Hsu FC, Robbins ME. PPARalpha ligands inhibit radiation-induced microglial inflammatory responses by negatively regulating NF-kappaB and AP-1 pathways. Free Radic Biol Med. 2008;45(12):1695-704.

27. Kyrkanides S, Olschowka JA, Williams JP, Hansen JT, O'Banion MK. TNFα and IL-1β mediate intercellular adhesion molecule-1 induction via microglia-astrocyte interaction in CNS radiation injury. Journal of Neuroimmunology. 1999;95(1-2):95-106.

28. Strober W. Trypan Blue Exclusion Test of Cell Viability. Curr Protoc Immunol. 2015;111(1):A3 B 1-A3 B

29. Poulose SM, Fisher DR, Larson J, Bielinski DF, Rimando AM, Carey AN, et al. Anthocyanin-rich acai (Euterpe oleracea Mart.) fruit pulp fractions attenuate inflammatory stress signaling in mouse brain BV-2 microglial cells. J Agric Food Chem. 2012;60(4):1084-93.

30. Cheng A, Han C, Fang X, Sun J, Chen X, Wan F. Extractable and non-extractable polyphenols from blueberries modulate LPS-induced expression of iNOS and COX-2 in RAW264.7 macrophages via the NF-kappaB signalling pathway. J Sci Food Agric. 2016;96(10):3393-400.

31. Bozic I, Savic D, Laketa D, Bjelobaba I, Milenkovic I, Pekovic S, et al. Benfotiamine attenuates inflammatory response in LPS stimulated BV-2 microglia. PLoS One. 2015;10(2):e0118372.

32. Acharya MM, Green KN, Allen BD, Najafi AR, Syage A, Minasyan H, et al. Elimination of microglia improves cognitive function following cranial irradiation. Sci Rep. 2016;6:31545.

33. Deng Z, Sui G, Rosa PM, Zhao W. Radiation-induced c-Jun activation depends on MEK1-ERK1/2 signaling pathway in microglial cells. PLoS One. 2012;7(5):e36739.

34. Schnegg CI, Kooshki M, Hsu FC, Sui G, Robbins ME. PPARdelta prevents radiation-induced proinflammatory responses in microglia via transrepression of NF-kappaB and inhibition of the PKCalpha/MEK1/2/ERK1/2/AP-1 pathway. Free Radic Biol Med. 2012;52(9):1734-43.

35. Kyrkanides S, Moore AH, Olschowka JA, Daeschner JC, Williams JP, Hansen JT, et al. Cyclooxygenase-2 modulates brain inflammation-related gene expression in central nervous system radiation injury. Brain Res Mol Brain Res. 2002;104(2):159-69.

36. Xue J, Dong JH, Huang GD, Qu XF, Wu G, Dong XR. NF-κB signaling modulates radiation-induced microglial activation. Oncology Reports. 2014;31(6):2555-60.

37. Liu JL, Tian DS, Li ZW, Qu WS, Zhan Y, Xie MJ, et al. Tamoxifen alleviates irradiation-induced brain injury by attenuating microglial inflammatory response in vitro and in vivo. Brain Research. 2010;1316:101-11.

38. Cekanaviciute E, Rosi S, Costes SV. Central Nervous System Responses to Simulated Galactic Cosmic Rays. Int J Mol Sci. 2018;19(11).

39. Cahoon DS, Shukitt-Hale B, Bielinski DF, Hawkins EM, Cacioppo AM, Rabin BM. Effects of partial- or whole-body exposures to 56Fe particles on brain function and cognitive performance in rats. Life Sciences in Space Research. 2020;27(July):56-63.

40. Cahoon DS, Rabin BM, Shukitt-Hale B. Effects of HZE particles exposure location and energy on brain inflammation and oxidative stress in rats. Radiation Research, Submitted February 2022.

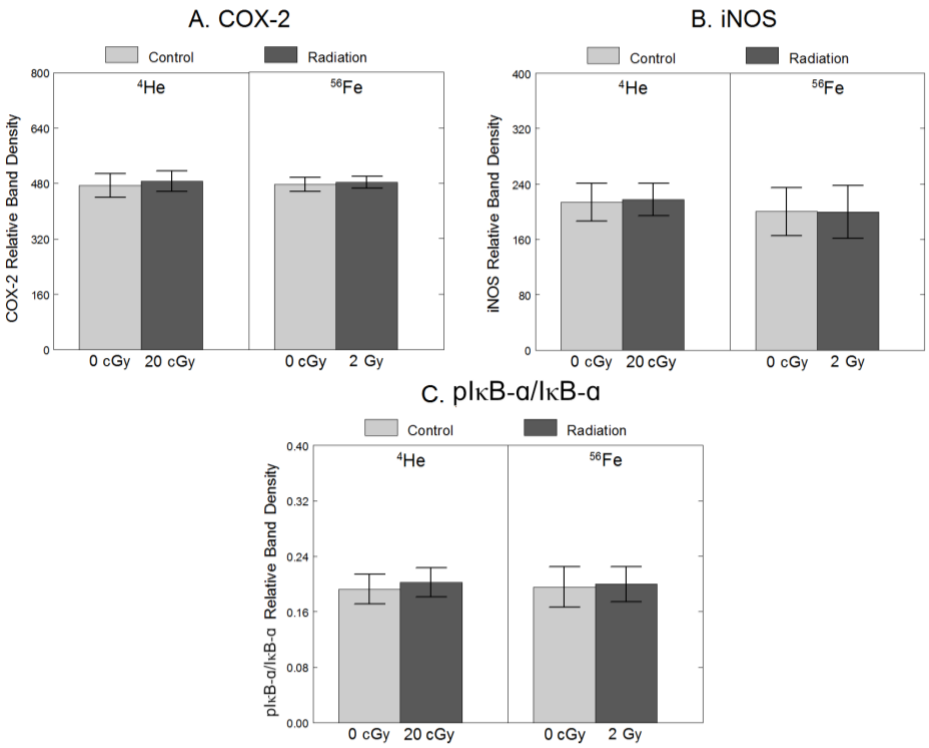

Figure 1. No significant effect of 20 cGy ^{4}He or 2 Gy ^{56}Fe on protein expression of pro-inflammatory enzymes in microglia.

HAPI rat microglia were exposed to no radiation (0 cGy), 20 cGy ^{4}He, or 2 Gy ^{56}Fe. The following outcomes were assessed 24 hours after irradiations using Western blot: A) COX-2 protein expression, B) iNOS protein expression, and C) phosphorylated IκB-α protein expression, expressed as a ratio of total IκB-α. Data are presented as the mean ± SEM of six independent experiments (i.e, flasks) assessed in triplicate.

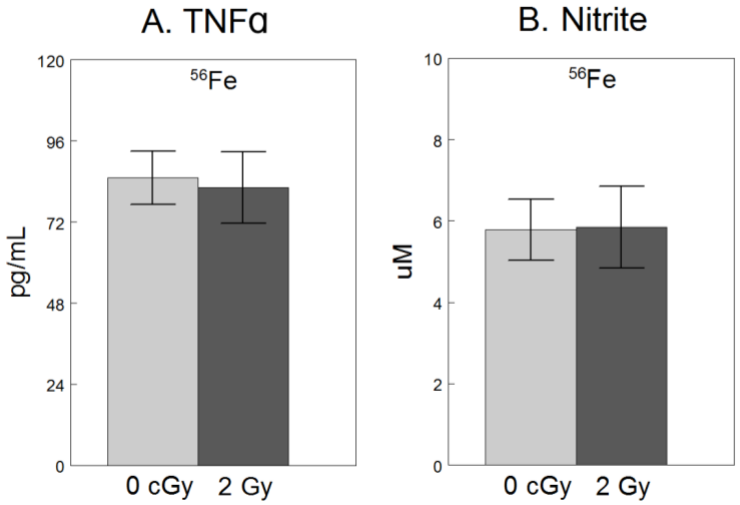

Figure 2. No significant effect of 2 Gy ^{56}Fe on extracellular release of soluble pro-inflammatory factors in microglia.

HAPI rat microglia were exposed to no radiation (0 cGy) or 2 Gy ^{56}Fe. The following outcomes were assessed 24 hours after irradiations in cell-conditioned supernatant A) TNFα concentrations determined by ELISA and B) nitrite concentrations determined by Griess methods. Data are presented as the mean ± SEM of six independent experiments (i.e, flasks) assessed in triplicate.

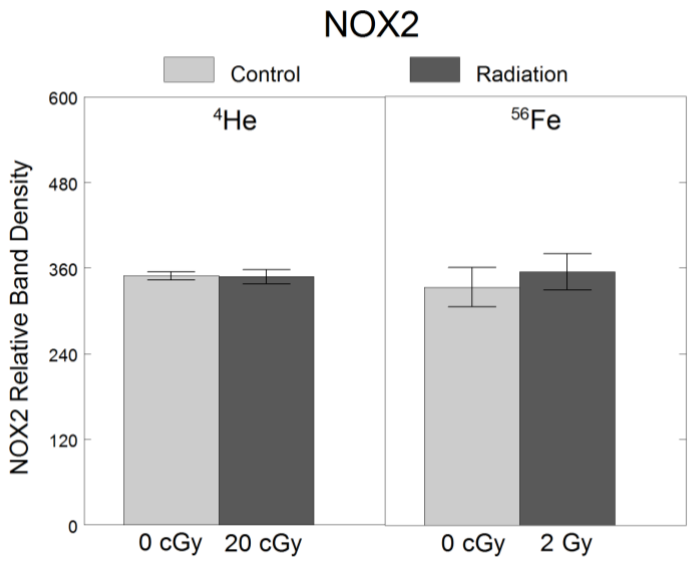

Figure 3. No significant effect of 20 cGy ^{4}He or 2 Gy ^{56}Fe on protein expression of oxidative stress-mediating enzyme NOX2 in microglia.

HAPI rat microglia were exposed to no radiation (0 cGy), 20 cGy ^{4}He, or 2 Gy ^{56}Fe. NOX2 protein expression was assessed 24 hours following irradiation using Western blot. Data are presented as the mean ± SEM of six independent experiments (i.e, flasks) assessed in triplicate.

3.3 Dietary blueberry before and/or after exposure to HZE particle radiation attenuates neuroinflammation, oxidative stress, and cognitive deficits in rats

Danielle S. Cahoon[a], Derek R. Fisher[a], Stefania Lamon-Fava[a], Tong Zheng[a], Dayong Wu[a], Bernard M. Rabin[b], and Barbara Shukitt-Hale[a,*]

[a] USDA-ARS, Jean Mayer Human Nutrition Research Center on Aging at Tufts University, Boston, MA, USA

[b] Department of Psychology, University of Maryland Baltimore County, Baltimore, MD, USA

Correspondence to:

Barbara Shukitt-Hale, Ph.D.

USDA, HNRCA at Tufts University

711 Washington Street

Boston, MA 02111

Tel: 617-556-3118; Fax: 617-556-3299

E-Mail: barbara.shukitthale@usda.gov

Abstract

On exploratory missions, astronauts will be exposed to particles of high energy and charge (HZE particles). HZE particle exposure produces neuroinflammation, oxidative stress (OS), and cognitive deficits, and is associated with increased risk for neurodegenerative disease. The molecular mechanisms underlying post-irradiation central nervous system (CNS) deficits are not fully understood, limiting the development of therapeutic strategies. Dietary interventions using foods with anti-inflammatory and antioxidant polyphenols, such as blueberries (BB), can attenuate neuroinflammation, OS, and cognitive deficits when administered to rodents before (i.e., pre-treatments) or continuously before and after HZE particle exposure. However, the effects and mechanistic targets of dietary interventions administered after HZE particle exposure (i.e., post-treatments) on these outcomes have not been established. The present experiment aimed to assess the differential efficacy and mechanistic targets of a BB-supplemented diet administered before and/or after HZE particle exposure on neuroinflammation, OS, and cognitive deficits.

Male Sprague-Dawley rats (n=120, 2 mo old) were randomized to consume a 2% BB diet or control diet for 45 days pre-irradiation. Animals were whole-body irradiated with 150 cGy ^{56}Fe or not irradiated (0 cGy). They were then fed either a 2% BB or control diet for 45 days post-irradiation to yield the following groups: 1) no BB (i.e., control diet only), 2) only pre-BB, 3) only post-BB, or 4) both pre- and post-BB. At the end of the post-irradiation period, the novel object recognition (NOR) test and radial arm water maze (RAWM) were performed to assess memory-related function. Following euthanasia, protein and/or mRNA levels of biomarkers for neuroinflammation (e.g., inducible nitric oxide synthase [iNOS], cyclooxygenase-2 [COX-2], phosphorylated IκB-α [pIκB-α], tumor necrosis factor [TNFα]), OS (e.g., NADPH oxidase [NOX2]), and glial cell activation (glial fibrillary acidic protein [GFAP] and CD68) were assessed in the frontal cortex and hippocampus of rat brains.

Irradiation with 150 cGy ^{56}Fe produced recognition memory deficits on the NOR task and increased the mRNA and/or protein expression of neuroinflammatory factors (iNOS, COX-2, TNFα, pIκB-α), one mediator of oxidative stress (NOX2), and glial cell activation indicators CD68 (microglia) and GFAP (astrocytes) in the frontal cortex and

hippocampus of rats. ^{56}Fe -induced increases in neuroinflammation, OS, and glial activation were positively correlated with each other and negatively correlated with recognition memory function. All BB treatments (pre-, post-, pre-/post-irradiation) were similarly effective at reducing ^{56}Fe -induced neuroinflammation, OS, glial activation, and memory deficits.

Results show that in addition to pre-treatments, BB post-treatments are effective at attenuating HZE particle-induced neuroinflammation, OS, and memory deficits, supporting the role of neuroinflammation and OS in the persistent effects of irradiation in the CNS. Furthermore, activated microglia and astrocytes are potential targets for dietary treatments, before and/or after activation by irradiation. Although mechanisms are not definitive, correlation analyses suggest that a feed-forward cycle of glial cell activation, neuroinflammation, and OS mediates or at least associates with HZE-particle-induced biochemical changes in the brain and memory deficits. These findings support the use of dietary post-treatments with antioxidant and anti-inflammatory properties to reduce the risk of neurodegenerative disease following neuroinflammatory/OS-inducing stressors, such as HZE particles in cosmic radiation on exploratory space missions.

Keywords: neuroinflammation, oxidative stress, polyphenolics, blueberry, memory, HZE particles, irradiation, microglia

Introduction

Astronauts on exploratory missions beyond the protection provided by the Earth's magnetic field, such as to Mars, will be exposed to ionizing radiation in galactic cosmic rays (GCRs). GCRs contain alpha particles, protons, and high energy and charge particles (HZE particles), which are densely ionizing and more damaging to biological tissues compared to terrestrial forms of radiation such as gamma rays and X-rays. HZE particles can penetrate both spacecraft shielding and human tissue (1, 2) to produce direct effects in irradiated tissues, in addition to formation of secondary radiation particles (e.g., neutrons and recoil nuclei) by nuclear reactions upon impact (3). Therefore, the ionization capacity of HZE particles makes them a major contributor to the biological risk of GCR exposures in space.

In rodents, HZE particle irradiation can induce acute and chronic deleterious effects in the central nervous system (CNS), such as neuroinflammation and oxidative stress (OS), as well as cognitive deficits (e.g., in learning and memory) (4-7). Additionally, exposure to HZE particles may produce 'accelerated aging' in the central nervous system (CNS), as irradiated young animals exhibit neuronal and cognitive changes similar to those observed in older animals (8). Because HZE particle exposures increase neuroinflammation and OS, both known to contribute to neurodegenerative disease development, HZE particle irradiation may increase risk for and/or exacerbate neurodegenerative disease (1). Therefore, countermeasures are necessary to mitigate the detrimental effects of HZE particle exposure on the CNS during and after mission completion. However, the cellular and molecular mediators of HZE particle-induced biochemical changes in the brain and cognitive deficits are not well established, limiting the development of radioprotective and radio-mitigating strategies. There are no established strategies to attenuate the cognitive deficits that progress after radiation exposure (9), and current treatments targeting putative molecular mediators such as inflammation and OS are associated with side effects, particularly with prolonged administration (10).

Nutritional strategies using whole foods with antioxidant and anti-inflammatory properties show potential to be safe, inexpensive, and easily accessible interventions to attenuate HZE particle-induced CNS deficits. For instance, blueberries (BB) contain some

of the highest levels of antioxidant and anti-inflammatory polyphenols, such as the flavonoid anthocyanin, relative to other plant species (11). Anthocyanins from dietary BB consumption can readily cross the blood-brain-barrier, and accumulation of anthocyanins in the brain has been associated with improved cognitive performance in aged rats (12). Previous studies have established the protective effects of berry-supplemented diets as pre-treatments (i.e., before irradiation only) on HZE particle-induced acute biochemical changes in the brain at 22-48 hours (4, 13, 14) and cognitive deficits at 2, 6, or 12 months after irradiation (5, 15). Berry-supplemented diets as pre-/post-treatments (i.e., fed both before and after irradiation) have also been shown to reduce HZE particle-induced biochemical changes in the brain (14) and cognitive deficits (16) one month after irradiation. These studies demonstrate that foods with antioxidant and anti-inflammatory properties, such as berries, can attenuate HZE particle-induced neuroinflammation, OS, and cognitive deficits. However, neither the isolated effects of post-treatments on biochemical changes in the brain (e.g., inflammation, OS) and cognitive outcomes, nor the persistent effects of pre-treatments on biochemical outcomes, have been assessed or compared to each other. Additionally, the effects of dietary interventions on persistent changes in gene expression of neuroinflammation/OS biomarkers and putative cellular mediators of HZE particle-induced CNS changes have not been assessed.

Post-treatments may be necessary countermeasures, particularly when radioprotective pre-treatments are not feasible as with unpredictable radiation surges in solar flares. Additionally, the adverse effects of HZE particles can persist and progress long after radiation exposure has ended, possibly mediated by a self-amplifying cycle of neuroinflammation, OS, glial cell activation, and other neuronal damage. Therefore, pre-treatments may not provide sufficient neuroprotection, as many therapeutics have short half-lives. Because post-treatments are delivered after the onset of irradiation-induced stress responses, a higher dose of active agent is available to interact with elevated neuroinflammation/OS, and could curb and/or reverse the progression of HZE-induced CNS deficits (17). Furthermore, investigating the effects of antioxidant/anti-inflammatory post-treatments can provide guidance for countermeasure development. Therefore, this study examined the effects of whole-body exposure to 150 cGy ^{56}Fe on neuroinflammation, OS, glial cell activation, and memory-related cognitive deficits 45 days after irradiation in

male Sprague-Dawley rats. We also examined whether persistent CNS changes could be attenuated by feeding a BB-supplemented diet post-irradiation, compared to no BB, BB before, or BB both before and after irradiation. ^{56}Fe particles were selected as the HZE particle in this study because they are estimated to be the largest effective dose contributor in the space radiation environment (3, 18).

Methods

Animals

The experimental design for this study is shown in **Figure 1.** Two-month old male Sprague-Dawley rats (Taconic; n=120) were weight-matched and randomly assigned to study groups (n=15/group) at the Human Nutrition Research Center on Aging at Tufts University (HNRCA). Male rats were used because previous studies suggest that males are more susceptible irradiation-induced neuroinflammation, OS, glial activation, and cognitive deficits than female rats (18, 19), potentially due to the neuroprotective effects of estrogen (20, 21). We used male rats in this work to ensure a sufficient stress response, without which, the differential effects of pre- and/or post-treatments could not be discerned. In the pre-treatment interval, rats were fed a 2% BB-supplemented or control diet for 45 days at the HNRCA. Then, animals were transported by vehicle to the NASA Space Radiation Laboratory (NSRL) at Brookhaven National Laboratory (BNL, Long Island, NY) for irradiation procedures. Following irradiation, rats were transported back to the HNRCA where they were fed a 2% BB-supplemented or control diet for an additional 45 days in the post-treatment interval. At both facilities, rats were maintained on a 12:12-h light/dark cycle with *ad libitum* access to food and water. Body weights were recorded every week throughout the study and food intake was assessed over a 24-hour period on the third week of feeding during both pre- and post-treatment intervals. All research protocols were approved by the Institutional Animal Care and Use Committees of the Tufts University and BNL and both facilities are AAALAC accredited.

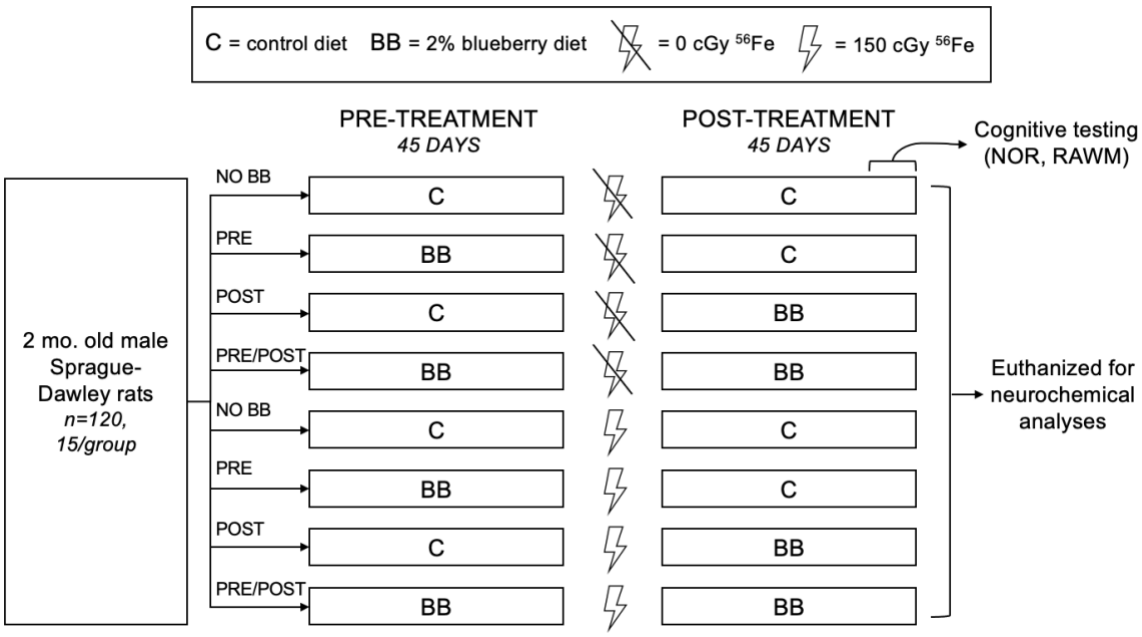

Figure 1. Experimental design.
Two-month old male Sprague-Dawley rats (n=120 total, 15/group) were randomized to consume a control (NIH-31) or BB diet for 45 days in the pre-treatment interval. Rats were exposed to a single dose of 150 cGy ^{56}Fe or were not irradiated, then consumed a C or BB diet for 45 days in the post-treatment interval. Cognitive performance and biochemical outcomes in the brain were assessed at the end of the post-treatment interval. C: control diet, BB: 2% blueberry diet, NOR: novel object recognition, RAWM: radial arm water maze. NO BB: neither pre- nor post-treatment with BB; PRE: only pre-treatment with BB; POST: only post-treatment with BB; PRE/POST: both pre- and post-treatment with BB.

Diets

Animals were fed *ad libitum* either a 2% BB diet or control diet (NIH-31 rodent chow) for 45 days during the pre-treatment interval and/or for a matched 45 days during the post-treatment interval. Therefore, animals consumed 1) no BB (i.e., only the control diet), 2) only pre-BB, 3) only post-BB, or 4) both pre- and post-BB. The details of the diet preparations have been described previously (22). In brief, blueberries were homogenized in water, centrifuged, lyophilized and added to NIH-31 rodent chow (20 g/kg diet, 2% w/w) at Envigo (Madison, WI). A 2% BB diet has been shown to protect against HZE-induced neuroinflammation, OS, and cognitive deficits when consumed before irradiation (5, 14). Further, a 2% diet for animals is approximately equivalent to a human serving of one cup of fresh berries/day (1). Corn was added to the control diet (NIH-31) to compensate for the additional volume of BB extract to the experimental diet.

Irradiation

Rats were whole-body (nose-tail) irradiated at the NSRL with a single dose of 150 cGy ^{56}Fe (1000 MeV/n) or not irradiated, according to study groups. Previous studies have shown that 150 cGy ^{56}Fe disrupts cognitive performance and produces biochemical changes in the brain of rats (13, 14, 16, 23). During irradiation, the animals were restrained in well-ventilated plastic holders (i.e., boxes) placed perpendicular to the beam. Location of the rat in the beam was verified by taking a computer image of the holder using the imager available at the beam line. Non-irradiated rats were taken to the NSRL and received the same confinement, transport, and handling as irradiated animals, but were not irradiated. Dosimetry was provided by the staff at BNL using parallel plate ionization chambers (24).

Cognitive Testing

At the end of the post-treatment interval, the novel object recognition task (NOR) and radial arm water maze (RAWM) were used to assess recognition and spatial memory, respectively. Due to the time required to perform the cognitive tests, the NOR was performed in the third and fourth week post-irradiation and the RAWM was performed in the fifth and sixth week post-irradiation. A 45 day post-irradiation interval was selected based on previous work demonstrating that ^{56}Fe exposure (150 cGy) produces cognitive deficits in memory (e.g., recognition memory assessed by NOR) 1-3 months post-irradiation in rats (5, 23, 25).

Novel Object Recognition Task

For the novel object recognition task, the rats were placed in an open field (93cm x 93cm). On the conditioning day there were two identical (familiar) stimulus objects placed in the field. The rat was allowed to explore the stimuli until it accumulated 25-30 sec total object exploration time (i.e., exploration of either object) or until 15 min had passed. On the test day, 24 hr later, the rat was placed back in the field with one familiar and one novel object and allowed to explore both stimuli until it had accumulated 25-30 sec of object exploration or until 15 min passed. Rats that did not meet the criterion of 25-30 sec exploration time were excluded from data analysis (n=8 animals). The number of animals achieving

criterion did not differ as a function of radiation exposure or BB treatment period (data not shown).

Radial Arm Water Maze

The RAWM was performed as described previously (26). Briefly, rats were placed in a pool of water with internal walls that form eight channels (arms) radiating from an open center area. The pool was surrounded by extramaze cues, which the rat used to navigate the maze. At the beginning of each trial (5 trials/day for 5 consecutive days), rats were randomized to start in one of the arms and swam to locate a submerged platform hidden in one of the arms. If the rat failed to locate the platform within 90 seconds, it was guided to the platform by the researcher. Rats remained on the platform for 15 seconds before being placed in a novel start location (trials 2-4). After the 4th trial, rats were towel-dried and returned to their home cage for 30 minutes, after which they were run on a 5th trial to test for retention. The platform was moved to a new arm daily without repetition, which forced the rats to unlearn the previous day's platform location and learn its new location. Latency (s) was obtained using image tracking software (HVS Image). The order of entry into the maze arms was scored manually to analyze the number of errors. Reference (long-term) memory errors are committed when a rat re-enters an arm that does not contain the platform (trial-independent) and working memory errors (short-term) are committed when a rat re-enters an arm previously explored during that trial (trial-dependent). Because trial 5 is a good assessment of short-term memory and memory consolidation, data from trial 5 were used for statistical analyses.

Neuroinflammation, Oxidative Stress, and Glial Cell Analyses

At the end of the post-treatment interval (45 days post-irradiation), all animals were euthanized by decapitation. Brains were bisected; the hippocampus and frontal cortex from one hemisphere were dissected, snap frozen in liquid nitrogen, and stored at -80°C for biochemical analysis. The other hemisphere of each animal was post-fixed in 4% paraformaldehyde and stored at 4°C for immunohistochemistry.

Western Blots

The hippocampus and frontal cortex of 9 animals/group were homogenized separately as described previously (27). The resultant supernatant lysate was used for blotting after total protein was quantified with the DC protein assay (BioRad, Hercules, CA). Western blot analysis was performed as described previously (28), except that 10% polyacrylamide gels were used. Primary antibodies were used at 1:1000 dilutions for the inflammatory markers cyclooxygenase-2 (COX-2, Santa Cruz, Dallas, TX), phosphorylated and total IκB-α (pIκB-α, IκB-α Santa Cruz, Dallas, TX), and inducible nitric oxide synthase (iNOS, Millipore, Billerica, MA), and oxidative stress markers NADPH oxidase (NOX2, Santa Cruz, Dallas, TX), nuclear factor erythroid 2-related factor 2 (Nrf2, Santa Cruz, Dallas, TX), and superoxide dismutase (Cu/Zn-SOD, Santa Cruz, Dallas, TX) for incubation overnight at 4°C. Glyceraldehyde 3-phosphate dehydrogenase (GAPDH, Santa Cruz, Dallas, TX) was used as a protein loading control marker. The signal was detected using an electrochemiluminescence (ECL) detection kit (BioRad, Hercules, CA) and the optical density of antibody-specific bands was analyzed by the VisionWorks LS image acquisition and analysis software (UVP, Upland, CA). Values were normalized to GAPDH protein levels.

Quantitative real-time PCR

The hippocampus and frontal cortex of the remaining 6 animals/group were homogenized and prepared for quantitative real-time PCR to analyze mRNA levels of inflammatory and OS markers. Total RNA was isolated from brain tissue using Rneasy Plus Mini Kit (Qiagen, Hilden, Germany) according to the manufacturer's instructions. Following extraction, the quality and quantity of RNA samples were determined using a NanoDrop 2000 Spectrophotometer (Thermofisher Scientific, Waltham, MA) with absorbance at A260/A280. The integrity of RNA samples was confirmed by agarose gel electrophoresis. First-strand cDNA was synthesized from 1 µg of total RNA using SuperScript III reverse transcriptase (Invitrogen, Carlsbad, CA) in a GeneAmp PCR System 9700 (Applied Biosystems, Foster City, CA) according to the manufacturer's instructions. The resulting cDNA templates were used for real-time PCR in 25 µl total volume with the SYBR Green PCR Master Mix (Applied Biosystems, Foster City, CA) on a QuantStudio 6 Flex Instrument (Applied Biosystems, Foster City, CA). Gene specific primers for amplification

(Qiagen, Hilden, Germany) were CD68 (QT00372204), COX-2 (QT00192934), iNOS (QT00178325), NOX2 (QT00195300), TNFα (QT00178717), and GAPDH (QT00079247). Relative gene expression was calculated using the comparative threshold cycle (CT) method with GAPDH as the endogenous reference and untreated animals (i.e., non-irradiated animals on a control diet) as the calibrator in the equation $2^{-\Delta\Delta Ct}$ (29).

Iba-1 Immunohistochemistry

One hemisphere of each animal was post-fixed in 4% paraformaldehyde and stored at 4°C. Brains were cryoprotected in 30% sucrose solutions and embedded in Optimal Cutting Temperature (OCT). For immunohistochemistry, brain hemispheres from 5 animals/group were sectioned coronally (30 μm) using a cryostat microtome (Cryocut 1800, Leica Biosystems, Buffalo Grove, IL) and collected in 96-well plates containing 200 uL/well of cryoprotective anti-freeze solution (25% Ethylene glycol, 25% glycerol, 0.05 M PBS). Every sixth section (i.e., 180 μm apart) for the frontal cortex and hippocampus was washed in phosphate buffered saline-Tween-20 (0.1% PBST, 3 x 5 minutes) and blocked with 10% fetal bovine serum (FBS) in PBST overnight at 4°C with gentle shaking. Then, sections were incubated with primary antibody for rabbit anti-Iba-1 (Wako, Richmond, VA) diluted 1:500 overnight at 4°C with gentle shaking. Sections were then washed with PBST (3 x 10 minutes) and incubated with secondary antibody (goat anti-rabbit conjugated with Alexa Fluor® 594, Thermofisher, Waltham, MA) prepared in PBST at 1:500 for 3 hours shaking at room temperature in darkness. Sections were washed, labeled with DAPI at 1:1000 by incubating for 10 minutes, and washed with PBST for 10 minutes. Sections were mounted using, dehydrated, and cover-slipped using Vectastain (Vector Laboratories, Burlingame, CA) for image capture. The images were taken using a Nikon Eclipse TE2000-U inverted fluorescence microscope at 20X magnification. For each brain, images were taken from layer three of the frontal cortex and the CA3 region of the hippocampus in 6 coronal sections per brain region. Numbers of Iba-1 immunolabeled cells in each image were counted using NIH ImageJ software. Only cells that were darkly stained (i.e., strong Iba-1 immunolabeling) across the majority of the soma were included in counts. For analysis, cell counts were averaged across sections for each brain.

Statistical Analysis

Statistical analyses were conducted in R (*v*3.8) using RStudio (*v*1.0.153) and results were considered statistically significant if the observed significance level was $P < 0.05$. All data were tested for normality using Shapiro test and log transformed for parametric analyses if not normally distributed. For body weight, food intake, and biochemical data, two-way analysis of variance (ANOVA) was conducted with ^{56}Fe exposure (0 cGy or 150 cGy ^{56}Fe) and BB treatment period (no BB, pre-BB, post-BB, pre-/post-BB) as experimental factors. If the ^{56}Fe exposure by BB treatment period interaction was significant, post-hoc testing was performed with Tukey's honestly significant difference test to adjust for multiple comparisons and determine differences among groups. Biochemical data for the frontal cortex and hippocampus were analyzed separately. For RAWM outcomes on trial 5, repeated measures ANOVA was performed with ^{56}Fe exposure (0 cGy or 150 cGy ^{56}Fe) and BB treatment period as between subject factors and testing day as the within subject factor. Recognition scores from the NOR were analyzed using t-tests to compare % time spent with novel object to 50%, as greater than 50% indicates intact cognitive function. To determine differences between irradiated groups, a one-way ANOVA was performed followed by Dunnett's test using irradiated animals on the control diet as the reference group. All data are expressed as mean ± standard error of the mean (SEM). Pearson's r correlations were performed to determine linear relationships between neuroinflammation, OS, glial cell activation, and cognitive outcomes.

Results

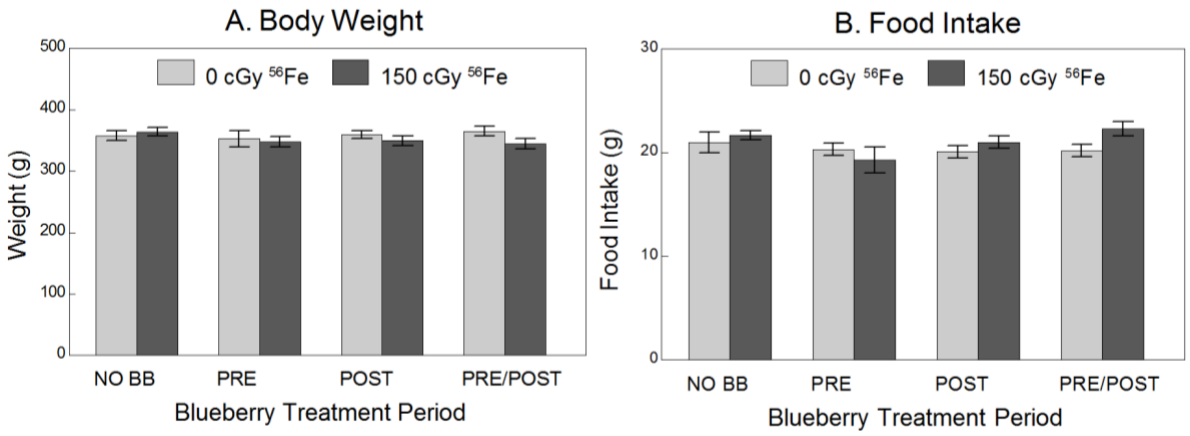

Figure 2. Body weight and food intake in non-irradiated and irradiated rats fed control and/or blueberry-supplemented diets.
Rats were fed with a control or a 2% BB diet for 45 days, received whole-body irradiation with 0 cGy or 150 cGy ^{56}Fe, then were fed with a control or a 2% BB diet for another 45 days. A) Body weight was recorded weekly and is reported as the average for each group across the study duration. B) Food intake was assessed over 24 hours in the pre-treatment and post-treatment interval and is reported as the average of both measures. There were no significant differences between groups in average body weight or food intake ($P > 0.05$). Data are presented as the mean ± SEM (n=15 animals/group). NO BB: neither pre- nor post-treatment with BB; PRE: only pre-treatment with BB; POST: only post-treatment with BB; PRE/POST: both pre- and post-treatment with BB.

Body Weights and Food Intake

There were no significant differences between groups in average body weight or food intake ($P > 0.05$) **(Figure 2).** Body weight was on average 355.39 ± 2.97 grams over the course of the study. Average food intake for the pre- and post-treatment periods was 20.80 ± 0.33 grams.

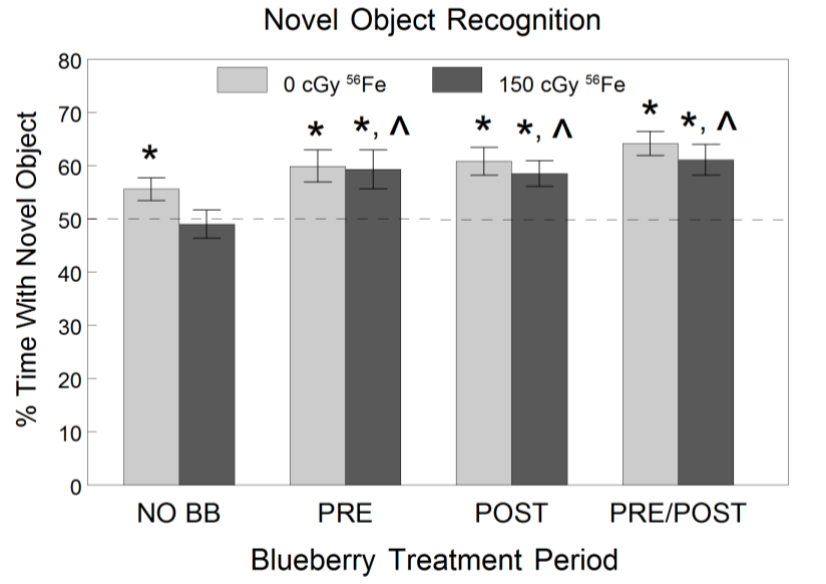

Figure 3. Effect of pre- and/or post-BB on novel object recognition performance in non-irradiated and irradiated rats.
Rats were fed a control or 2% BB diet for 45 days, received whole-body irradiation with 0 cGy or 150 cGy ^{56}Fe, then were fed a control or 2% BB diet for 45 days. Recognition memory was assessed using the novel object recognition task at the end of the post-treatment period (3-4 weeks post-irradiation) and performance is reported as percent of total exploration time spent with the novel object. Data are presented as the mean ± SEM (n=13-15 animals/group). * = significantly different than 50% (t-test, $P < 0.05$). ^ = within ^{56}Fe irradiated animals, significantly different than NO BB (Dunnett's test, $P < 0.05$). NO

BB: neither pre- nor post-treatment with BB; PRE: only pre-treatment with BB; POST: only post-treatment with BB; PRE/POST: both pre- and post-treatment with BB.

NOR

Percent time spent with the novel object was significantly greater than 50% for all groups ($P < 0.05$) except irradiated animals with no BB ($P = 0.71$), indicating that non-irradiated animals on the control diet and all animals on the BB diet distinguished the novel from the familiar object (**Figure 3)**. Within irradiated animals, there was a significant effect of BB treatment group ($F_{3,52} = 3.12$, $P < 0.05$), and recognition scores for all BB groups were significantly greater than no BB ($P < 0.05$).

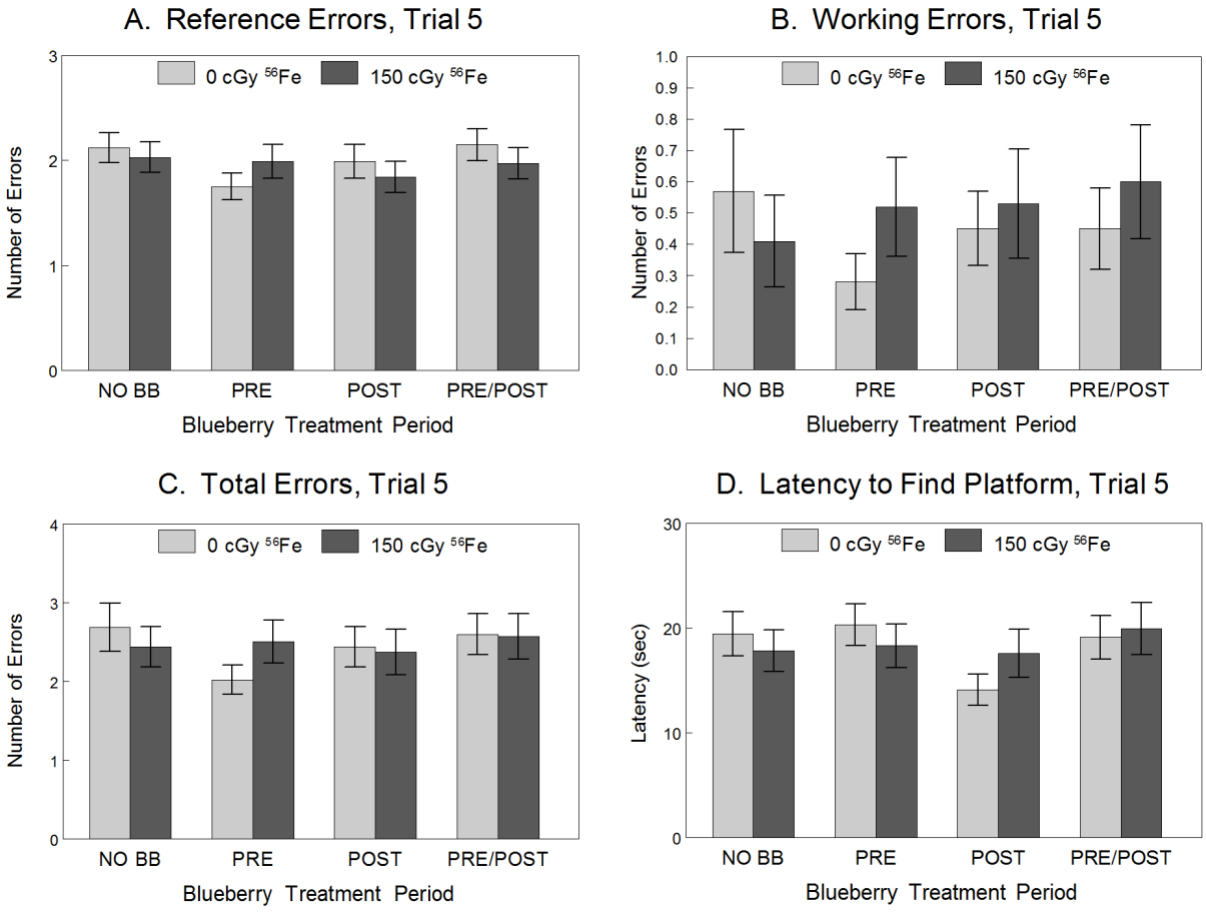

Figure 4. No effect of ^{56}Fe irradiation or of pre- and/or post-BB on RAWM performance on trial 5 in non-irradiated and irradiated rats.
Rats were fed a control or 2% BB diet for 45 days, received whole-body irradiation with 0 cGy or 150 cGy ^{56}Fe, then were fed a control or 2% BB diet for 45 days. At the end of the post-treatment period (5-6 weeks post-irradiation), the RAWM was performed to assess

spatial memory using A) reference memory errors, B) working memory errors, C) total errors, and D) latency to find the platform on trial 5. Data are presented as the mean ± SEM (n=15 animals/group). There were no significant differences between groups on RAWM performance measures on trial 5 ($P > 0.05$). NO BB: neither pre- nor post-treatment with BB; PRE: only pre-treatment with BB; POST: only post-treatment with BB; PRE/POST: both pre- and post-treatment with BB.

RAWM

There were no significant effects of irradiation, BB treatment period, or their interaction on reference memory errors, working memory errors, total errors, or latency to find the platform on trial 5 ($P > 0.05$) **(Figure 4),** indicating that neither irradiation nor diet affected spatial memory. On average, trial 5 reference errors were 1.98 ± 0.05, working errors were 1.32 ± 0.05, total errors were 2.3 ± 0.09, and latency to find the platform was 18.3 ± 0.74 seconds. All groups of rats learned the task and improved performance over the trials and testing days **(Supplemental Figure 1).**

Effects of ^{56}Fe irradiation and BB on the protein expression of neuroinflammation, glial cell (astrocyte) activation, and OS markers in the frontal cortex and hippocampus

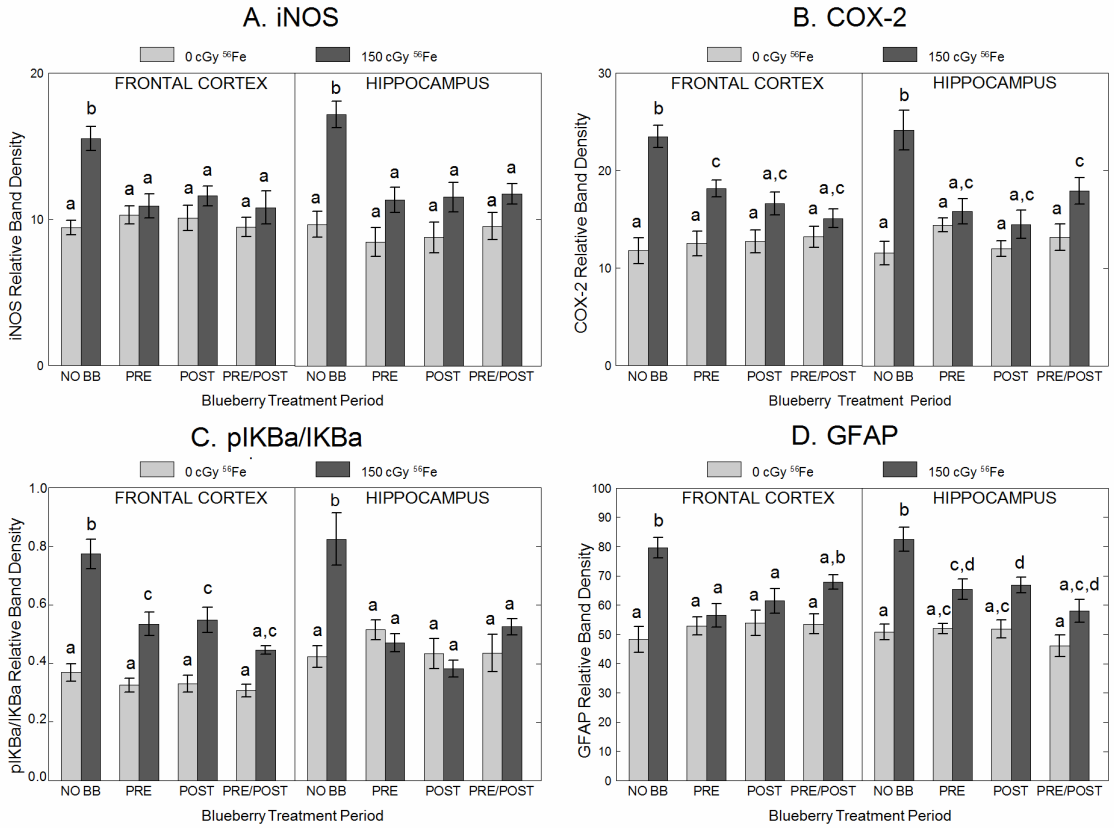

Figure 5. Effect of pre- and/or post-BB on ^{56}Fe -induced protein expression of inducible inflammatory factors, iNOS, COX-2, and pIκB-α, and an indicator of astrocyte activation, GFAP in the frontal cortex and hippocampus.
Rats were fed a control or 2% BB diet for 45 days, received whole-body irradiation with 0 cGy or 150 cGy ^{56}Fe, then were fed a control or 2% BB diet for 45 days. The following markers for neuroinflammation were assessed after the post-treatment interval using Western blot: A) iNOS protein expression, B) COX-2 protein expression, C) phosphorylated IκB-α protein expression, expressed as a ratio of total IκB-α, and D) GFAP protein expression. Data are presented as the mean ± SEM (n=9 animals/group). Bars with different letters are significantly different from each other ($P < 0.05$). NO BB: neither pre- nor post-treatment with BB; PRE: only pre-treatment with BB; POST: only post-treatment with BB; PRE/POST: both pre- and post-treatment with BB.

Neuroinflammation

iNOS Protein

In the frontal cortex, there were significant main effects of ^{56}Fe exposure ($F_{1,64} = 18.62$, $P < 0.001$) and BB ($F_{3,64} = 3.44$, $P < 0.05$), and a ^{56}Fe x BB interaction ($F_{3,64} = 5.20$, $P < 0.01$) on iNOS protein expression. In the hippocampus, there were also significant main effects of ^{56}Fe exposure ($F_{1,64} = 34.97$, $P < 0.001$) and BB ($F_{3,64} = 6.28$, $P < 0.001$), and a ^{56}Fe x BB interaction ($F_{3,64} = 3.60$, $P < 0.05$) on iNOS protein expression. Post-hoc testing showed that in both regions, ^{56}Fe exposure significantly increased iNOS expression compared to no radiation ($P < 0.001$) **(Figure 5A),** and BB treatment before and/or after ^{56}Fe exposure significantly reduced iNOS expression compared to no BB ($P < 0.05$). Additionally, within each BB treatment group, iNOS expression was not significantly different between irradiated and non-irradiated animals, indicating that BB treatments reversed the effects of radiation on iNOS expression. The timing of BB administration did not alter ^{56}Fe-induced iNOS expression as its levels following pre-, post-, and pre-/post-radiation BB treatments were not significantly different.

COX-2 Protein

In the frontal cortex, there were significant main effects of ^{56}Fe exposure ($F_{1,64} = 52.44$, $P < 0.001$) and BB ($F_{3,64} = 3.68$, $P < 0.05$), and a ^{56}Fe x BB interaction ($F_{3,64} = 7.03$, $P < 0.001$) on COX-2 protein expression. In the hippocampus, there were also significant main effects of ^{56}Fe exposure ($F_{1,64} = 31.57$, $P < 0.001$) and BB

($F_{3,64} = 4.01$, $P < 0.05$), and a ^{56}Fe x BB interaction ($F_{3,64} = 7.22$, $P < 0.001$) on COX-2 protein expression. Post-hoc testing showed that in both regions, ^{56}Fe exposure significantly increased COX-2 expression compared to no radiation ($P < 0.001$) **(Figure 5B),** and BB treatment before and/or after ^{56}Fe exposure significantly reduced COX-2 expression compared to no BB ($P < 0.05$). The timing of BB administration did not alter ^{56}Fe-induced COX-2 expression as its levels following pre-, post-, and pre-/post-radiation BB treatments were not significantly different from each other. Moreover, within post- and pre-/post-treatments in the frontal cortex and pre- and post-treatments in the hippocampus, COX-2 expression was not significantly different between irradiated and non-irradiated animals, indicating that BB treatments reversed the effects of radiation on COX-2 expression in these groups.

Phosphorylated IκB-a (pIκB-a/total IκB-a) Protein

Phosphorylation of IκB-α indicates greater availability of the transcription factor NF-κB to translocate to the nucleus where it induces the transcription of inflammatory genes such as iNOS and COX-2. In the frontal cortex, there were significant main effects of ^{56}Fe exposure ($F_{1,64} = 106.22$, $P < 0.001$) and BB ($F_{3,64} = 12.27$, $P < 0.001$), and a ^{56}Fe x BB interaction ($F_{3,64} = 5.81$, $P < 0.01$) on the ratio of phosphorylated to total IκB-α protein expression. In the hippocampus, there were also significant main effects of ^{56}Fe exposure ($F_{1,64} = 7.94$, $P < 0.01$) and BB ($F_{3,64} = 6.56$, $P < 0.001$), and a ^{56}Fe x BB interaction ($F_{3,64} = 9.10$, $P < 0.001$) on IκB-α phosphorylation. Post-hoc testing showed that in both regions, ^{56}Fe exposure significantly increased IκB-α phosphorylation compared to no radiation ($P < 0.001$) **(Figure 5C),** and BB treatment before and/or after ^{56}Fe exposure significantly reduced IκB-α expression compared to no BB ($P < 0.001$). The timing of BB administration did not alter ^{56}Fe-induced IκB-α phosphorylation as its levels following pre-, post-, and pre-/post-radiation BB treatments were not significantly different from each other. Moreover, within pre-/post-treatments in the frontal cortex and all BB treatments in the hippocampus, pIκB-α expression was not significantly different between irradiated and non-irradiated animals, indicating that BB treatments reversed the effects of radiation on IκB-α expression in these groups.

Astrocyte activation

GFAP Protein

In the frontal cortex, there was a significant main effect of ^{56}Fe exposure ($F_{1,64} = 28.80$, $P < 0.001$) and a ^{56}Fe x BB interaction ($F_{3,64} = 5.40$, $P < 0.01$) on GFAP protein expression. In the hippocampus, there were significant main effects of ^{56}Fe exposure ($F_{1,64} = 60.17$, $P < 0.001$) and BB ($F_{3,64} = 6.62$, $P < 0.001$), and a ^{56}Fe x BB interaction ($F_{3,64} = 3.86$, $P < 0.05$) on GFAP expression. Post-hoc testing showed that in both regions, ^{56}Fe exposure significantly increased GFAP expression compared to no radiation ($P < 0.001$) **(Figure 5D).** BB treatment before and/or after ^{56}Fe exposure significantly reduced GFAP expression compared to no BB ($P < 0.05$), except pre-/post-treatment in the frontal cortex ($P > 0.05$). The timing of BB administration did not alter ^{56}Fe-induced GFAP expression as its levels following pre-, post-, and pre-/post-radiation BB were not significantly different from each other. Moreover, within all BB treatment groups in the frontal cortex and pre- and pre-/post-BB in the hippocampus, GFAP expression was not significantly different between irradiated and non-irradiated animals, indicating that BB treatments reversed the effects of radiation on GFAP expression in these groups.

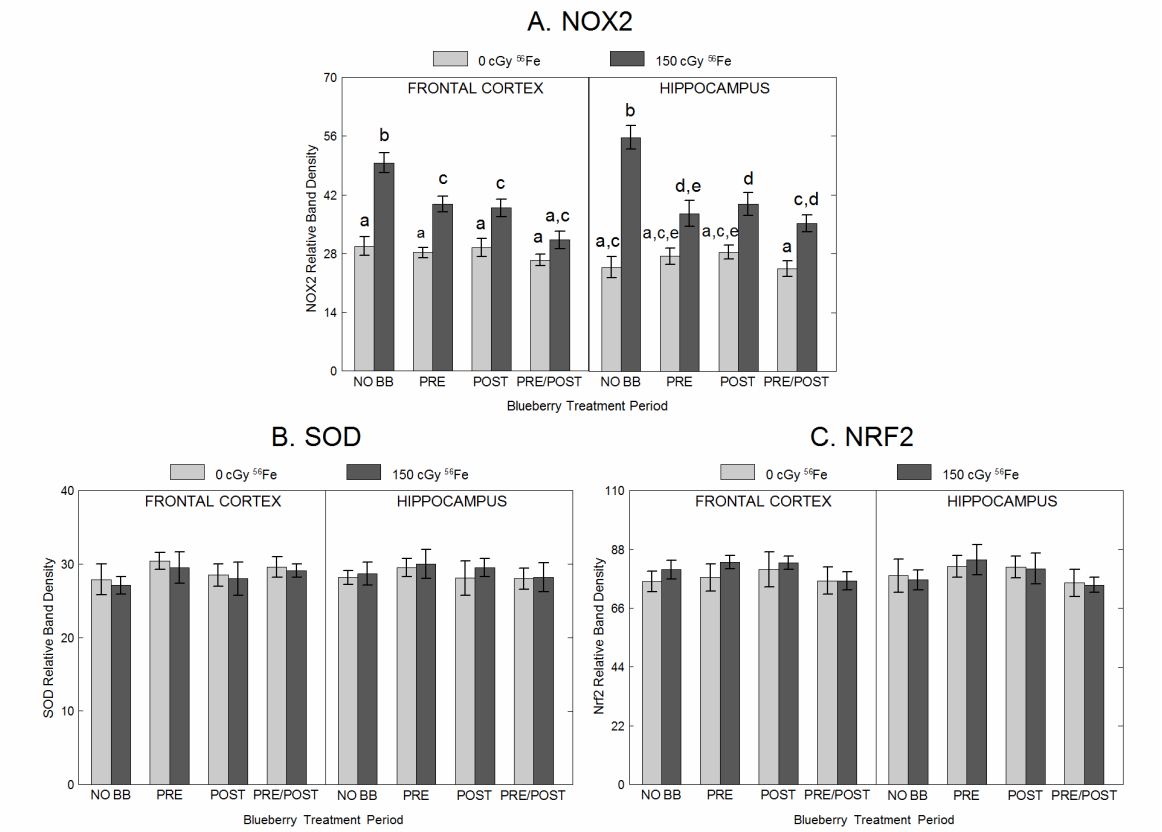

Figure 6. Effect of pre- and/or post-BB on ^{56}Fe-induced protein expression of oxidative stresses mediators, NOX2, SOD, and Nrf2 in the frontal cortex and hippocampus.

Rats were fed a control or 2% BB diet for 45 days, received whole-body irradiation with 0 cGy or 150 cGy ^{56}Fe, then were fed a control or 2% BB diet for 45 days. The following markers for OS were assessed after the post-treatment interval using Western blot: A) NOX2 protein expression, B) SOD protein expression, and C) Nrf2 protein expression. Data are presented as the mean ± SEM (n=9 animals/group). Bars with different letters are significantly different from each other ($P < 0.05$). NO BB: neither pre- nor post-treatment with BB; PRE: only pre-treatment with BB; POST: only post-treatment with BB; PRE/POST: both pre- and post-treatment with BB.

Oxidative Stress

NOX2 Protein

In the frontal cortex, there were significant main effects of ^{56}Fe exposure ($F_{1,64} = 66.41$, $P < 0.001$) and BB ($F_{3,64} = 9.95$, $P < 0.001$), and a ^{56}Fe x BB interaction ($F_{3,64} = 5.04$, $P < 0.01$) on NOX2 protein expression. In the hippocampus, there were also significant main effects of ^{56}Fe exposure ($F_{1,64} = 88.42$, $P < 0.001$) and BB ($F_{3,64} = 6.88$, $P < 0.001$), and a ^{56}Fe x BB interaction ($F_{3,64} = 8.91$, $P < 0.001$) on NOX2

expression. Post-hoc testing showed that in both regions, ^{56}Fe exposure significantly increased NOX2 expression compared to no radiation ($P < 0.001$) **(Figure 6A).** BB treatment before and/or after ^{56}Fe exposure significantly reduced NOX2 expression compared to no BB ($P < 0.05$). The timing of BB administration did not alter ^{56}Fe-induced NOX2 expression as its levels following pre-, post-, and pre-/post-radiation BB were not significantly different from each other, although in the frontal cortex, there was a trend for reduced NOX2 expression with pre-/post-treatment compared to pre-treatment ($P = 0.059$). Within pre-/post-treatment in the frontal cortex and pre-BB in the hippocampus, NOX2 expression was not significantly different between irradiated and non-irradiated animals, indicating that BB treatments reversed the effects of radiation on NOX2 expression in these groups.

SOD Protein

In the frontal cortex, neither ^{56}Fe ($F_{1,64} = 0.32$, $P = 0.57$) nor BB ($F_{3,64} = 0.85$, $P = 0.47$) caused significant changes in SOD expression **(Figure 6B).** Likewise, in the hippocampus, neither ^{56}Fe ($F_{1,64} = 0.32$, $P = 0.57$) nor BB ($F_{3,64} = 0.38$, $P = 0.77$) caused significant changes in SOD expression.

Nrf2 Protein

As with SOD, in the frontal cortex, neither ^{56}Fe ($F_{1,64} = 1.06$, $P = 0.31$) nor BB ($F_{3,64} = 0.64$, $P = 0.59$) caused significant changes in Nrf2 expression **(Figure 6C).** Likewise, in the hippocampus, neither ^{56}Fe ($F_{1,64} = 0.001$, $P = 0.98$) nor BB ($F_{3,64} = 1.07$, $P = 0.37$) caused significant changes in SOD expression.

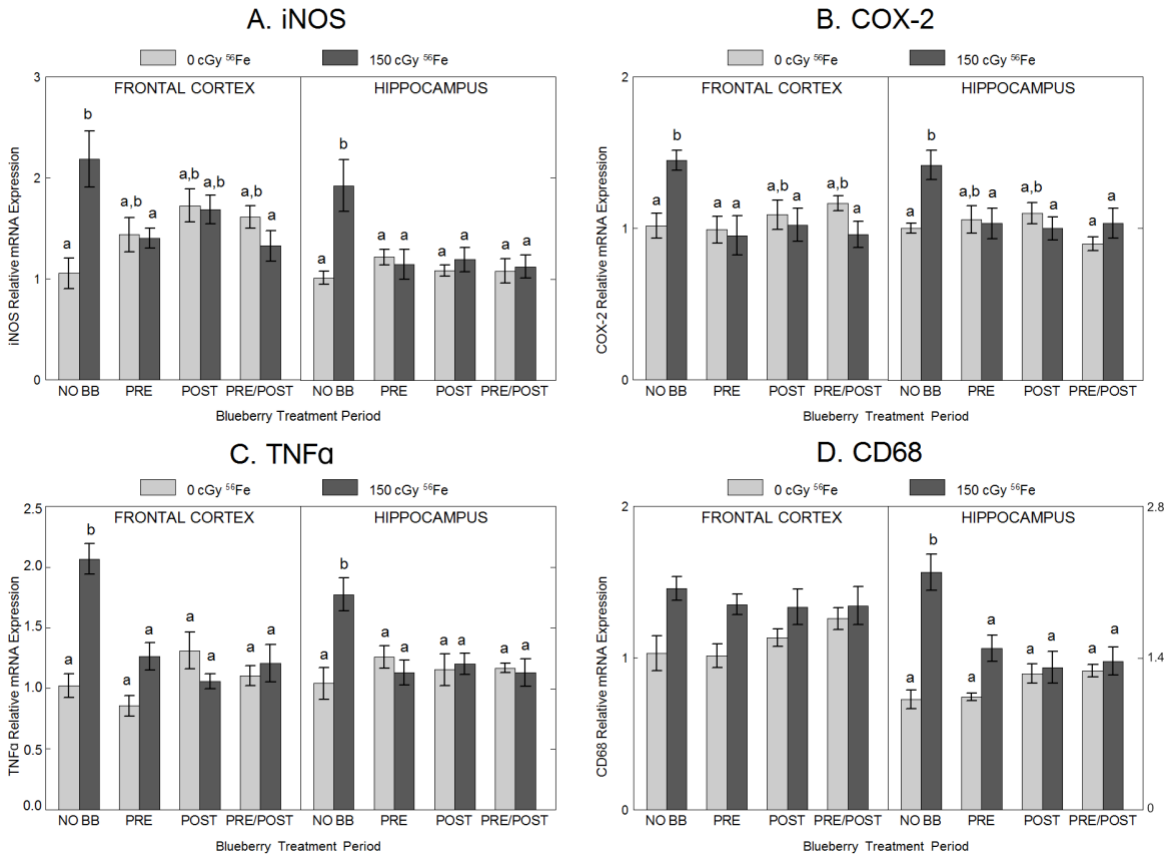

Figure 7. Effect of pre- and/or post-BB on ^{56}Fe-induced relative mRNA levels of inducible inflammatory enzymes, iNOS, COX-2, pro-inflammatory cytokine TNFα, and an indicator of microglia activation, CD68 in the frontal cortex and hippocampus. Rats were fed a control or 2% BB diet for 45 days, received whole-body irradiation with 0 cGy or 150 cGy ^{56}Fe, then were fed a control or 2% BB diet for 45 days. The following outcomes were assessed after the post-treatment interval using quantitative real-time PCR: A) iNOS mRNA, B) COX-2 mRNA, C) TNFα mRNA, and D) CD68 mRNA. Data are presented as the mean ± SEM (n=6 animals/group). Bars with different letters are significantly different from each other ($P < 0.05$). NO BB: neither pre- nor post-treatment with BB; PRE: only pre-treatment with BB; POST: only post-treatment with BB; PRE/POST: both pre- and post-treatment with BB.

Effects of ^{56}Fe irradiation and BB on the relative mRNA levels of neuroinflammation, glial cell activation (microglia), and OS markers in the frontal cortex and hippocampus

Neuroinflammation

iNOS mRNA

In the frontal cortex, there was a significant ^{56}Fe x BB interaction ($F_{3,40} = 7.30$, $P < 0.001$) on iNOS mRNA expression, although the main effects of ^{56}Fe exposure ($F_{1,40} = 2.68$, $P = 0.11$) and BB ($F_{3,40} = 1.28$, $P = 0.29$) were not significant.

However, post-hoc testing showed that in animals fed only the control diet (i.e., no BB), ^{56}Fe exposure increased iNOS mRNA compared to no irradiation ($P < 0.001$) **(Figure 7A)**. Within irradiated animals, pre-BB and pre-/post-BB reduced iNOS mRNA levels compared to no BB ($P < 0.05$), although post-BB did not have a significant effect. INOS mRNA levels were not significantly different between irradiated and non-irradiated animals within each BB group, including post-BB, indicating that BB treatments reversed the effects of radiation on iNOS mRNA in these groups.

In the hippocampus, there were significant main effects of ^{56}Fe exposure ($F_{1,39} = 7.47$, $P < 0.01$) and BB ($F_{3,39} = 3.22$, $P < 0.05$), and a ^{56}Fe x BB interaction ($F_{3,39} = 5.31$, $P < 0.01$) on iNOS mRNA. Post-hoc testing showed that ^{56}Fe exposure significantly increased iNOS mRNA compared to no radiation ($P < 0.01$). BB treatment before and/or after ^{56}Fe exposure significantly reduced iNOS mRNA compared to no BB ($P < 0.05$), and the timing of BB administration did not alter its inhibitory effect on ^{56}Fe-induced iNOS expression as levels following pre-, post-, and pre-/post-radiation BB were not different from each other. Within all BB treatment groups in the hippocampus, iNOS mRNA was not significantly different between irradiated and non-irradiated animals, indicating that BB treatments reversed the effects of radiation on iNOS mRNA.

COX-2 mRNA

In the frontal cortex, there were significant main effects of BB ($F_{3,40} = 2.92$, $P < 0.05$) and a ^{56}Fe x BB interaction ($F_{3,40} = 4.61$, $P < 0.01$) on COX-2 mRNA expression. Similarly, in the hippocampus there were significant main effects of BB ($F_{3,40} = 3.06$, $P < 0.05$) and a ^{56}Fe x BB interaction ($F_{3,40} = 4.20$, $P < 0.05$) on COX-2 mRNA expression. Although the main effect of ^{56}Fe exposure on COX-2 mRNA was not significant in the frontal cortex ($F_{3,40} = 0.22$, $P = 0.64$) or hippocampus ($F_{3,40} = 3.04$, $P = 0.09$), post-hoc testing showed that in animals fed only the control diet (i.e., no BB), ^{56}Fe exposure increased COX-2 mRNA compared to no irradiation ($P < 0.05$) **(Figure 7B)**. In both regions, BB treatment before and/or after ^{56}Fe exposure significantly reduced COX-2 mRNA expression compared to no BB ($P < 0.05$). Additionally, within each BB treatment group, COX-2 mRNA was not significantly different between irradiated and non-irradiated animals, indicating that BB treatments reversed the effects of radiation on COX-2 mRNA. The

timing of BB administration did not alter its inhibitory effect on ^{56}Fe-induced COX-2 expression as levels following pre-, post-, and pre-/post-radiation BB treatments were not significantly different from each other.

TNFα mRNA

In the frontal cortex, there were significant main effects of ^{56}Fe exposure ($F_{1,40} = 13.92$, $P < 0.001$) and BB ($F_{3,40} = 4.74$, $P < 0.01$), and a ^{56}Fe x BB interaction ($F_{3,40} = 8.88$, $P < 0.001$) on TNFα mRNA expression. In the hippocampus, there was a significant main effect of ^{56}Fe exposure ($F_{1,39} = 4.17$, $P < 0.05$) and a ^{56}Fe x BB interaction ($F_{3,39} = 6.39$, $P < 0.01$) on TNFα expression, although the main effect of BB treatment period was not significant ($F_{3,39} = 2.43$, $P = 0.08$). Post-hoc testing showed that in both regions, ^{56}Fe exposure significantly increased TNFα mRNA compared to no radiation ($P < 0.05$) **(Figure 7C),** and BB treatment before and/or after ^{56}Fe exposure significantly reduced TNFα mRNA compared to no BB ($P < 0.05$). Additionally, within each BB treatment group, TNFα expression was not significantly different between irradiated and non-irradiated animals, indicating that BB treatments reversed the effects of radiation on TNFα expression. The timing of BB administration did not alter ^{56}Fe-induced TNFα expression as levels following pre-, post-, and pre-/post-radiation BB treatments were not significantly different.

Glial cell (microglia) activation

CD68 mRNA

In the frontal cortex, there was a significant main effect of ^{56}Fe exposure ($F_{1,40} = 16.19$, $P < 0.001$) on CD68 mRNA. However, the main effect of BB ($F_{3,40} = 0.54$, $P = 0.65$) and the ^{56}Fe x BB interaction ($F_{3,40} = 1.34$, $P = 0.27$) on CD68 mRNA were not significant. Post-hoc testing showed that ^{56}Fe exposure significantly increased CD68 expression compared to no irradiation ($P < 0.001$) **(Figure 7D)**. In the hippocampus, there was a significant main effect of ^{56}Fe exposure ($F_{1,39} = 22.82$, $P < 0.001$) and a ^{56}Fe x BB interaction ($F_{3,39} = 8.32$, $P < 0.001$) on CD68 expression, although the main effect of BB treatment period was not significant ($F_{3,39} = 1.65$, $P = 0.19$). Post-hoc testing showed that ^{56}Fe exposure significantly increased

CD68 mRNA compared to no radiation ($P < 0.001$), and BB treatment before and/or after ^{56}Fe exposure significantly reduced CD68 compared to no BB ($P < 0.05$). Additionally, within each BB treatment group, CD68 mRNA was not significantly different between irradiated and non-irradiated animals, indicating that BB treatments reversed the effects of radiation on CD68 mRNA expression in the hippocampus. The timing of BB administration did not alter ^{56}Fe-induced CD68 mRNA expression as levels following pre-, post-, and pre-/post-radiation BB treatments were not significantly different.

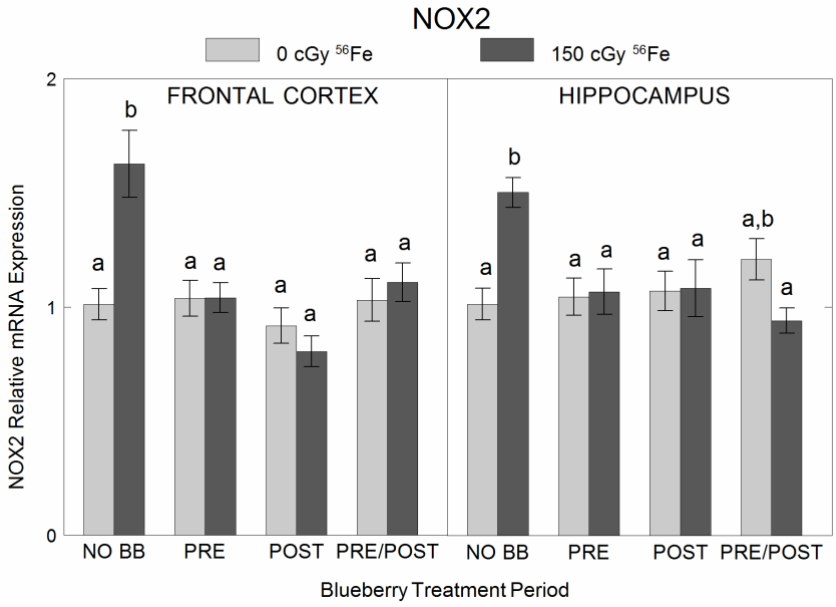

Figure 8. Effect of pre- and/or post-BB on ^{56}Fe-induced relative mRNA expression of oxidative stress marker, NOX2 in the frontal cortex and hippocampus.
Rats were fed a control or 2% BB diet for 45 days, received whole-body irradiation with 0 cGy or 150 cGy ^{56}Fe, then were fed a control or 2% BB diet for 45 days. Relative mRNA expression NOX2 was assessed using quantitative real-time PCR. Data are presented as the mean ± SEM (n=9 animals/group). Bars with different letters are significantly different from each other ($P < 0.05$). NO BB: neither pre- nor post-treatment with BB; PRE: only pre-treatment with BB; POST: only post-treatment with BB; PRE/POST: both pre- and post-treatment with BB.

Oxidative stress

NOX2 mRNA

In the frontal cortex, there were significant main effects of ^{56}Fe exposure ($F_{1,40} = 5.38$, $P < 0.05$) and BB ($F_{3,40} = 9.00$, $P < 0.001$), and a ^{56}Fe x BB interaction ($F_{3,40} = 6.60$, $P < 0.001$) on NOX2 mRNA. Post-hoc testing showed that ^{56}Fe exposure

significantly increased NOX2 mRNA compared to no radiation ($P < 0.001$) **(Figure 8),** and BB treatment before and/or after ^{56}Fe exposure significantly reduced NOX2 mRNA compared to no BB ($P < 0.05$). In the hippocampus, there was a significant ^{56}Fe x BB interaction ($F_{3,39} = 6.65$, $P < 0.001$) on NOX2 mRNA, although the main effects of ^{56}Fe ($F_{3,39} = 1.00$, $P = 0.32$) and BB ($F_{3,39} = 2.41$, $P = 0.08$) were not significant. However, post-hoc testing showed that in animals fed only the control diet (i.e., no BB), ^{56}Fe exposure increased NOX2 mRNA in the hippocampus compared to no irradiation ($P < 0.01$). Within irradiated animals, all BB treatments reduced NOX2 mRNA compared to no BB ($P < 0.05$), and the attenuating effects of BB treatments were not different from each other. In both the frontal cortex and hippocampus, NOX2 mRNA levels were not different between irradiated and non-irradiated animals within each BB group, indicating that BB treatments reversed the effects of radiation on NOX2 mRNA induction in these groups.

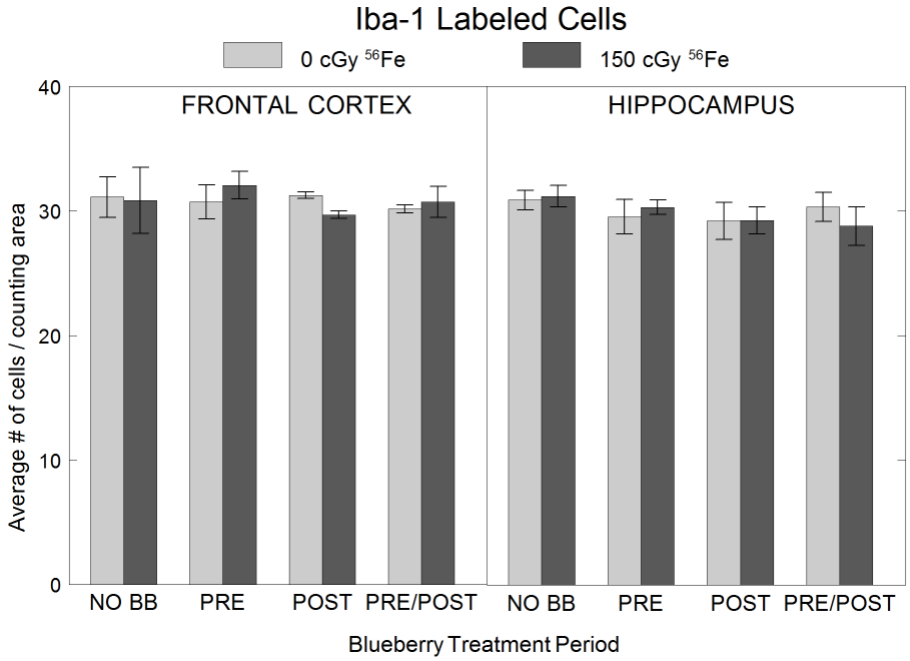

Figure 9. No effect of ^{56}Fe irradiation or of pre- and/or post-BB on Iba-1 immunolabeled microglia in the frontal cortex and hippocampus
Rats were fed a control or 2% BB diet for 45 days, received whole-body irradiation with 0 cGy or 150 cGy ^{56}Fe, then were fed a control or 2% BB diet for 45 days. The number of microglia immunolabeled with Iba-1 were counted quantified in the frontal cortex and hippocampus. Data are presented as the mean ± SEM (n=6 animals/group). NO BB: neither pre- nor post-treatment with BB; PRE: only pre-treatment with BB; POST: only post-treatment with BB; PRE/POST: both pre- and post-treatment with BB.

No effect of ^{56}Fe irradiation or of pre- and/or post-BB on the number of Iba-1 immunolabeled microglia in the frontal cortex and hippocampus

In the frontal cortex, neither ^{56}Fe ($F_{1,26} = 0.008$, $P = 0.93$) nor BB ($F_{3,26} = 0.20$, $P = 0.90$) caused significant changes in the number of Iba-1 labeled microglia **(Figure 9, Supplemental Figure 2).** Likewise, in the hippocampus, neither ^{56}Fe ($F_{1,26} = 0.002$, $P = 0.88$) nor BB ($F_{3,26} = 1.08$, $P = 0.37$) caused significant changes in the number of Iba-1 labeled microglia. The average number of Iba-1 labeled microglia in each counting frame was 30.88 ± 0.52 in the frontal cortex and 29.96 ± 0.41 in the hippocampus.

Frontal Cortex		mRNA				Protein					
		COX2	iNOS	NOX2	TNFα	GFAP	pIκBa	COX2	iNOS	NOX2	NOR
mRNA	CD68	0.23^	0.29	0.29	0.43	0.33	0.31	0.38	0.26^	0.32	-0.11
	COX2		0.34	0.38	0.55	0.29	0.28	0.28^	0.23	0.29	-0.26^
	iNOS			0.24^	0.42	0.35	0.29	0.36	0.36	0.36	-0.16
	NOX2				0.60	0.10	0.24	0.33	0.39	0.34	-0.42
	TNFα					0.34	0.36	0.38	0.30	0.35	-0.42
Protein	GFAP						0.42	0.37	0.28	0.28	-0.34
	pIκBa							0.70	0.49	0.78	-0.42
	COX2								0.69	0.77	-0.33
	iNOS									0.62	-0.24
	NOX2										-0.30

Table 1. Correlation between indicators of neuroinflammation, OS, and glial cell activation in the frontal cortex, and memory function.

Pearson r values are reported for analyses including all 8 study groups (n = 48 rats for correlations with mRNA, n = 72 rats for all other correlations). Blue = significant positive correlation ($P < 0.05$); red = significant negative correlation ($P < 0.05$); white = non-significant correlation; ^ = trend for correlation ($0.05 \leq P < 0.1$). Darker shading indicates stronger correlations. NOR = novel object recognition score (% time with novel object).

Hippocampus		mRNA				Protein					
		COX2	iNOS	NOX2	TNFα	GFAP	pIκBa	COX2	iNOS	NOX2	NOR
mRNA	CD68	0.59	0.59	0.61	0.51	0.61	0.27^	0.63	0.54	0.63	-0.45
	COX2		0.53	0.49	0.41	0.41	0.32	0.43	0.32	0.44	-0.26^
	iNOS			0.49	0.48	0.46	0.39	0.63	0.33	0.41	-0.34
	NOX2				0.56	0.35	0.41	0.38	0.38	0.36	-0.28^
	TNFα					0.52	0.34	0.43	0.41	0.61	-0.37
Protein	GFAP						0.31	0.32	0.48	0.69	-0.34
	pIκBa							0.31	0.30	0.39	-0.30
	COX2								0.46	0.42	-0.35
	iNOS									0.59	-0.45
	NOX2										-0.36

Table 2. Correlation between indicators of neuroinflammation, OS, and glial cell activation in the hippocampus, and memory function.
Pearson r values are reported for analyses including all 8 study groups (n = 48 rats for correlations with mRNA, n = 72 rats for all other correlations). Blue = significant positive correlation ($P < 0.05$); red = significant negative correlation ($P < 0.05$); white = non-significant correlation; ^ = trend for correlation ($0.05 \leq P \leq 0.10$). Darker shading indicates stronger correlations (r = 0 to 1). NOR = novel object recognition score (% time with novel object).

Correlation analyses

The correlation analyses presented in **Table 1** (frontal cortex), **Table 2** (hippocampus), and results below include animals in all 8 study groups (n = 48 observation pairs for correlations with mRNA, n = 72 observation pairs for all other correlations). Significant correlations between neuroinflammation/OS, glial cell activation, and recognition memory were also observed among animals fed only the control diet (i.e., irradiated and non-irradiated, without BB), presented in **Supplemental Table S1** (frontal cortex) and **Supplemental Table S2** (hippocampus). Pearson r values and p-values for all correlation analyses are available in **Supplemental Table S3**.

Positive correlations between neuroinflammation and OS mediators

In the frontal cortex and hippocampus, iNOS and NOX2 mRNA levels were significantly positively correlated with the respective protein expression levels ($P < 0.05$). COX-2 protein was positively associated with COX-2 mRNA in the hippocampus (r = 0.43, $P < 0.01$), and there was a trend for a positive association between COX-2 mRNA and protein in the frontal cortex (r = 0.28, $P = 0.05$). In both brain regions, iNOS, NOX2, and COX-2

were significantly positively correlated with mRNA and protein levels of each other ($P < 0.05$), except a non-significant correlation between COX-2 mRNA and iNOS protein in the frontal cortex (r = 0.23, $P = 0.12$), and a trend between NOX2 mRNA and iNOS mRNA in the frontal cortex (r = 0.24, $P = 0.09$). In both regions, pIκB-α was significantly positively correlated with TNFα mRNA and with the mRNA and protein expression of COX-2, iNOS, and NOX2 ($P < 0.05$). TNFα mRNA was also significantly positively associated the mRNA and protein expression of COX-2, iNOS, and NOX-2 ($P < 0.05$).

Positive correlations between glial activation and neuroinflammation/OS mediators

In the frontal cortex and hippocampus, CD68 mRNA, a marker of microglial activation was significantly positively correlated with mRNA and protein levels of NOX2, mRNA of iNOS, protein of COX-2, and mRNA of TNFα ($P < 0.05$). There was a significant positive correlation between CD68 mRNA and iNOS protein in the hippocampus (r = 0.54, $P < 0.001$), and also a trend in the frontal cortex (r = 0.26, $P = 0.08$). Likewise, a significant positive correlation between CD68 mRNA and COX-2 mRNA was observed in the hippocampus (r = 0.60, $P < 0.001$), and a trend in the frontal cortex (r = 0.23, $P = 0.10$). In the frontal cortex, CD68 mRNA was significantly associated with pIκB-α protein (r = 0.31, $P < 0.05$), and a strong trend for a positive correlation was observed in the hippocampus (r = 0.27, $P = 0.06$). In both brain regions, GFAP protein, a marker of astrocytes, was significantly positively correlated with mRNA and protein levels of iNOS, COX-2, and NOX2, protein of pIκB-α, and mRNA of TNFα ($P < 0.05$). Furthermore, CD68 mRNA and GFAP protein were significantly positively correlated in both the frontal cortex (r = 0.33, $P < 0.05$) and hippocampus (r = 0.61, $P < 0.001$).

Negative correlations between recognition memory (NOR) and glial activation or neuroinflammation/OS mediators

Recognition memory function was assessed on the NOR task as percent time spent exploring the novel object; greater than 50% of time with the novel object indicates intact recognition memory function, while $\leq$ 50% of time with the novel object indicates impaired recognition memory. In the frontal cortex and hippocampus, mRNA levels of TNFα and protein expression of GFAP, pIκB-α, COX-2, iNOS, and NOX2 were

significantly negatively associated with recognition memory ($P < 0.05$). CD68 mRNA in the hippocampus was significantly negatively associated with recognition memory (r = -0.45, $P < 0.01$), but a significant correlation was not observed with CD68 mRNA in the frontal cortex (r = -0.11, $P = 0.45$). Likewise, iNOS mRNA in the hippocampus was significantly negatively associated with recognition memory (r = -0.34, $P < 0.05$), but a significant correlation was not observed with iNOS mRNA in the frontal cortex (r = -0.16, $P = 0.28$). There was a trend for a negative correlation between COX-2 mRNA in the frontal cortex or hippocampus and recognition memory (r = -0.26, $P = 0.07$). Lastly, NOX2 mRNA in the frontal cortex was significantly negatively correlated with recognition memory (r = -0.42, $P < 0.01$), and there was a trend for a negative correlation with NOX2 mRNA in the hippocampus (r = -0.28, $P = 06$). **Supplemental Figures S3, S4, and S5** show that irradiated animals on the no BB diets tended to cluster at higher neuroinflammation/OS and glial activation and lower % time spent with the novel object, while all other groups (irradiated and non-irradiated on BB diets) clustered at lower neuroinflammation/OS and glial activation and higher % time with novel object.

Discussion

Previous work has established that HZE particle exposure causes prolonged detrimental changes in the CNS, including neuroinflammation, OS, and associated cognitive deficits, particularly in memory. These effects pose risks to the CNS of astronauts on exploratory missions, both during missions and upon return to Earth. However, the cellular and molecular mechanisms responsible for the detrimental CNS changes that occur post-irradiation are not clear. There are no clinically established strategies to attenuate the cognitive deficits that progress after radiation exposure, and putative (i.e., pre-clinical) countermeasures are limited and associated with side effects (9, 10).

Our study showed that whole-body exposure to 150 cGy ^{56}Fe produced recognition memory deficits on the NOR task and increased the mRNA and/or protein expression of neuroinflammatory factors (iNOS, COX-2, TNFα, pIκB-α), one mediator of oxidative stress (NOX2), and glial cell activation indicators CD68 (microglia) and GFAP (astrocytes) in the frontal cortex and hippocampus of rats 45 days after irradiation. Changes in neuroinflammation, OS, and glial activation were positively correlated with each other, and

negatively correlated with recognition memory function. All BB treatments (pre-, post-, pre-/post-irradiation) reduced ^{56}Fe-induced neuroinflammation, OS, glial activation, and recognition memory deficits.

Dietary interventions are a safe and accessible strategy to mitigate age and/or stressor-induced neuroinflammation, OS, and cognitive deficits. However, the effects of dietary interventions on HZE particle-induced CNS deficits have been minimally assessed. Of the few studies, the majority have investigated berry-supplemented diets and focused on the protective effects of berries as pre-treatments on HZE particle-induced acute neuroinflammation/OS (4, 13, 14) and prolonged cognitive deficits (5, 15), and on pre-/post-treatments on biochemical changes in the brain (14) and cognitive deficits (16). The biological effects of flavonoids (e.g., anthocyanins in BBs) have primarily been attributed to antioxidant and anti-inflammatory mechanisms such as directly scavenging ROS and inhibiting or modulating the expression of OS/inflammation-producing enzymes (11, 30). Therefore, to further characterize the mechanisms contributing to persistent HZE particle-induced neurodegenerative effects (i.e., neuroinflammation, OS, and cognitive deficits), BBs were selected as the dietary intervention for pre-, post-, and pre-/post-treatments in this study. The efficacy of antioxidant/anti-inflammatory BB supports the role of inflammation/OS in persistent ^{56}Fe -induced CNS changes and establishes cellular mechanisms responsive to pre- and/or post- irradiation dietary countermeasures.

In the present study, whole-body irradiation with 150 cGy ^{56}Fe produced deficits in recognition memory, assessed by the NOR task at 1-2 months post-irradiation, replicating prior findings (5, 25). We previously demonstrated that pre-feeding a BB supplemented diet for 2 months, followed by ^{56}Fe irradiation, and an un-supplemented control diet starting 1 week post-irradiation for 2-3 months can protect against deficits on the NOR task (5). In the present study, we found that post-treatment with a BB-supplemented diet can also attenuate ^{56}Fe-induced deficits in recognition memory, and that effects were similar to a pre-, and pre-/post-BB diet. These findings support the persistent role of neuroinflammation/OS in the development of memory deficits after irradiation, and demonstrate that treatments do not need to be present before irradiation for beneficial effects on recognition memory.

We did not find effects of ^{56}Fe irradiation and/or BB on RAWM performance (i.e., spatial memory) 1-2 months after irradiation. To our knowledge, the effects of HZE particle exposure on RAWM performance had not been previously assessed. However, similar maze tests have shown mixed effects of HZE particle exposure on spatial memory, which may depend on factors such as testing protocols, rodent age and sex, post-irradiation timepoint, and irradiation dose. For example, in studies using male rats on the radial arm maze, spatial deficits in reference memory, but not working memory or latency, were observed 2 months after 150 cGy ^{56}Fe (23), and deficits in several, but not all parameters (e.g., irradiated rats made more errors on the first 4 choices, but not total errors) were found 9 months after 100 cGy ^{56}Fe (31). In apoE3 mice, 3 Gy ^{56}Fe impaired water maze performance in females, but not males, 13 months after irradiation (32). On the Morris Water Maze, spatial memory deficits were observed in male rats one month after 150 cGy ^{56}Fe (16, 33).

Because the NOR and RAWM tasks both assess memory function mediated by the hippocampus and frontal cortex, it was somewhat unexpected that no irradiation-induced changes in RAWM performance were observed. A discrepancy in the effects of ^{56}Fe irradiation on recognition memory (NOR) and spatial memory (RAWM) may be due to differences in the types of memory and cognitive systems employed in each task. The NOR relies on a novelty spontaneous preference paradigm, while the RAWM relies on motivation to escape the water, speed, and accuracy of spatial navigation (34). Additionally, as latency to find the platform and number of errors made were low for all animals, it is possible that the RAWM was not sensitive enough to capture irradiation-induced deficits in spatial memory in the present study. Compared to aged rats (20-months old) (26), the animals in the current study found the platform faster, and committed about half the number of errors in finding the platform. Therefore, rats used in this study may have performed too well on the RAWM to detect changes between irradiated and non-irradiated groups. This observation could also be due to the amount of training involved in the RAWM (i.e. 5 trials/day for 5 days). A previous study demonstrated that mild impairments on the radial arm maze were eliminated with additional training (35). Finally, the RAWM was performed after the NOR task, and rats may have gained the ability to

process environmental information through NOR trials. Nonetheless, with too few deficits (i.e., errors) to attenuate, BB supplementation is unlikely to produce changes.

In the present study, exposure to 150 cGy ^{56}Fe increased the mRNA and protein expression of iNOS and COX-2 in the frontal cortex and hippocampus of rats 45 days after irradiation. INOS and COX-2 are enzymes induced by inflammatory insults to produce the pro-inflammatory molecules nitric oxide (NO) and prostaglandins (e.g., PGE_2), respectively. ^{56}Fe irradiation has been shown to increase brain protein expression of iNOS at 36 hours and 30 days, and of COX-2 up to three days post-irradiation (4, 14, 36). In these previous studies, pre-treatment with berry-supplemented diets attenuated the acute (22-48 hours) effects of ^{56}Fe on COX-2 protein (4), but not iNOS protein (14), and pre-/post-treatment attenuated ^{56}Fe -induced iNOS protein 30 days post-irradiation (14). In the present study, pre- and/or post-treatment with a 2% BB diet attenuated both protein and mRNA expression of iNOS and COX-2 in rat brains 45 days after ^{56}Fe irradiation. Therefore, the effects of pre-treatments on iNOS may manifest at later post-irradiation durations (e.g., 45 days in the current study), and post-treatments can have similar beneficial effects on iNOS and COX-2. Furthermore, our data indicate that BBs can target both gene and protein irradiation-induced upregulation of iNOS and COX-2 at the level of gene expression.

In addition to upregulating inflammatory enzymes, ^{56}Fe exposure increased brain mRNA levels of the pro-inflammatory cytokine TNFα 45 days after irradiation. Previous studies have shown mixed effects of HZE particle exposure on TNFα expression. Increased TNFα protein levels were found 1 month after combined exposure to proton and ^{56}Fe, but not ^{56}Fe alone (50 cGy) in the hippocampus of mice (37), and no changes in protein levels were observed 6 months after 100 cGy ^{56}Fe in the hippocampus of APP/PS1 mice (7). As with iNOS and COX-2, pre- and/or post-treatment with BB attenuated mRNA levels of TNFα in the frontal cortex and hippocampus of rat brains, indicating that TNFα can be targeted with anti-inflammatory/antioxidant dietary countermeasures, even after expression is initiated with irradiation.

To further investigate the molecular pathway responsible for changes in pro-inflammatory mediators, we assessed protein expression of IκB-α, and found increased phosphorylation 45 days after ^{56}Fe irradiation. When phosphorylated for degradation, IκB-

α releases transcription factor NF-κB to enter the nucleus where it initiates transcription of inflammatory genes, including COX-2, iNOS, and TNFα (38). The observed increase in phosphorylated IκB-α suggests that ^{56}Fe-induced upregulation of COX-2, iNOS, and TNFα may be mediated by increased translocation of NF-κB to the nucleus for gene expression. In support of this hypothesis, pIκB-α protein and COX-2, iNOS, and TNFα mRNA were significantly positively correlated. In the present study, pre- and/or post-treatment with BB attenuated ^{56}Fe-induced IκB-α phosphorylation, indicating reduced degradation of this NF-κB inhibitor. Therefore, BB may attenuate mRNA and protein expression of inflammatory mediators by targeting upstream regulators of gene transcription (i.e., IκB-α).

We observed that ^{56}Fe irradiation increased mRNA and protein expression of NOX2, an enzyme responsible for producing the free radical superoxide, which contributes to OS. Previous studies have also demonstrated ^{56}Fe -induced increases in NOX2 protein at 22-48 hours, attenuated by berry pre-treatments (4, 14) and 30 days post-irradiation, attenuated by berry pre-/post-treatments (14). In the present study, pre- and/or post-treatment with BB attenuated ^{56}Fe -induced NOX2 mRNA and protein expression 45 days after irradiation, demonstrating that dietary compounds can downregulate transcription and translation of this enzyme, and that treatments do not need to be present before irradiation for beneficial effects.

Neither radiation nor BB induced significant changes in Nrf2, an antioxidant transcription factor (39) or Cu/Zn-SOD, a cytoplasmic antioxidant enzyme (40). Previous work has shown that ^{56}Fe exposure increased Nrf2 in the hippocampus of rats 22-48 hours after irradiation (4), but did not produce changes 2 months after irradiation (41). Similarly, ^{56}Fe exposure increased brain levels of Cu/Zn-SOD at 36 hours, but not 30 days following irradiation (14). Therefore, endogenous antioxidant enzymes may increase shortly after radiation exposure as a defense mechanism to counteract excessive free radical production (e.g., by NOX2 and iNOS), but return to baseline levels by 30 days (14).

Studies using alternate stressor models and systems have shown that inflammation and OS can exacerbate each other in a reciprocal manner, resulting in a self-propelling cycle of tissue damage long after the initial stress response dissipates. High levels of NOX2-derived superoxide, iNOS-derived NO, and TNFα can induce NF-κB signaling to increase transcription of these mediators (40, 42), and NO can modulate NOX2 activity in

a feed-forward process (43). Our correlation analyses suggest that irradiation induces this cycle of neuroinflammation/OS, as significant positive correlations were found between NOX2 (i.e., OS) and TNFα, iNOS, COX-2, and pIκB-α (i.e., neuroinflammation), in addition to the pro-inflammatory correlations previously discussed.

The cellular mediators of HZE particle-induced neuroinflammation, OS, and other neurodegenerative effects have not been established, although glial cells (e.g., microglia and astrocytes) are thought to play a role (44). In particular, as the primary immune cells of the CNS, microglia are key regulators of neuroinflammation and OS, and have been implicated in the development of CNS deficits and risks for neurodegeneration following many stressors (30). Through a cycle known as reactive gliosis, danger/damage signals (e.g., inflammatory cytokines and ROS/RNS) cause microglia to change from a quiescent phenotype to an activated phenotype, prompting the upregulation of inflammatory/OS-inducing enzymes. The resulting production of cytotoxic factors such as TNFα, ROS/RNS, and PGE_2 perpetuates glial cell activation and neuronal damage, leading to chronic detrimental processes (45). Given that neuroinflammation and OS increase following HZE particle exposures, glial cells in reactive gliosis are one of the putative targets in mediating HZE particle-induced CNS changes.

In the present study, 150 cGy ^{56}Fe increased CD68 mRNA, a scavenger receptor indicative of activated microglia (46, 47) in the frontal cortex and hippocampus of rats 45 days after exposures. CD68 mRNA was positively correlated with mRNA and/or protein expression of iNOS, COX-2, TNFα and NOX2, suggesting that ^{56}Fe may induce reactive gliosis as a cause and/or result of neuroinflammation/OS. Previous research on microglial responses to HZE particles is both limited and equivocal, and alterations may be sex-specific. Several studies in male mice have demonstrated HZE particle-induced increases in microglia activation, as indicated by CD68/ED-1 expression from 1 to 9 months post-irradiation (48, 49), and depletion of microglia can limit irradiation-induced biochemical change in the brain and cognitive deficits (50). However, other studies in male mice did not find HZE particle-induced changes in CD68/ED-1 (7, 18, 47, 51, 52) using a similar range of doses, HZE-particles, and post-irradiation durations. Reasons for the discrepancy in findings are unclear.

We observed that pre- and/or post-treatment with BB attenuated ^{56}Fe -induced increases in CD68 mRNA, although only in the hippocampus. A non-significant effect of BB on CD68 mRNA in the frontal cortex could be due to region specific alterations in irradiation-induced pro-inflammatory environments, as previously reported (53), inter-animal variability in the effects of BB on CD68 mRNA expression, or a less detrimental radiation effect to attenuate in the frontal cortex. Our findings suggest that microglia are involved in the neuroinflammatory/OS-inducing effects of HZE particle exposure, and are one of the cellular targets responsive to dietary strategies even after activation. In a recent *in vitro* study, we demonstrated that pre-, post-, and pre-/post-BB can attenuate LPS-induced neuroinflammation and OS in microglia (54). Therefore, antioxidant/anti-inflammatory treatments may act through direct mechanisms to reduce microglial activation and/or exert effects indirectly, such as by downregulating activation signals in the surrounding environment (e.g., neuroinflammation/OS mediators in reactive gliosis).

In addition to adopting an activated phenotype, microglia respond to stressors by accumulating in a site of stress. Iba-1 is an indicator for all microglia (activated and non-activated) (55), and can therefore demonstrate infiltration and/or proliferation of microglia to the frontal cortex or hippocampus. Unlike CD68, we did not find differences in the number of Iba-1 labeled cells between irradiated and non-irradiated animals, or changes with BB 45 days after ^{56}Fe exposure. Previous studies have observed increases in Iba-1 immunolabeling at 6 hours (56), but not at 24 hours, 3 weeks, or 2 months after ^{56}Fe irradiation in brain regions of male mice (7, 18, 56). Therefore, it is possible that microglia proliferate and/or infiltrate immediately after irradiation in the resolution phase of the immune response (45).

We observed that ^{56}Fe irradiation also induced astrocyte activity, as indicated by increased GFAP protein, which has been previously demonstrated following HZE particle exposures at acute (57, 58) and long-term post-irradiation timepoints (57, 59). As with microglia, activated astrocytes release pro-inflammatory cytokines, ROS, and RNS to perpetuate reactive gliosis and neuronal damage (45) following stressors. In support of the hypothesized role of reactive gliosis in HZE particle-induced effects, we found significant positive correlations between CD68 mRNA and GFAP protein, and between GFAP and TNFα, COX-2, iNOS, and NOX2. Although stressor-induced reactive gliosis involves both

microglia and astrocytes, it is hypothesized that astrocyte activation requires microglial-derived soluble factors. An *in vitro* study found that X-ray irradiation produced no effect on astrocyte activation, but incubating astrocytes with cell conditioned media from irradiated microglia increased GFAP immunostaining and produced morphological changes indicating a reactive state (60). Similar changes were observed by incubating astrocytes with PGE_2 (produced by COX-2) and TNFα, indicating that these pro-inflammatory molecules released from microglia may induce astrocyte activation following irradiation. We found that pre- and/or post-treatment with antioxidant/anti-inflammatory BBs reduced ^{56}Fe-induced GFAP expression, further suggesting that astrocytes are involved in the neuroinflammatory/OS-inducing effects of HZE particle exposure, and are responsive to dietary strategies.

Findings from the current study combined with previous work demonstrate that the effects of HZE particles on the CNS are the result of multicellular and multifactorial processes. Biochemical results show that ^{56}Fe irradiation produces persistent neuroinflammation, OS, and glial cell activation 45 days after irradiation, and these changes are correlated with each other. The current observation that BB post-treatment attenuated ^{56}Fe -induced neuroinflammation, OS, and glial cell activation indicates that these processes remain active targets for countermeasures after the immediate response to irradiation, which may be due to reactive gliosis. Additionally, recognition memory scores were significantly negatively correlated with CD68 mRNA (hippocampus only), TNFα mRNA, and the mRNA and/or protein expression of NOX2, COX-2, iNOS, GFAP, and pIκB-α. Similarly, previous work has found negative correlations between numbers of newly born activated microglia in the hippocampus and novel object recognition (37) scores in mice, and between brain OS and radial arm maze performance (i.e., reference memory) in rats exposed to HZE particles. These associations indicate that neuroinflammation and OS are involved in the development of memory deficits, which may be mediated by activated microglia and astrocytes through reactive gliosis.

Although speculative at the time, we hypothesize that ^{56}Fe irradiation initiates reactive gliosis by activating the NF-κB pathway through IκB-α phosphorylation, resulting in the expression of pro-inflammatory enzymes and cytokines (e.g., COX-2, iNOS, TNFα) **(Figure 10).** The production of soluble pro-inflammatory factors such as PGE_2 and NO by

these enzymes, in addition to TNFα, may occur initially in microglia, which then induces astrocyte activation and further microglial activation. We propose that inflammatory mediators upregulate NOX2 to exacerbate OS, and these processes continue in a positive feedback loop, resulting in neurodegeneration and cognitive decline. BB may act by directly blocking the transcription of inflammatory factors (e.g., by reducing IκB-α degradation) and/or indirectly by scavenging downstream mediators (e.g., ROS, NO) to intercept the cycle of reactive gliosis. Therefore, countermeasures targeting the expression of neuroinflammatory and OS mediators, at the level of transcription and/or translation, may attenuate the HZE particle-induced neuroinflammation, OS, cognitive deficits, and other mechanisms associated with neurodegeneration.

When the effects of irradiation and BB were significant, pre- and/or post-treatment did not produce differential effects on ^{56}Fe-induced neuroinflammation, OS, or recognition memory deficits. As such, the cellular and molecular targets in this study can be attenuated by preventative and therapeutic strategies. This may be because the same pathways and mechanisms are involved in the immediate and longer-term effects of HZE particle irradiation (e.g., reactive gliosis). Additionally, the beneficial effects of BB may occur early after initiation of the stress response. Although we administered post-treatments for 45 days after HZE-irradiation, early attenuation of pathogenic mechanisms may be necessary to prevent the propagation of detrimental CNS effects long-term after stressors. For example, it has been hypothesized that reducing initial damage from radiotherapy to the brain vasculature and parenchyma prevents the progression of damage, even though the most severe residual effects of radiotherapy are observed months to years after exposures (61). Although it is unknown how long BB metabolites are retained in the brain, it is unlikely that BB pre-treatments were fully metabolized by the time irradiation occurred in this study. Therefore, pre- and post-treatments may have produced similar effects because sufficient BB was available to target an early critical period.

As pre-/post-treatments did not provide additional benefit beyond pre- or post-treatments, there may be a dose and/or duration threshold for the beneficial effects of BBs. For some outcomes, pre- or post-treatment fully ameliorated the effects of irradiation (i.e., within pre- or post-BB, no difference between irradiated and non-irradiated animals).

Because basal levels of neuroinflammation and OS are necessary to maintain homeostasis in the brain, additional BB consumption with pre-/post-treatments could not attenuate these outcomes further without potentially producing a deleterious effect. Future investigation on the therapeutic window required for the beneficial effects of antioxidant/anti-inflammatory foods on irradiation-induced CNS deficits is warranted.

Overall, findings from this study add to the body of literature on the effects of HZE particles in cosmic radiation on the CNS and potential targets responsive to countermeasures. However, several limitations exist. The dose of ^{56}Fe used in this study (150 cGy) is higher than expected HZE particle exposures expected on exploratory space missions. Future studies should assess the effects of antioxidant/anti-inflammatory post-treatments on CNS deficits induced by additional HZE particles, doses, and combinations of particles. While this study suggests that microglia and astrocytes are involved in HZE-induced neuroinflammation and OS via correlation analyses, the causality of these effects remain to be established. In other words, it is not clear from this study if activated microglia and/or astrocytes are the initial cause of HZE particle-induced neuroinflammation/OS, become activated in response to neuroinflammation/OS originating elsewhere (e.g., damaged neurons), or both. Determining whether antioxidant/anti-inflammatory treatments reduce glial activation by attenuating endogenously produced signals and/or signals originating from other cells would optimize countermeasure efficacy. Nonetheless, this work establishes glial cells as putative potential targets for countermeasures administered before and/or after HZE particle exposure. Finally, irradiation-induced alterations in additional processes such as apoptosis, demyelination, inhibition of neurogenesis, changes in neurotransmission, and damage to the blood-brain-barrier likely also contribute to and/or result from the increases in neuroinflammation, OS, and glial activation observed in this study. Evaluating the effects of post-treatments on these multi-factorial and multi-cellular responses is necessary to advance understanding of mechanisms and therapeutic targets for HZE particle-induced CNS damage.

To conclude, we found that persistent increases in ^{56}Fe-induced neuroinflammation, OS, glial cell activation, and recognition memory deficits can be attenuated by administering BB before, after, or both before and after ^{56}Fe exposure. The mitigating effects of BB post-treatments supports the role of neuroinflammation and OS in

stressor-induced CNS deficits, including memory deficits at 45 days post-irradiation. Furthermore, microglia and astrocytes are targets for dietary treatments, before and/or after activation by irradiation. Although mechanisms are not definitive, correlation analyses suggest that a feed-forward cycle of glial cell activation, neuroinflammation, and OS mediates HZE-particle induced CNS deficits. These findings support the use of dietary intervention with antioxidant and anti-inflammatory properties even after neuroinflammation and OS are initiated. Therefore, dietary post-treatments can contribute to reducing the risk of neurodegenerative disease following HZE exposure in cosmic radiation, and may provide therapeutic value following other neuroinflammation and OS-inducing stressors (e.g., stroke, traumatic brain injury). Future studies *in vivo* using animal models and in the clinical setting are necessary to evaluate the therapeutic potential and mechanistic targets of dietary post-treatments as countermeasures for the detrimental CNS effects of HZE particles and other stressors.

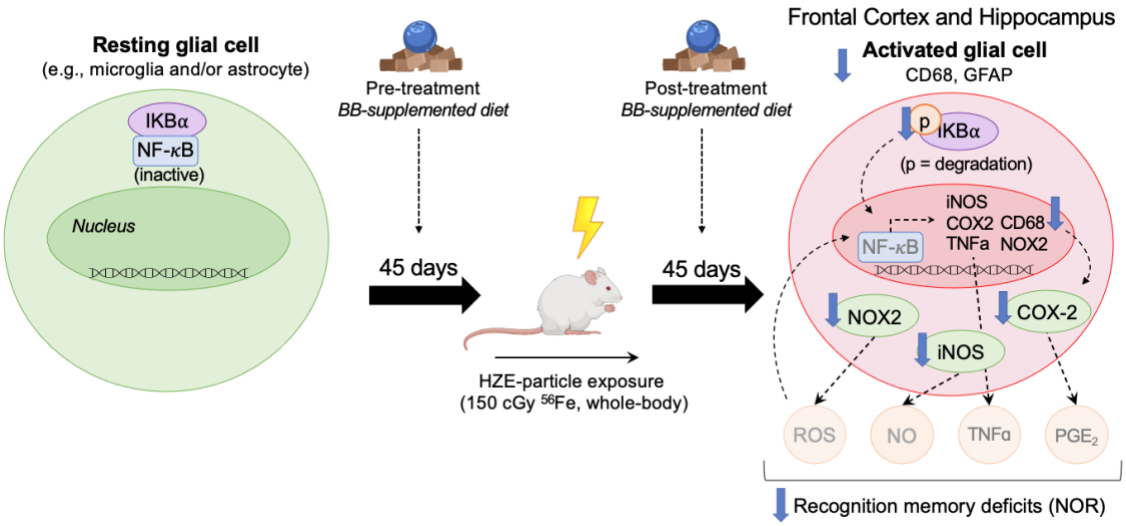

Figure 10. Cascade of neuroinflammatory and OS-inducing events associated with ^{56}Fe irradiation and the attenuating effects of pre- and/or post-^{56}Fe BB.
The effects of blueberry (2% supplemented diet) administered before and/or after 150 cGy ^{56}Fe on neuroinflammation and OS indices are shown in blue arrows. Factors in grey were not assessed in this study. BB, blueberry; COX-2, cyclooxygenase-2; IκB-α, inhibitor kappa-B-α; iNOS, inducible nitric oxide synthase; NF-κB, nuclear factor kappa-B; NO, nitric oxide; NOX2, NADPH oxidase; OS, oxidative stress; PGE_2, prostaglandin E_2; ROS, reactive oxygen species; TNFα, tumor necrosis factor-α

Financial Support

This work was supported by USDA intramural funding and NASA Grants NNJ16HP45I and NNX16AE06G.

Disclosure of Interest

The authors report no conflict of interest.

Data Availability Statement

All data are available upon request.

References

1. Rabin BM, Shukitt-Hale B. A voyage to Mars: Space radiation, aging, and nutrition. Nutrition and Aging 2014;2(4):233-41. doi: 10.3233/nua-140045.
2. Norbury JW, Slaba TC. Space radiation accelerator experiments - The role of neutrons and light ions. Life Sciences in Space Research 2014;3:90-4. doi: 10.1016/j.lssr.2014.09.006.
3. Durante M, Cucinotta FA. Heavy ion carcinogenesis and human space exploration. Nature Reviews Cancer 2008;8(6):465-72. doi: 10.1038/nrc2391.
4. Poulose SM, Rabin BM, Bielinski DF, Kelly ME, Miller MG, Thanthaeng N, Shukitt-Hale B. Neurochemical differences in learning and memory paradigms among rats supplemented with anthocyanin-rich blueberry diets and exposed to acute doses of (56)Fe particles. Life Sciences in Space Research 2017;12:16-23. doi: 10.1016/j.lssr.2016.12.002.
5. Rabin BM, Carrihill-Knoll K, Hinchman M, Shukitt-Hale B, Joseph JA, Foster BC. Effects of heavy particle irradiation and diet on object recognition memory in rats. Advances in Space Research 2009;43(8):1193-9. doi: 10.1016/j.asr.2009.01.015.
6. Britten RA, Davis LK, Jewell JS, Miller VD, Hadley MM, Sanford LD, Machida M, Lonart G. Exposure to mission relevant doses of 1 GeV/Nucleon 56Fe particles leads to impairment of attentional set-shifting performance in socially mature rats. Radiation Research 2014;182(3):292-8. doi: 10.1667/RR3766.1.

7. Cherry JD, Liu B, Frost JL, Lemere CA, Williams JP, Olschowka JA, O'Banion MK. Galactic cosmic radiation leads to cognitive impairment and increased abeta plaque accumulation in a mouse model of Alzheimer's disease. PLoS ONE 2012;7(12):e53275. doi: 10.1371/journal.pone.0053275.
8. Parihar VK, Maroso M, Syage A, Allen BD, Angulo MC, Soltesz I, Limoli CL. Persistent nature of alterations in cognition and neuronal circuit excitability after exposure to simulated cosmic radiation in mice. Neuroscience Letters 2018;305(2018):44-55. doi: 10.1016/j.expneurol.2018.03.009.
9. Stone HB, Moulder JE, Coleman CN, Ang KK, Anscher MS, Barcellos-Hoff MH, Dynan WS, Fike JR, Grdina DJ, Greenberger JS, et al. Models for Evaluating Agents Intended for the Prophylaxis, Mitigation and Treatment of Radiation Injuries Report of an NCI Workshop. Radiation Research 2006;162(6):711-28. doi: 10.1667/rr3276.
10. Pariset E, Malkani S, Cekanaviciute E, Costes SV. Ionizing radiation-induced risks to the central nervous system and countermeasures in cellular and rodent models. International Journal of Radiation Biology 2021;97(sup1):S132-S50. doi: 10.1080/09553002.2020.1820598.
11. Debnath-Canning M, Unruh S, Vyas P, Daneshtalab N, Igamberdiev AU, Weber JT. Fruits and leaves from wild blueberry plants contain diverse polyphenols and decrease neuroinflammatory responses in microglia. Journal of Functional Foods 2020;68(2020). doi: 10.1016/j.jff.2020.103906.
12. Andres-Lacueva C, Shukitt-Hale B, Galli RL, Jauregui O, Lamuela-Raventos RM, Joseph JA. Anthocyanins in aged blueberry-fed rats are found centrally and may enhance memory. Nutritional Neuroscience 2005;8(2):111-20. doi: 10.1080/10284150500078117.
13. Shukitt-Hale B, C. Lau F, Cheng V, Luskin K, N. Carey A, Carrihill-Knoll K, M. Rabin B, A. Joseph J. Changes in Gene Expression in the Rat Hippocampus Following Exposure to 56Fe Particles and Protection by Berry Diets. Central Nervous System Agents in Medicinal Chemistry 2013;13(1):36-42. doi: 10.2174/1871524911313010006.

14. Poulose SM, Bielinski DF, Carrihill-Knoll KL, Rabin BM, Shukitt-Hale B. Protective effects of blueberry- and strawberry diets on neuronal stress following exposure to 56Fe particles. Brain Research 2014;1593:9-18. doi: 10.1016/j.brainres.2014.10.028.
15. Rabin BM, Joseph JA, Shukitt-Hale B. Effects of age and diet on the heavy particle-induced disruption of operant responding produced by a ground-based model for exposure to cosmic rays. Brain Research 2005;1036(1-2):122-9. doi: 10.1016/j.brainres.2004.12.041.
16. Shukitt-Hale B, Carey AN, Jenkins D, Rabin BM, Joseph JA. Beneficial effects of fruit extracts on neuronal function and behavior in a rodent model of accelerated aging. Neurobiology of Aging 2007;28(8):1187-94. doi: 10.1016/j.neurobiolaging.2006.05.031.
17. Limoli CL, Giedzinski E, Baure J, Rola R, Fike JR. Redox changes induced in hippocampal precursor cells by heavy ion irradiation. Radiat Environ Biophys 2007;46(2):167-72. doi: 10.1007/s00411-006-0077-9.
18. Liu B, Hinshaw RG, Le KX, Park MA, Wang S, Belanger AP, Dubey S, Frost JL, Shi Q, Holton P, et al. Space-like 56Fe irradiation manifests mild, early sex-specific behavioral and neuropathological changes in wildtype and Alzheimer's-like transgenic mice. Scientific Reports 2019;9(1):1-17. doi: 10.1038/s41598-019-48615-1.
19. Krukowski K, Grue K, Frias ES, Pietrykowski J, Jones T, Nelson G, Rosi S. Female mice are protected from space radiation-induced maladaptive responses. Brain, Behavior, and Immunity 2018;74(August):106-20. doi: 10.1016/j.bbi.2018.08.008.
20. Rabin BM, Carrihill-Knoll KL, Long LV, Pitts SC, Hale BS. Effects of 17B-Estradiol on Cognitive Performance of Ovariectomized Female Rats Exposed to Space Radiation. Journal of Behavioral and Brain Science 2013;03(01):67-73. doi: 10.4236/jbbs.2013.31007.
21. Rabin BM, Miller MG, Larsen A, Spadafora C, Zolnerowich NN, Dell'Acqua LA, Shukitt-Hale B. Effects of exposure to 12C and 4He particles on cognitive

performance of intact and ovariectomized female rats. Life Sciences in Space Research 2019;22(June):47-54. doi: 10.1016/j.lssr.2019.07.005.

22. Youdim KA, Shukitt-Hale B, Martin A, Wang H, Denisova N, Bickford PC, Joseph JA. Short-Term Dietary Supplementation of Blueberry Polyphenolics: Beneficial Effects on Aging Brain Performance and Peripheral Tissue Function. Nutritional Neuroscience 2000;3(6):383-97. doi: 10.1080/1028415X.2000.11747338.
23. Denisova NA, Shukitt-Hale B, Rabin BM, Joseph JA. Brain signaling and behavioral responses induced by exposure to 56Fe-particle radiation. Radiation Research 2002;158(6):725-34. doi: 10.1667/0033-7587(2002)158[0725:BSABRI]2.0.CO;2.
24. La Tessa C, Sivertz M, Chiang IH, Lowenstein D, Rusek A. Overview of the NASA space radiation laboratory. Life Sciences in Space Research 2016;11:18-23. doi: 10.1016/j.lssr.2016.10.002.
25. Casadesus G, Shukitt-Hale B, Cantuti-Castelvetri I, Rabin BM, Joseph JA. The effects of heavy particle irradiation on exploration and response to environmental change. Advances in Space Research 2004;33(8):1340-6. doi: 10.1016/j.asr.2003.12.011.
26. Shukitt-Hale B, Thangthaeng N, Miller MG, Poulose SM, Carey AN, Fisher DR. Blueberries Improve Neuroinflammation and Cognition differentially Depending on Individual Cognitive baseline Status. Journals of Gerontology - Series A Biological Sciences and Medical Sciences 2019;74(7):977-83. doi: 10.1093/gerona/glz048.
27. Poulose SM, Bielinski DF, Carey A, Schauss AG, Shukitt-Hale B. Modulation of oxidative stress, inflammation, autophagy and expression of Nrf2 in hippocampus and frontal cortex of rats fed with açaí-enriched diets. Nutritional Neuroscience 2017;20(5):305-15. doi: 10.1080/1028415X.2015.1125654.
28. Poulose SM, Fisher DR, Larson J, Bielinski DF, Rimando AM, Carey AN, Schauss AG, Shukitt-Hale B. Anthocyanin-rich acai (Euterpe oleracea Mart.) fruit pulp fractions attenuate inflammatory stress signaling in mouse brain BV-2

microglial cells. J Agric Food Chem 2012;60(4):1084-93. doi: 10.1021/jf203989k.

29. Livak KJ, Schmittgen TD. Analysis of relative gene expression data using real-time quantitative PCR and the 2-ΔΔCT method. Methods 2001;25(4):402-8. doi: 10.1006/meth.2001.1262.
30. Cianciulli A, Porro C, Calvello R, Trotta T, Lofrumento DD, Panaro MA. Microglia mediated neuroinflammation: Focus on PI3K modulation. Biomolecules 2020;10(1):1-19. doi: 10.3390/biom10010137.
31. Shukitt-Hale B, Casadesus G, Cantuti-Castelvetri I, Rabin BM, Joseph JA. Cognitive deficits induced by 56Fe radiation exposure. Advances in Space Research 2003;31(1):119-26. doi: 10.1016/s0273-1177(02)00878-5.
32. Villasana LE, Benice TS, Raber J. Long-term effects of 56Fe irradiation on spatial memory of mice: role of sex and apolipoprotein E isoform. International Journal of Radiation Oncology, Biology, Physics 2011;80(2):567-73. doi: 10.1016/j.ijrobp.2010.12.034.
33. Shukitt-Hale B, Casadesus G, McEwen JJ, Rabin BM, Joseph JA. Spatial Learning and Memory Deficits Induced by Exposure to Iron-56-Particle Radiation. Radiation Research 2000;154(1):28-33. doi: 10.1667/0033-7587(2000)154[0028:Slamdi]2.0.Co;2.
34. Belarbi K, Jopson T, Tweedie D, Arellano C, Luo W, Greig NH, Rosi S. TNF-alpha protein synthesis inhibitor restores neuronal function and reverses cognitive deficits induced by chronic neuroinflammation. Journal of Neuroinflammation 2012;9:23. doi: 10.1186/1742-2094-9-23.
35. Rosi S, Belarbi K, Ferguson RA, Fishman K, Obenaus A, Raber J, Fike JR. Trauma-induced alterations in cognition and Arc expression are reduced by previous exposure to 56Fe irradiation. Hippocampus 2012;22(3):544-54. doi: 10.1002/hipo.20920.
36. Rabin BM, Poulose SM, Carrihill-Knoll KL, Ramirez F, Bielinski DF, Heroux N, Shukitt-Hale B. Acute Effects of Exposure to 56Fe and 16O Particles on Learning and Memory. Radiation Research 2015;184(2):143-50. doi: 10.1667/rr13935.1.

37. Raber J, Allen AR, Sharma S, Allen B, Rosi S, Olsen RH, Davis MJ, Eiwaz M, Fike JR, Nelson GA. Effects of Proton and Combined Proton and (56)Fe Radiation on the Hippocampus. Radiation Research 2016;185(1):20-30. doi: 10.1667/RR14222.1.

38. Cheng A, Han C, Fang X, Sun J, Chen X, Wan F. Extractable and non-extractable polyphenols from blueberries modulate LPS-induced expression of iNOS and COX-2 in RAW264.7 macrophages via the NF-kappaB signalling pathway. Journal of the Science of Food and Agriculture 2016;96(10):3393-400. doi: 10.1002/jsfa.7519.

39. Sun GY, Chen Z, Jasmer KJ, Chuang DY, Gu Z, Hannink M, Simonyi A. Quercetin Attenuates Inflammatory Responses in BV-2 Microglial Cells: Role of MAPKs on the Nrf2 Pathway and Induction of Heme Oxygenase-1. PLoS ONE 2015;10(10):e0141509. doi: 10.1371/journal.pone.0141509.

40. Dringen R. Oxidative and antioxidative potential of brain microglial cells. Antioxidants & Redox Signaling 2005;7(9-10):1223-33. doi: 10.1089/ars.2005.7.1223.

41. Cahoon DS, Shukitt-Hale B, Bielinski DF, Hawkins EM, Cacioppo AM, Rabin BM. Effects of partial- or whole-body exposures to 56Fe particles on brain function and cognitive performance in rats. Life Sciences in Space Research 2020;27(July):56-63. doi: 10.1016/j.lssr.2020.07.006.

42. Bozic I, Savic D, Laketa D, Bjelobaba I, Milenkovic I, Pekovic S, Nedeljkovic N, Lavrnja I. Benfotiamine attenuates inflammatory response in LPS stimulated BV-2 microglia. PLoS ONE 2015;10(2):e0118372. doi: 10.1371/journal.pone.0118372.

43. Lijia Z, Zhao S, Wang X, Wu C, Yang J. A self-propelling cycle mediated by reactive oxide species and nitric oxide exists in LPS-activated microglia. Neurochemistry International 2012;61(7):1220-30. doi: 10.1016/j.neuint.2012.09.002.

44. Pazzaglia S, Briganti G, Mancuso M, Saran A. Neurocognitive Decline Following Radiotherapy: Mechanisms and Therapeutic Implications. Cancers (Basel) 2020;12(1). doi: 10.3390/cancers12010146.

45. Lumniczky K, Szatmári T, Sáfrány G. Ionizing radiation-induced immune and inflammatory reactions in the brain. Frontiers in Immunology 2017;8(MAY):1-13. doi: 10.3389/fimmu.2017.00517.

46. Perry VH, Teeling J. Microglia and macrophages of the central nervous system: The contribution of microglia priming and systemic inflammation to chronic neurodegeneration. Seminars in immunopathology 2013;35:601-12. doi: 10.1007/s00281-013-0382-8.

47. Raber J, Yamazaki J, Torres ERS, Kirchoff N, Stagaman K, Sharpton T, Turker MS, Kronenberg A. Combined Effects of Three High-Energy Charged Particle Beams Important for Space Flight on Brain, Behavioral and Cognitive Endpoints in B6D2F1 Female and Male Mice. Frontiers in Physiology 2019;10:179. doi: 10.3389/fphys.2019.00179.

48. Parihar VK, Allen BD, Caressi C, Kwok S, Chu E, Tran KK, Chmielewski NN, Giedzinski E, Acharya MM, Britten RA, et al. Cosmic radiation exposure and persistent cognitive dysfunction. Scientific Reports 2016;6(June):1-14. doi: 10.1038/srep34774.

49. Rola R, Sarkissian V, Obenaus A, Nelson GA, Otsuka S, Limoli CL, Fike JR. High-LET radiation induces inflammation and persistent changes in markers of hippocampal neurogenesis. Radiation Research 2005;164(4 Pt 2):556-60. doi: 10.1667/rr3412.1.

50. Acharya MM, Green KN, Allen BD, Najafi AR, Syage A, Minasyan H, Le MT, Kawashita T, Giedzinski E, Parihar VK, et al. Elimination of microglia improves cognitive function following cranial irradiation. Scientific Reports 2016;6:31545. doi: 10.1038/srep31545.

51. Rola R, Fishman K, Baure J, Rosi S, Lamborn KR, Obenaus A, Nelson GA, Fike JR. Hippocampal Neurogenesis and Neuroinflammation after Cranial Irradiation with 56Fe Particles. Radiation Research 2008;169(6):626-32. doi: 10.1667/rr1263.1.

52. Raber J, Fuentes Anaya A, Torres ERS, Lee J, Boutros S, Grygoryev D, Hammer A, Kasschau KD, Sharpton TJ, Turker MS, et al. Effects of Six Sequential Charged Particle Beams on Behavioral and Cognitive Performance in B6D2F1

Female and Male Mice. Frontiers in Physiology 2020;11:959. doi: 10.3389/fphys.2020.00959.

53. Lee WH, Sonntag WE, Mitschelen M, Yan H, Lee YW. Irradiation induces regionally specific alterations in pro-inflammatory environments in rat brain. International Journal of Radiation Biology 2010;86(2):132-44. doi: 10.3109/09553000903419346.

54. Cahoon DS, Fisher DR, Lamon-Fava S, Wu D, Zheng T, Shukitt-Hale B. Blueberry treatment administered before and/or after lipopolysaccharide stimulation attenuates inflammation and oxidative stress in rat microglial cells. Nutritional Neuroscience 2022:1-11. doi: 10.1080/1028415x.2021.2020404.

55. Walker DG, Lue LF. Immune phenotypes of microglia in human neurodegenerative disease: Challenges to detecting microglial polarization in human brains. Alzheimer's Research and Therapy 2015;7(1):1-9. doi: 10.1186/s13195-015-0139-9.

56. Encinas JM, Vazquez ME, Switzer RC, Chamberland DW, Nick H, Levine HG, Scarpa PJ, Enikolopov G, Steindler DA. Quiescent adult neural stem cells are exceptionally sensitive to cosmic radiation. Experimental Neurology 2008;210(1):274-9. doi: 10.1016/j.expneurol.2007.10.021.

57. Poulose SM, Bielinski DF, Carrihill-Knoll K, Rabin BM, Shukitt-Hale B. Exposure to 16 O-Particle Radiation Causes Aging-Like Decrements in Rats through Increased Oxidative Stress, Inflammation and Loss of Autophagy. Radiation Research 2011;176(6):761-9. doi: 10.1667/rr2605.1.

58. Cahoon DS, Rabin BM, Shukitt-Hale B. Effects of HZE particles exposure location and energy on brain inflammation and oxidative stress in rats. Radiation Research, Submitted February 2022.

59. Suman S, Rodriguez OC, Winters TA, Fornace AJ, Albanese C, Datta K. Therapeutic and space radiation exposure of mouse brain causes impaired dna repair response and premature senescence by chronic oxidant production. Aging 2013;5(8):607-22. doi: 10.18632/aging.100587.

60. Hwang SY, Jung JS, Kim TH, Lim SJ, Oh ES, Kim JY, Ji KA, Joe EH, Cho KH, Han IO. Ionizing radiation induces astrocyte gliosis through microglia activation. Neurobiology of Disease 2006;21(3):457-67. doi: 10.1016/j.nbd.2005.08.006.

61. Constanzo J, Midavaine É, Fouquet J, Lepage M, Descoteaux M, Kirby K, Tremblay L, Masson-Côté L, Geha S, Longpré JM, et al. Brain irradiation leads to persistent neuroinflammation and long-term neurocognitive dysfunction in a region-specific manner. Progress in Neuro-Psychopharmacology and Biological Psychiatry 2020;102(April):109954-. doi: 10.1016/j.pnpbp.2020.109954.

Supplemental Material

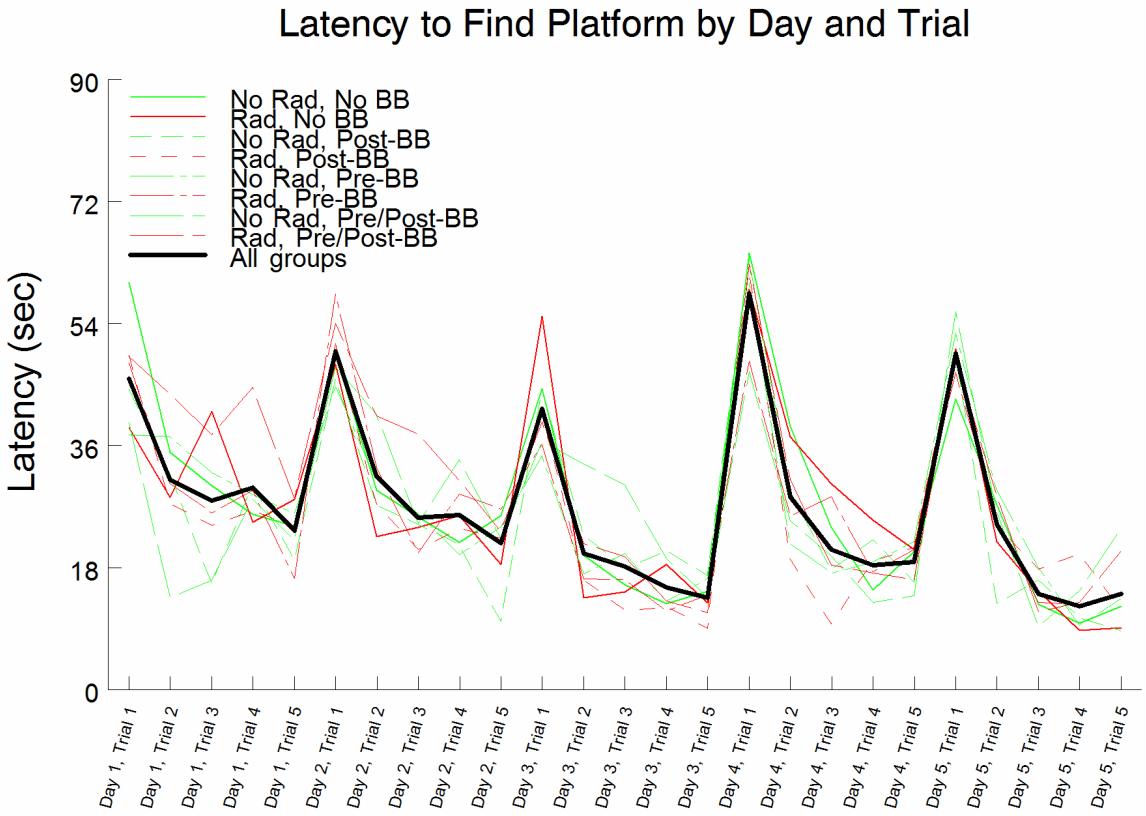

Figure S1. Latency to find the platform on the RAWM task by trial and day.

No Rad = 0 cGy ^{56}Fe, Rad = 150 cGy ^{56}Fe, No BB = neither pre- nor post-treatment with BB, Pre = only pre-treatment with BB, Post = only post-treatment with BB = Pre/Post, both pre- and post-treatment with BB.

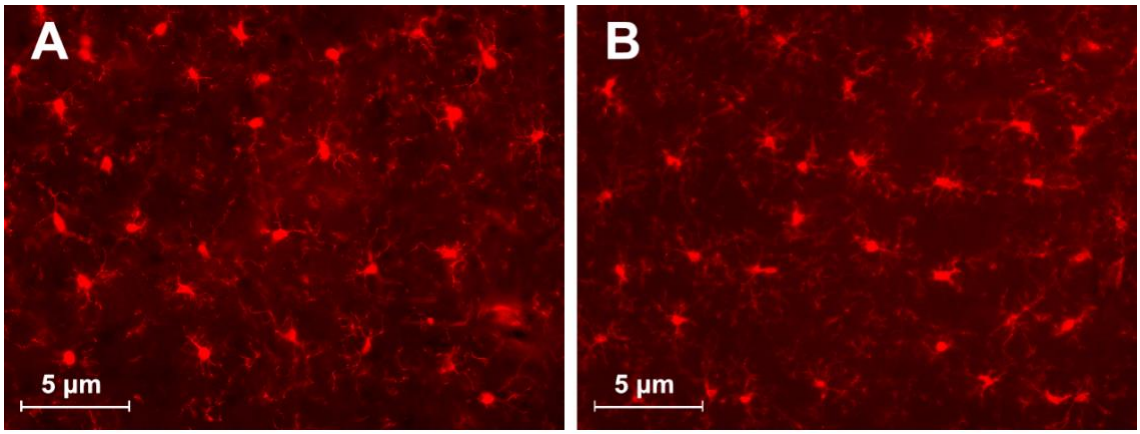

Figure S2. Iba-1 labeled microglia in the A) frontal cortex and B) hippocampus.

No Rad = 0 cGy ^{56}Fe, Rad = 150 cGy ^{56}Fe, No BB = neither pre- nor post-treatment with BB, Pre = only pre-treatment with BB, Post = only post-treatment with BB = Pre/Post, both pre- and post-treatment with BB.

Frontal Cortex		mRNA				Protein					
		COX2	iNOS	NOX2	TNFα	GFAP	pIKBα	COX2	iNOS	NOX2	NOR
mRNA	CD68	0.59	0.63	0.49^	0.65	0.50^	0.41	0.56^	0.69	0.64	-0.44
	COX2		0.60	0.57^	0.85	0.88	0.66	0.71	0.60	0.61	-0.42
	iNOS			0.58	0.76	0.56^	0.41	0.58	0.67	0.61	-0.30
	NOX2				0.70	0.71	0.69	0.75	0.64	0.65	-0.29
	TNFα					0.92	0.69	0.77	0.71	0.70	-0.46
Protein	GFAP						0.73	0.69	0.59	0.49	-0.68
	pIκBα							0.83	0.61	0.81	-0.61
	COX2								0.74	0.82	-0.63
	iNOS									0.77	-0.48
	NOX2										-0.47

Table S1. Correlation between indicators of neuroinflammation, OS, and glial cell activation in the frontal cortex, and memory function.

Pearson r values are reported for analyses including irradiated and non-irradiated animals on the control diet (n = 12 for correlations with mRNA, n = 18 for all other correlations). Blue = significant positive correlation ($P < 0.05$); red = significant negative correlation ($P < 0.05$); white = non-significant correlation; ^ = trend for correlation ($0.05 \leq P \leq 0.10$). Darker shading indicates stronger correlations (r = 0 to 1). NOR = novel object recognition score (% time with novel object).

Hippocampus		mRNA				Protein					
		COX2	iNOS	NOX2	TNFα	GFAP	pIKBα	COX2	iNOS	NOX	NOR
mRNA	CD68	0.80	0.73	0.75	0.70	0.79	0.66	0.85	0.59	0.79	-0.47^
	COX2		0.80	0.75	0.78	0.82	0.50^	0.91	0.59	0.75	-0.42
	iNOS			0.78	0.61	0.62	0.55^	0.90	0.41	0.53^	-0.42
	NOX2				0.81	0.61	0.84	0.77	0.70	0.72	-0.47
	TNFα					0.69	0.73	0.66	0.64	0.79	-0.38
Protein	GFAP						0.58	0.67	0.62	0.78	-0.64
	pIκBα							0.40^	0.59	0.58	-0.44^
	COX2								0.53	0.62	-0.54
	iNOS									0.79	-0.71
	NOX2										-0.58

Table S2. Correlation between indicators of neuroinflammation, OS, and glial cell activation in the hippocampus, and memory function.

Pearson r values are reported for analyses including irradiated and non-irradiated animals on the control diet (n = 12 for correlations with mRNA, n = 18 for all other correlations). Blue = significant positive correlation ($P < 0.05$); red = significant negative correlation ($P < 0.05$); white = non-significant correlation; * = trend for correlation ($0.05 \leq P \leq 0.10$). Darker shading indicates stronger correlations (r = 0 to 1). NOR = novel object recognition score (% time with novel object).

Parameter 1	Parameter 2	N (all grps)	FC all groups		HP all groups		N (no BB)	FC no BB		HP no BB	
			r	P	r	P		r	P	r	P
COX2 protein	iNOS protein	72	0.692	<0.001	0.456	<0.001	18	0.745	<0.001	0.530	0.024
COX2 protein	NOX2 protein	72	0.774	<0.001	0.428	<0.001	18	0.824	<0.001	0.624	0.006
COX2 protein	pIKBα protein	72	0.705	<0.001	0.313	0.007	18	0.831	<0.001	0.404	0.096
COX2 protein	GFAP protein	72	0.368	0.001	0.325	0.005	18	0.688	0.002	0.670	0.002
COX2 protein	NOR	72	-0.330	0.005	-0.351	0.002	18	-0.630	0.005	-0.538	0.021
iNOS protein	NOX2 protein	72	0.619	<0.001	0.594	<0.001	18	0.772	<0.001	0.791	<0.001
iNOS protein	pIKBα protein	72	0.490	<0.001	0.305	0.009	18	0.610	0.007	0.590	0.010
iNOS protein	GFAP protein	72	0.282	0.017	0.482	<0.001	18	0.590	0.010	0.623	0.006
iNOS protein	NOR	72	-0.236	0.046	-0.454	<0.001	18	-0.475	0.046	-0.710	0.001
NOX2 protein	pIKBα protein	72	0.780	<0.001	0.386	0.001	18	0.813	<0.001	0.583	0.011
NOX2 protein	GFAP protein	72	0.279	0.018	0.697	<0.001	18	0.490	0.039	0.781	<0.001
NOX2 protein	NOR	72	-0.297	0.011	-0.360	0.002	18	-0.470	0.049	-0.577	0.012
pIKBα protein	GFAP protein	72	0.416	<0.001	0.316	0.007	18	0.732	0.001	0.579	0.012
pIKBα protein	NOR	72	-0.419	<0.001	-0.303	0.010	18	-0.611	0.007	-0.444	0.065
GFAP protein	NOR	72	-0.339	0.004	-0.336	0.004	18	-0.675	0.002	-0.643	0.004
CD68 mRNA	COX2 mRNA	48	0.234	0.110	0.586	<0.001	12	0.586	0.045	0.800	0.002
CD68 mRNA	iNOS mRNA	48	0.288	0.047	0.589	<0.001	12	0.636	0.026	0.733	0.007
CD68 mRNA	NOX2 mRNA	48	0.293	0.043	0.614	<0.001	12	0.493	0.103	0.753	0.005
CD68 mRNA	TNFα mRNA	48	0.433	0.002	0.507	<0.001	12	0.652	0.022	0.689	0.013
CD68 mRNA	COX2 protein	48	0.376	0.008	0.627	<0.001	12	0.559	0.059	0.852	<0.001
CD68 mRNA	iNOS protein	48	0.257	0.078	0.536	<0.001	12	0.687	0.014	0.587	0.045
CD68 mRNA	NOX2 protein	48	0.320	0.027	0.631	<0.001	12	0.639	0.025	0.785	0.002
CD68 mRNA	pIKBα protein	48	0.311	0.031	0.272	0.062	12	0.412	0.184	0.658	0.020

CD68 mRNA	GFAP protein	48	0.332	0.021	0.609	<0.001	12	0.504	0.095	0.791	0.002
CD68 mRNA	NOR	48	-0.112	0.450	-0.452	0.001	12	-0.437	0.155	-0.473	0.121
COX2 mRNA	iNOS mRNA	48	0.344	0.017	0.534	<0.001	12	0.599	0.040	0.796	0.002
COX2 mRNA	NOX2 mRNA	48	0.387	0.007	0.493	<0.001	12	0.567	0.054	0.779	0.003
COX2 mRNA	TNFα mRNA	48	0.554	<0.001	0.405	0.004	12	0.852	<0.001	0.779	0.003
COX2 mRNA	COX2 protein	48	0.279	0.055	0.429	0.002	12	0.708	0.010	0.787	0.002
COX2 mRNA	iNOS protein	48	0.227	0.121	0.325	0.024	12	0.596	0.041	0.594	0.042
COX2 mRNA	NOX2 protein	48	0.288	0.047	0.441	0.002	12	0.607	0.036	0.750	0.005
COX2 mRNA	pIKBα protein	48	0.285	0.049	0.321	0.026	12	0.662	0.019	0.497	0.100
COX2 mRNA	GFAP protein	48	0.300	0.039	0.413	0.004	12	0.881	<0.001	0.819	0.001
COX2 mRNA	NOR	48	-0.262	0.072	-0.259	0.075	12	-0.421	0.173	-0.418	0.176
iNOS mRNA	NOX2 mRNA	48	0.242	0.097	0.491	<0.001	12	0.580	0.048	0.779	0.003
iNOS mRNA	TNFα mRNA	48	0.417	0.003	0.476	0.001	12	0.759	0.004	0.608	0.036
iNOS mRNA	COX2 protein	48	0.359	0.012	0.628	<0.001	12	0.580	0.048	0.907	<0.001
iNOS mRNA	iNOS protein	48	0.368	0.010	0.330	0.022	12	0.666	0.018	0.411	0.184
iNOS mRNA	NOX2 protein	48	0.359	0.012	0.414	0.003	12	0.615	0.033	0.528	0.077
iNOS mRNA	pIKBα protein	48	0.295	0.042	0.388	0.006	12	0.412	0.183	0.553	0.062
iNOS mRNA	GFAP protein	48	0.353	0.014	0.464	0.001	12	0.557	0.060	0.618	0.032
iNOS mRNA	NOR	48	-0.158	0.283	-0.335	0.020	12	-0.297	0.349	-0.422	0.172
NOX2 mRNA	TNFα mRNA	48	0.600	<0.001	0.557	<0.001	12	0.701	0.011	0.805	0.002
NOX2 mRNA	COX2 protein	48	0.326	0.024	0.385	0.007	12	0.747	0.005	0.772	0.003
NOX2 mRNA	iNOS protein	48	0.390	0.006	0.376	0.008	12	0.644	0.024	0.704	0.011
NOX2 mRNA	NOX2 protein	48	0.339	0.018	0.357	0.013	12	0.653	0.021	0.722	0.008
NOX2 mRNA	pIKBα protein	48	0.238	0.103	0.410	0.004	12	0.646	0.023	0.838	0.001
NOX2 mRNA	GFAP protein	48	0.103	0.485	0.349	0.015	12	0.710	0.010	0.606	0.037
NOX2 mRNA	NOR	48	-0.421	0.003	-0.276	0.057	12	-0.291	0.358	-0.472	0.121

TNFα mRNA	COX2 protein	48	0.376	0.008	0.432	0.002	12	0.766	0.004	0.658	0.020
TNFα mRNA	iNOS protein	48	0.297	0.040	0.413	0.004	12	0.710	0.010	0.634	0.027
TNFα mRNA	NOX2 protein	48	0.354	0.014	0.613	<0.001	12	0.699	0.011	0.787	0.002
TNFα mRNA	pIKBα protein	48	0.367	0.010	0.338	0.019	12	0.685	0.014	0.728	0.007
TNFα mRNA	GFAP protein	48	0.345	0.016	0.520	<0.001	12	0.918	<0.001	0.690	0.013
TNFα mRNA	NOR	48	-0.419	0.003	-0.366	0.011	12	-0.464	0.128	-0.385	0.216

Legend				
Highly significant	Significant	Moderately significant	Trend for significance	Not significant
$P < 0.001$	$0.001 \leq P < 0.01$	$0.01 \leq P < 0.05$	$0.05 \leq P < 0.10$	$P \leq 0.10$

Table S3. All data for correlations between indicators of neuroinflammation, OS, glial cell activation, and memory function Error! Not a valid bookmark self-reference.

'All groups' = analyses including all 8 study groups (n = 48 for correlations with mRNA, n = 72 for all other correlations). 'No BB' = analyses including irradiated and non-irradiated animals on the control diet (n = 48 for correlations with mRNA, n = 72 for all other correlations). BB = blueberry, FC = frontal cortex, HP = hippocampus, N = number of observation pairs, NOR = novel object recognition score (% time with novel object).

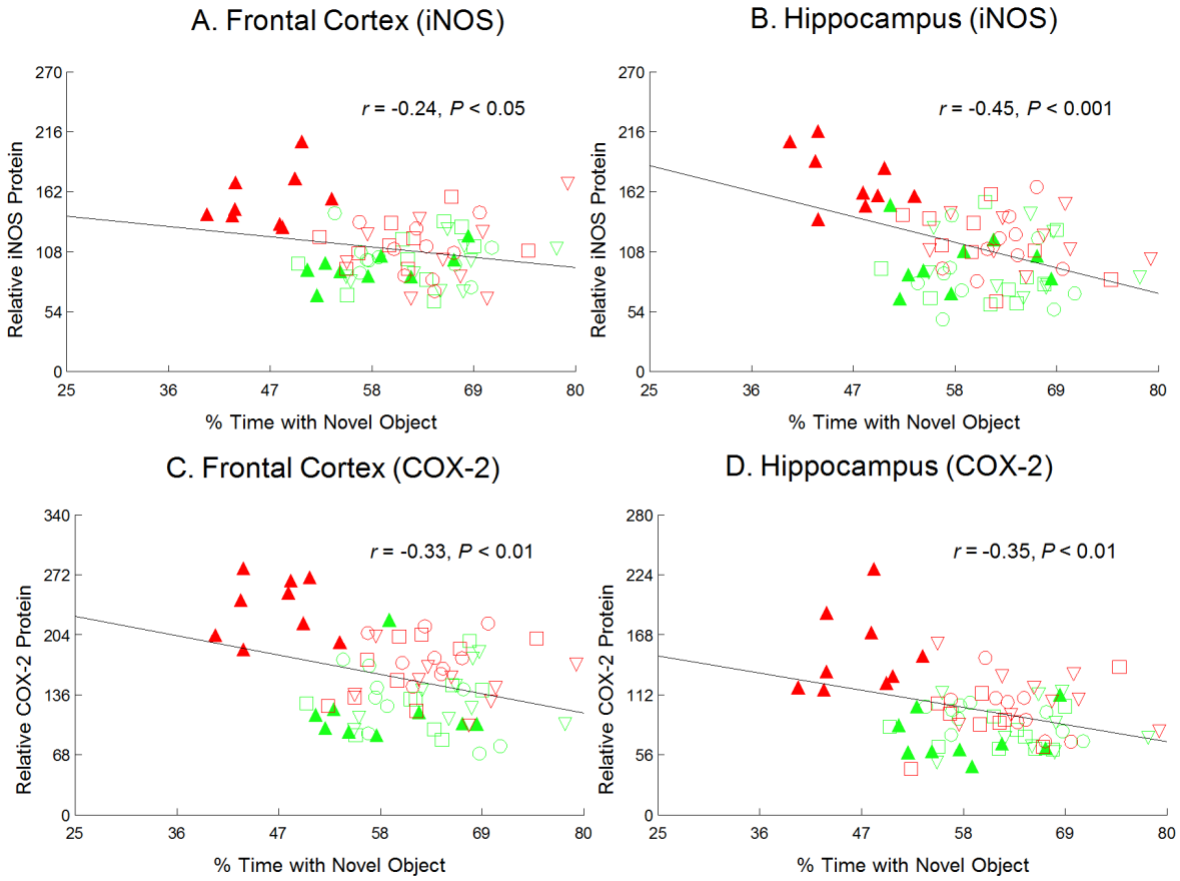

Figure S3. Correlation between protein expression of neuroinflammatory enzymes and recognition memory function.

Negative correlations between percent time with novel object on the NOR task and protein expression of A) iNOS in the frontal cortex, B) iNOS in the hippocampus, C) COX-2 in the frontal cortex and D) COX-2 in the hippocampus. Each correlation analysis included animals in all 8 study groups (n = 72 observation pairs). No BB = neither pre- nor post-treatment with BB (▲ No Rad [0 cGy ^{56}Fe], ▲ Rad [150 cGy ^{56}Fe]), Pre = only pre-treatment with BB (○ No Rad, ○ Rad), Post = only post-treatment with BB (□ No Rad, □ Rad), Pre/Post, both pre- and post-treatment with BB (▽ No Rad, ▽ Rad).

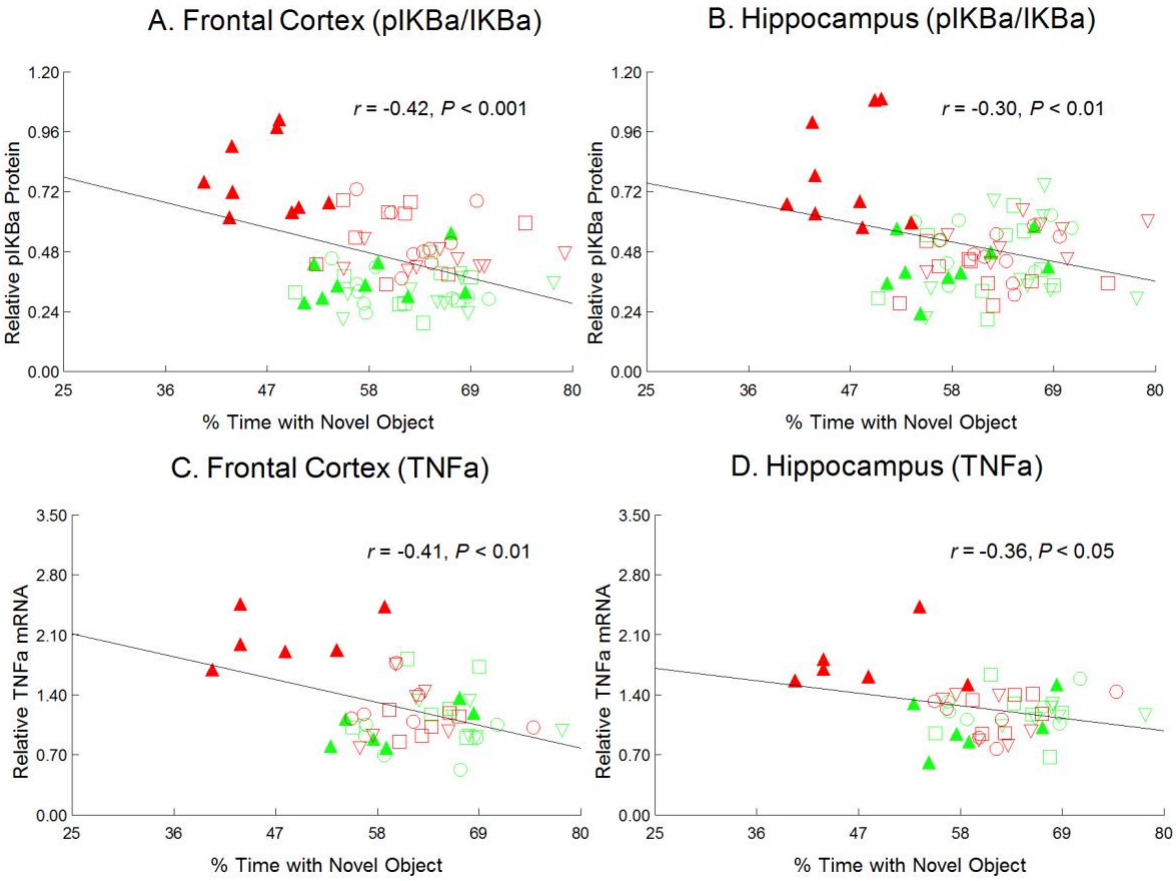

Figure S4. Correlation between protein expression of neuroinflammatory transcriptional regulator pIκB-α or mRNA levels of pro-inflammatory cytokine TNFα and recognition memory function.

Negative correlations between percent time with novel object on the NOR task and A) pIκB-α/IκB-α protein in the frontal cortex, B) pIκB-α/IκB-α protein in the hippocampus, C) TNFα mRNA in the frontal cortex and D) TNFα mRNA in the hippocampus. Each correlation analysis included animals in all 8 study groups (n = 72 observation pairs for pIκB-α/IκB-α protein, n = 48 observation pairs for TNFα mRNA). No BB = neither pre- nor post-treatment with BB (▲ No Rad [0 cGy ^{56}Fe], ▲ Rad [150 cGy ^{56}Fe]), Pre = only pre-treatment with BB (○ No Rad, ○ Rad), Post = only post-treatment with BB (□ No Rad, □ Rad), Pre/Post, both pre- and post-treatment with BB (▽ No Rad, ▽ Rad).

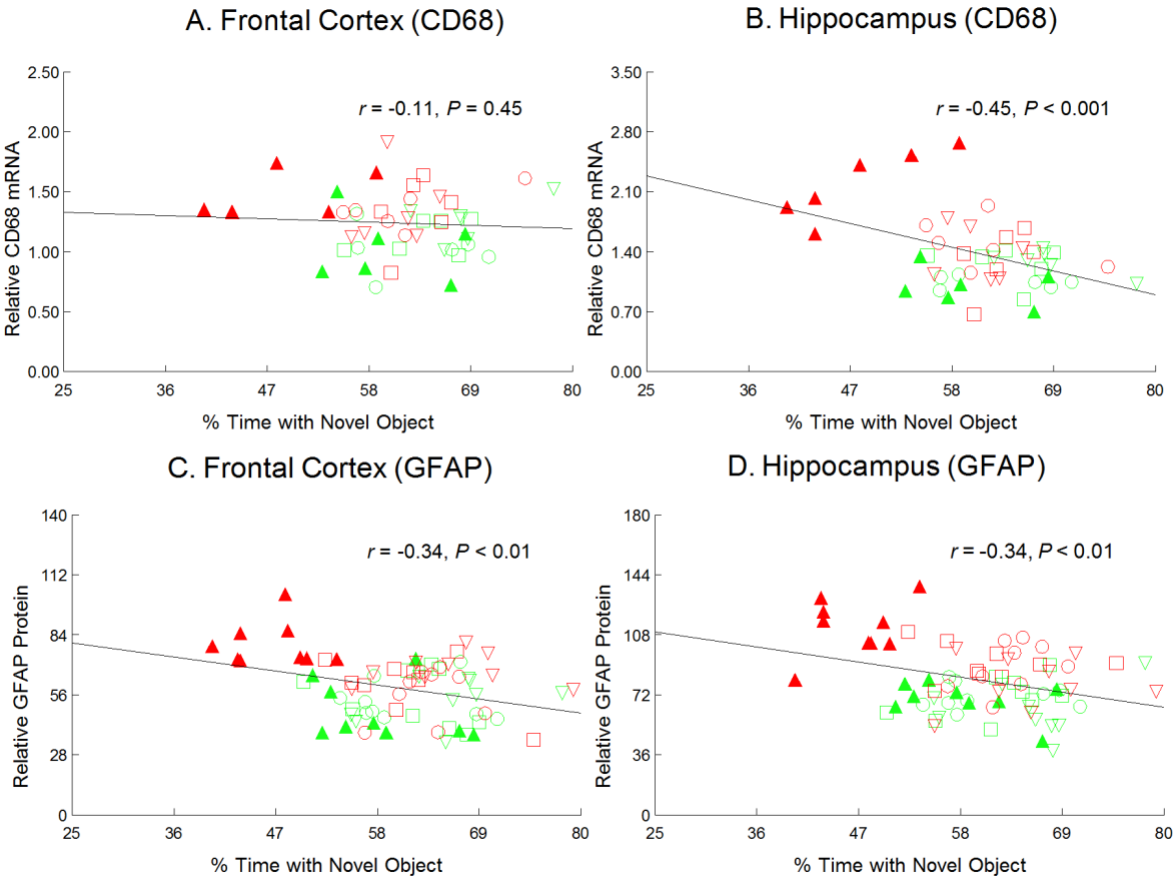

Figure S5. Correlation between glial cell activation indicators and recognition memory function.

Negative correlations between percent time with novel object on the NOR task and A) CD68 mRNA in the frontal cortex, B) CD68 mRNA in the hippocampus, C) GFAP protein in the frontal cortex and D) GFAP protein in the hippocampus. Each correlation analysis included animals in all 8 study groups (n = 48 observation pairs for CD68 mRNA, n = 72 observation pairs for GFAP protein). No BB = neither pre- nor post-treatment with BB (▲ No Rad [0 cGy ^{56}Fe], ▲ Rad [150 cGy ^{56}Fe]), Pre = only pre-treatment with BB (○ No Rad, ○ Rad), Post = only post-treatment with BB (□ No Rad, □ Rad), Pre/Post, both pre- and post-treatment with BB (▽ No Rad, ▽ Rad).

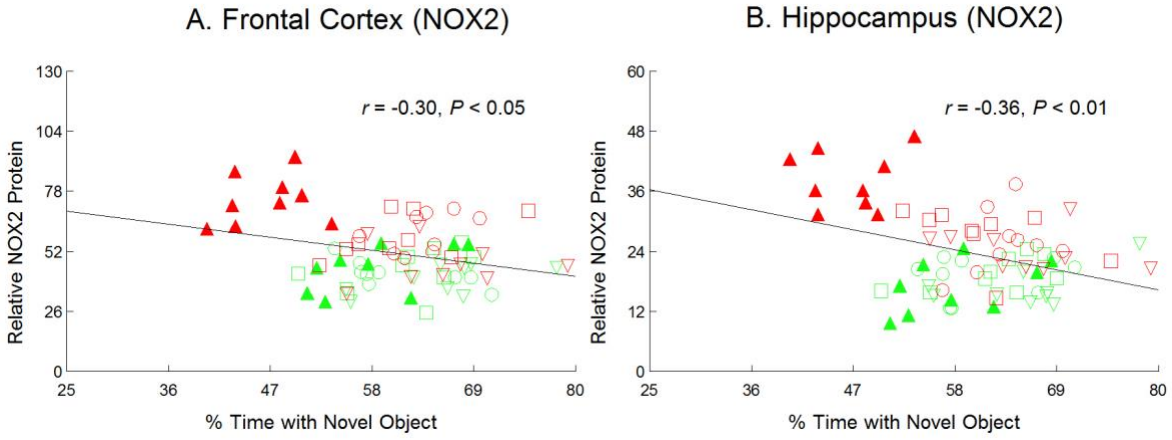

Figure S6. Correlation between OS-inducing enzyme NOX2 and recognition memory function.

Negative correlations between percent time with novel object on the NOR task and A) NOX2 protein in the frontal cortex and B) NOX2 protein in the hippocampus. Each correlation analysis included animals in all 8 study groups (n = 72 observation pairs). No BB = neither pre- nor post-treatment with BB (▲ No Rad [0 cGy ^{56}Fe], ▲ Rad [150 cGy ^{56}Fe]), Pre = only pre-treatment with BB (○ No Rad, ○ Rad), Post = only post-treatment with BB (□ No Rad, □ Rad), Pre/Post, both pre- and post-treatment with BB (▽ No Rad, ▽ Rad).

4 SUMMARY AND DISCUSSION

4.1 Research summary

Neuroinflammation and OS have been implicated as key risk factors involved in the development of neurodegeneration, and both increase with age and following exposure to acute neuropathological stressors. As the primary immune cells of the CNS, microglia are thought to regulate the production of inflammatory molecules and ROS/RNS in the brain to maintain homeostasis. However, excess and/or uncontrolled microglial activation can perpetuate neuroinflammation, OS, and neuronal damage, and the vicious cycle of reactive gliosis may be involved in the development of neurogenerative disease following stressors. Therefore, targeting neuroinflammation, OS, and activated microglia after stressor exposures may curb the progression of neurodegenerative processes leading to cognitive decline. Post-stressor nutritional treatments using foods with antioxidant and anti-inflammatory properties could be implemented as a safe and accessible long-term neuroprotective lifestyle strategy.

The objective of this work was to evaluate the effects and mechanistic targets of post-stressor BB, relative to no BB, pre-BB, and pre-/post-BB on neuroinflammation, OS, and cognitive deficits. We used both *in vitro* (microglia) and *in vivo* (rodents) models to address this objective. With the *in vitro* model, we assessed the effects of pre- and/or post-BB on the protein expression of stressor-induced inflammation and OS biomarkers in rat microglia using LPS and HZE particle irradiation as stressors. With the *in vivo* model, we assessed the effects of dietary BB- supplementation as a pre- and/or post-treatment on cognitive function (spatial and recognition memory) in male Sprague-Dawley rats exposed to ^{56}Fe or no radiation. Additionally, we assessed the mRNA and/or protein expression of neuroinflammation, OS, and glial cell activation indicators in the frontal cortex and hippocampus.

First, we showed that in microglia, LPS exposure *in vitro* increased the protein expression of inflammatory factors (NO_2^-, iNOS, COX-2, TNFα, pIκB-α), and one mediator of oxidative stress (NOX2) when assessed 24 hours after LPS washout. All BB treatment periods (pre-, post-, and pre-/post) attenuated LPS-induced increases in inflammation and OS markers. Therefore, BB not only produced a preventative anti-inflammatory/antioxidant effect, but it was also able to attenuate the stressor response when

administered after initiation of neuroinflammation and OS. We found that pre-BB was more effective than post- or pre-/post-BB at attenuating LPS-induced NO_2^- and TNFα, while for all other markers, BB treatments at different timepoints were similarly effective. The differential efficacy of pre- and post- or pre-/post-BB *in vitro* could be due to differences in transcriptional modulation, protein degradation, and/or hormetic effects, although mechanisms are unclear. Nonetheless, because LPS is a potent activator of microglia, these findings have provided insight on the molecular mechanisms involved in microglial responses to stressors. This study established a model for assessing the effects of pre- and/or post-treatments on stressor-induced inflammation/OS in microglia, and for identifying further molecular mechanisms responsive to dietary antioxidant/anti-inflammatory treatments.

Next, we assessed the effects of HZE particle irradiation on inflammation and OS in microglia using the same model and experimental design as aim 1a. Unlike LPS, previous findings on the effects of HZE particles on inflammation and OS in microglia had not been previously investigated *in vitro,* and the effect on microglial responses *in vivo* are equivocal. Somewhat unexpectedly, results showed that HZE particle irradiation (^{4}He or ^{56}Fe) did not increase the protein expression of COX-2, iNOS, pIκB-α, TNFα, NO_2^- or NOX2 compared to non-irradiated control conditions in microglial cells. Findings suggest that without signal from other cell types, microglia may not be the primary cause of neuroinflammation and OS following HZE particle exposures. Without a stress response induced by HZE particle exposure, BB treatments did not produce effects on inflammation or OS biomarkers in microglia, which should be maintained at basal levels (see Appendix 5.2).

Finally, we demonstrated that whole-body HZE particle (^{56}Fe) irradiation increased the mRNA and/or protein expression of inflammatory factors (iNOS, COX-2, TNFα, pIκB-α), one mediator of OS (NOX2), and glial activation indicators CD68 (microglia) and GFAP (astrocytes) 45 days after radiation exposure in the hippocampus and frontal cortex of male Sprague-Dawley rats. ^{56}Fe-induced increases in neuroinflammation, OS, and glial activation were positively correlated with each other and negatively correlated with recognition memory function, assessed by the NOR task. We found that BB treatments before, after, or both before and after irradiation reduced ^{56}Fe-induced increases in

neuroinflammation, OS, glial activation, and memory deficits, supporting the role of neuroinflammation and OS in stressor-induced CNS deficits. All BB treatments (pre-, post-, pre-/post-irradiation) were similarly effective at reducing neuroinflammation, OS, glial activation, and cognitive deficits, suggesting that similar processes are targeted before and after irradiation, and there may be a dose and/or time threshold effect for the attenuating effects of BB.

In summary, we determined that microglia are involved in stressor-induced neuroinflammation and OS. Further, microglia are one of the targets responsive to dietary antioxidant/anti-inflammatory treatments, even after stressor-induced activation occurs. A comparison of *in vitro* and *in vivo* approaches suggests that microglial responses to HZE particle irradiation may depend on signals from the brain's microenvironment. Therefore, dietary anti-inflammatory/antioxidant compounds may attenuate stressor-induced microglial activation by directly targeting microglia and/or by altering the surrounding signals. Nonetheless, these results demonstrate that neuroinflammation and OS can be attenuated by nutritional strategies even after these processes are initiated by stressors such as LPS *in vitro* and HZE particles *in vivo.* The proposed effects of stressors on neuroinflammation, OS, and cognitive deficits, and relationships between these factors are shown in **Figure 1.** The attenuating effects of BB on cellular and molecular mediators observed in this work are shown in blue arrows.

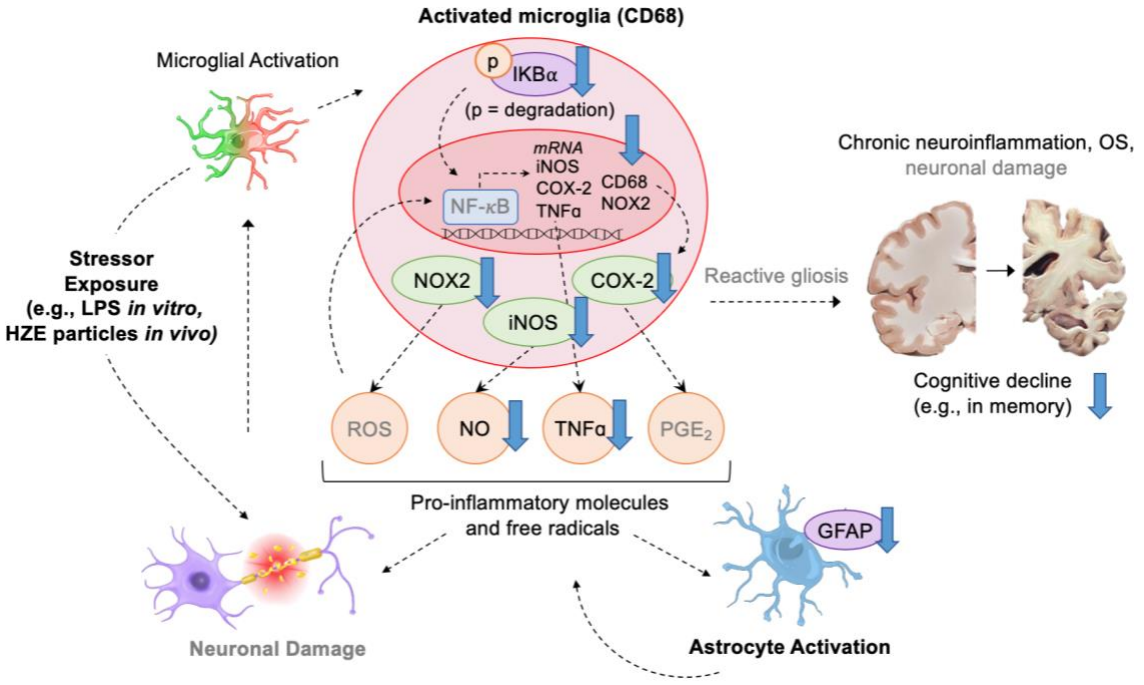

Figure 1. Proposed mechanisms for stressor-induced neuroinflammation, OS, and cognitive decline, mediated by reactive gliosis, and the observed attenuating effects of BB.

The observed effects of BB administered before and/or after LPS to microglia *in vitro* or 150 cGy ^{56}Fe in rats on neuroinflammation and OS indices are shown in blue arrows. Outcomes in grey were not directly measured in this work (NF-κB, ROS, PGE_2, and neuronal damage). BB, blueberry; COX-2, cyclooxygenase-2; GFAP, glial fibrillary acidic protein; IκB-α, inhibitor kappa-B-α; iNOS, inducible nitric oxide synthase; LPS, lipopolysaccharide; NF-κB, nuclear factor kappa-B; NO, nitric oxide; NOX2, NADPH oxidase; OS, oxidative stress; PGE_2, prostaglandin E_2; ROS, reactive oxygen species; TNFα, tumor necrosis factor-α.

4.2 Discussion and future directions

Common mechanisms involving neuroinflammation, OS, and associated changes in various neuronal cell types (e.g., microglia and astrocytes) have been identified in the development of neurodegeneration and other CNS deficits (1). In our work, we observed associations between HZE particle-induced neuroinflammation, OS, glial activation, and memory deficits, and demonstrated that these changes can be attenuated by BB pre- and/or

post-treatments, suggesting that a self-propelling cycle exists. However, the relationship (e.g., causality and directionality) between neuroinflammation, OS, and various cell types in the common response to neuropathological stressors remains unclear.

The observed discrepancy in microglial responses to HZE particles *in vitro* and *in vivo* suggests that microglia in isolation are not sufficient for initiation of neuroinflammation/OS following HZE particle irradiation. Nonetheless, we demonstrated that activated microglia, as demonstrated by inflammatory hallmarks of activation *in vitro* and CD68 *in vivo* are involved in the persistent stressor response (i.e., following stressor removal) to LPS *in vitro* and HZE particle irradiation *in vivo*, and can be targeted by nutritional treatments to reduce neuroinflammation and OS, even after activation occurs. Therefore, the mechanisms involved in microglial activation, particularly following HZE irradiation, and those targeted by pre-and/or post-treatments to reduce activation, require further investigation.

In a quiescent state, microglia monitor the CNS environment through ramified processes that survey the environment for pathogens or danger/damage signals. Microglia can be activated in response to 1) direct interactions with pathogens (e.g., neurotoxins, LPS bind surface receptors), 2) exogenous signals originating from other cells (e.g., damage-associated molecular patterns, DAMPs), and/or 3) endogenously produced microglial signals (e.g., DNA strand breaks induce NF-κB transcription). Microglia recognize pathogens and external signals through a variety of cell-surface receptors such as TLRs, scavenger receptors, and cytokine receptors. A well-characterized route for microglial activation is through ligand binding of TLR4, for which LPS is the prototypic ligand. Therefore, TLR4 activation was likely the initial cause of microglial activation, and the production of inflammation and OS mediators in our aim 1a study using LPS as an *in vitro* stressor. The mechanisms leading to microglial activation, and the role of TLR4 when the stressor itself is not a ligand, such as with HZE particle exposure, are less established.

When microglia are not directly exposed to the initiating pathogenic stimulus, damaged or dead cells produce signaling molecules such as cytokines, chemokines, and DAMPS, which bind specific receptors on microglia to induce activation. As discussed, pro-inflammatory molecules and free radicals originating from neurons, astrocytes, and other sites of damage can activate microglia through these receptors to perpetuate reactive

gliosis. The precise mechanisms, including primary ligands and receptors activated, and the overall contribution of reactive gliosis to stressor-induced neurodegeneration require further study. For example, emerging evidence shows that high-mobility group protein 1 (HMGB1), an endogenous LPS-like molecule produced as a danger signal under cellular stress, can also bind TLR4 (1). Therefore, even though HZE particles do not act as ligands, it is possible that TLR4 binding mediates HZE-induced microglial activation *in vivo*. Studies have shown that HMGB1 may promote microglial activation and neuroinflammation by binding to TLR4 following acute stress conditions such as TBI, ischemic injury, and neurotoxin exposure (1). HMGB1 can also bind pro-inflammatory cytokines to amplify inflammatory signaling (2). The role of TLR4 and HMGB1 in microglial activation following HZE particle exposure and other stressors, and response to dietary treatments is an avenue for future investigation.

Peripheral insults outside of the CNS can also induce microglial activation. For example, peripherally administered LPS cannot cross the BBB (if intact), and therefore, does not directly activate microglia *in vivo*. Instead, LPS binds TLR4 on endothelial cells of the BBB which transmit pro-inflammatory signals to the brain where they can activate microglia. Systemic inflammatory molecules such as cytokines may also activate microglia through receptors on the BBB or induce neuroinflammation through the vagus nerve (3). To understand the contribution of peripheral exposures to microglial activation, and mechanisms involved, future work should assess serum levels of inflammation/OS following stressors such as whole-body HZE particle exposure, and whether these are associated with glial activation. Due to the interplay between central and peripheral inflammation, countermeasures could attenuate microglial activation by downregulating central and/or peripheral inflammation/OS. Dietary strategies provide a safe and practical opportunity to target systemic mechanisms for neuroprotection.

In addition to external factors, the intracellular signaling pathways involved in stressor-induced glial cell activation, neuroinflammation, and OS, and those targeted by dietary pre- and/or post-treatments should be further examined. Our work suggests that NF-κB is induced by LPS and HZE particle irradiation, as indicated by IκB-α phosphorylation, and can be attenuated by BB before and/or after stressor exposure. However, microglial activation and the downstream production of inflammation and OS may be mediated by

other signal transduction pathways including MAPKs, STATs, and PI3K/Akt, and interactions between these pathways (4). Additionally, although BB pre- and post-treatments produced similar effects on glial cell activation, neuroinflammation, and OS *in vivo*, they could act on different pathways and/or at different stages within the same signal transduction pathway. Studies using pathway-specific inhibitors should be conducted to better elucidate the stressor-induced response and precise anti-inflammatory/antioxidant mechanisms of dietary strategies.

Overall, the mechanisms involved in microglial activation, particularly following HZE particle irradiation require further study. Although we found that glial cell activation is involved in HZE particle-induced inflammation and OS via correlation analyses, the directionality and causality of these effects remain to be established. It is not clear whether activated microglia are the initial cause of HZE particle-induced inflammation/OS, become activated in response to inflammation/OS originating elsewhere, or both. The contributions of reactive astrocytes to these processes, and whether astrocytes could be one of the primary targets for countermeasures requires investigation. Similar questions remain about the role of glial cells, neuroinflammation, OS, and neurodegeneration following other stressors. Further evaluating the effects of post-treatments on these multi-factorial and multi-cellular responses is necessary to advance understanding of mechanisms and therapeutic targets for the CNS deficits of HZE particles and other neuropathological stressors. Additionally, whether antioxidant/anti-inflammatory dietary treatments reduce microglial activation by attenuating endogenously produced microglial signals and/or exogenous signals originating from other cells should be assessed to optimize countermeasure efficacy.

In our work, we found that post-treatments starting immediately after LPS removal for 24 hours reduced inflammation/OS in microglia, and post-treatments administered to rats immediately after HZE particle exposure for 45 days reduced neuroinflammation, OS, and cognitive deficits. The timing of post-treatment interventions required for efficacy is an avenue for future investigation. Although our post-treatments were administered for 24 hours or 45 days after stressors, it is possible that the beneficial effects occur early after stressor-induced initiation of the inflammatory response. A recent *in vitro* study using microglia found that post-treatment with an acetone extract of Spirulina reduced LPS-

induced IL-1β, TNFα, and iNOS when administered 2 hours after LPS stimulation, but the attenuating effects were diminished when administered 4 hours after LPS, potentially due to a progressive increase in inflammation (5). However, in this study, post-treatments were co-administered with LPS, representing a sustained stressor exposure, rather than targeting the residual mechanisms that continue after stressor removal, as in our studies. Nonetheless, early attenuation of pathogenic mechanisms may be necessary to prevent the propagation of detrimental CNS effects, such as neurodegeneration long-term after stressors. For example, it has been hypothesized that attenuating early damage to the brain vasculature and parenchyma resulting from radiotherapy could prevent propagation of damage, even though the most severe residual effects of radiotherapy are observed months to years after exposures (6). The importance of targeting early pathogenic mechanisms could also explain why pre- and post-treatments did not produce differential effects on HZE-induced damage.

Furthermore, there may be a dose/duration threshold for the beneficial effects of antioxidant/anti-inflammatory treatments on stressor-induced neuroinflammation, OS, and cognitive deficits. Unexpectedly, we found that pre-/post-treatments (i.e., for 24 hours before and after LPS and 45 days before and after ^{56}Fe) did not produce greater attenuating effects than pre- or post-treatment on stressor-induced deficits, despite a higher overall dose and longer exposure of BB. In support of a threshold effect, for some outcomes, pre- or post-treatment was sufficient to fully ameliorate the effects of irradiation (i.e., no difference between irradiated and non-irradiated animal consuming pre-BB). Because basal levels of neuroinflammation and free radicals are necessary to maintain homeostasis in the brain, additional BB consumption with continuous pre-/post-BB could not attenuate these outcomes further without potentially producing a deleterious effect. Future investigation on the therapeutic window and dose for the beneficial effects of antioxidant/anti-inflammatory foods on stressor-induced CNS deficits is warranted.

Although not pursued in this work, there appear to be sex differences in stressor-induced neuroinflammation, OS, glial activation, and cognitive deficits. Males may be more susceptible to the biochemical changes in the brain and cognitive deficits of irradiation exposure (7, 8). These differences could be due to sex-specific mechanisms related to memory formation (9), or differences in glucocorticoids, which are critical

mediators of stress-induced microglial responses (2). Furthermore, estrogen has been shown to have a neuroprotective effect against irradiation-induced CNS changes (10, 11). We used male rats in this work to ensure a sufficient stress response, without which, the differential effects of pre- and/or post-treatments could not be discerned. However, the efficacy of post-stressor treatments on neuroinflammation, OS, glial activation, and cognitive deficits in females, and the potential role and of sex hormones in these processes, should be assessed.

Finally, it is known that stressor exposures associated with neurodegenerative disease risk, including HZE particles can alter processes in the CNS in addition to inflammation/OS. Stressor-induced apoptosis, demyelination, inhibition of neurogenesis and autophagy, and damage to the blood-brain-barrier likely contribute to and/or result from increases in neuroinflammation, OS, and glial activation. The downstream declines in cognitive function are therefore a result of multicellular and multifactorial processes. The effects of dietary post-treatments on these processes should be investigated in future studies.

To conclude, the attenuating effects of BB treatments, even when administered after LPS or HZE particle exposures, supports the role of neuroinflammation and OS in stressor-induced CNS deficits. Microglia are cellular mechanisms involved in stressor-induced neuroinflammation and OS, and can be targeted by nutritional treatments even after activation occurs. However, the intercellular and intracellular mechanisms involved in microglial activation, and the relationship to chronic and progressive neuroinflammation, OS, and cognitive deficits, require further investigation. A better understanding of whether and how reactive gliosis contributes to stressor-induced neurodegeneration, the primary targets of antioxidant/anti-inflammatory post-treatments, and the post-stressor therapeutic window to administer treatments will optimize countermeasure development. Overall, our findings support the use of dietary post-treatments to reduce the risk of neurodegenerative disease following neuroinflammatory/OS-inducing stressors, such as HZE particle irradiation, and potentially other unpredictable insults involving neuroinflammation and OS such as stroke and traumatic brain injury.

References

1. Lumniczky K, Szatmári T, Sáfrány G. Ionizing radiation-induced immune and inflammatory reactions in the brain. Frontiers in Immunology 2017;8(MAY):1-13. doi: 10.3389/fimmu.2017.00517.
2. Frank MG, Fonken LK, Watkins LR, Maier SF. Microglia: Neuroimmune-sensors of stress. Seminars in Cell and Developmental Biology 2019;94(December 2018):176-85. doi: 10.1016/j.semcdb.2019.01.001.
3. Perry VH, Teeling J. Microglia and macrophages of the central nervous system: The contribution of microglia priming and systemic inflammation to chronic neurodegeneration. Seminars in immunopathology 2013;35:601-12. doi: 10.1007/s00281-013-0382-8.
4. Cianciulli A, Porro C, Calvello R, Trotta T, Lofrumento DD, Panaro MA. Microglia mediated neuroinflammation: Focus on PI3K modulation. Biomolecules 2020;10(1):1-19. doi: 10.3390/biom10010137.
5. Piovan A, Battaglia J, Filippini R, Dalla Costa V, Facci L, Argentini C, Pagetta A, Giusti P, Zusso M. Pre- and Early Post-treatment With Arthrospira platensis (Spirulina) Extract Impedes Lipopolysaccharide-triggered Neuroinflammation in Microglia. Frontiers in Pharmacology 2021;12:724993. doi: 10.3389/fphar.2021.724993.
6. Constanzo J, Midavaine É, Fouquet J, Lepage M, Descoteaux M, Kirby K, Tremblay L, Masson-Côté L, Geha S, Longpré JM, et al. Brain irradiation leads to persistent neuroinflammation and long-term neurocognitive dysfunction in a region-specific manner. Progress in Neuro-Psychopharmacology and Biological Psychiatry 2020;102(April):109954-. doi: 10.1016/j.pnpbp.2020.109954.
7. Krukowski K, Grue K, Frias ES, Pietrykowski J, Jones T, Nelson G, Rosi S. Female mice are protected from space radiation-induced maladaptive responses. Brain, Behavior, and Immunity 2018;74(August):106-20. doi: 10.1016/j.bbi.2018.08.008.
8. Liu B, Hinshaw RG, Le KX, Park MA, Wang S, Belanger AP, Dubey S, Frost JL, Shi Q, Holton P, et al. Space-like 56Fe irradiation manifests mild, early sex-specific behavioral and neuropathological changes in wildtype and Alzheimer's-

like transgenic mice. Scientific Reports 2019;9(1):1-17. doi: 10.1038/s41598-019-48615-1.

9. Arone A, Ivaldi T, Loganovsky K, Palermo S, Parra E, Flamini W, Marazziti D. The Burden of Space Exploration on the Mental Health of Astronauts: A Narrative Review. Clinical Neuropsychiatry 2021;18(5):237-46. doi: 10.36131/cnfioritieditore20210502.
10. Rabin BM, Carrihill-Knoll KL, Long LV, Pitts SC, Hale BS. Effects of 17B-Estradiol on Cognitive Performance of Ovariectomized Female Rats Exposed to Space Radiation. Journal of Behavioral and Brain Science 2013;03(01):67-73. doi: 10.4236/jbbs.2013.31007.
11. Rabin BM, Miller MG, Larsen A, Spadafora C, Zolnerowich NN, Dell'Acqua LA, Shukitt-Hale B. Effects of exposure to 12C and 4He particles on cognitive performance of intact and ovariectomized female rats. Life Sciences in Space Research 2019;22(June):47-54. doi: 10.1016/j.lssr.2019.07.005.

5 APPENDICES

5.1 Dose-response effects of blueberry on LPS-induced nitric oxide release in rat microglia

This preliminary dose-response experiment was performed to determine a minimum BB dose for aim 1a and 1b experiments by examining LPS-induced nitrite production in microglia. Nitrite (NO_2^-) is a stable breakdown product of the free radical nitric oxide (NO) and a well-known indicator of microglia activation (1). A 24 hour pre/post-stressor treatment interval was selected because a previous study showed that indicators of inflammation/OS, including nitrite, were increased 24 hours after LPS stimulation in microglia (1).

The experimental design and methods for this dose-response experiment are described in Chapter 3.1, except 4 doses of BB for pre- and/or post-treatments were used and all groups were stressed with LPS (i.e., no unstressed control cells). In brief, HAPI rat microglia were incubated with media containing no BB (i.e., control) or with freeze-dried BB diluted in media at 0.125, 0.25, 0.5, or 1.0 mg/mL for 24 hours **(Figure 1**). Pre-treatment media was removed and cells were incubated with 200 ng/mL LPS for 18 hours. Then, cells were post-treated with control or BB media for 24 hours. Nitrite production was assessed in the cell conditioned supernatant using Griess reagent. All doses and pre/post groups were assayed in duplicate in three separate experiments.

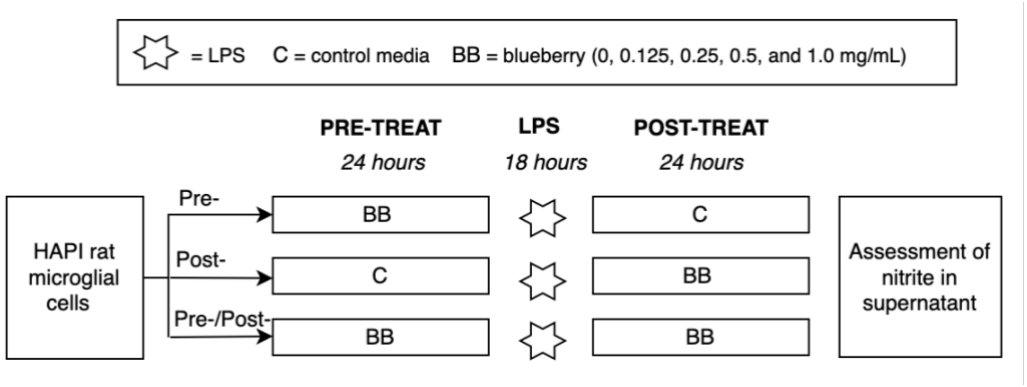

Figure 1. Experimental design of dose-response experiment to determine the minimum optimal dose of BB that reduces LPS-induced nitrite production in microglia.

Data were analyzed using a two-way ANOVA with BB dose (0, 0.125, 0.25, 0.5, and 1.0 mg/mL) and BB treatment period (pre, BB/LPS/C; post, C/LPS/BB; pre/post,

BB/LPS/BB) as experimental factors. Post-hoc testing was performed with Tukey's test. Results showed a significant effect of dose ($F_{4, 30} = 4.09$, $P < 0.01$), and the effects of BB treatment period and the treatment period x dose interaction were not significant ($P > 0.05$). Post-hoc testing showed that both 0.5 mg/mL and 1.0 mg/mL BB significantly lowered nitrite relative to no BB ($P < 0.05$) (**Figure 2)**. We selected the lower dose (0.5 mg/mL) to minimize representation of supraphysiological effects and to represent a closer application to human consumption. Additionally, previous studies from our laboratory demonstrated that 0.5 mg/mL BB administered for 45 mins (2) and 1 hr (3) significantly reduced LPS-induced nitrite production in microglia with no cytotoxic effects.

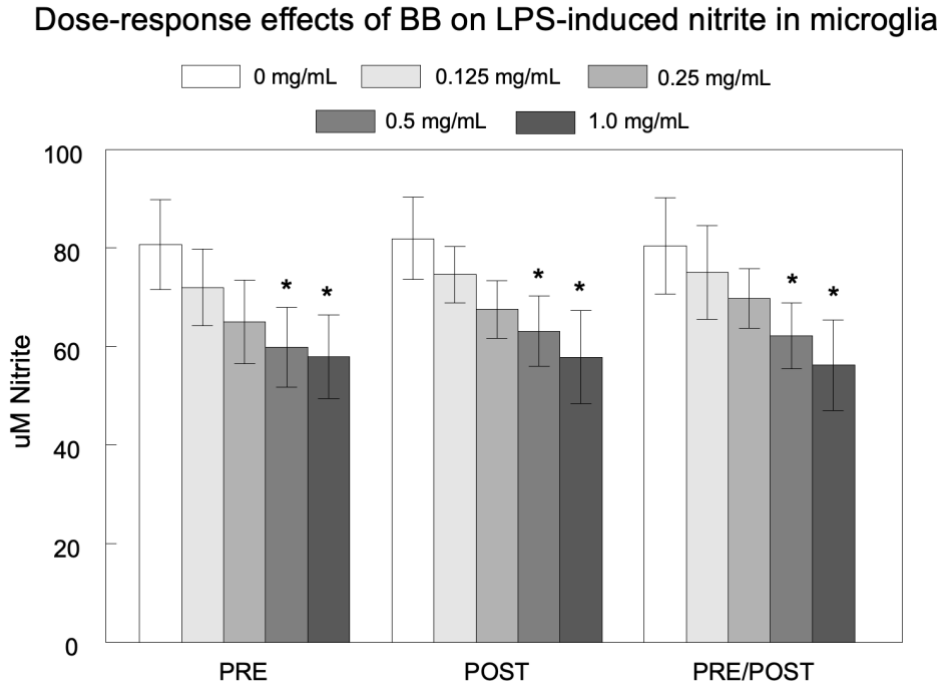

Figure 2. The effects of 0, 0.125, 0.25, 0.5, 1.0 and 2.0 mg/mL BB administered before and/or after LPS on nitrite production in microglia.
* = significantly different from 0 mg/mL ($P < 0.05$). C = control, BB = blueberry, LPS = lipopolysaccharide, PRE: only pre-treatment with BB; POST, only post-treatment with BB; PRE/POST, both pre- and post-treatment with BB.

References:

1. Lijia Z, Zhao S, Wang X, Wu C, Yang J. A self-propelling cycle mediated by reactive oxide species and nitric oxide exists in LPS-activated microglia. Neurochemistry International 2012;61(7):1220-30. doi: 10.1016/j.neuint.2012.09.002.

2. Lau FC, Bielinski DF, Joseph JA. Inhibitory effects of blueberry extract on the production of inflammatory mediators in lipopolysaccharide-activated BV2 microglia. Journal of Neuroscience Research 2007;85(5):1010-7. doi: 10.1002/jnr.21205.
3. Carey AN, Fisher DR, Rimando AM, Gomes SM, Bielinski DF, Shukitt-Hale B. Stilbenes and anthocyanins reduce stress signaling in BV-2 mouse microglia. Journal of Agricultural and Food Chemistry 2013;61(25):5979-86. doi: 10.1021/jf400342g.

5.2 Without a radiation effect, pre- and/or post-treatment with blueberry does not alter inflammation or oxidative stress biomarkers in rat microglia exposed to ^{56}Fe *in vitro*

Background & Methods:

Aim 1b of this thesis work was to evaluate whether post-stressor BB reduces HZE-particle induced inflammation and OS, relative to no BB, pre-stressor BB or pre-/post-stressor BB, in rat microglial cells. To meet this objective, we conducted *in vitro* experiments using the same experimental design and methods as aim 1a, described in Chapter 3.1, except that cells were exposed to ^{56}Fe irradiation or no irradiation instead of LPS.

Prior to this experiment, the effects of high-LET ionizing radiation (IoR) particles, such as ^{56}Fe, had not been investigated. Instead, previous work on microglial responses to ionizing radiation *in vitro* had been limited to high dose x-ray or γ-ray exposures. Nonetheless, in order to meet our objective of assessing the pre- and/or post-HZE particle effects of BB on microglia *in vitro*, a significant stress response (e.g., inflammation and OS) was necessary. Therefore, prior to experimental irradiations, we conducted a dose-response experiment using ^{56}Fe doses within the ranges of *in vivo* studies demonstrating increased microglial activation, while minimizing the time required for flasks to be upended at room-temperature for irradiations. Nitrite (NO_2^-) was used as the inflammatory/OS indicator for irradiation dose-response experiments. Unexpectedly, we did not find effects of ^{56}Fe irradiation up to 2 Gy on NO_2^- release. Therefore, we decided to use the highest dose tested, 2 Gy for experimental irradiations with the hypothesis that irradiation may be altering intracellular enzymes (e.g., COX-2, iNOS, pIκB-α, NOX2) rather than soluble factors released from microglia.

In brief, HAPI rat microglial cells were pre-treated in the absence (control) or presence of BB (0.5 mg/mL) for 24 hours. Then, cells were exposed to a single dose of 2 Gy (600 MeV/n) ^{56}Fe or were not irradiated, as described in Chapter 3.2. Media was removed and cells were post-treated in the absence (control) or presence of BB (0.5 mg/mL) for 24 hours. The protein expression of inflammation/OS-mediators were assessed using Western blot following the post-treatment period and data were analyzed using two-

way ANOVAs with ^{56}Fe exposure (0 or 2 Gy) and BB treatment period (no BB, pre-BB, post-BB, pre-/post-BB) as experimental factors.

Results:

As reported in Chapter 3.2, we determined that that irradiation with 2 Gy ^{56}Fe did not produce significant effects on the protein expression of inflammation (COX-2, iNOS, pIκB-α) and OS (NOX2) biomarkers ($P > 0.05$). The overall ANOVAs also showed that there were no significant effects of BB treatment period or an interaction between ^{56}Fe exposure and BB treatment period on COX-2, iNOS, pIκB-α, or NOX2 ($P > 0.05$, **Figure 3**).

Discussion:

Evaluating the effects of antioxidant/anti-inflammatory compounds, such as in BBs, on stressor-induced CNS changes can help identify mechanisms and mediators involved (or not involved) in the stress response. We hypothesized that microglia are primarily responsible for HZE particle-induced neuroinflammation and OS *in vivo,* and would increase the production of inflammatory and OS mediators in response to HZE particle exposure *in vitro*. However, HZE particle irradiation did not increase inflammation and OS outcomes in microglia in our work. Given that BBs contain antioxidant/anti-inflammatory polyphenols, the observation that BB treatments did not produce significant effects in irradiated microglia relative to no BB on inflammation and OS biomarkers further confirms that these processes are not involved in microglial responses to ^{56}Fe when isolated *in vitro*.

At physiological levels, inflammatory mediators and ROS/RNS serve as important signaling molecules to maintain cell functions and homeostasis. Therefore, as demonstrated in previous studies, in unstressed conditions, BB typically does not produce attenuating effects on these processes relative to control treatments (i.e., no BB) *in vitro* (1) and *in vivo* (2, 3). Similarly, in aim 1a studies in microglia exposed to 200 ng/mL LPS, and aim 2 studies in rats irradiated with 150 cGy ^{56}Fe, pre- and/or post-BB did not produce significant effects relative to no BB on neuroinflammation, OS, and cognitive performance when the stressor did not induce significant changes (e.g., Nrf2, SOD, RAWM, Iba-1).

Additionally, BB treatments did not produce significant effects on inflammation, OS, and cognitive performance, relative to no BB in cells or animals not exposed to the stressor. Findings from this study confirm those presented in Chapter 3.2, i.e., that a significant stress response involving inflammation and OS was not induced by HZE particle exposure in microglia *in vitro*. However, the limitations discussed in Chapter 3.2 should be considered when interpreting these findings.

As presented in Chapter 3.3, our aim 2 study showed that pre and/or post-BB attenuates HZE particle-induced microglial activation (CD68 mRNA) in the hippocampus. Therefore, future work is necessary to determine which molecular factors BBs target to attenuate HZE particle-induced microglial activation. The multicellular and multifactorial cycle of reactive gliosis could be a therapeutic target, and selective inhibitor experiments could determine how BBs intercept these processes.

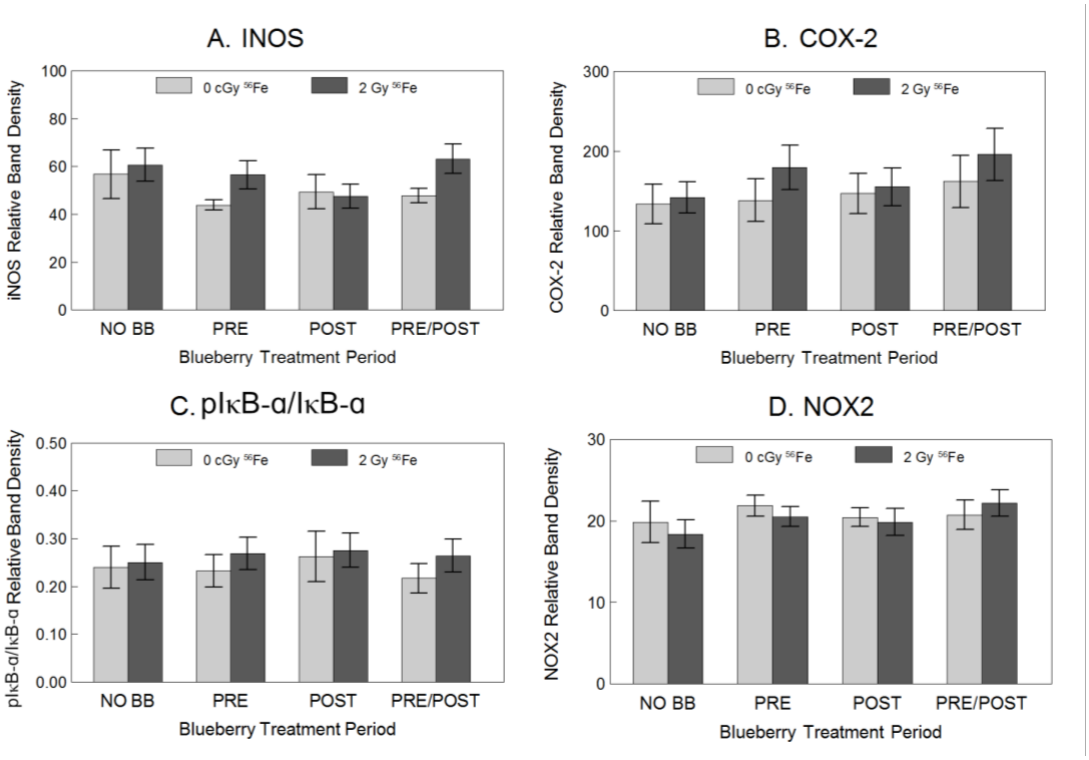

Figure 5.3. Neither irradiation with ^{56}Fe nor 0.5 mg/mL BB (pre- and/or post-treatment) produces significant effects on protein expression of inflammation and oxidative stress biomarkers in microglia.

HAPI rat microglia were pre-treated in the absence or presence of BB (0.5 mg/mL), exposed to no irradiation (0 cGy ^{56}Fe) or 150 cGy ^{56}Fe , and post-treated with or without BB. Protein expression levels of the following mediators were assessed after the post-treatment period using Western blot: A) iNOS, B) COX-2, C) phosphorylated IκB-α, expressed as a ratio of total IκB-α, and D) NOX2. Data are presented as the mean ± SEM of six independent experiments (i.e, flasks) assessed in triplicate. NO BB, neither pre- nor post-treatment with BB; PRE: only pre-treatment with BB; POST, only post-treatment with BB; PRE/POST, both pre- and post-treatment with BB.

References

1. Cheng A, Han C, Fang X, Sun J, Chen X, Wan F. Extractable and non-extractable polyphenols from blueberries modulate LPS-induced expression of iNOS and COX-2 in RAW264.7 macrophages via the NF-kappaB signalling pathway. Journal of the Science of Food and Agriculture 2016;96(10):3393-400. doi: 10.1002/jsfa.7519.
2. Shukitt-Hale B, Lau FC, Carey AN, Galli RL, Spangler EL, Ingram DK, Joseph JA. Blueberry polyphenols attenuate kainic acid-induced decrements in cognition and alter inflammatory gene expression in rat hippocampus. Nutritional Neuroscience 2008;11(4):172-82. doi: 10.1179/147683008X301487.
3. Poulose SM, Bielinski DF, Carrihill-Knoll KL, Rabin BM, Shukitt-Hale B. Protective effects of blueberry- and strawberry diets on neuronal stress following exposure to 56Fe particles. Brain Research 2014;1593:9-18. doi: 10.1016/j.brainres.2014.10.028.

5.3 Animal diet composition

The macronutrient composition of control and 2% BB diets is shown in **Table 1**.

Table 1. Macronutrient composition of control and 2% BB diets				
	NIH-31 Control		*2% BB Suppl.*	
	% kcal	**% by weight**	**% kcal**	**% by weight**
Protein	25.6	17.9	25.4	17.8
Carbohydrate[a]	61.5	43.0	62.0	43.4
Fat	12.9	4.0	12.7	3.9
Kcal/g	2.8		2.8	

[a] Estimated digestible carbohydrate

The ingredient composition of control and 2% BB diets is shown in **Table 2,** replicated from Youdim et al. 2000 (1). Average food intake was 20.8 grams/day (Chapter 3.3). Therefore, rats on the 2% diet consumed approximately 420 mg of BB extract/day. Our laboratory has previously described that 1 kg of whole BB yields 110 g of BB extract. Therefore, rats in this thesis work consumed the equivalent of approximately 4 g of whole BB/day.

Table 2. Ingredient composition of control and 2% BB diets		
	Diet Composition (g/kg)	
Ingredient	Control diet	2% BB diet
Wheat, Hard ground	355.50	355.50
Wheat Middlings	99.96	99.96
Oats, ground	99.96	99.96
Fish Meal, Menhaden, 60%	89.96	89.96
Soybean Meal, 48%	49.98	49.98
Alfalfa Meal, Dehydrated, 17%	19.99	19.99
Corn Gluten Meal, 60%	19.99	19.99
Dicalcium Phosphate, 18.5%	14.99	14.99
Soybean oil	10.00	10.00
Brewer's Yeast Dried	5.00	5.00
Salt, Iodized NaCl	4.75	4.75
Calcium Carbonate, 38%	4.75	4.75
Vitamin Mix, NIH-31[a]	3.50	3.50
Mineral Mix, NIH-31[b]	1.50	1.50
Corn, yellow ground	209.92	189.92
Tif-blue Blueberry Extract	-	20.00
TOTAL	1000	1000

[a]Vitamin mix contains (in g/kg vitamin mix): Corn ground (316.24), Choline Chloride (423.50), MSB Complex (135.30), Thiamin mononitrate (25.26), Calcium Panthothenate

(24.37), Vitamin B12 (19.05), Vitamin E (17.15), Niacin (12.65), Vitamin A Acetate (10.65), Riboflavin (7.14), Biotin (3.78) Vitamin D3 (2.99) Folic Acid (0.32), Pyridoxine HCL (1.60).

[b]Mineral mix contains (in g/kg mineral mix): magnesium oxide (487.10), Calcium Carbonate (219.23), Ferrous Sulfate (146.85), Manganous Oxide (122.40), Copper Sulfate (11.84), Zinc Oxide (10.20), Calcium Iodate (1.74), Cobalt Carbonate (0.64).

Reference

1. Youdim KA, Shukitt-Hale B, Martin A, Wang H, Denisova N, Bickford PC, Joseph JA. Short-Term Dietary Supplementation of Blueberry Polyphenolics: Beneficial Effects on Aging Brain Performance and Peripheral Tissue Function. Nutritional Neuroscience 2000;3(6):383-97. doi: 10.1080/1028415X.2000.11747338.

5.4 Sample size calculation for adequate power *in vivo*

Rabin et al. 2019 demonstrated that whole-body exposure to 0.05 cGy ^{4}He significantly worsened performance on the NOR (% time with novel object) in male Sprague-Dawley rats relative to non-irradiated rats by 14% two months post-irradiation (1). Using parameters of $\alpha = 0.05$, power=80%, effect size = 14%, and standard deviation = 11%, it was determined that n = 11 animals/group are necessary to detect significance for the effect of radiation on NOR. To account for the comparison of multiple means and unexpected loss, and to further detect the hypothesized effect of diet, we added 4 animals/group for a total of n = 15/group and 120 animals overall. We chose to calculate sample size based on a radiation effect because without a significant stressor response, the pre- vs. post-irradiation effects of blueberry cannot be determined.

Poulose et al. 2014 demonstrated that whole-body exposure to 150 cGy ^{56}Fe significantly increased the expression of NOX2 in the hippocampus of male Sprague-Dawley rats 30 days post-irradiation relative to non-irradiated animals (relative band density effect size = 327, 215, and standard deviation = 42,214) (2). NOX2 was used to determine sample size for biochemical outcomes because NOX2 is a main source of endogenous free radicals in the brain and an indicator of neuroinflammation (2). Using parameters of $\alpha = 0.05$, power=80%, and to account for the comparison of multiple means and further detect the potential effects of diet, we chose to analyze n=9 animals/group for Western blot outcomes. The remaining 6 animals/group were used for mRNA analyses.

References

1. Rabin BM, Poulose SM, Bielinski DF, Shukitt-Hale B. Effects of head-only or whole-body exposure to very low doses of 4He (1000 MeV/n) particles on neuronal function and cognitive performance. Life Sciences in Space Research 2019;20(August):85-92. doi: 10.1016/j.lssr.2019.02.001.
2. Poulose SM, Bielinski DF, Carrihill-Knoll KL, Rabin BM, Shukitt-Hale B. Protective effects of blueberry- and strawberry diets on neuronal stress following exposure to 56Fe particles. Brain Research 2014;1593:9-18. doi: 10.1016/j.brainres.2014.10.028.

5.5 Methods

5.5.1 Cell culture procedure and pre-/post-LPS BB treatments in HAPI microglia

Cell culture

1. Turn on blower and open cabinet up (maximum height is noted on cabinet side). Clean hood with 70% ethanol.
2. Turn on water bath (37 °C).
3. Make complete medium
    a. Dulbecco's modified Eagle's medium (DMEM, Invitrogen, Grand Island, NY) supplemented with 10% fetal bovine serum (FBS), 100 U/ mL penicillin, and 100 μg/mL streptomycin e.g., to 534 mL DMEM, add 60 mL of FBS and 6 mL of penstrep.
4. Starting cells (HAPI rat microglia)
    a. Rapid thaw vial at 37 °C (water bath).
    b. Add vial to 10 mL complete medium on 100 mm plate.
    c. Put plate in at 37 °C in a humidified incubator under 5% CO2. Allow cells to attach for 1 hour.
    d. Remove media (to eliminate DMSO) and add 10 mL complete medium to plate. Put plate in at 37 °C in a humidified incubator under 5% CO2.
    e. Clean hood with 70% ethanol, close and turn light off
5. Counting cells
    a. Remove media, add trypsin (100 mm plate: 2 mL, T25 flask: 2 mL, T75 flask: 3 mL). Sit for 5 minutes for detachment.
    b. Rinse plate to remove cells. Add 50 uL of cell suspension to microcentrifuge tube → add 50 uL trypan blue → mix and add microliter amount (10 uL) to hemacytometer
    c. Count cells in each of four big corner squares and center big square (5 squares total).
        i. (average of 5 squares) x 2 x (10^4) x (X mL of trypsin) = amount of cells you have total
            1. 2 = dilution factor (50 uL cells in 100 uL total)
            2. 10^4 = amount in 1 mL (specified by hemacytometer)
            3. X = mL of trypsin (total cell suspension)

Aim 1a experiments

6. Maintain cells in 100 mm plates and then split into T25 flasks at a seeding density of 2.5×10^5 cells/flask in DMEM with phenol red.
    a. 5 mL/flask in T25 flask x 8 groups = 40 mL total
    b. $\frac{\#\ cells\ you\ WANT}{\#\ cells\ you\ HAVE\ in\ 1\ mL}\ x\ 1000 = uL\ cell\ suspension\ needed$
        i. Want 250,000 cells/flask x 8 flasks = 2,000,000 cells total (in 40 mL media)
        ii. E.g., 10,000,000 cells in confluent 100 mm plate. Add 2 mL trypsin → 5,000,000 in 1 mL
        iii. $\frac{2{,}000{,}000}{5{,}000{,}000}\ x\ 1000 = 400\ uL\ cell\ suspension\ needed\ in\ 40\ mL$

   c. Add 400 uL cell suspension to Falcon tube containing 40 mL DMEM. Add 5 mL to each T25 flask.
7. Allow cells to grow for 3 days to reach 2.5×10^6 cells/flask for experimental treatments.
8. For pre-treatments, incubate cells in the absence (control) or presence of freeze-dried BB extract (Tif-blue BB) diluted in media to a concentration of 0.5 mg/mL for 24 h.
   a. Make 10 mg/mL BB stock solution in clear media (i.e., DMEM without phenol red)
      i. 2000 mg/200 mL = 2 grams of BB in 200 mL
   b. 4x control flasks (5 mL/flask) → 20 mL clear media
   c. 4x 0.5 mg/mL BB flasks (5 mL/flask) → 20 mL 0.5 mg/mL BB in clear media
      i. 10 mg/mL stock (X) = 0.5 mg/mL(20 mL)
      ii. Add 1 mL 10 mg/mL BB stock to 19 mL media
9. Remove pre-treatment media and incubate cells in the absence (unstressed control) or presence of LPS (Sigma-Aldrich, St Louis, MO) in serum-free DMEM without phenol red at 200 ng/mL for 18 h.
   a. LPS aliquots = 1 mg/mL, 25 uL
   b. Add 225ul of DMEM (serum free, no phenol red) to the 25ul aliquot of 1 mg/mL LPS = 0.1 mg/mL = 100 ug/mL
   c. Make to final concentration of 200 ng/mL depending on total volume you need
      i. 20 mL (0.200 ug/mL) = X mL (100 ug/mL) → 40 ug / (100 ug/mL) =
      ii. eg. so for 20ml use 40ul from the 250)
10. Remove LPS/control media. Add post-treatments prepared as above → incubate for 24 hours.

<u>Preparing cell lysates</u>

1. Setup
   a. Have a tray of ice ready with a 50 mL Falcon tube filled with cold sterile PBS (1x).
   b. Add PMSF (a protease inhibitor, from aliquot of 200 mM in isopropanol) to Lysis Buffer (CelLytic-M Cell Lysis Reagent from Sigma) and keep on ice.
      i. 20 uL PMSF to each 10ml of CelLytic Lysis buffer.
      ii. Use 100ul/well of a 12-well plate, 1 mL/T25 flask
2. Keep plates/flasks on ice while transferring cell-conditioned media (CCM) into microcentrifuge tubes for nitrite/ELISA assay. After removing CCM, wash by adding ~1 mL ice-cold PBS to each flask using transfer pipette.
   a. Keep plate covered unless immediately adding the PBS; do not let cells dry out.
2. Remove PBS, rinse 3x. Cover plate and place on ice again.
3. Add Lysis Buffer/PMSF to each flask (1 mL/flask) → rock for 15 minutes in cold room
   a. You can briefly check under the microscope to see that the cells are detached. Then, put the plates/flasks back on ice.

4. With a P1000 pipetman, changing tips between flasks, triturate the cells by pipetting up & down a few times, then transfer the lysed cells to a labeled eppendorf tube on ice.
5. Spin in the eppendorf centrifuge for 10 minutes at 14K rpm to pellet cell membranes.
6. Transfer the supernatants (lysates) into a new set of labeled eppendorf tubes; discard pellets. Freeze the lysates at -80C.

5.5.2 Nitrite Assay

Purpose: To assess the production of free radical nitric oxide (NO) from HAPI cells, the extracellular release of nitrite (NO_2^-), a stable and nonvolatile breakdown product of NO, is measured in cell-conditioned supernatant by Greiss reagent kit (Cat # G7921, Thermofisher, Waltham, MA).

Reagents Supplied (store at 2-6 C, protected from light)

- N-(1-naphthyl)ethylenediamine dihydrochloride (Component A), 25 mL of a 0.1% (1 mg/mL) solution, sealed under argon
- Sulfanilic acid (Component B), 25 mL of a 1% (10 mg/mL) solution in 5% phosphoric acid
- Nitrite standard solution (Component C), 1.0 mL of 1.0 mM sodium nitrite in deionized water

Protocol

1. Place samples containing cell conditioned media (CCM, i.e., supernatants) on ice to thaw.
2. Prepare nitrite standards in 8 microcentrifuge tubes with a serial dilution from 0-100 uM using Component C.
    a. Add 450 uL of DMEM without Phenol Red to the first tube and 250uL to the remaining 7 tubes.
    b. To the first tube, add 50uL of Component C for a 100uM solution.
    c. Perform a serial dilution by pipetting 250 uL from the first tube into the second tube. Repeat this step for tubes 2-7, leaving the last tube blank.
3. Add 100 uL of each standard in duplicate to a 96-well plate in increasing concentration (using tubes 1-8 from right to left).
4. Add 100 µl of CCM supernatant from each sample in duplicate to a 96-well plate.
5. Mix equal volumes of component A and component B in a beaker to make Griess reagent (~35 drops of each for 1x 96-well plate).
6. Add 25 µl of Griess reagent to each well using a repeater pipette and incubate at room temperature for 15 min.
7. Turn on the BioTek ELx800 plate reader and open the Gen5 program.
8. Select new experiment, then 'Nitrite protocol' for absorbance at 548 nm.
9. Put plate on plate reader and press run. Export results to Excel file.
10. Generate standard curve of nitrite concentration using standard values.
    a. Average duplicates for each standard value.
    b. Plot a standard curve of nitrite concentration (x-axis) using values 0, 1.562, 3.125, 6.25, 12.5, 25, 50, 1000 against absorbance (y-axis) and generate linear equation.
11. Calculate the concentration of NO_2^- in each sample using the linear equation derived from the standard curve generated by known concentrations of NO_2^-.
    a. Average the duplicates for each sample
    b. Divide the result from the slope of the curve generated from the standards for each sample to obtain uM of Nitrite

12. Normalize values by total protein levels in cell lysates quantified with the DC protein assay (BioRad, Hercules, CA).
    a. To calculate protein ratio, divide all protein values by median.
    b. Divide each nitrite value by protein ratio for that sample

5.5.3 TNFa ELISA

Purpose: To measure the production of pro-inflammatory cytokine TNFα in HAPI cells is measured in cell-conditioned supernatant using a Rat TNFα ELISA kit (Cat #88-7340-88, Invitrogen, Waltham, MA).

Reagents Supplied (Kit stored at 4°C and protected from light)

- **Capture Antibody:** 500 uL (250X) of Pre-titrated, purified anti rat TNF alpha antibody.
- **Detection Antibody:** 500 uL (250X) of Pre-titrated, biotin-conjugated anti rat TNF alpha antibody.
- **Standard:** Recombinant rat TNFα for generating standard curve.
- **Coating Buffer:** 12 mL (10X) Phosphate Buffer Saline Concentrate.
- **ELISA/ELISPOT Diluent:** 150 mL (5X) Diluent Concentrate.
- **Enzyme:** 500 uL (250X) pre-titrated Avidin-HRP Concentrate.
- **Substrate Solution:** 100 mL of Tetramethylbenzidine (TMB) Solution.

Other Materials Needed

Supplies:

- Multi-Channel Pipettors and tips
- Reagent Reservoirs
- 96-well plates (Corning™ Costar™ 9017) & Plate Sealers
- 15 mL and 50 mL Falcon tubes to prepare reagents
- 96-well microplate reader (BioTek ELx800)

Reagent Preparation:

Reagent	When to make	How to Make	Protocol
Wash buffer (4 L) *1X PBS, 0.05% Tween™-20*	Day before, store at 4°C	• 4 L diH2O • 20 PBS tablets (5 tablets/L) • 2 mL tween (0.05%)	150 uL/well
Coating buffer (120 mL) *1:10 dilution of 10X coating buffer in diH_2O*	Day before, store at 4°C	• 12 mL 10X coating buffer • 108 mL diH2O	Used to make capture antibody (12 mL/plate)
Standard *Reconstitute at 2000 pg/mL*	Just before use	• 730 uL diH_2O and mix gently. • Allow to sit for 10 minutes before making dilutions	200 uL/well
Assay diluent buffer (250 mL) *Dilute 5X concentrate 1:5 in diH2O*	Just before use	• 50 mL 5X AD • 200 mL diH2O	200 uL/well for 1 hour to block.
Capture antibody (12 mL/plate) *Dilute capture antibody 1:250 in Coating Buffer*	Just before use	• 48 uL of 250X antibody in 12 mL 1X coating buffer per plate	100 uL/ well O/N

Detection antibody (12 mL/plate) *Dilute 1:250 in AD*	Just before use	• 48 uL of 250X antibody in 12 mL 1X assay diluent per plate	100 uL/well 1 hour
AVD/HRP Enzyme (12 mL/plate) *Dilute HRP concentrate 1:250 in AD*	Just before use	• 48 uL 250X AVD/HRP in 12 mL 1X assay diluent per plate	100 uL/cells for 30 mins
Substrate solution	Just before use	• 1X TMB substrate solution comes in kit	100 uL/well for 15 mins → turns blue
Stop solution (100 mL): 1 M H_3PO_4	Just before use	• 93 mL diH2O • 7 mL phosphoric acid	50 uL/well

Protocol

1. Coat 96-well plates with 100 uL/well of the capture antibody in Coating Buffer as described in the reagent preparation. Seal the plate and incubate overnight at 4°C.
2. Aspirate the wells and wash 3 times with 150 uL/well of Wash Buffer. Let sit for 1 minute during each wash to increase the effectiveness of the washes. Blot the plate on absorbent paper to remove excess buffer (do this for subsequent washes as well).
3. Block plate with 200 uL/well of 1X Assay Diluent and incubate for 1 hour at room temperature. During this time, thaw all samples on ice.
4. Following blocking, aspirate each well and wash 3 times with Wash Buffer.
5. Reconstitute standards as noted in the reagent preparation. Perform a serial dilution in duplicate of the standards to make a standard curve for a total of 8 points.
    a. Add 100 ul of 1X Assay Diluent to the wells leaving the first wells empty. Add 200 uL/well of the top standard into the first two empty wells (A1/A2). Transfer 100 uL of the top standard from A1/A2 into wells B1/B2. Mix well and continue this process for the remainder of the column.
6. For the samples, add 65 uL of Assay Diluent to each well and 35 uL of sample to the appropriate wells. Save two blank wells for each plate and add 100 uL Assay Diluent.
    a. Note: The protocol calls for 100 uL of sample mixed with assay diluent/well and to adjust accordingly depending on how concentrated the samples are. We have found this dilution (35 uL sample/65 uL AD) to work well for LPS-treated HAPI cells. The dilution factor is considered during calculations at the end.
7. Seal the plates and incubate for 2 hours at room temperature. This step can also be done overnight at 4°C.
8. Prepare the detection antibody as described in the reagent preparation.
9. Aspirate and wash each plate 3 times as in step 2.

10. Add 100 uL/well of the diluted Detection Antibody.
11. Seal the plate and incubate at room temperature for 1 hour.
12. Prepare the Avidin-HRP as described in the reagent preparation.
13. Aspirate and wash each plate 3 times as in previous steps.
14. Add 100 uL/well of the diluted Avidin-HRP.
15. Seal the plate and incubate for 30 minutes.
16. Aspirate and wash the plate 5 times as in previous steps.
17. Add 100 uL/well of 1X TMB Substrate Solution and incubate at room temperature for 15 minutes.
18. Add 50 uL/well of Stop Solution.
19. Read each plate using Gen5 software at 450 nm and 550 nm and export to Excel.
    a. Subtract 550 nm values from 450 nm.
20. Generate standard curve of TNFα concentration (pg/mL) using standard values.
    a. Average duplicates for each standard value.
    b. Plot a standard curve of TNFα concentration (x-axis) using values of 7.8125, 15.625, 31.25, 62.5, 125, 250, 500, 1000 against absorbance (y-axis) and generate linear equation (y=mx+b)
21. Calculate the concentration of TNF alpha in pg/ml in each sample using the linear equation derived from the standard curve. Be sure to take into account the dilutions factor of the samples in the final analyses.
    a. Average duplicates for each sample = 'X'
    b. To obtain pg/mL TNFα, calculate (x-b)/m
22. Normalize values by total protein levels in cell lysates quantified with the DC protein assay (BioRad, Hercules, CA).
    a. To calculate protein ratio, divide all protein values by median.
    b. Divide each TNFα value by protein ratio for that sample

5.5.4 Western blot

Protein Assay
***DC*™ Protein Assay Kit II** Biorad # 5000112

Kit contents

- 250 ml REAGENT A, an alkaline copper tartrate solution
- 2000 ml REAGENT B, a dilute Folin Reagent
- 5 ml REAGENT S

1. Prepare standards
    a. Prepare 3 - 5 dilutions of a protein standard containing from 0.2 mg/ml to about 1.5 mg/ml protein. A standard curve should be prepared each time the assay is performed. For best results, the standard should be prepared in the same buffer as the sample.
2. Add 5 uL standard to each well in duplicate in first two columns of 96-well plate.
3. Add 5 uL cell lysate to 20 uL diH2O in microcentrifuge tubes. Vortex and spin down.
4. Add 5 uL sample to each well in duplicate.
5. Prepare working reagent A' (add 20 uL reagent S to each mL of reagent A)
    a. ~2.5 mL for full 96-well plate. Add 50 uL S to 2.5 mL A in 15 mL Falcon tube and vortex.
6. Add 25 uL reagent A' to each well using repeater pipette.
7. Add 200 uL reaegent B to each well using repeater pipette.
8. Gently agitate the plate to mix the reagents. If bubbles form, pop them with a clean, dry pipet tip. Be careful to avoid cross-contamination of sample wells.
9. Allow the plate to sit for 15 minutes, then read absorbance at 750 nm.
10. Calculate amount of protein in each sample and amount needed for Western blot samples.
    a. Mg/mL calculation = (X-b)/m (m = slope, b = intercept)
    b. Multiply by 5 (dilution factor if added 5 uL sample to 20 uL H2O in protein assay)
    c. To get uL sample/20ug protein, divide 20 by mg/mL value
    d. Multiply by 4 so that you have enough to run each sample at least 4 times
    e. 50 uL – (uL/80 ug) to get amount of buffer you need

Prepare Western blot samples

1. Add 50 uL BME to 450 uL 6x Laemmli sample buffer = SB
2. Poke holes in top of tubes with needle,
3. For 60 uL total sample, Add 10 uL SB to 50 uL sample
4. Spin down, Heat samples at 95C for 3 minutes
5. When running blots, load 20 ug protein prepared from lysates (15 uL sample/well)

Recipe for 6X SDS Sample Buffer (10 mL):

- 7ml 4X Tris-Cl/SDS, pH 6.8 (0.28M)
- 3ml glycerol

- 1g SDS
- 1.2 mg Bromophenol Blue

Prepare, load, and run gel:

1. **Setup plates:**
    a. Wash glass plates with soap & hot tap water; dry with kimwipes, lay plates on bench, wipe surface (only the surface facing up – spacers up on large plate) with ethanol (70% or 95%); also wipe spacers (usually 1mm in width) with ethanol.
    b. Assemble a large plate with a small plate (avoid nicked plate edges at the bottom), with the ethanol-wiped surfaces facing each other; place into casting stand with short plate/clamps in front. Check to make sure plates are flush to ensure gel-bottom will be leak-proof and clamp
    c. Can get samples out to thaw on ice now or while gels polymerize (also get rainbow markers, pooled sample, APS to thaw).

2. **Prepare gel mixtures** in beaker, swirling the mixture after adding each ingredient:

FOR 4 MINI GELS:	**10% Lower Gel**	**12.5% Lower Gel**	**Upper/Stacking Gel** *can add 15 ul bromophenol blue (16 mg/mL)
Water (HPLC H2O)	10.3 ml	10.6 ml	6 ml
30% Acrylamide solution	8.4 ml	13.4 ml	1.5 ml
4X Lower Gel Buffer	6.25 ml	8.0 ml	--
4X Upper Gel Buffer	--	--	2.5 ml
10% APS (ammonium persulfate)*	156.25 ul	200 ul	120 ul
TEMED*	15.625 ul	20 ul	12 ul

*Note: DO NOT add APS and TEMED until you are absolutely ready to pour the gel.

3. **Pour gels:**
    a. Transfer lower gel mixture to space between two plates (up to between black line and top edge of clamp); on the top of the gel, gently overlay a small amount of HPLC water or isopropanol using a transfer pipette to even out mixture
        i. Use transfer pipette to pick up remainder of gel mixture in beaker to determine when gel has polymerized **(~30 minutes).** Pipette rest of mixture into serological pipette and throw away.
    b. Prepare the upper/stacking gel mixture. Do not add APS and Temed until:
        i. Combs are wiped with ethanol and dried;
        ii. Pipetmen for APS & TEMED have tips on them and set for the correct volume;
        iii. The water or isopropanol on top of the gels is poured off and the last drop is wiped off with kimwipe while the gels are inverted.

c. Pour the stacker: immediately after adding the APS & TEMED and briefly swirling, pipet the gel mixture, filling the space to the very top of the plates. **Make sure there are no bubbles.** Then immediately insert combs into the stacking gel (horizontal ridge of combs facing you), being careful not to create bubbles → polymerize for 15-30 min.

4. Dilute 10X Running Buffer to 1X with deionized water
   a. For 4 mini-gels (run in two boxes i.e. 'chambers'), **make 1600 mL** (want extra in case leaking happens, can save any remaining for leaks in future gels)
      i. 4 mini gels: **1440 mL DI water + 160 mL 10x running buffer**
      ii. 2 mini gels: 720 mL DI water + 80 mL 10x RB
   b. Thaw gel samples if not done already.

5. Carefully remove combs, pulling straight up. Clear off excess gel on top of plate with kimwipe. If any lanes are crooked, fill the lanes with some gel running buffer using a small transfer pipet, then straighten the lanes (or can do this after in chamber boxes). Remove gels from the casting stand.

6. Set up chamber boxes
   a. Attach plates to each side of the gel apparatus (small plates face in), hold plates in place and clamp both sides at the same time. Put the apparatus into the chamber (match electrodes – red to red and black to black)
   b. Pour 1X running buffer into the gel apparatus, then rest of the chamber up to black line. Clean out each of the wells in the stacking gel by squirting into them with running buffer using a small transfer pipet inserted into each well.

7. Load gels with rainbow markers, gel samples, and pooled samples
   a. 4-5ul/well of rainbow for a mini-gel → can add on both sides if cutting blots
   b. 15 uL of gel samples (rainbow first, then 12 gel samples, 1 PS, blank) → write out order
   c. Vortex each sample before loading, being careful to load exact amount of sample into appropriate wells. Pull out pipette tip as you see bubble (to make sure you load all sample).
   d. ***make sure to keep track of gel numbers (1, 2, 3, 4), and which gels are in which chamber (chambers are labeled 1 and 2). I keep gels 1 and 2 in chamber #1 on the left and gels 3 and 4 in chamber #2 on the right.

8. Connect electrical probes (red to red and black to black), turn on power supply.
   a. For mini-gels, **run at 150V constant through stacker gel, then can turn up to 175-200 V** for the rest of the gel. Run until the blue dye front is almost at bottom edge of plates (takes about 1-1.5 hr). Make sure you see bubbles coming from the bottom when you turn on.
   b. ***Make sure the gels remain covered by running buffer. If level leaks below top of glass plates, blue line of samples will become slanted. PAUSE the power supply, add more running buffer to the top and start.

Transfer method:

1. Make fresh 1X Tris-Glycine Transfer Buffer: 10x transfer buffer + deionized water in a beaker, stirring it for a while in the cold-room on stir-plate before adding cold methanol and continuing to stir (covering the beaker with saran wrap).
    - **a.** For 2 gels (1 transfer box) → 1L Transfer Buffer 100ml 10x transfer buffer + 700 mL DI water + 200 mL cold methanol in cold room
    - b. For 4 gels (2 transfer boxes) → 1.5L TB: 150 mL 10X transfer buffer, 1050 mL DI water, 300 mL cold methanol
    - **c.** Can bring transfer boxes (with stir bars) and ice packs into cold room at this time. Can bring jug of used transfer buffer from cold room into lab.

2. Get transfer cassettes, sponge pads, blotting paper cut to the size of the pads (or less, but not more), glass tray and used transfer buffer; set the open cassettes in the tray with the clear (or red) side lying down in the tray, sponge pad on each side of the cassette, blotting paper on each pad. Clip top cassette (black side) to glass tray to keep it secured.
    - a. Pour used transfer buffer into the tray. Will want PVDF to be submerged; also pour some used transfer buffer into a plastic tray for gel-soaking.

3. With gloves on, get PVDF (8.5 x 5 cm), cut a small slash off the bottom right corner of the membrane, mark the corner with a syringe-needle hole (# holes to correspond to gel 1, 2, 3 and no holes in 4)
    - a. 'activate' membranes by soaking in 10 mL methanol (room temp) on shaker for 1-3 mins
    - b. place PVDF on the blotting paper that's on the clear (or) side (bottom of tray). Bottom right corner should be top left (rainbow markers of gel will be on right) when looking down at it.

4. Remove gels from the apparatus; carefully pry the plates apart using the "wedge" (I place short place facing down with rainbow markers on the right)
    - a. quickly (without letting the gel dry out) cut the stacking gel off to discard;
    - b. Can cut a small slash off the bottom right corner (opposite from rainbow markers) to designate orientation of the gel; gel can be wetted with some of the used transfer buffer from the tray if the cutting goes slowly.

5. Pick up the gels by two corners and fully immerse them in the plastic tray with used transfer buffer, remember to differentiate the gels by #; leave gels to equilibrate for about 10 minutes.
    - a. Meanwhile, clean up the gel equipment (rinse plates, spacers, clamps, apparatus, chamber in hot tap water; give the apparatus, spacers & chamber a rinse in deionized water, too – *or can put everything in hot water/soap to soak until later*).

6. Assemble the "sandwich": place gel on top of the corresponding membrane in the correct orientation (bottom of the gel is at the top with rainbow markers on the righ side); **again, make sure there are no bubbles,** especially between the gel and

membrane by using the "roller" pressed gently across the gel surface; place the blotting paper over the gel and re-use the roller to ensure no bubbles; place the sponge-pad on top and close the cassette.

7. Take the tray into the cold room where the transfer apparatus (chamber & lid), "ice-pack," and fresh transfer buffer (don't forget to add methanol if you haven't already). Add transfer buffer to chambers with stir-bar spinning on a stir-plate. Place the cassettes in the tank with the clear side (or red) of each cassette toward the red side of the chamber (and black side to black side).

8. Cover the chamber with the lid containing electrode connections (again, red to red and black to black); plug the electrodes into the Bio-Rad power supply, turn it on and set it for **100V for 1hr and 15 min (1 hr is sufficient for the mini-gel transfer apparatus);** press "Run" and the transfer will proceed and automatically shut off after the set time elapses.

9. After transfer, put blots in 1x rapid block or superblock (depending on the antibody – check chart) for ~10 mins. Then add 10 mL primary antibody (check chart for dilutions) → cold room O/N on rocker or room temperature for 1 hour. Can put rat sponge pad over pour bucket to remind you not to throw away primary antibody when incubation is done.
    a. Save fresh transfer buffer after transfer by pouring into 'used transfer' bottle.

<u>Antibody incubation:</u>

1. After overnight incubation with primary antibody, add primary antibody back into falcon tube (labeled in fridge)
2. **Wash 3-4x with 1X TBST** (50 mL 20x TBST + 950 mL diH2O) at room temp
    a. 10 min/wash on shaker, 10 mL/blot
3. While washing, **make 2ndary antibody dilution in 1x RapidBlock (or superblock depending on which the primary antibody was in)**
    a. Small blots → 10 mL/blot
        i. Make separate Falcon tube w/ 20 mL of 2ndary for each species
        ii. 2ndary antibodies are in -20 freezer
    b. Anti-rabbit = 1:5000 *(NFKB, iNOS, CREB, SOD, Nrf2)*
        i. Ex. for NFKB: add 4 uL anti-rabbit to 20 mL RB
    c. Anti-goat = 1:2500 (*GFAP, Actin, Cox2, GAPDH)*
    d. Anti-mouse: 1:2500 (*NOX2, GST)*
        i. Ex. for NOX2: add 8 uL anti-mouse to 20 mL RB
4. **Add 2ndary** antibodies to blots (10 mL/blot), **shake for 1 hour** at room temperature
5. Discard 2ndary in same Falcon tube you made it in
6. **Wash 3-4x with 1X TBST**

<u>Develop blot:</u>

1. While on wash 2-3, **plug in camera to cool** (cools for 10-15 mins), open UVP software (purple logo)
2. **Make ECL** in 15 mL Falcon tube (while blots are still in TBST)
    a. For 2 large blots, add 3.2 mL brown + 3.2 mL clear bottle (change tips)
    b. Keep tube in drawer until washes are done
3. **Cut transparencies** (in half on longer side 'hamburger'), 1 full transparency per blot
4. **Add ECL reagents, rock for 5 minutes**
    a. First pour off TBST, dab kimwipe at one corner to get it all off
    b. Add ECL 1.6 mL/blot
    c. Put blots on rocker on belly dancer, make sure all of blot is being covered (can rock by hand at first)
5. After 5 mins, develop blot 1 (blot 2 can stay rocking or you can stagger the 5 mins)
    a. Pour off ECL back into 15 mL Falcon, dab corner with kimwipes
    b. Use tweezers on bottom right corner and roll blot onto transparency
    c. Roll other half of transparency on top (no bubbles)
    d. In UVP: acquisition → preview → 0 min, 0 sec to position blot in frame
    e. End preview, set to 5 mins first for each → capture
6. During capture 1, prepare blot 2
7. During capture 2, wash blot boxes, fill with diH2O, get gentle review strip buffer out (fridge door)
    a. Add strip buffer to Falcon tube (20 mL/blot) → *confirm with Donna*
    b. warm in water bath for 5-10 mins
8. Wash both blots briefly with diH2O
9. Add strip buffer, put blots in water bath and rock for 30-45 mins
10. Wash with TBST 3-4x
11. RapidBlock
12. Primary antibody O/N

5.5.5 Immunohistochemistry for fluorescent labeling of glial cells in rat brains

Reagents:

- 1L 1x PBS:
    - 1 tablet per 200 mL → 5 tablets in 1 L water
    - Or 100 mL 10x PBS in 900 mL water
- 500 mL PBST (0.1% tween):
    - Add 500 uL tween to 500 mL 1x PBS
    - Keep 50 mL at room temperature for use, store rest in refrigerator
- Blocking buffer (2 mL/vial)
    - 10% FBS in PBST: 1.8 mL PBST + 200 uL FBS per vial

Day 1

Note: realistic to start 4 brains at once

1. Label vials on cap and base with brain number and brain region (HP, FC)
2. Add 2 mL blocking buffer/vial
3. Pour PBST into dish on black box (easier to see)
4. Remove sections from 96 well plate using paintbrush
    a. Remove sections from 2 columns per plate, 6 columns apart (e.g., 1 and 7, 2 and 8)
    b. Add to dish containing PBST on black box
    c. Uncurl sections in dish using two paintbrushes
    d. Add FC to one vial, HP to another vial
5. Put vials in cardboard box and add paper towels around so that they can't fall over
6. Put box on shaker in cold room overnight (4 degrees)

Day 2

1. Add primary antibody directly to the 2 mL blocking buffer already in vial
    a. GFAP 1:1000 → 2 uL in 2 mL
    b. CD68 1:100 → 20 uL in 2 mL
    c. *Note: can double label if using different colors and species e.g., GFAP mouse green with Iba rabbit red*
2. Swirl to collect any sections stuck to the side and put back on shaker in cold room overnight

Day 3

1. Wash with PBST x3
    a. Use transfer pipette to collect blocking buffer and put into discard container. Make sure you don't pick up any sections.
    b. Add 4 mL PBST/vial → 10 minutes on shaker at room temperature
2. Add secondary antibody into 2 mL blocking buffer (10% FBS/PBST)/vial at 1:500
    a. E.g., for 1 brain, two vials (HP and FC), add 8 uL secondary antibody into 4 mL blocking buffer, then add 2 mL to each vial
    b. Cover box so that light can't enter. Place on shaker at room temperature for 3 hours
3. Wash with PBST as in step 1 x3

4. Add DAPI at 1:1000 (2 uL in 2 mL PBST → 2 mL/vial)
5. Wash 1x with PBST → can place in fridge for mounting later or mount now

Mounting sections

1. Label slide on frosted white part with experiment, brain number, antibodies, brain region, slide number, date, your initials (e.g., NSRL21A #1 GFAP FC-1 1/1/2021 DC)
2. Fill dish with PBST and pour all sections from one vial into dish
3. I like to organize the sections now – place them in order to the left of the dish and orient them so that midline is on the right
4. Angle slide in the dish so that white part is on the right (if you are a lefty) resting on the top edge of the dish. Use paintbrush to wet slide.
5. Slide sections onto the slide with the brush in two rows. Can fit 6-12 sections/slide
6. Put in black box or under foil to dry overnight

5.5.6 RNA isolation from brain tissue and RT-qPCR for mRNA quantification

Brain RNA isolation using the RNAesy Lipid Tissue mini kit (Qiagen, 74804)

- Materials:
  - RNeasy Lipid Tissue Mini Kit (50 preps)
    - Add 4 volumes (44 mL) of 96-100% ethanol to 11 mL RPE buffer
  - Tissue homogenizer
  - 200 uL Chloroform/sample
  - 70% and 96-100% ethanol
  - Sterile, RNase-free pipette tips
  - 1.5 mL, 2 mL sterile microcentrifuge tubes
  - 2 centrifuges: 4C, 15-25C
  - RNase-Free DNase Set (Qiagen, 79254)
    - Make DNase I stock: Add 550 uL of RNAse-free water (provided) using RNase-free needle and syringe. Do not vortex! → pipette into microcentrifuge tube and label for future use

Protocol:

1. When starting new kits, make RPE buffer and DNAse I stock solutions (see above)
   - *Realistic to prepare 12 samples at once (takes ~3-4 hours before agarose gel)*
   - *Keep samples on ice until lysis reagent is added*

2. Homogenize ≤100 mg fatty tissue (≤50 mg other tissue) in **1 ml QIAzol Lysis Reage**nt using tissue homogenizer
   - Transfer tissues to 2 mL RNAse free/sterile microcentrifuge tubes (wide/round bottom) using pipette tip
   - Prepare 4x 15 mL tubes with ~10 mL of: 10% bleach, RNAse-free water x2, 70% ethanol → clean homogenizer in-between each sample by washing in solutions

3. Incubate the homogenate at room temperature for 5 min
   - *Promotes dissociation of nucleoprotein complexes*

4. Add **200 µl chloroform**, and shake vigorously for 15 s (thorough for phase separation).

5. Incubate sample at room temperature for 2–3 min.

6. Centrifuge at 12,000 x g (~13,500 rpm) for 15 min at 4°C (centrifuge in cold room).

7. Transfer upper, aqueous phase (clear) to a new labeled tube (not supplied). Be careful to avoid the interphase. Add **1 volume of 70% ethanol**, and vortex. Do not centrifuge. Proceed at once to step 7.

8. **Transfer up to 700 µl of the sample** to labeled RNeasy Mini spin column in 2 ml

collection tube (supplied). Close the lid, centrifuge at room temperature for 15 s at ≥8000 x g (10,000 rpm) and discard flow-through (whatever is in the tube → beaker).

9. Using the same collection tube, repeat step 7 using the remainder of the sample *(if you have more than 700 uL total).* Discard the flow-through.

10. Add **350 µl Buffer RW1** to the RNeasy Mini spin column. Close the lid gently and centrifuge for 15 s at 8000 x *g* (10,000 rpm) to wash the membrane. Discard the flow-through.

11. DNAse digestion: **Add 10 µl DNase I stock solution** (prepared as above) **to 70 µl Buffer RDD** (for 1 sample). Mix by gently inverting the tube, and centrifuge briefly to collect residual liquid from the sides of the tube.
    - Need 80 uL total/sample, so make extra
    - *Note: DNase I is especially sensitive to physical denaturation. Mixing should only be carried out by gently inverting the tube. Do not vortex.*

12. Add **80 uL DNase I incubation mix** directly to the RNeasy Mini spin column membrane, and place on the benchtop (15–25°C) for 15 min.
    - *Note: Be sure to add the DNase I incubation mix directly to the RNeasy Mini spin column membrane (looking from directly above column on the bench). DNase digestion will be incomplete if part of the mix sticks to the walls or the O-ring of the spin column. If it sticks to the side, re-pipette into the center.*

13. Add **350 µl Buffer RW1** to the RNeasy Mini spin column. Close the lid gently and centrifuge for 15 s at 8000 x *g* (10,000 rpm). Discard the flow-through.

14. Add **500 µl Buffer RPE** to RNeasy column. Close lid, centrifuge for 15 s at ≥8000 x g and discard flow-through.
    - *Be sure to add 4 volumes of 96-100% ethanol to RPE when opening a new kit (see above)*

15. Add **500 µl Buffer RPE** to RNeasy column. Close lid and centrifuge for 2 min at ≥8000 x g.
    - *Note: The long centrifugation dries the spin column membrane, ensuring that no ethanol is carried over during RNA elution. Residual ethanol may interfere with downstream reactions. After centrifugation, carefully remove the RNeasy Mini spin column from the collection tube so that the column does not contact the flow-through. Otherwise, carryover of ethanol will occur.*

16. Place RNeasy column in a new labeled 1.5 ml tube with cap (supplied). **Add 30–50 µl RNase-free water,** close lid and centrifuge for 1 min at ≥8000 x g.

17. Keep purified RNA on ice when aliquots are pipetted for downstream applications or

store at -80 C.

Quantify RNA NanoDrop-1000 (4th floor)

- Clean nanodrop with diH20 (NOT ethanol). Open program on the computer. Press 'nucleic acid'. Remove kimwipe and put top down to calibrate. Then add 1 uL RNAse free water and press 'blank'. Wipe with diH20 and add 1 uL of sample (remember to enter sample number). Put handle down and press 'measure'.
- Record for each sample: concentration (ng/uL), 260nm, 280 nm, 260/280 ratio
    - *Note: Pure RNA ratio should be ~2.0. If lower, it may indicate the presence of protein, phenol or other contaminants that absorb strongly at or near 280 nm*
- Gives concentration in ng/uL → calculate uL for 1 ug
    - There are 1000 ng in 1 ug, so…
    - $\frac{650\ ng}{1\ uL} = \frac{1000\ ng\ (i.e.,1\ ug)}{x\ uL}$ → solve for X by dividing 1000 by concentration in ng/uL.
    - E.g., X = 1000/650 = 1.538 uL for 1 ug RNA

Assessing RNA Quality

- Materials
    - Agarose
    - TBE Buffer (5x)
    - RNA Loading buffer
    - RNase*Zap*™ RNase Decontamination Solution x 1 (Thermo, Sigma)
    - RNAse free water, flask, gel equipment

1. Prepare 300 mL TBE buffer
    - 5X to 1X → add 60 mL 5X TBE to 240 mL RNAse free water in sterile bottle
    - Spray gel equipment with RNaseZap and let sit. Then wash with distilled water.
2. Prepare agarose gel
    - Measure 0.5 grams of agarose using sterile scoop
    - Add to flask of 50 mL TBE buffer and put on hot plate. Once boiling, remove (using gloves). Add 3-5 uL ethidium bromide and swirl. Pour into gel box and add combs.
3. Add samples
    - Prepare samples by adding 1 ug RNA (calculated above), 5 uL RNAse-free water, 2 uL sample loading buffer/dye into microcentrifuge tube.
    - Once gel is polymerized, turn orientation of gel to run left to right
    - Add samples to wells. Be careful not to break gel by putting tip too far to the bottom or samples will leak out.
4. Run at 80-90 V
5. Visualize (UVP system)
    - Turn 'emission filter' to ethidium bromide. Turn UV on. Set time and capture.

- Partially degraded RNA will have a smeared appearance, will lack the sharp rRNA bands, or will not exhibit a 2:1 ratio.

Synthesize cDNA (RT reaction)
SuperScript III First Strand (Thermofisher, cat #18080-051)
Sufficient for 50 reactions, based on a 20 µl reaction size

Additional materials:

- 0.2 mL PCR strips, sterile tips
- GeneAmp PCR system 9700

Protocol:

1. Mix and briefly centrifuge each component before use.
    a. Thaw RNA samples on ice
    b. Keep enzymes in freezer until you need them
        • SuperScript III RT, RNaseOUT, E. coli RNase H
    c. Room temp to thaw
        • DEPC-treated water, Random hexamers, 10X RT buffer, 0.1 M DTT, 25 mM magnesium chloride, 10 mM dNTP mix
    d. Calculate amount of RNA (1 ug) and water (up to 10 uL)
2. Prepare RNA mixture in sterile PCR tubes and no RT control (see below)
    a. Pipette to the bottom of tube, then add cap and spin down after everything is added
3. Using GeneAmp PCR system 9700, incubate at 65°C for 5 min, then place in ice for 1+ min. "Stacey –> cDNA-1"

RNA mixture	Sample	No RT control
dH_2O	to 10µL	8 µL
dNTPs	1µL	1µL
Random Hexamers	1µL	1µL
RNA	1 µg	0 µg
Total	**10µL**	**10µL**

Temperature	**Time**
65ºC	5 minutes
4ºC	1 minute

4. For each reaction, prepare following cDNA reaction mix in single tube:
    a. e.g., for 4 samples, make enough for 4.5 samples → keep on ice
    b. With PCR strip on ice, add 10 uL of cDNA reaction mix to each tube (total 20 uL). Mix gently and centrifuge briefy.

cDNA reaction mix	
10x RT Buffer	2µL
25mM $MgCl_2$	4µL
0.1M DTT	2µL
RNase Out	1µL
SuperScript III RT	1µL
Total	**10µL**

Temperature	**Time**
25ºC	10 minutes
42ºC	50 minutes
85ºC	5 minutes
4ºC	∞

5. Add strip to GeneAmp PCR system 9700 → "Stacey cDNA-2"
    a. Incubate at 25°C for 10 min.
    b. 50°C for 50 min.
    c. Terminate reaction at 85°C for 5 min, then chill on ice.
6. Add 1 µL of Rnase H to each tube and incubate at 37°C for 20 min → "Stacey cDNA-3"
7. Proceed to PCR or freeze at –20°C (label strip with tape).
    a. Dilute cDNA 1:10 (add 180 uL distilled H20 to 20 uL cDNA)
    b. Note: now we don't have any RNA left (RNAse H degrades it) → don't need to keep on ice when using

Real-Time qPCR

- Optical 96-well PCR reaction plates (Applied Biosystems, No. N801-0560)
- Optical adhesive 96-well reaction plate covers (Applied Biosystems, No 4311971)
- Power SYBR Green PCR Master Mix (Applied Biosystems, No. 4367659)

1. Prepare reaction mix in microcentrifuge tube
    a. Make enough for each sample in triplicate + 1 extra (e.g., 4 samples x3=12, make enough for 13)

Reagent	**Volume (1x)**
SYBR Green PCR Master Mix	12.5µL
dH_2O	2.5µL
10x Primer	2.5µL
Total (w/o cDNA)	**20µL**

2. Add 20µL mix to optical plate (on black plate holder) → pipette to the bottom of each well
3. Add 5µL of cDNA to plate in triplicate, avoid bubbles
4. Cover plate adhesive film and rub kimwipe over to seal
5. Check for bubbles in wells → if so, centrifuge for <1 minute
6. Using applied Biosystems 7300 instrument, set up plate, identify all wells, change volume of reaction to 25 µl, and add the dissociation stage. Start.

Calculation

1. Average triplicates for each sample (e.g., COX-2)
2. Subtract GAPDH average for each sample from COX-2 average = ^Ct
3. To calculate mRNA expression relative to a reference group (e.g., non-irradiated, control diet), subtract the average ^Ct of the reference group from ^Ct of each sample (^Ct of rat #1 - $^{\wedge}$Ct average reference group) = ^^Ct
4. Calculate $2^{-\wedge\wedge Ct}$ for each sample. Compute group averages and SD/SE. The average $2^{-\wedge\wedge Ct}$ for reference group should be ~1 and all other values are expressed relative to this reference group (e.g., 1.4 = 1.4 fold higher mRNA expression).

5.5.7 Novel object recognition (NOR)

Overview: This task assesses the rat's ability to remember an object by observing reaction to a novel object compared to a previously viewed (i.e., familiar) object. During the conditioning day, rats are exposed to two identical objects and have the opportunity to explore the objects and become familiar with them. On the testing day, one of the familiar objects and one novel object are presented. Rats are expected to spend more time investigating the novel object than the familiar object, showing they remember the familiar object from the conditioning day (i.e., demonstrating recognition memory).

Materials:

- Open field arena (93 x 93 cm)
- 70% ETOH
- 2 sets of identical objects (e.g., 2 dragons, 2 turtles)
- 3 stopwatches that do not make noise: 1) time up to 15 minutes 2) exploration of object 1 3) exploration of object 2

Protocol:

1. Rats are tested in a dimly lit an open field arena (93 x 93 cm) using stimulus objects that vary in color and shape affixed to the bottom of the arena with velcro. On the conditioning day (training trial), add two identical objects (familiar) to the arena equidistant from the sides.
2. Record the starting time and place the rat in the arena facing the front wall (closest to you) away from the objects. Start stopwatch #1 (to track total time up to 15 minutes).
3. Hold stopwatch #2 in one hand and stopwatch #3 in the other hand. Record the amount of time the rat explores each object ('left' and 'right' on the datasheet). The rat will be allowed to explore both stimuli until it has explored either object for 30 seconds or until 15 minutes have passed.
    a. Exploration is defined as when the head of the animal is 0.5 cm from the object or when it touched the object, but not when an animal climbs onto an object or uses it as a support to explore the environment. In other words whenever it is engaged in active exploration (e.g., sniffing or manipulating) of the object.
    b. The data sheet also has a place to record notes, of anything that happens during the session that is of note (rat chewing the object, loud noise in the hall, etc).

		Trial 1					Trial 2			
Rat	Familiar Object	Start Time	Left	Right	Novel Object	L/R Novel	Start Time	Left	Right	Notes
7	Leprechaun				Dragon	R				
8	Leprechaun				Dragon	R				

4. Return the rat to its home cage. Disinfect objects and the arena with 70% ETOH after each rat to clean the apparatus and remove olfactory cues. Place the next rat into the arena; the order in which the rats are run are counterbalanced across groups (one rat from each group is run, then the second rat from each group is run, etc.).
5. Twenty-four hours later, on the testing day, add one familiar object (i.e., object using during conditioning day) and one novel object to the arena.

    a. The objects are counterbalanced between groups, test session, and whether they are novel or familiar objects.
6. Place the rat into the arena and record exploration time as above.
    a. Note: If during the conditioning day, a rat did not explore either object for 30 seconds within 15 minutes, they will not be tested on the testing day.
7. Recognition memory will be evaluated based on the amount of time spent exploring the familiar and novel objects
    a. rats that remember the object presented on the conditioning day will spend a disproportionate amount of time exploring the novel object, relative to the familiar object, while rats that do not remember the object (impaired recognition memory) will spend an equivalent amount of time exploring both the novel and familiar object.
8. Data analysis
    a. Recognition scores will be reported as percentage of total exploration time spent with novel object calculated as: (seconds spent with novel object − seconds spent with familiar object)/(total time spent with both objects) x 100.
    b. Lower scores indicate impaired recognition memory.
    c. Can compare each group to 50% using one-sample t-test and/or compare recognition scores between groups (e.g., using ANOVA).

5.5.8 Radial Arm Water Maze (RAWM)

Overview:

Rats are placed in a pool of water with internal walls that form eight channels (arms) radiating from an open center area. The pool is surrounded by extramaze cues, which the rat must use to navigate the maze. At the beginning of each trial (5 trials/day for 5 consecutive days), rats are randomized to start in one of the arms and must swim to locate a submerged platform hidden in one of the arms. If the rat fails to locate the platform within 90 seconds, it is guided to the platform by the researcher. Rats remain on the platform for 15 seconds before being placed in a novel start location (trials 2-4). After the 4th trial, rats are returned to their home cage for 30 minutes, after which they are run on a 5th trial to test for retention. The platform is moved to a new arm daily without repetition, which forces the rats to unlearn the previous day's platform location and learn its new location. Latency (s) is obtained using image tracking software (HVS Image). The order of entry into the maze arms is scored manually to analyze the number of errors. Reference (long-term) memory errors are committed when a rat re-enters an arm that does not contain the platform (trial-independent) and working memory errors (short-term) are committed when a rat re-enters an arm previously explored during that trial (trial-dependent). Because trial 5 is a good assessment of short-term memory and memory consolidation, data from trial 5 is used for statistical analyses.

Setup:

1. Turn all ceiling lights off except by the door. Manually turn on 3 plugged in lights, plug in camera, and turn on computer. Open HVS image program and load file created for that day which shows order of rats.
2. Fill pool to ruler mark (1 cm) above platform
3. Water temperature at ~23 °C
4. Platform in different arm each day
5. Cues = posters, hanging mouse, green chair, soda bottle

Maze protocol

1. Place rat in starting arm specified by the datasheet and computer program (different each trial) and squeeze clicker ball to start recording time/swim path.
2. Manually record each arm (1-8) the rat enters (full body) on the datasheet until he either finds platform or 90 seconds passes. If the rat doesn't find the platform in 90 seconds, guide him to the platform.
3. Allow the rat to stay on platform for 15 seconds (so that he can look around and remember spatial cues for the platform location). Place the rat in a new starting arm for the next trial x 4 trials total. Then start timer for 30 minutes.
    a. Note: you will need 3-4 timers to keep track of the 30 minutes between trial 4 and 5 for multiple rats.
4. Dry off rat with a towel and place back in cage for 30 minutes before trial 5.
5. New platform location each day for 5 days. Weigh rats before starting trial 1 on days 2 and 4.

Shutdown

1. Turn off manual lights. Turn room lights off, then press up arrow 6 times.

2. Unplug camera, turn off computer.
3. Take 5-6 buckets of water out of maze.
4. Hang towels to dry.

Data analysis:

1. Enter all values from datasheet into Excel file programmed to calculate reference, working, and total errors. A second researcher can manually score errors to check calculations.
2. Reference (long-term) memory errors are committed when a rat re-enters an arm that does not contain the platform (trial-independent) and working memory errors (short-term) are committed when a rat re-enters an arm previously explored during that trial (trial-dependent).
    a. E.g., for rat 1 below, the platform was in arm 1. On trial 1, he was placed in arm 3 to start, and made 2 reference errors by entering arms 2 and 7. He made 2 working errors by re-visiting arms 2 and 3, which did not contain the platform.

Rat #	Weight	Group	Start	Choices														
	(gr)			1	2	3	4	5	6	7	8	9	10	11	12	13	14	15
1	493		3	2	7	2	3	1										
1			5	7	8	1												
1			2	4	2	6	2	1										
1			6	2	1													

3. Score errors for all trials and days. Because trial 5 is a good assessment of short-term memory and memory consolidation, data from trial 5 is used for statistical analyses.
4. Perform a repeated measures ANOVA using testing day as the within subject factor to analyze trial 5 latency to find the platform (seconds), and reference, working, and total errors.